REPUBLIQUE DU CAMEROUN
Paix – Travail – Patrie
****
UNIVERSITE DE YAOUNDE I
FACULTE DES SCIENCES
DEPARTEMENT DE PHYSIQUE
****
CENTRE DE RECHERCHE ET DE FORMATION DOCTORALE EN SCIENCES, TECHNOLOGIES ET GEOSCIENCES

REPUBLIC OF CAMEROUN
Peace – Work – Fatherland
****
UNIVERSITY OF YAOUNDE I
FACULTY OF SCIENCE
DEPARTMENT OF PHYSICS
****
POSTGRADUATE SCHOOL OF SCIENCE, TECHNOLOGY AND GEOSCIENCE

MULTI-OBJECTIVE ANALYSIS AND OPTIMIZATION OF PERFORMANCE OF A MULTI-IRREVERSIBLE ABSORPTION HEAT PUMP

Thesis submitted to the Faculty of Sciences, Department of Physics under the theme In view of obtaining a Doctorate/PhD degree of physics

Par : **FOSSI NEMOGNE Rodrigue Léo**
Master ès Physics

Sous la direction de
TCHINDA Réné
Professor,
University of Dschang

Année Académique : 2021

UNIVERSITÉ DE YAOUNDÉ I
THE UNIVERSITY OF YAOUNDE I

FACULTÉ DES SCIENCES
FACULTY OF SCIENCE

DÉPARTEMENT DE PHYSIQUE
DEPARTMENT OF PHYSICS

ATTESTATION DE CORRECTION DE LA THÈSE DE DOCTORAT/Ph.D

Nous, Professeur **OWONA ANGUE Marie Louise Clotilde épouse OWONO OWONO** et Professeur **TCHAWOUA Clément**, respectivement Examinateur et Président du jury de la Thèse de Doctorat/Ph.D de Monsieur **FOSSI NEMOGNE Rodrigue Léo**, Matricule 07W263, préparée sous la direction du Professeur **TCHINDA Réné** intitulée : « **Multi-objective analysis and optimization of performance of a multi-irreversible absorption heat pump** », soutenue le Jeudi, **08 Avril 2021**, en vue de l'obtention du grade de Docteur/Ph.D en Physique, Spécialité **Energie, Systèmes électriques et électroniques,** Option **Energie et environnement,** attestons que toutes les corrections demandées par le jury de soutenance ont été effectuées.

En foi de quoi, la présente attestation lui est délivrée pour servir et valoir ce que de droit.

Fait à Yaoundé, le 06 Mai 2021

Examinateur	Le Chef de Département de Physique	Le Président du jury
Pr OWONA ANGUE Marie Louise Clotilde épouse OWONO OWONO	Pr NDJAKA Jean-Marie Bienvenu	Pr TCHAWOUA Clément

REPUBLIQUE DU CAMEROUN
Paix-Travail-Patrie
****
UNIVERSITE DE YAOUNDE I
****
CENTRE DE RECHERCHE ET DE FORMATION DOCTORALE EN SCIENCES, TECHNOLOGIES ET GEOSCIENCES
****
UNITE DE RECHERCHE ET DE FORMATION DOCTORALE PHYSIQUE ET APPLICATIONS
****
B.P. 812 Yaoundé
Email: crfd_stg@uy1.uninet.cm

REPUBLIC OF CAMEROON
Peace-Work-Fatherland
****
UNIVERSITY OF YAOUNDE I
****
POSTGRADUATE SCHOOL OF SCIENCE, TECHNOLOGY AND GEOSCIENCES
****
RESEARCH AND POSTGRADUATE TRAINING UNIT FOR PHYSICS AND APPLICATIONS
****
P.O. BOX 812 Yaounde
Email: crfd_stg@uy1.uninet.cm

Energy, Electrical Systems and Electronics laboratory

Thesis submitted to the Faculty of Sciences, Department of Physics under the theme

MULTI-OBJECTIVE ANALYSIS AND OPTIMIZATION OF PERFORMANCE OF A MULTI-IRREVERSIBLE ABSORPTION HEAT PUMP

In view of obtaining a Doctorate/PhD degree of physics

Specialty: **Energy, Electrical Systems and Electronics**
Option: **Energy and environment**

Written and presented by:
FOSSI NEMOGNE Rodrigue Léo
Registration number: **07W263**
Master ès Sciences
Under the Supervision of:
TCHINDA Réné
Professor,
University of Dschang

Jury:

President: TCHAWOUA Clément, Professor, University of Yaounde I;
Supervisor: TCHINDA Réné, Professor, University of Dschang;
Members: - MEUKAM Pierre, Professor, University of Yaounde I;
- DJONGYANG Noël, Professor, University of Maroua;
- VONDOU Debertini Appolinaire, Associate Professor, University of Yaounde I;
- OWONA ANGUE Marie-Louise Wife OWONO OWONO, Associate Professor, University of Yaounde I.

Year 2021

DEDICATION

I dedicate this thesis to FOSSI'S family

ACKNOWLEDGEMENTS

A thesis is the result of many years of work, hope and sacrifice. It is therefore difficult to achieve without the support of family, friends, colleagues and of course your supervisors.

On this occasion, I wish to express my deepest gratitude to:

• Chancellor of the University of Yaounde 1, Pr. SOSSO Aurelien, for the user-friendly and appropriate environment of the “LMD” course,

• Dean of the Faculty of Sciences, Pr. TCHOUANKEU Jean Claude, for the training and the framework during my course,

• Vice-Dean, Pr. DONGO Etienne, for support and advice in the academic setting,

• Head of Physics Department, Pr. NDJAKA Jean Marie Bienvenu, for the training and his availability,

• Pr. TCHINDA Réné, to have accepted to supervise me in Master Degree and to have directed this thesis. I am grateful for his availability and his advices,

• Pr. KOFANE Timoléon Crépin, for his guidance and edifying advices,

• Pr. ELE Pierre for his advices,

• Dr. MEDJO NOUADJE Brigitte Astrid and Dr. NGOUATEU WOUAGFACK Paiguy Armand, who were great seniors by their generosity, their advices and their availability,

• Pr. TCHAWOUA Clément, who has agreed to chair my jury,

• Pr. MEUKAM Pierre, Pr. DJONGYANG Noel, Associate Professor VONDOU Debertini Appolinaire, Associate Professor OWONA ANGUE Marie Louise wife OWONO OWONO who agreed to be the members of my jury.

However, I wish to express my gratefulness to the family and friends who without them all this would have not been accomplished.

• My parents Mr. and Mrs. FOSSI who supported me from the first day in a continuous and encouraging way. Their sacrifices allowed the completion of this work. "Thanks to dad and to mom",

• My Sisters and Brother, FOSSI MAKAMWE Anne Laure, FOSSI MEVOUTSA Durelle Yolande, FOSSI DJOUMESSI Victoire Doriane, FOSSI MBA Ulrich Sorel, and NGUETSA KUATE Jiresse Loic and KEMBOU Ernest Lin. They have not always been exemplary but their affection and support both emotionally and financially have reversed the trend,

• RABIATOU BEN ABDOUL AZIZ Farida my niece and FOSSI ONGUENE Raphael Claire-Mathis my nephew for their joy of living by denoting a glimmer of hope,

• The KUATE family who welcomed me, hosted and supported me during my stay in Bafoussam since 2014. "Thank you aunty",
• The TSOPGNI Family, who has always supported me, especially financially. "Thank you Priva for the costume of my defense of Master degree",
• The ASSONGFACK Family, who has always supported me, especially financially,
• The BOPDA family, who welcomed me and hosted me during my stay in Bandjoun since 2017. "Thank you late father BOP" and Mother BOP,
• The AGOKEN family, who welcomed me and hosted me during my stay in Douala in 2018,
• Mr. and Mrs. Agoken for their unconditional support for more than ten years,
• The rest of the big family, Kembou and Nemogne,
• My wonderful companion for her emotional and moral support,
• My loyal friends FOUELEFACK TILALIENNE Gasi Paulidor and CHEGAM Armel Leger for their emotional support and well again including their advices for more than a decade,
• My brother-in-law ONGUENE Simon Pierre Claver, for his financial support,
• My friends EFFA Helene, BIOLO Berenice, Audrey Muriel, TOUKAM TONPOUWO Leticia Audrey, MASSO Aimé Suffis, Isabelle, WANJI Philomène, NGO KANGA Léa, TSIEMI TCHONANG Linda Doriane and FOYEN Priscal Jaseline for their comfort at a time in my life. "Thanks FOYEN",
• My childhood friends TEGUIA Gilles, SIANG ATIBOUM Roussel, MBIA Pierre Emmanuel, BITANG A ZIEM Daniel Cassidy, ZE OHANDJA Midinette, YOMI Arlette, KOUANDOU Arouna, AYINA NKE Franck for these moments of childhood and transition,
• My little LANDRY Tcheho Noune who brought unconditional linguistic expertise to this work.
• Dad KAMDEM CHOUPE and Mom Augustine the direct neighbors for their affection,
• Mom EVELINE for her joie de vivre and her honesty,
• JANVIER the shopkeeper in Yaounde-Ngousso, always open and welcoming,
• SUMO Patrick for his availability and welcome concerning the reproduction of my documents in the cradat during all this time,
• The colleagues of the UIT of Douala for their welcome,
• Energy, Electrical Systems and Electronics Laboratory and Research Unit in Industrial Systems and the Environment for their welcome,
• All who did not believe in me, because they made me even stronger and conquering,
• And finally GOD the father who is the beginning and the end.

CONTENTS

LIST OF FIGURES

LIST OF TABLES

NOMENCLATURE

Symbols

A	heat-transfer area	m^2
C	cost, heat capacitance rate	ncu, WK^{-1}
CE	conductance on condenser side	WK^{-1}
COP	coefficient of performance	-
E	exergy-based ecological criterion	W
EE	conductance on evaporator side	WK^{-1}
$ECOP$	ecological coefficient of performance	-
EPC	exergetic performance criterion	-
ex	exergetic efficiency	-
$\dot{EX}$	exergy rate	W
EX	exergy	J
F	thermo-economic criterion	-
h	specific enthalpy	Jkg^{-1}
HE	conductance on hot side reservoir	WK^{-1}
I	internal irreversibility parameter	-
k	conductance/thermo-economic parameter	WK^{-1}/ -
L	lagrangian operator	-
LE	conductance on cold side reservoir	WK^{-1}
K	thermal conductance	WK^{-1}
$LMTD$	log mean temperature difference	-
m	distribution of the total rate of rejected heat between the absorber and the condenser	-
$\dot{m}$	mass flow rate	Kgs^{-1}
q	specific heating load	Wm^{-2}
$\dot{Q}$	heat transfer rate	W
Q	heat transfer	J
R	refrigeration	-
S	specific entropy generation rate	$WK^{-1}m^{-2}$
t, t_{cycle}	total/cycle time	s
T	temperature	K
U	heat-transfer coefficient	$WK^{-1}m^{-2}$

W	work input/output	J

Abbreviations

AHP	absorption heat pump
AHT	absorption heat transformer
AR	absorption refrigeration
CCHP	combined cooling, heating and power
COP	coefficient of performance
ECOP	ecological coefficient of performance
EPC	exergetic performance criterion
FTT	finite time thermodynamics
FTL	four-temperature-level
GAX	generator-absorber heat exchange
HP	heat pump
HT	heat transformer
LMTD	log mean temperature difference
M	mach number
ncu	national current unit
NSGA II	non dominated sorting genetic algorithm of second generation
NTU	number of transfer units
PHE	plate heat exchanger
PTC	parabolic trough collector
RHX	refrigerant heat exchanger
SHC	solar heating and cooling
SHX	solution heat exchanger
THR	three-heat-reservoir
VCR	vapour compression refrigeration

Greek symbols

α, β	thermal conductance	WK^{-1}
γ	specific heat rate	-
ε	effectiveness/overall performance/coefficient of performance	-
η	thermal efficiency	
λ, μ	lagrangian multipliers	-
ξ	heat leakage coefficient	$WK^{-1}m^{-2}$

π	heating load	W
$\dot{\sigma}$	entropy generation rate	WK^{-1}
ψ	coefficient of performance	-

Subscripts

1	inlet/working fluid in generator/capital cost for the unit heat-transfer area
2	outlet/working fluid in evaporator/unit cost of energy
3	working fluid in absorber and condenser, working fluid in condenser
4	working fluid in absorber
a	absorber side
A	absorber
c	condenser side
C	condenser/heat sink side
C-A	Curzon-Ahlborn
CAR, Carnot	Carnot cycle
cycle	cycle
D	destruction
e	energy consumed
E	evaporator/heat source side/at maximum of ecological criterion
env	environment
EPC	at maximum *EPC*
f	fluid
F	at maximum *F*
g	generator side
G	generator
h	heat source reservoir side
H	high temperature/hot side reservoir
i	investment
in	input
l	sink/cold side
L, L1, L2	low temperature/cold side reservoir/heat leakage
max	maximum
min	minimum
O	absorber and condenser

op, opt	optimal
out, o	output/optimal
p	pressure
R	refrigeration
s	source
rev	reversible
real	real
w	warm/hot side
wf	working fluid

superscripts

HP	heat pump
o, a	environment/ambient

ABSTRACT

In this work, a theoretical analysis and a multi-objective optimization of three-heat-reservoir absorption heat pump (THR AHP) and four-temperature-level absorption heat pump (FTL AHP) were carried out under real operating conditions. It highlights the different thermodynamic cycles including the inversed Carnot, Brayton, Stirling and Ericsson cycles. In fact, the non-insignificant increase in absorption systems such as refrigeration, air conditioning and heat pump which is the subject of our attention is presented as ecological, economical and environment-friendly systems. In addition, multi-objective optimization, particularly for AHP, is established by first considering the thermo-ecological criterion for THR AHP, then the exergetic criterion for FTL AHP. Futhermore, the simultaneous analysis of ecological, exergetic and economic criteria is considered. Indeed, the different criteria are highlighted analytically using finite time thermodynamics (FTT). This made it possible to determine the optimal operating points of the system by minimizing exergy destruction rate, entropy generation rate, the environmental impact and the costs of capital and energy consumed. Also, the parameters taken into account influencing the performance of the absorption heat pump are the finite heat resistances, the heat leakages, the thermo-economic parameter, the ratio of heat rejected between the absorber and the condenser for FTL and the two internal irreversibility factors in particular that between the evaporator-condenser assembly for THR. However, the flowchart optimization methodology made it possible to deduce that the system has a significant advantage at the maxima of the thermo-economic and exergetic criteria in terms of coefficient of performance. Nevertheless, THR AHP presents a significant advantage at the maximum of the exergetic criterion in terms of exergy destruction rate and at the maximum of the ecological criterion in terms of specific heating load and exergy output rate. These results could make it possible to improve the design and sizing of AHP, especially on the nature of the materials used and the difference in the temperature-level of the working fluid circulating in the absorber and the condenser.

Keywords: *multi-objective optimization, flowchart optimization, ecological coefficient of performance, absorption heat pump, exergy-based ecological function, exergetic performance criterion, thermo-economic criterion.*

RESUME

Dans l'organisation de ce travail, il a été effectué une analyse théorique et une optimisation multiobjective des pompes à chaleur à absorption avec trois et à quatre réservoirs thermiques dans les conditions réelles de fonctionnement. Il est mis en relief les différents cycles thermodynamiques notamment les cycles inversés de Carnot, Brayton, Stirling et Ericsson. En effet l'accroissement non négligeable des systèmes à absorption, réfrigération, air conditionnée et pompe à chaleur qui fait l'objet de notre attention est présenté comme systèmes écologiques, économes et soucieux de l'environnement. Par ailleurs, l'optimisation multiobjective particulièrement des AHP est établie en considérant tout d'abords le critère thermo-écologique pour les pompes à chaleur à absorption avec trois réservoirs thermiques (THR AHP), ensuite le critère exergétique pour les pompes à chaleur à absorption avec quatre réservoirs thermiques (FTL AHP). Plus encore l'analyse simultanée des critères écologique, exergétique et économique est considérée. En effet, ces différents critères sont mis en évidence analytiquement en utilisant la thermodynamique des temps finis (FTT). Ceci a permis de déterminer les points de fonctionnement optimaux du système en minimisant le taux d'exergie destruite, le taux d'entropie généré, l'impact environnemental et les coûts du capital et de l'énergie consommée. De plus, les paramètres pris en compte influençant les performances de la pompe à chaleur à absorption sont les résistances thermiques finies, les fuites de chaleur, le paramètre thermo-économique, le rapport de chaleur rejetée entre l'absorbeur et le condenseur pour FTL et les deux facteurs d'irréversibilité internes notamment celui entre l'ensemble évaporateur-condenseur pour THR. Cependant, la méthodologie d'optimisation flowchart a permis de déduire que le système présente un avantage significatif au maximum des critères thermo-économique et exergétique en termes de coefficient de performance. Néanmoins, la THR AHP présente un avantage significatif au maximum du critère exergétique en termes de taux d'exergie détruite et au maximum du critère écologique en termes de puissance spécifique de chauffage et du taux d'exergie à la sortie. Ces résultats pourront permettre d'améliorer la conception et le dimensionnement des AHP notamment sur la nature des matériaux utilisés et la différence du niveau de température du fluide circulant dans l'absorbeur et le condenseur.

Mots clés : *optimisation multi-objective, optimisation flowchart, pompe à chaleur à absorption, coefficient de performance écologique, fonction écologique, critère exergétique de performance, critère thermo-économique*

GENERAL INTRODUCTION

Increasing global warming over the last decade has led to the use of heating, cooling and air conditioning systems in industries, transportation and building, which are more concerned with the environment. What led researchers and engineers to develop systems for producing cold and heating (Sieniutycz and Salamon, 1990; Bejan, 1996; Chen et al., 1999; Chen and Sun, 2004; Feidt, 2010, 2013; Andresen, 2011; Qin et al., 2013; Ngouateu Wouagfack and Tchinda, 2013; Rivera et al., 2015; Ge et al., 2016; Su et al., 2017; Chaves Fortes et al., 2018; Wang et al., 2019) which include Carnot, vapour compression refrigeration, cascade and multistage refrigeration, gas refrigeration (Brayton, Ericsson and Stirling), adsorption, desiccation and absorption cycles. However, given that the most used cycles are vapour compression cycles because they are more efficient, have drawbacks such as the high consumption of electricity and their refrigerants are pollutants which participate in climate change. As a result, the refrigeration industry has developed other systems to address these problems. One of these systems is the absorption machine environmental friendly while using renewable energy sources (solar, geothermal and biomass, etc.). In addition to using small amounts of energy, absorption cycles can operate from energy sources from industrial heat losses. Absorption machines use thermal energy (absorber-desorber or generator) and no mechanical or electrical energy in the driving part of the cycle. The fluids used in an absorption cycle are composed of a refrigerant and of an absorbent. Thus, the system requires a rectification column and/or a pre-condenser (rectifier) to purify the vapour leaving the desorber as illustrated in **Fig. 1** (Lostec et al., 2010). The high pressure refrigerant liquid (2) leaving the condenser is sub-cooled in the refrigerant heat exchanger (RHX). The liquid (11) is expanded (3) and then evaporated in the evaporator. The resulting vapour (4) is superheated in the RHX. It is then necessary to compress this vapour before reinjecting it into the condenser. For this purpose the superheated vapour (12) is absorbed in a weak refrigerant-absorbent mixture (5) in the absorber and then compressed by the pump from (6) to (7). The generator or desorber and rectification column separate the refrigerant from the absorbent to complete the cycle. States 23 and 24 are the outlet and inlet to the rectification column while states 8 and 9 are the inlet and outlet to the desorber or generator. The solution heat exchanger (SHX) permits an internal recovery of thermal energy, thus lowering the evacuated energy at the absorber and the energy provided to the generator or desorber. External streams indicated by discontinuous lines in **Fig. 1** act as heat sources or sinks in the condenser, evaporator, absorber, desorber or generator and pre-condenser.

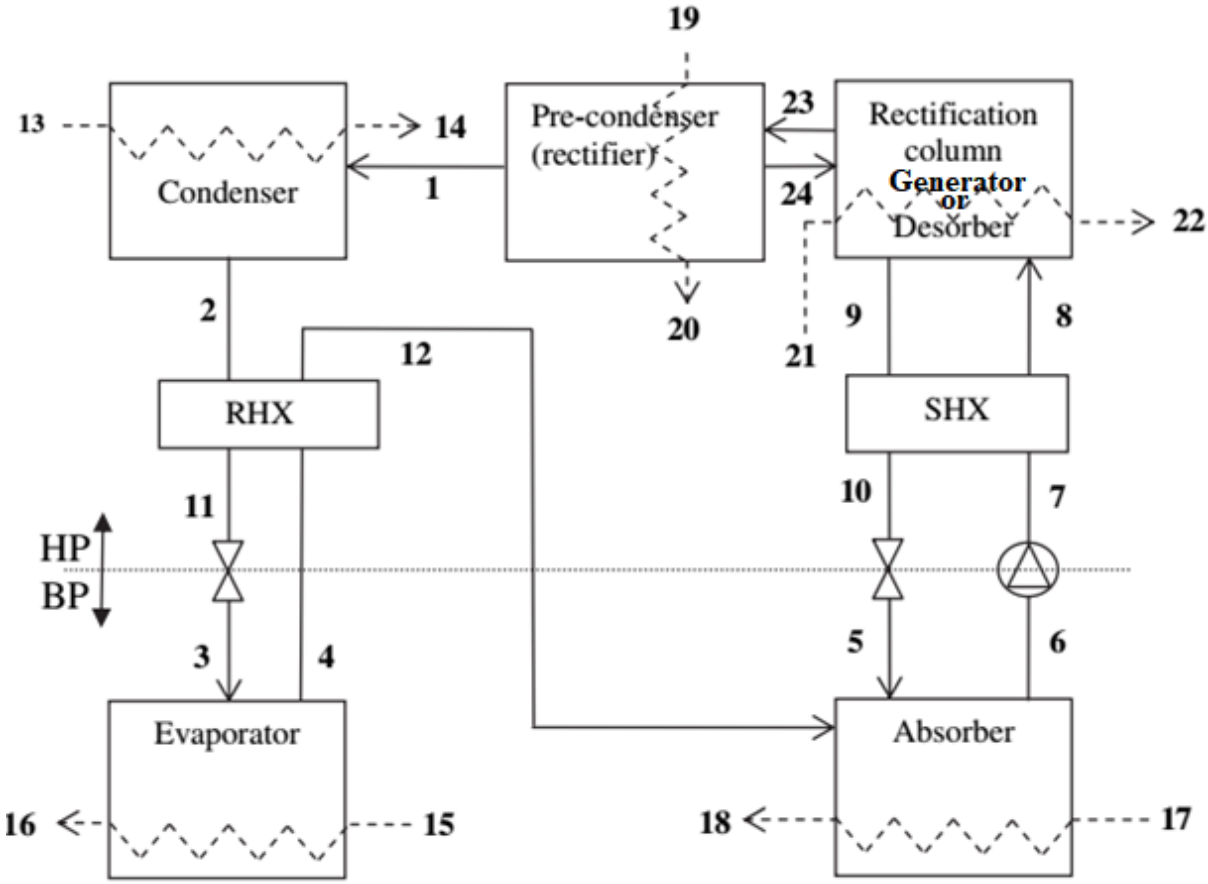

Fig. 1. Schematic representation of the absorption system single effect (Lostec et al., 2010).

Moreover, because absorption systems are more energy efficient, they are also environmentally conscious with less polluting and use more environmentally friendly working fluids (Ally and Sharma, 2018; Hu et al., 2018; Sarbu, 2014). Moreover, the optimization of AHP and other thermal systems becomes crucial for research because the demand is increasing, especially in the industry with the use of renewable energy sources as a source of power (Mastrullo and Renno, 2010; Li et al., 2013; Dixit et al., 2017; Leonzio, 2017; Yuksel and Ozturk, 2017; Wang et al., 2018). This being so, the combined optimization approach by the several decisive objective functions *EPC*, *E*, *EPC* and *F* using finite time thermodynamics (FTT) aims to significantly improve the design and operation of AHP. These criteria are each characterized by:

(i) The thermo-ecological function (ECOP), which is the ratio between the specific heating load and the loss rate of available (product of the entropy generation rate and the temperature of the environment).

(ii) The exergetic performance criterion (EPC), which is the exergy output rate per unit exergy destruction rate or loss rate of availability.

(iii) The ecological function (E) which is the difference between exergy output rate and the loss rate of availability.

(iv) The thermo-economic function (F) which is the specific heating or cooling or mechanical load per unit sum of cost on the investment and the cost of the energy consumed.

However, research has systematically evolved towards optimization using the FTT. Therefore, Chen (1999), Kato et al. (2005), Chen et al. (2005a), Qin et al. (2006, 2007, 2015), Xia et al. (2007), Bi et al. (2008), Huang et al. (2008) and Xiling et al. (2011) on AHP, Wei et al. (2011) on magnetic HP of Ericsson, Bhardwaj et al. (2003, 2005), Zheng et al. (2004), Chen et al. (2005b, 2006), Qin et al. (2010) and Kaushik et al. (2018) on AR, Qin et al. (2004a, 2004b, 2008) and Chen et al. (2007a) on AHT, have analyzed these endoreversible and irreversible systems using the coefficient of performance, the specific heating load and the specific cooling load as objective functions. Then, the performances are studied considering the environmental impact with the heat losses, the heat leakage and the heat resistances in the various components. These parameters are derived from the second law of thermodynamics and initiated by Ust et al. (2006a, 2006b) on irreversible Brayton heat engines using the thermo-ecological criterion. They are followed by Ngouateu Wouagfack and Tchinda (2011a, 2011b, 2014), Medjo Nouadje et al. (2014, 2016) and Ahmadi and Ahmadi (2016) with the irreversible ARs, then Ngouateu Wouagfack and Tchinda (2012a, 2012b) and Ahmadi et al. (2015) with irreversible AHP and Ahmadi et al. (2016) with an inverse Brayton cycle. At the same time, the ecological criterion (E) based on the same considerations is first used by Angulo-Brown (1991) and followed by Sun et al. (2005), Chen et al. (2007b, 2019), Qin et al. (2017) and Frikha and Abid (2016). Moreover, the exergetic approach in addition to the previous considerations takes into account the useful energy consumed by the thermodynamic cycle (Sahin et al., 1997; Talbi and Agnew, 2000; Kilic and Kaynakli, 2007; Kaushik and Arora, 2009; Lostec et al., 2010; Farshi et al., 2013) and the exergetic performance criterion (*EPC*) used by Ust et al. (2007) on a dual cycle cogeneration system and Ust et Karakurt (2014) on a cascade refrigeration system. However, the optimization of thermal systems by the thermo-economic approach makes use of the cost on the investment with the parameters such as the areas of heat exchange, the thermal capacities and the cost on the consumption with the load rate consumed. Kodal et al. (2000, 2002, 2003) used this approach on AHP and two-stage AHP, followed by Silveira and Tuna (2003, 2004) on combined heat and power systems. Then, Misra et al. (2003, 2005) on single-effect and double-effect H2O/LiBr, Qin et al. (2005) on endoreversible AR, Durmayaz et al. (2004) on thermal systems, Wu et al. (2005) on irreversible AHP, Qureshi and Syed (2015) on AHP and AR. Zare et al. (2012) and Ahmadi et al. (2014b) conducting a thermo-economic and exergy study on an ammonia-water power/cooling cogeneration cycle and on multi-generation systems respectively using the evolutionary genetic algorithm. Therefore, each approach has been examined using each time an optimization criterion. Nevertheless, it is

important to consider simultaneously the influences of two internal irreversibilities due to heat losses (Xiling et al., 2011 using COP and specific heating load as objective functions and Medjo Nouadje et al., 2014 using the thermo-ecological criterion as objective function on THR AR), of the overall external irreversibility due to heat leakages and heat resistances. This being the case, the consideration multi-objective brings the limitation and the advantages presented by the optimization of each objective function.

In this thesis, we will from the FTT, determine the optimal operating points of a THR AHP and of a FTL AHP corresponding to the maximum of each respective objective function thermo-ecological, ecological, exergetic and thermo-economic and discuss, while using the Maple software and Flowchart optimization algorithm (Su et al., 2017; Chen et al., 2019). In order to carry out this study, this work is divided into three chapters.

In the first chapter, we will expose the approaches already studied, the current trends and the applications of the future in the absorption process. However, the different methods analysis technical and optimization will be based essentially on finite time thermodynamics or even non-equilibrium thermodynamics. This review is grouped into several parts: a part about to the basic principles of FTT, including thermodynamic cycles; a part on optimization by objective functions such as the coefficient of performance, the heating load, the cooling load and the mechanical power; a part on ecological and thermo-economic analysis; a part on exergetic analysis and a part on applications.

In the second chapter, we will use the FTT, the Maple software (Maple 13) and a flowchart algorithm, analytically establish the expressions of the objective functions, determine their maximum values and obtain the corresponding optimal performance parameters, respectively.

In the third chapter it will be a question of understanding and determining the optimal operating ranges of a THR AHP and FTL AHP single effect system by considering real hypotheses. This being so, we will in the following plot the curves of the objective functions *ECOP* for the THR cycle and *EPC* for a FTL cycle with respect to the temperatures of the working fluid and the heat exchange surfaces areas in the various components, coefficient of performance specific heating load and entropy generation rate. Then we will make a comparative study of the ecological, exergy and economic criteria for the THR and FTL cycles compared to performance indices such as the Coefficient of performance, exergy output rate and exergy destruction rate. Finally we will discuss these results in order to find a suitable compromise.

CHAPTER 1: REVIEW OF FINITE TIME THERMODYNAMICS OPTIMIZATION ON THE ABSORPTION HEAT PUMPS AND NEW TRENDS

1.1. Introduction

In recent years, the heat transformation with absorption systems has attracted increasing attention, in particular with absorption heat pumps (AHP) although vapor-compression systems are still the most used. In this chapter, we will expose the approaches already studied, the current trends and the applications of the future in the absorption process. However, the different methods, technical analysis and optimization will be based essentially on finite time thermodynamics (FTT) or even non- equilibrium thermodynamics. This review is grouped into several parts: a part about to the basic principles of FTT, including thermodynamic cycles; a part on optimization by objective functions such as the coefficient of performance, the heating load, the cooling load and the mechanical power; a part on thermo-economic, ecological and exergetic analysis and optimization, and a part on applications.

1.2. Finite time thermodynamics approach

1.2.1. Development and concept of irreversible finite time thermodynamics

A system is said to have a reversible process if at the conclusion of the process it leaves no change anywhere within the system or with the surrounding. A reversible process is hypothetical which can never be attained in practice but can be approximated as close as reversible process. Such processes are defined in the limit of infinitely slow execution. So the real thermodynamic process should proceed in finite time or limited time which causes a change between the system and its surrounding and is known as irreversible process. All real/actual processes are irreversible which means there is some entropy generation, which is a measure of irreversibility. Thus, irreversibility can be defined as lost opportunities to do work. It represents the entropy generation that could have been converted into work but was not. The smaller the irreversibility associated with the cycle, the greater the work that will be produced by the heat engine cycle (or smaller work will be consumed by the refrigeration cycle). To improve the performance of thermodynamic systems, one should reduce the primary source of irreversibility associated with each component of the systems. For a closed system, the irreversibility is the difference of the reversible and real work, i.e.

$$I = W_{rev} - W_{real} \tag{1.1}$$

For energy-producing devices, like heat engines, the actual output work (W_{real}) will be less, while, for energy-consuming devices like RAC and HP systems, the actual input work (W_{real}) will be more than the reversible input work, i.e.

For heat engine cycles $I = W_{rev} - (W_{real})$ (1.2)

For RAC and HP cycles $I = W_{real} - W_{rev}$ (1.3)

The irreversible thermodynamics in general deals with irreversibility of any kind in the system. The finite time thermodynamics deals with external irreversibility due to source/sink reservoirs, while the internal irreversibility deals with thermodynamic processes (including friction, etc.) within the cycle. Irreversibility in any system cannot be removed completely; however, it can be minimized up to some extent. The irreversible thermodynamics has become an increasing powerful tool for energy conversion systems. Thus, the concept of finite time thermodynamics came into existence after the novel work of Curzon and Ahlborn (1975) which not only answer the above questions but also solved the problems of heat transfer and energy conversion systems.

Heat is a kind of energy, which can be transferred from one body to another because of temperature difference between them, but finite temperature difference makes the process irreversible. Therefore, the heat transfer process approaches a reversible one as the temperature difference between two bodies reaches zero. However, transfer of finite amount of heat through infinitesimal temperature difference would take infinite time or infinite heat transfer area. As we know from the heat transfer theory, the amount of heat (Q) transfer between two bodies is proportional to the temperature difference, the contact area, and the time taken, i.e.

$$Q = UA(\Delta T)(\Delta t),\ Q \propto A(\Delta T)(\Delta t) \quad (1.4)$$

where U is the overall heat transfer coefficient, A is the heat transfer area, ΔT is the temperature difference between the bodies, and Δt is the time taken in the process.

For infinitesimal temperature difference i.e. $\Delta T \to 0$.

Then $A \to \infty$ or $\Delta t \to \infty$ or $U \to \infty$.

But due to the finite conductivity of materials U will be finite, thus the only possibility is that either $A \to \infty$ or $\Delta t \to \infty$, again:

i) If $A \to \infty$ means the heat exchanger area is infinite, the heat engine/heat transfer unit becomes economically unviable, since the heat exchanger units are quite expensive.

(ii) If $\Delta t \to \infty$ means it takes infinite time to produce the finite amount of work, the power (which is work per unit time, i.e. $P = W/t \to 0$ as $\Delta t \to \infty$) will tend to zero.

Thus, the very purpose of power generation is nullified, since no engineer wants to design such type of machine whose output power is zero. Also the prime object of the machine is to produce power, which means finite amount of work in finite time rather than finite work in infinite time. This means we need finite heat transfer in finite time, which produces irreversibility. In the real engineering world, every machine has some power, which means the production of finite

amount of work in finite time. This requires that there should be a finite temperature difference between the working fluid and the external reservoirs. Thus, irreversible heat transfer due to finite temperature difference is known as 'finite time thermodynamics' and/or 'finite temperature difference thermodynamics'. Curzon and Ahlborn (1975) proposed that due to finite conductivity of materials, the heat transfer to and from the heat engine is flowing through a finite temperature difference. They applied the idea in Carnot heat engine whose efficiency was found lower than the well-known Carnot efficiency.

$$\eta_{Carnot} = 1-\left(T_L/T_H\right) \text{ while } \eta_{C-A} = 1-\sqrt{T_L/T_H} \;\Rightarrow\; \eta_{C-A} < \eta_{Carnot} = 1-\sqrt{T_L/T_H}\,. \tag{1.5}$$

where T_L and T_H are the temperatures of sink and source reservoirs, respectively. The main objectif of finite time thermodynamics is to understand irreversible finite time processes and to establish bonds on efficiency and maximum power for such processes. Further, it seeks to establish general operating principle for system, which serves as a model for real processes. The real processes can be associated with two kinds of irreversibilities, as below: External irreversibilities and internal irreversibilities.

The external irreversibilities are due to finite temperature difference and the direct heat leakage from source to sink (heat engines) and/or from sink to source (RAC and HP systems) and can be found using finite time thermodynamics methodology. The internal irreversibilities are due to non-isentropic compression/ expansion, friction, and entropy generation in the machine and can be determined using exergy analysis and irreversible thermodynamics. Thus, the concept of exergy should be used to review the performance of energy conversion systems, because exergy is the maximum possible work that can be extracted from a given system in a given state by a process, which brings it into equilibrium with environment. Thus, exergetic analysis is the true mission to calculate the real performance of real energy conversion devices.

1.2.2. Application of finite time thermodynamics

There are three main power cycles being used in power generation sector, and different options are characterized by the type of the working fluid and/or the thermodynamic cycles followed by a particular heat engine. The power cycles mainly used in power generation sector are, namely, Rankine cycle, Brayton cycle and Stirling cycle. The Rankine cycle is most commonly used for power generation and basically a steam/vapour power cycle. This cycle comprises the constant pressure heat addition and rejection processes along with the isentropic expansion and pumping processes and utilizes the working fluids, which change the phase during the heat addition processes to provide essentially isothermal heat addition and rejection. The other power cycles, such as Brayton, Stirling, and Ericsson cycles, are gas power cycles and utilize the

gas or air as the working fluid and are preferred for higher temperature applications. On one hand, the Brayton cycle combines the adiabatic compression and expansion along with the isobaric heat addition and rejection processes, while on the other hand, the Stirling cycle combines the isothermal heat addition and rejection along with the isochoric compression and expansion processes. Whereas the Ericsson cycle combines the isobaric compression and expansion along with the isothermal heat addition and rejection processes, respectively. Finite time thermodynamic analysis of various cycles. Rankine, Brayton, Stirling, and Ericsson, vapour compression, vapour absorption, etc. have been carried in detail with different possible options from a simple to a more complex version for both power generation and refrigeration applications. All these three cycles offer higher performance, and hence, attention on these cycles is increasing nowadays.

However, improving the performance of these cycles has led physicists and engineers to design more energy and exergy efficient systems and environmentally friendly (Sieniutycz and Salamon, 1990; Bejan, 1996; Chen et al., 1999a; Ziegler, 2002; Chen and Sun, 2004; Feidt, 2010, 2013; Andresen, 2011; Qin et al., 2013; Ngouateu Wouagfack and Tchinda, 2013; Rivera et al., 2015; Ge et al., 2016; Su et al., 2017; Chaves Fortes et al., 2018; Dai et al., 2019; Wang et al., 2019).

1.2.3. Boundary between classical thermodynamics and finite time thermodynamics

From the above, in contrary to classical thermodynamics stated by Carnot-Clausius-Kelvin and Gibbs, the difference between classical thermodynamics and finite time thermodynamics is the approach to the concept of processes such as reversible, endoreversible, exoreversible, irreversible, equilibrium, quasi-static equilibrium and non-quasi-static equilibrium. This means that finite time thermodynamics (FTT), which can combine heat transfer and thermodynamics of non-equilibrium processes, is a very valuable tool for the analysis and optimization of thermodynamic systems. In other words, the concept of classical thermodynamics calls for thermodynamic equilibrium, i.e. the temperature of the working fluid is the same as that of the heat reservoirs and the heat exchangers during the process, which is not the case for finite time thermodynamics which deals with thermodynamic non-equilibrium systems. Furthermore, in classical thermodynamics the heat exchange between the system and the environment is done in an infinitely long time, on the other hand in FTT, the temperature difference between the system and the environment is finished and the heat exchanges are done to finite time cycles.

However, experimental observations have shown that heat cannot be transferred from a low-temperature reservoir to a high-temperature reservoir without external energy input or work. Therefore, the device that extracts heat from low-temperature reservoir and rejects or transfers it to high-temperature reservoir is called a refrigerator or heat pump, and the cycle followed by the

device or system is called refrigeration cycle. These devices are cyclic devices, and the working fluid flowing through the device is called a refrigerant. Refrigerator and heat pump are essentially the same device and follow the same thermodynamic cycle, but they differ in their objective function. However, the production of heat is the objective of a heat pump, and extraction of heat from low-temperature medium is only a necessary part of this operation in such system.

There are several types of refrigeration cycles; some of the main cycles are as below:

- The reverse cycle of Carnot
- Vapour compression refrigeration cycle
- Cascade and multistage refrigeration cycle
- Vapour absorption refrigeration cycle
- Gas refrigeration cycles (Brayton, Stirling and Ericsson)

1.2.4. Analysis of thermodynamic cycles

1.2.4.1. Carnot cycle coupled heat pump

In 1824, Carnot showed that no heat engine operating between two temperature levels can work better than the ideal Carnot engine (reversible). This Carnot heat engine follows the Carnot cycle which is completely a reversible cycle composed of two isothermal transformations and two reversible isentropic transformations. It has maximum thermal efficiency for given temperature limits, and it also serves as a standard against which the actual power cycle can be compared. However, the reversibility of this cycle gives the four thermodynamic processes to be reversed in a cycle called "Carnot reverse cycle" (Tyagi et al., 2004a). This is commonly called Carnot refrigeration or heat pump which is shown in **Fig 1.1.** and characteristic *T*-*s* of **Fig. 1.2.** The reversed Carnot cycle is executed within the saturation dome of a refrigerant as can be seen clearly from **Fig. 1.2.** The refrigerant absorbs heat Q_L during process 1–2 at constant temperature T_L from a low-temperature source and is compressed isentropically to state point 3, and as a result its temperature rises to T_H. The refrigerant rejects heat Q_H at constant temperature T_H to a high-temperature sink during process 3–4 and then converts into saturated liquid and expands isentropically to state point 1 and cools down to low temperature T_L, thereby completing the cycle. The coefficient of performance of Carnot heat pump can be expressed in terms of temperature as below (Cengel and Boles, 2006):

$$COP_{HP} = Q_H / W_{in} = T_H / (T_H - T_L) = 1 / (1 - (T_L / T_H)) \quad (1.6)$$

where W_{in} is the work input of the Carnot cycle

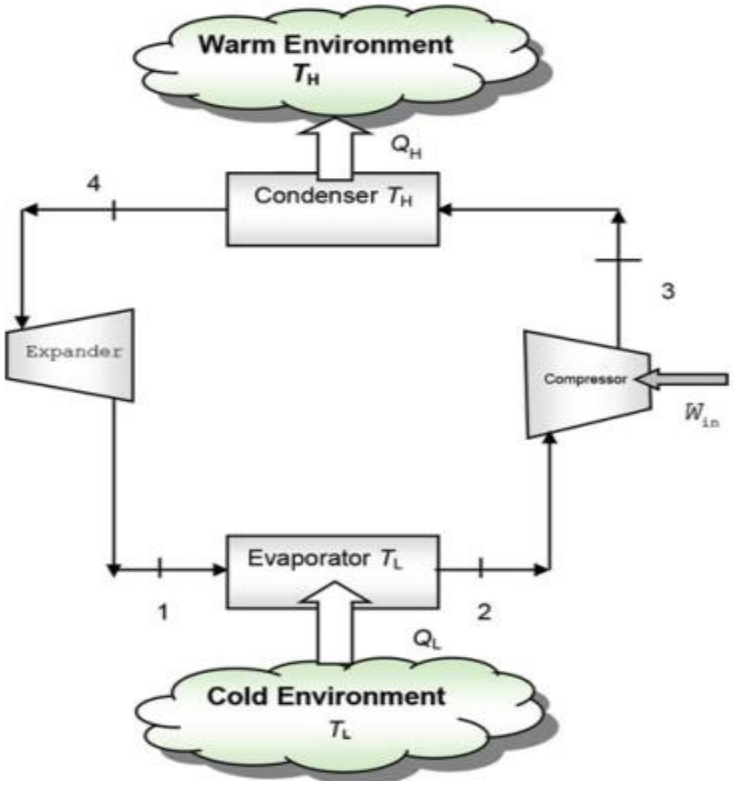

Fig. 1.1. Schematic diagram of the reversed Carnot cycle (Cengel and Boles, 2006).

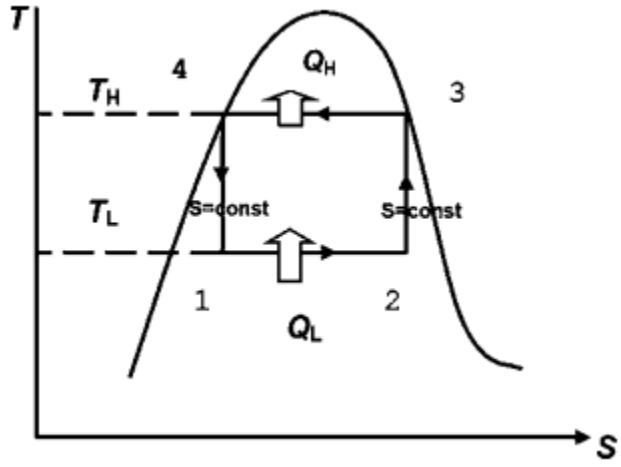

Fig. 1.2. *T-s* diagram of the reversed Carnot cycle (Cengel and Boles, 2006).

In reversed Carnot cycle (ideal Carnot cycle), temperature difference between the refrigerant and surrounding is zero; hence, heat transfer is zero. So to get a non-zero heat transfer, either heat transfer time is infinitely long or heat exchanger area is infinitely large, but both conditions are impractical. It turns out that reversible processes are only defined within the limits of an infinitely slow execution. Reversible isentropic compression/expansion processes 2–3 and 4–1 cannot be approximated closely in practice. Among others, major challenges for this cycle are: Process 2–3 requires compression of liquid–vapour mixture to be compressed which requires a

compressor that handles two phases. Process 4–1 involves the expansion of high moisture content refrigerant and requires a turbine that can expand the saturated liquid, and either of the two processes is difficult to obtain in the real practice. So there is a need to execute the cycle out of the saturation curve limit, but then the cycle cannot maintain the two isothermal processes 1–2 and 3-4 (Cengel and Boles, 2006). Therefore, the reversed Carnot cycle is not a practical cycle, while it can serve as the standard against which a real refrigeration cycle may be compared.

However, vaporizing the refrigerant before it is being compressed in the compressor and replacing the turbine by a throttling device such as expansion valve and capillary tube. The modified cycle becomes a practical cycle called a reversible vapor compression refrigeration (VCR) cycle as shown in **Fig. 1.3 (a), (b).** The VCR cycle widely used for cooling and heating applications is composed of the following processes:

Process 1–2: Isobaric heat extraction from the space to be cooled

Process 2–3: Isentropic compression in a compressor

Process 3–4: Isobaric heat rejection to the surroundings

Process 4–1: Isenthalpic expansion in the expansion valve

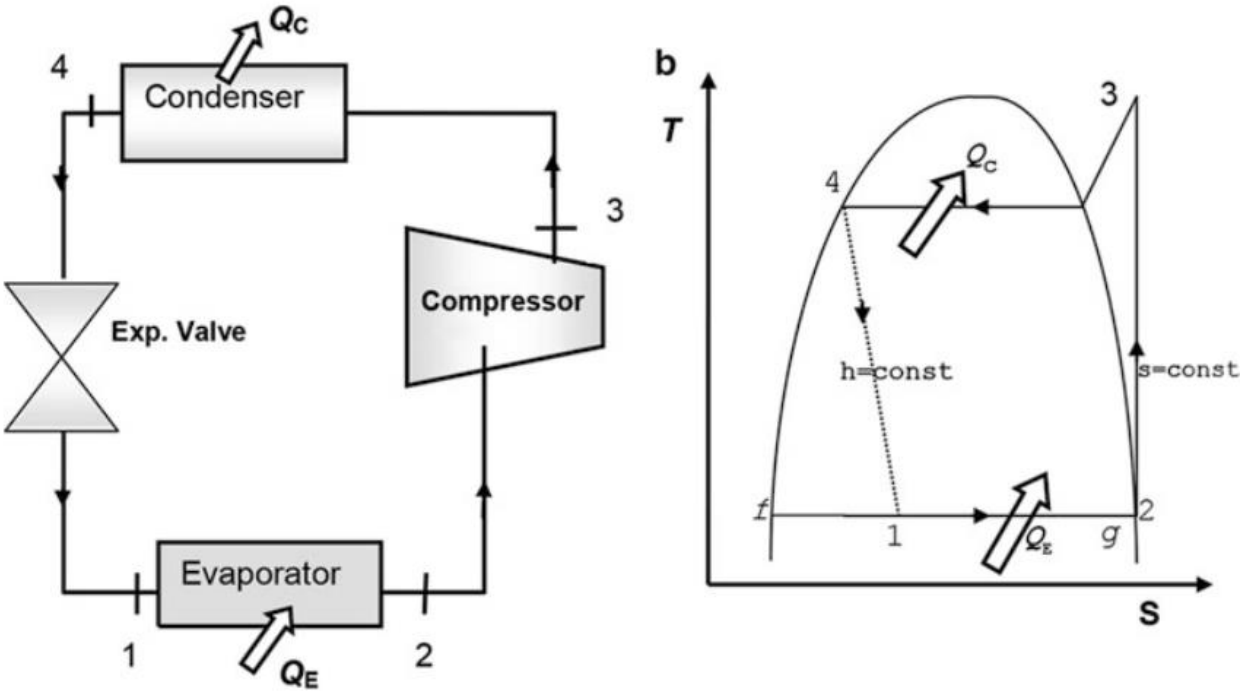

Fig. 1.3. (a) Schematic and (b) *T-s* diagrams of a basic VCR cycle (Cengel and Boles, 2006).

The previous processes are described such as, the saturated vapour enters the compressor at state point 2 as shown in **Fig. 1.3** and is compressed to state point 3 isentropically at compressor discharge pressure, and the temperature of the refrigerant also increased. The high-temperature

high-pressure (superheated) refrigerant vapour enters the condenser at state point 3. In the condenser, heat is rejected isobarically to the surrounding and cools down to saturated liquid to state point 4 where it expands to state point 1 while the enthalpy of the liquid remains constant (isenthalpic process). Again, the refrigerant enters the evaporator where it absorbs heat isobarically from the place to be cooled and converts into saturated vapour, thereby completing the cycle. All the four components associated with a VCR cycle are steady-state flow devices; hence, all the four components that make up the cycle can be analyzed as steady-state processes. The changes in the kinetic and potential energy are very small as compared to the heat transfer and work terms and hence neglected while evaluating a VCR cycle. Thus, for steady-state flow, energy equation can be written as (Cengel and Boles, 2006):

$$\dot{Q}_E = \dot{m}\left(h_2 - h_1\right),\ \dot{Q}_C = \dot{m}\left(h_3 - h_4\right),\ \dot{W}_{in} = \dot{m}\left(h_3 - h_2\right) \tag{1.7}$$

$$COP_{HP} = \dot{Q}_C \Big/ \dot{W}_{in} = \dot{m}\left(h_3 - h_4\right) \Big/ \dot{m}\left(h_3 - h_2\right) = \left(h_3 - h_4\right) / \left(h_3 - h_2\right) \tag{1.8}$$

where $\dot{m}$ is the mass flow rate of the refrigerant, h_1 and h_2 are the specific enthalpy at state points 1 and 2 which are located at low pressure line and h_3 and h_4 are the specific enthalpy values at state points 3 and 4, located at high pressure lines.

1.2.4.2. Rankine cycle coupled heat pump

The Rankine cycle is very often found in power plants where water/steam is used as the working fluid due to its easy availability, low cost and safety. However, the ideal Rankine cycle is a practical attempt to approach the Carnot cycle. The Rankine cycle heat pump system is considered as a heat engine driving a heat pump system. In this section, Rankine cycle HP systems will be analyzed and coupled with external heat reservoirs of finite heat capacity and having both external and internal irreversibilities (Kaushik et al., 1999, 2000; Bhardwaj et al., 2001, 2003a). The basic components of a Rankine heat engine are the pump, constant pressure steam generator, turbine, and constant pressure condenser. **Fig. 1.4** shows a schematic diagram of a Rankine cycle heat pump system. The output work of heat engine is used as input work to the heat pump cycle. The equivalent cycle model of a Rankine cycle airconditioning/heat pump system is shown in **Fig. 1.5**. Thermal reservoirs of finite heat capacity are coupled with the system, so temperatures of these will vary as shown in **Fig. 1.5.**

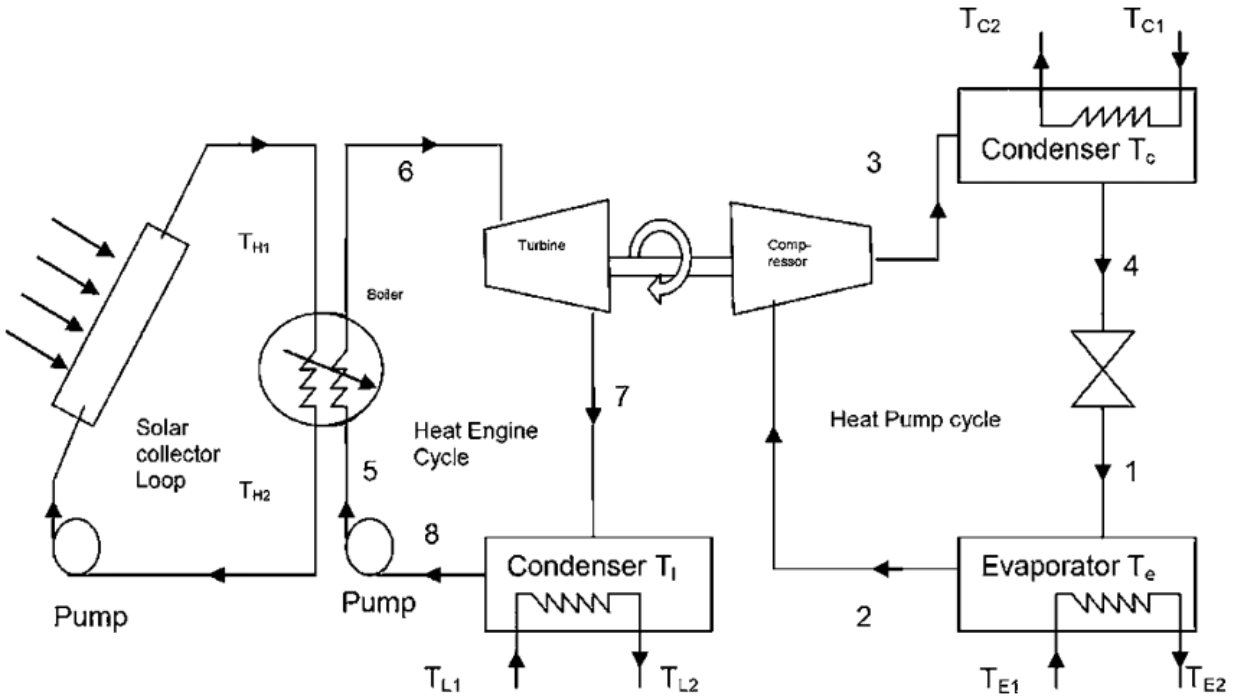

Fig. 1.4. Schematic diagram of Rankine heat engine heat pump system (Kaushik et al., 2018).

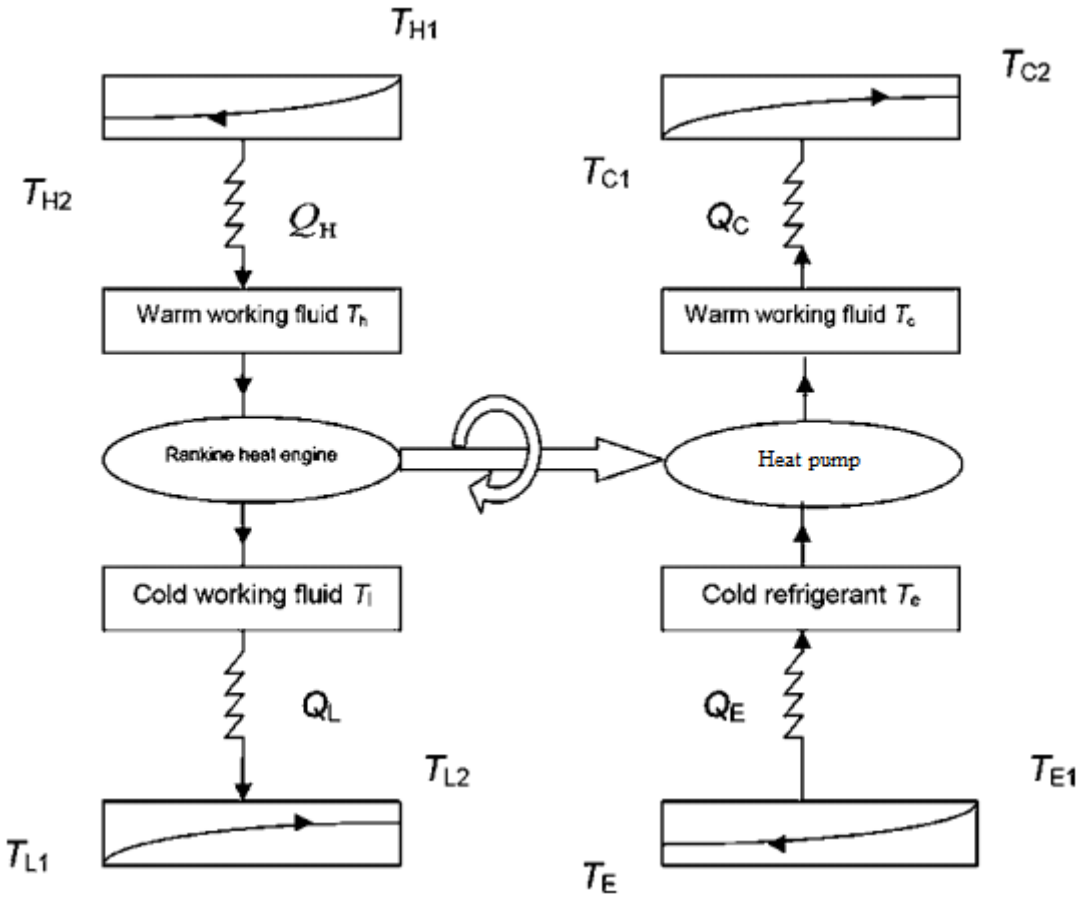

Fig. 1.5. Equivalent cycle diagram of Rankine heat pump system (Kaushik et al., 2018).

1.2.4.2.1. Heat engine cycle analysis

The heat input rate from heat source to the system and the heat rejection rate from system to the heat sink, respectively (Bhardwaj et al., 2003a, Chen et al., 2004) are given by:

$$\dot{Q}_H = \frac{Q_H}{t_H} = U_H A_H \left(\text{LMTD}\right)_H = \dot{m}_H C_{PH} \left(T_{H1} - T_{H2}\right)$$

$$\text{and } \dot{Q}_L = \frac{Q_L}{t_L} = U_L A_L \left(\text{LMTD}\right)_L = \dot{m}_L C_{PL} \left(T_{L2} - T_{L1}\right) \tag{1.9}$$

$$\text{where, } \left(\text{LMTD}\right)_H = \frac{\left(T_{H1} - T_h\right) - \left(T_{H2} - T_h\right)}{\ln\left(\frac{T_{H1} - T_h}{T_{H2} - T_h}\right)} \text{ and } \left(\text{LMTD}\right)_L = \frac{\left(T_l - T_{L1}\right) - \left(T_l - T_{L2}\right)}{\ln\left(\frac{T_l - T_{L1}}{T_l - T_{L2}}\right)} \tag{1.10}$$

Using LMTD expression in **Eq. (1.9)**, they were able to get:

$$Q_H = HE\left(T_{H1} - T_h\right)t_H \text{ and } Q_L = LE\left(T_1 - T_{L1}\right)t_L \tag{1.11}$$

where, $HE = C_H \varepsilon_H$ is the conductance on hot side reservoir, $LE = C_L \varepsilon_L$ is the conductance on cold side reservoir, $C_H = m_H C_{PH}$, $C_L = m_L C_{PL}$, $\varepsilon_H = 1 - \exp\left(-\frac{U_H A_H}{\dot{m}_H C_{PH}}\right)$ and $\varepsilon_L = 1 - \exp\left(-\frac{U_L A_L}{\dot{m}_L C_{PL}}\right)$.

They were able to get the work output of the heat engine cycle (first law of thermodynamics)

$$W = HE\left(T_{H1} - T_h\right)t_H - LE\left(T_l - T_L\right)t_L \tag{1.12}$$

and using the second law of thermodynamics and internal irreversibility parameter is introduced as:

$$\Delta S = \frac{Q_H}{t_h} - I\frac{Q_L}{t_l} = 0 \tag{1.13}$$

$I = 1$ for endoreversible and $I < 1$ for internal irreversible system. For given input heat in the boiler, output work of heat engine can be maximized by defining the modified Lagrangian operator as given by:

$$L = W - \lambda Q_H - \mu \Delta S \tag{1.14}$$

where λ and μ are Lagrangian multipliers.

The optimal values of T_h and T_l are obtained from the resolution of the differential equations $\frac{\partial L}{\partial T_h}=0$ and $\frac{\partial L}{\partial T_1}=0$. Now, using the optimal value of T_l into **Eq. (1.11)**, (Chen et al., 2004) were able to get the thermal efficiency at maximum work output of heat engine:

$$\eta = 1 - \frac{I^{-1}T_{L1}}{\left(T_{H1} - \frac{Q_H}{HE.t_H} - \frac{Q_H}{I^{-1}LE.t_L}\right)} \tag{1.15}$$

$\frac{\partial \eta}{\partial t_H}=0$ and $\frac{\partial \eta}{\partial t_L}=0$ give the optimal values of τ_H and τ_L. Now, after substituting these optimal values of the cycle times into **Eq. (1.15)**, we have the optimal efficiency of the heat engine at maximum work output:

$$\eta = 1 - \frac{I^{-1}T_{L1}}{\left(T_{H1} - \frac{P_H}{K_1}\right)} \tag{1.16}$$

where,

$$P_H = \frac{Q_H}{\tau_1},\ \tau_1 = t_H + t_L \text{ and } K_1 = \frac{I.HE.LE}{\left(\sqrt{HE} + \sqrt{I.LE}\right)^2} \tag{1.17}$$

1.2.4.2.2. Heat pump cycle analysis

By analogy of the previous paragraph we can obtain the optimal COP of an irreversible heat pump operating between reservoirs at temperatures T_{E1} and T_{C1}.

$$COP = \left(1 - \frac{\left(I^{'}\right)^{-1}T_{E1}}{\left(T_{C1} - \frac{P_H}{K_2}\right)}\right)^{-1} \tag{1.18}$$

$$P_H = \frac{Q_C}{\tau_2},\ \tau_2 = t_E + t_C \text{ and } K_2 = \frac{EE.CE}{\left(\sqrt{EE} + \sqrt{I^{'}.CE}\right)^2} \tag{1.19}$$

where, $EE = C_E\varepsilon_E$ is the conductance on evaporator side and $CE = C_C\varepsilon_C$ is the conductance on condenser side.

Under the circumstances of the given Q_C, τ_1 and τ_2, the optimal overall coefficient of performance of an irreversible Rankine cycle heat pump system is given by:

$$\varepsilon = \left(1 - \frac{I^{-1}T_{L1}}{\left(T_{H1} - \frac{Q_C}{\varepsilon\tau_1 K_1}\right)}\right)\left(1 - \frac{\left(I^{-1}\right)' T_{E1}}{\left(T_{C1} - \frac{Q_C}{\tau_2 K_2}\right)}\right)^{-1} \tag{1.20}$$

Now, let τ_1 and τ_2 vary, while Q_C and $\tau = (\tau_1 + \tau_2)$ remain unvaried. Under this constraint conditions, we take ε as objective function and find its optimum. For this reason, we introduce the Lagrangian operator:

$$L = \varepsilon + \lambda(\tau - \tau_1 - \tau_2) \tag{1.21}$$

From the Euler-Lagrangian equations (Kaushik et al., 2002b), $\frac{\partial L}{\partial \tau_1} = 0$ and $\frac{\partial L}{\partial \tau_2} = 0$ give the optimal value of τ_1 and τ_2. After substituting these optimal values into **Eq. (1.20)**, Chen et al. (2004) obtained the optimal coefficient of performance of an irreversible Rankine cycle heat pump system, which satisfies the equation:

$$\varepsilon = \frac{1 - \frac{T_{L1}}{IT_{H1}} - \frac{R_H}{\varepsilon T_{H1} T_{C1}}\left(\frac{\varepsilon T_{H1}}{K_2} + \frac{\varepsilon T_{C1}}{K_1 K_2^{1/2}}\left(\sqrt{I^{-1}T_{L1} I' T_{E1}}\frac{1}{\sqrt{K_1}} + \frac{T_{L1}}{I\sqrt{K_2}}\right)\right)}{\left(1 - \frac{I' T_{E1}}{T_{C1}}\right) + \frac{R_H}{\varepsilon T_{H1} T_{C1}}\left(\frac{\varepsilon T_{H1}}{K_2} + \frac{T_{C1}}{K_1} - \frac{1}{K_1^{1/2}}\left(\frac{I' T_{E1}}{K_1^{1/2}} + \frac{1}{K_2^{1/2}}\sqrt{I' T_{E1} I^{-1} T_{L1}}\right)\right)} \tag{1.22}$$

where heating load $R_H = Q_C / t$.

Rearranging **Eq. (1.22)**, we have:

$$R_H = \frac{K_1(\varepsilon_R - \varepsilon)T_{H1}\left(T_{C1} - I' T_{E1}\right)}{\left(\frac{T_{H1}K_1}{K_2}(\varepsilon - 1) + T_{C1}\left(\varepsilon^{-1} - 1\right) + 2\sqrt{I' T_{E1} I^{-1} T_{L1}\frac{K_1}{K_2}} - \frac{K_1}{K_2} I^{-1} T_{L1} + I' T_{E1}\right)} \tag{1.23}$$

where $\varepsilon_R = \frac{T_{C1}\left(T_{H1} - I^{-1}T_{L1}\right)}{T_{H1}\left(T_{C1} - I' T_{E1}\right)}$

$\frac{\partial R_H}{\partial \varepsilon} = 0$ gives the value of the coefficient of performance of heat pump:

$$\varepsilon_m = \frac{-T_{C1} \pm \sqrt{{T_{C1}}^2 + \left(\frac{T_{H1}K_1}{K_2}(\varepsilon_R - 1) + 2\sqrt{I' T_{E1} I^{-1} T_{L1}\frac{K_1}{K_2}} + \frac{K_1}{K_2} I^{-1} T_{L1} + I' T_{E1} - T_{C1}\right)\varepsilon_R T_{C1}}}{\frac{T_{H1}K_1}{K_2}(\varepsilon_R - 1) + 2\sqrt{I' T_{E1} I^{-1} T_{L1}\frac{K_1}{K_2}} + \frac{K_1}{K_2} I^{-1} T_{L1} + I' T_{E1} - T_{C1}} \tag{1.24}$$

at which the rate of heating R_H attains the maximum:

$$\left(R_H\right)_m = \frac{K_1\left(\varepsilon_R - \varepsilon_m\right)T_{H1}\left(T_{C1} - I^{'}T_{E1}\right)}{\frac{T_{H1}K_1}{K_2}\left(\varepsilon_m - 1\right) + T_{C1}\left(\varepsilon_m{}^{-1} - 1\right) + 2\sqrt{I^{'}T_{E1}I^{-1}T_{L1}\frac{K_1}{K_2}} + \frac{K_1}{K_2}I^{-1}T_{L1} + I^{'}T_{E1}} \tag{1.25}$$

The maximum objective functions relating to the irreversible Rankine cycle heat pump system are therefore the maximum heating load $\left(R_H\right)_m$ and the maximum COP (ε_m). However, by evaluating the case of the reversible Rankine cycle HP system, the heating load is taken $R_H = 0$ and the internal irreversibility parameters are taken $I = I^{'} = 0$. It can be seen from **Eq. (1.22)** that optimal overall coefficient of performance of irreversible Rankine cycle heat pump system reduces to Carnot coefficient of performance which is given by:

$$\varepsilon_{CAR} = \frac{T_{C1}\left(T_{H1} - T_{L1}\right)}{T_{H1}\left(T_{C1} - T_{E1}\right)} \tag{1.26}$$

The results obtained allowing the performance of such a system to be discussed from the finite time thermodynamic analysis take into account the following numerical examples (Chen et al., 2004): $T_{H1} = 385\text{K}$, $T_{L1} = 318\text{K}$, $T_{E1} = 285\text{K}$, $T_{C1} = 318\text{K}$, $\text{C}_H = \text{C}_L = \text{C}_E = \text{C}_C = 1.0\,\text{kW/K}$, $\varepsilon_H = \varepsilon_L = \varepsilon_E = \varepsilon_C = 0.75$, $I = I^{'} = 1.0$ and $R_H = 1.2\text{kW}$.

From **Eq. (1.23)**, it is seen that, one R_H corresponds to two ε (say ε_I and ε_{II}); where one is smaller than ε_m (say ε_I), the other is larger than ε_I (say ε_{II}), which is sketchily shown in **Fig. 1.6.** Obviously, the optimal value of *COP* is ε_{II} (larger than ε_m) and not ε_I (smaller than ε_m). The important significance of ε_m lies in that it not only shows the optimal value at maximum heating load but also determines a lower limit to the optimal coefficient of performance. In parametric study, the effect of various input parameters has been studied, and it is found that the internal irreversibility is more prominent for performance reduction than the external irreversibility. For the above typical operating conditions, the COP of a completely reversible system is found to be $\varepsilon_{CAR} = 1.68$. The optimal overall coefficient of performance of a completely irreversible Rankine cycle heat pump system is calculated using **Eq. (1.22)**, and for $I = I^{'} = 0.97$, it is found to be $\varepsilon_{II} = 0.64$, whereas for endoreversible system ($I = I^{'} = 1.0$), it is found to be $\varepsilon_{II} = 1.07$.

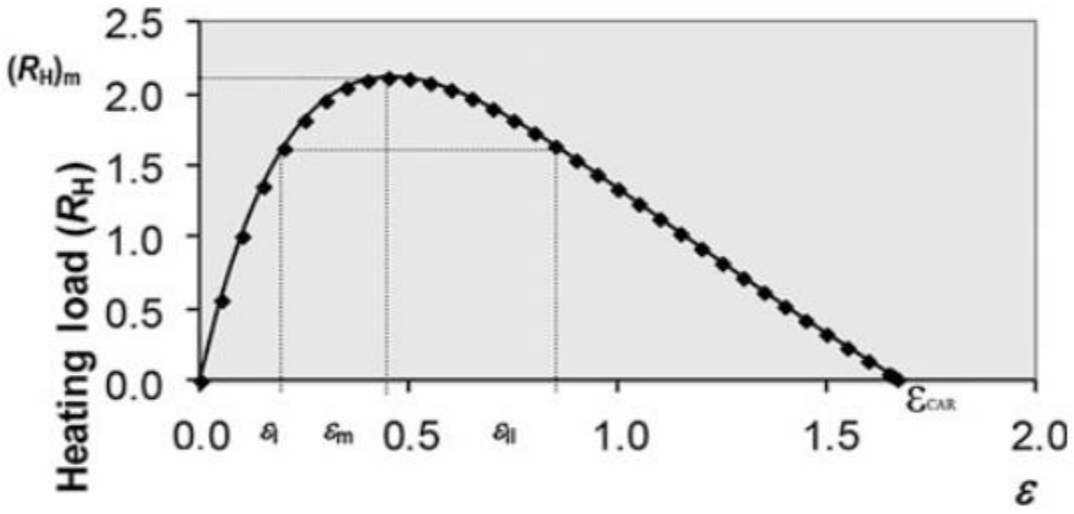

Fig. 1.6. Heating load with respect to the coefficient of performance (Chen et al., 2004).

1.2.4.3. Brayton cycle coupled heat pump

Unlike the refrigeration cycles studied previously, the Brayton refrigeration cycle like the Stirling/Ericsson refrigeration cycle is a gas refrigeration cycle, that is to say the working fluid remains in the gaseous state all along the cycle. Also, the heat transfer during the gas cycle is not isothermal and therefore the temperature varies considerably. Consequently, the gas refrigeration cycle has much lower coefficient of performance (COP) as compared to the VCR and reversed Carnot cycle (Chen et al., 1999c, Ni et al., (1999), Kaushik and Tyagi, 2002, Tyagi et al., 2004c). Nevertheless, gas refrigeration systems have a number of important applications over the vapour compression, vapour absorption, and hybrid refrigeration systems. Some of them are used to achieve very low temperature for many important applications, such as liquefaction of gases/air, aircraft cabin cooling, superconductivity-related R&D works, and other specialized applications. Among others, the Brayton refrigeration cycle is one of the important gas refrigeration cycles being used for space airconditioning applications with its unique application for aircraft cooling, liquefaction of gases, and cryogenic applications. We will present and analyze in the following first the ideal Brayton refrigeration cycle then the irreversible Brayton refrigeration cycle.

In the first place, the Brayton refrigeration cycle is a reverse of closed Brayton power cycle as shown on the schematic and *T*–*s* diagrams of **Figs. 1.7 and 1.8**, respectively. The refrigerant gas, which may be air, enters the compressor at state point 1, where the temperature is somewhat below the temperature of the cold region (i.e. heat source) T_L and is compressed in the compressor to state point 2. The gas then cooled up to state point 3, where the temperature of the gas refrigerant

approaches to the temperature of the sink/warm region, T_H. After releasing the heat to the sink/surroundings, the gas refrigerant is expanded in an expander up to the state point 4, where the exit temperature is well below than that of the cold region/heat source (T_L) as can be seen from **Fig. 1.8**. At state point 4, the gas starts absorbing heat from the heat source (cold region) as it passes from state 4 to state 1, thereby, completing the cycle. Thus, the ideal Brayton refrigeration cycle shown on the *T*–*s* diagram of **Fig. 1.8** is denoted by 1–2–3–4–1 in which all the processes in the compressor and expander (turbine) are assumed to be adiabatic. However, the actual compression and expansion processes, in general, are not adiabatic because there is some less useful work during the actual processes (3–4), respectively (Kaushik and Tyagi, 2002). But, for simplicity of the analysis, the irreversibilities due to pressure drops have been ignored in this particular model of Brayton refrigeration cycle. Thus, for steady-state operation, the heat transfer rates to and from the cycle, power consumption by compression, and power production by expander are given below (Kaushik and Tyagi, 2002):

$$\dot{Q}_{in} = \dot{m}\left(h_1 - h_4\right) = \dot{m} C_P \left(T_1 - T_4\right),\ \dot{Q}_{out} = \dot{m}\left(h_2 - h_3\right) = \dot{m} C_P \left(T_2 - T_3\right),$$

$$W_c = \dot{m}\left(h_2 - h_1\right) = \dot{m} C_P \left(T_2 - T_1\right) \text{ and } W_t = \dot{m}\left(h_3 - h_4\right) = \dot{m} C_P \left(T_3 - T_4\right) \tag{1.27}$$

where $\dot{m}$ is the mass flow rate and C_P is the specific heat of the working/air being used in the cycle. Also, the net work input and COP of the cycle are given as below:

$$W_{net} = W_c - W_t = \dot{m} C_P \left(\left(T_2 - T_1\right) - \left(T_3 - T_4\right)\right)$$

$$\text{and } COP_{HP} = \frac{\dot{Q}_{out}}{W_{net}} = \frac{h_1 - h_4}{\left(h_2 - h_1\right) - \left(h_3 - h_4\right)} = \frac{T_1 - T_4}{\left(T_2 - T_1\right) - \left(T_3 - T_4\right)} \tag{1.28}$$

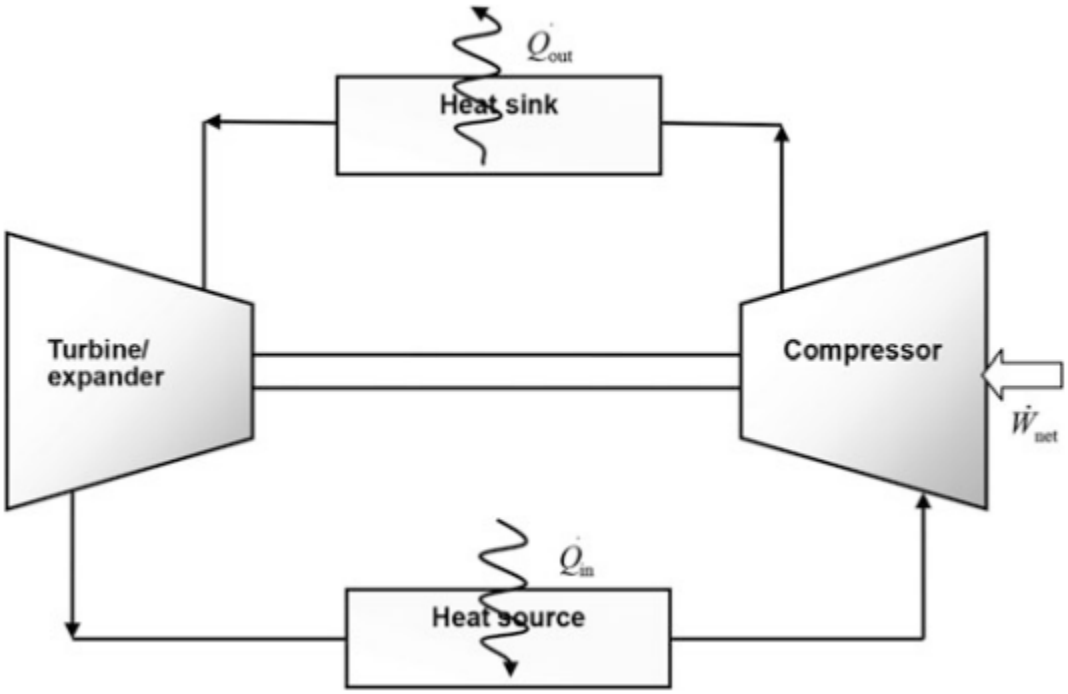

Fig. 1.7. Schematic of an ideal Brayton refrigeration cycle (Kaushik and Tyagi, 2002).

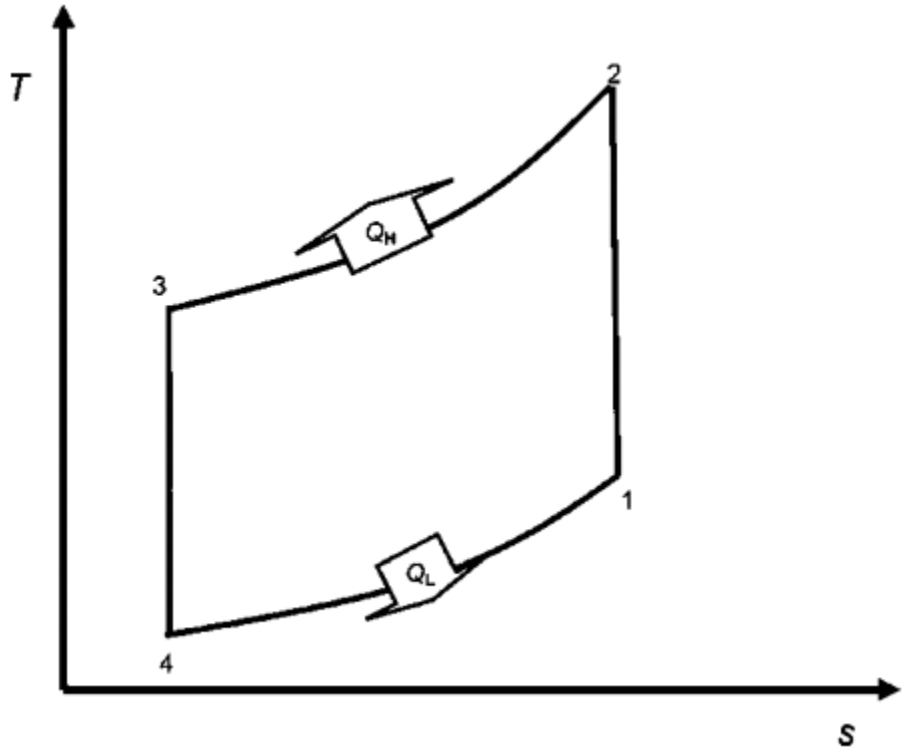

Fig. 1.8. *T-s* diagram of an ideal Brayton refrigeration cycle (Kaushik and Tyagi, 2002).

The two particular advantages of this cycle are the light weight of the components and the fact that it can integrate regeneration. In this ideal cooling/heating system, the isothermal heating and cooling processes must be carried out infinitely slowly so that the working substance is in thermal equilibrium with the heat source and sink.

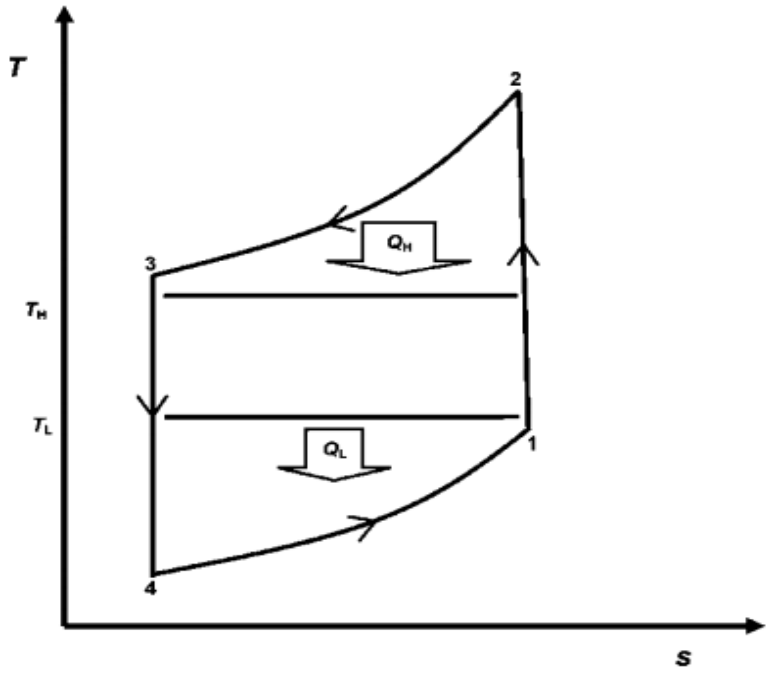

Fig. 1.9. *T-s* diagram of finite time Brayton refrigeration cycle (Tyagi et al., 2004c).

Among other things, **Fig. 1.9** shows the modified Brayton refrigeration cycle, i.e. there is now a finite temperature difference between the working fluid and the thermal reservoirs.

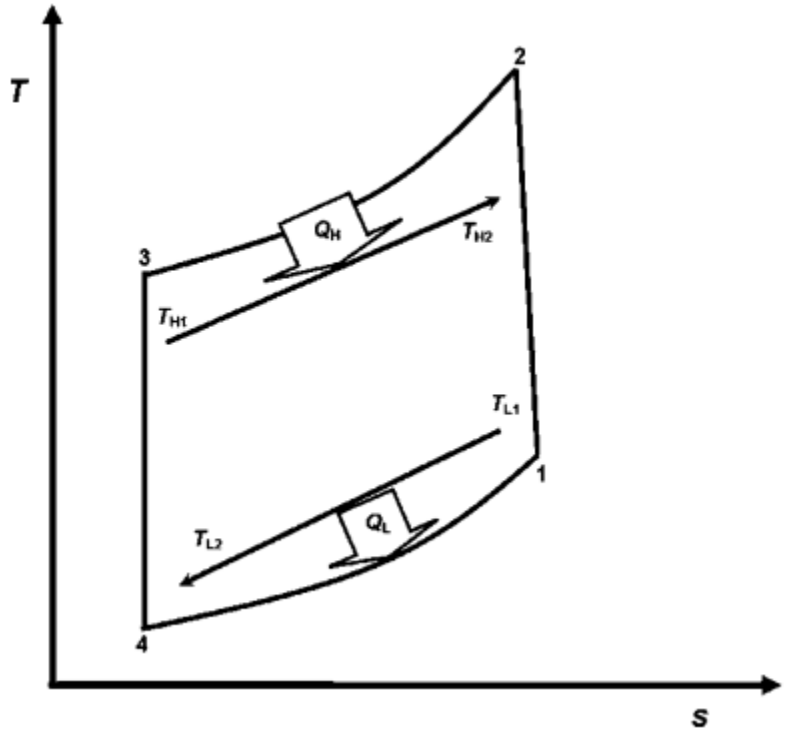

Fig. 1.10. *T-s* diagram of finite heat capacity Brayton refrigeration cycle (Tyagi et al., 2004c).

On the other hand in **Fig. 1.10** in addition to the heat exchange in finite time between the working fluid and the heat reservoirs during the refrigeration process, there is also heat exchange between the heat reservoirs and the environment.

As it is well known that at the exit of the heat sink (space to be heated), the temperature of the refrigerant is much higher than that of the inlet of the heat source. In order to further reduce the exit temperature of the expander and/or to reduce the temperature at the entrance of the heat source, a regenerator may be included in the Brayton cycle (Kaushik and Tyagi, 2002) as shown in **Fig. 1.9**. This did not only enhance the cooling load and indirectly increased the heating load, but also reduced the compressor input power, thereby, enhancing the overall COP of the system. In this case of Brayton refrigeration system, the refrigerant enters the compressor at state point 1 and is compressed in the compressor to state point 2/2S in a real/ideal compressor. The gas then cooled up to state point 3 by rejecting the heat to the heat sink of finite heat capacity whose temperature remains constant at temperature T_H. After releasing the heat to the sink/surroundings, the gas refrigerant is expanded in an expander up to the state point 4S/4 in a real/ideal expander. At state point 4, the gas enters the heat exchanger and starts absorbing heat from the heat source (cold region) of infinite heat capacity whose temperature remains constant at temperature T_L, as it passes from state 4 to state 4R. Finally, the working fluid enters the regenerator where it gets heated to state point 1, thereby, completing the cycle.

Thus, the real Brayton refrigeration cycle shown on the *T*–*s* diagram of **Fig. 1.10** is denoted by 1–2–3–4–1 in which compression and expansion are assumed to be non-isentropic, due to the fact that in general, all real processes are non-adiabatic as there is always some loss of useful work during the actual processes. However, for simplicity the irreversibility due to pressure drop has been ignored. The heat transfer rates (Q_L and Q_H) to and from the cycle can be written as (Kaushik and Tyagi, 2002):

$$\dot{Q}_H = C_{wf}\left(T_3 - T_{3R}\right) = \left(UA\right)_H \left(LMTD\right)_H = C_H\left(T_{H2} - T_{H1}\right) = C_{H,\min}\varepsilon_H\left(T_3 - T_{H1}\right)$$

$$\text{and } \dot{Q}_L = C_{wf}\left(T_{1R} - T_1\right) = \left(UA\right)_L \left(LMTD\right)_L = C_L\left(T_{L1} - T_{L2}\right) = C_{L,\min}\varepsilon_L\left(T_{L1} - T_1\right) \tag{1.29}$$

where $\left(LMTD\right)_H$ and $\left(LMTD\right)_L$ are the Log Mean Temperature Differences and ε_H and ε_L are the effectiveness of the source and sink-side heat exchangers, respectively. Also $C_{H,\min}$, $C_{L,\min}$, $C_{H,\max}$ and $C_{L,\max}$ are the minimum and the maximum heat capacitance rates of the external fluids on the source and sink-side, respectively, and for counter flow heat exchangers are given as below (Kaushik and Tyagi, 2002, Tyagi et al., 2004c):

$$(LMTD)_H = \frac{(T_{H1}-T_2)-(T_{H2}-T_3)}{\ln\left((T_{H1}-T_2)/(T_{H2}-T_3)\right)} \quad \text{and} \quad (LMTD)_L = \frac{(T_4-T_{L2})-(T_1-T_{L1})}{\ln\left((T_4-T_{L2})/(T_1-T_{L1})\right)} \tag{1.30}$$

$$\varepsilon_H = \frac{1-\exp\left(-NTU_H\left(1-\frac{C_{H,\min}}{C_{H,\max}}\right)\right)}{1-\frac{C_{H,\min}}{C_{H,\max}}\exp\left(-NTU_H\left(1-\frac{C_{H,\min}}{C_{H,\max}}\right)\right)}, \quad \varepsilon_L = \frac{1-\exp\left(-NTU_L\left(1-\frac{C_{L,\min}}{C_{L,\max}}\right)\right)}{1-\frac{C_{L,\min}}{C_{L,\max}}\exp\left(-NTU_L\left(1-\frac{C_{L,\min}}{C_{L,\max}}\right)\right)} \quad \text{and} \quad \varepsilon_R = \frac{NTU_R}{1+NTU_R}$$

(1.31)

$$\text{Also,} \begin{pmatrix} C_{H,\min} = \min\left(C_{wf}, C_H\right) \\ C_{H,\max} = \max\left(C_{wf}, C_H\right) \end{pmatrix} \text{ and } \begin{pmatrix} C_{L,\min} = \min\left(C_{wf}, C_L\right) \\ C_{L,\max} = \max\left(C_{wf}, C_L\right) \end{pmatrix} \tag{1.32}$$

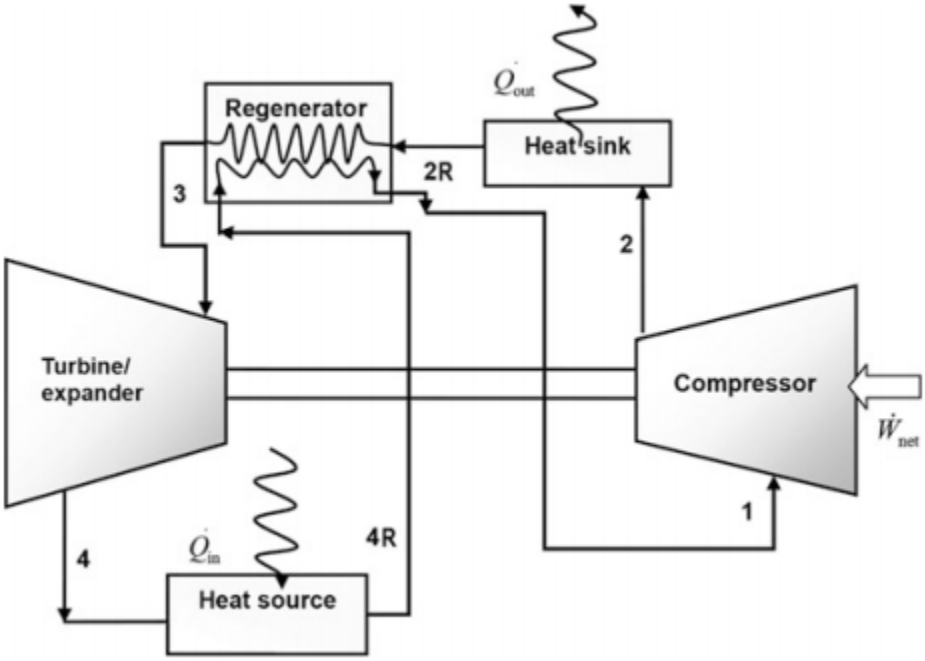

Fig. 1.11. Schematic of an irreversible regenerative Brayton refrigeration cycle (Ni et al., 1999).

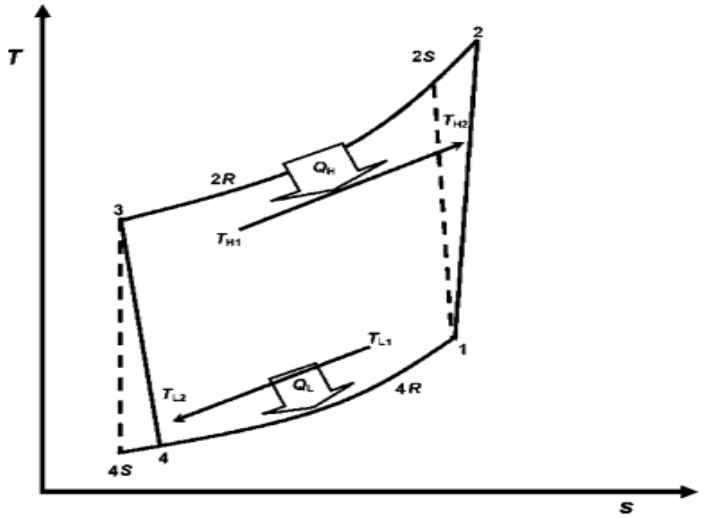

Fig. 1.12. *T-s* diagram of an irreversible regenerative Brayton refrigeration cycle (Ni et al., 1999).

Using *T-s* diagram, the expression and compression efficiencies of the cycle can also be expressed, as below (Ni et al., 1999):

$$\eta_e = \frac{C_w\left(T_4 - T_1\right)}{C_w\left(T_4 - T_1\right)} \text{ and } \eta_c = \frac{C_w\left(T_3 - T_{2S}\right)}{C_w\left(T_3 - T_2\right)} \tag{1.33}$$

Using the second law of thermodynamics in this case of Brayton cycle yields (Ni et al., 1999):

$$C_{wf}\ln\left(T_{3S}/T_2\right) - C_{wf}\ln\left(T_4/T_{1S}\right) = 0 \Rightarrow T_{3S}/T_2 = T_4/T_{1S} = X = \left(R_P\right)^{(\gamma-1)/\gamma} \tag{1.34}$$

where X and R_P are, respectively, the temperature and pressure ratios of the cycle and γ is the heat capacity ratio of the working fluid. Following **Eq. (1.29)** for this case yieds:

$$T_4 = \left(1-\varepsilon_R\right)T_{3R} + \varepsilon_R T_{1R}, \qquad T_2 = \left(1-\varepsilon_R\right)T_{1R} + \varepsilon_R T_{3R}, \qquad T_{1R} = \left(1-a_2\right)T_1 + a_2 T_{L1} \text{ and}$$

$$T_{3R} = \left(1-a_1\right)T_3 + a_1 T_{H1} \tag{1.35}$$

where $a_1 = \varepsilon_H C_{H,\min}/C_w$ and $a_2 = \varepsilon_H C_{L,\min}/C_w$.

Using the first law of thermodynamics to obtain the power input and the COP, in this case of Brayton cycle yield (Ni et al., 1999):

$$P = Q_L - Q_H,\ COP_{ref} = Q_L/P \text{ and } COP_{HP} = Q_H/P \tag{1.36}$$

From the above, it follows that the optimal values of the performance parameter can be calculated for different set of operating conditions with respect to the cycle temperature ratio (X) using Lagrangian multiplier method (Kaushik et al., 2002b; Tyagi et al., 2004a, 2004b, 2004c). The objective function can be given as below:

$$L = P + \lambda Q_L \tag{1.37}$$

1.2.4.4. Stirling/Ericsson cycle coupled heat pump

1.2.4.4.1. System description

The Stirling and Ericsson cycles are among the important cycle models of refrigerators, air-conditionning and heat pump systems for the production of very low temperature and desirable temperature, especially in the cryogenic range. These cycles have been utilized by a number of engineering firms in the construction of practical systems and have promoted the development of new design of these cycles for different applications (Chen, 1998, Kaushik and Kumar, 2000a, Kaushik et al., 2002a, Tyagi et al., 1999). The reversed Stirling and Ericsson cycles are also called gas refrigeration cycle as gas/air being the working fluid and are very similar to each other. The basic Stirling and Ericsson refrigeration cycles are very similar to each other. These refrigeration

cycles also slightly deviate from the reverse Carnot cycle because the adiabatic processes of the latter replaced with the isochoric processes in the Stirling cycle and with the isobaric processes in the Ericsson cycle involving a regenerator for heat transfer during the operation of these cycles. Also the performance of these cycles approaches to the Carnot cycle, as the regenerator efficiency tends to unify with it, which seldom happens in real practice. Hence, the performance of Stirling and Ericsson cycles is always lesser than that of a Carnot cycle for the same set of operating parameters. It is therefore necessary to study the Stirling/Ericsson refrigeration cycles through their relevant applications. We will first study the ideal cycle, then the irreversible cycles thereafter by considering the finite and infinite heat capacities.

1.2.4.4.2. Ideal Stirling/Ericsson heat pump cycle

The fundamental ideal Stirling/Ericsson cycle (internal reversibility and external reversibility) consists of a compressor, a regenerator, and an expander as shown in the schematic diagram of **Fig. 1.13 (**Kaushik et al., 2002a). The refrigerant, which may be air or a gas, enters the compressor at state point 1, where the temperature is somewhat below the temperature of the cold region, i.e. heat source temperature (T_L), and is compressed in the compressor to state point 2. The gas then cooled up to state point 3, where the temperature of the gas refrigerant approaches to the temperature of the sink/warm region (T_H). After releasing the heat to the sink/surroundings, the gas refrigerant is expanded in an expander up to the state point 4, where the exit temperature is well below than that of the cold region/heat source (T_L) as can be seen from **Fig. 1.14 (**Kaushik and Kumar, 2000a). At state point 4, the gas enters the low-temperature heat exchanger and starts absorbing heat from the heat source (cold region) as it passes from state 4 to state 1, thereby completing the cycle. Thus, the ideal Stirling/Ericsson refrigeration cycle shown in **Fig. 1.14** is denoted by 1–2–3–4–1. In these cycles, heat rejection processes (4–1 and 2–3) are isothermal, while the expansion (3–4) and compression (1–2) processes are isochoric in Stirling cycle, whereas they are isobaric in the Ericsson cycle, respectively (**Fig. 1.15**, Kaushik and et al., 2002a). For ideal cycle, the heat transferred to the regenerator during the compression process (1–2) is fully recovered during the expansion process (3–4), as can be seen from the T–s diagram of **Fig. 1.14.**

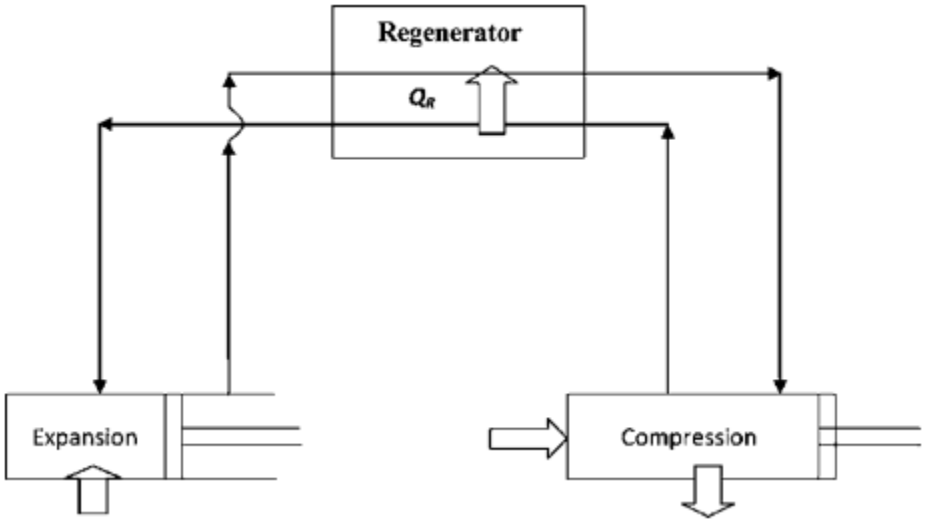

Fig. 1.13. Line diagram of Stirling/Ericsson heat pump cycle (Kaushik et al., 2002a).

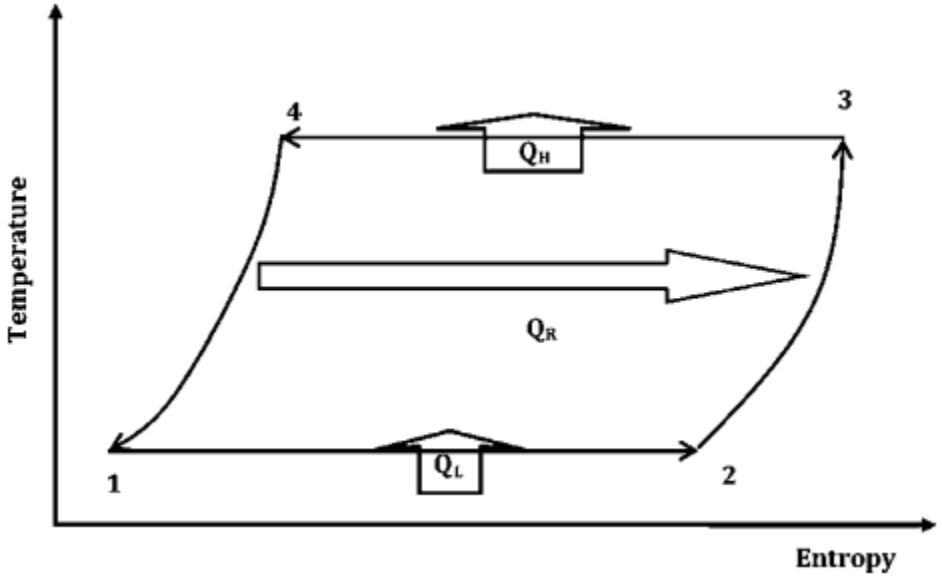

Fig. 1.14. *T-s* diagram of ideal Stirling heat pump cycle (Kaushik and Kumar, 2000a).

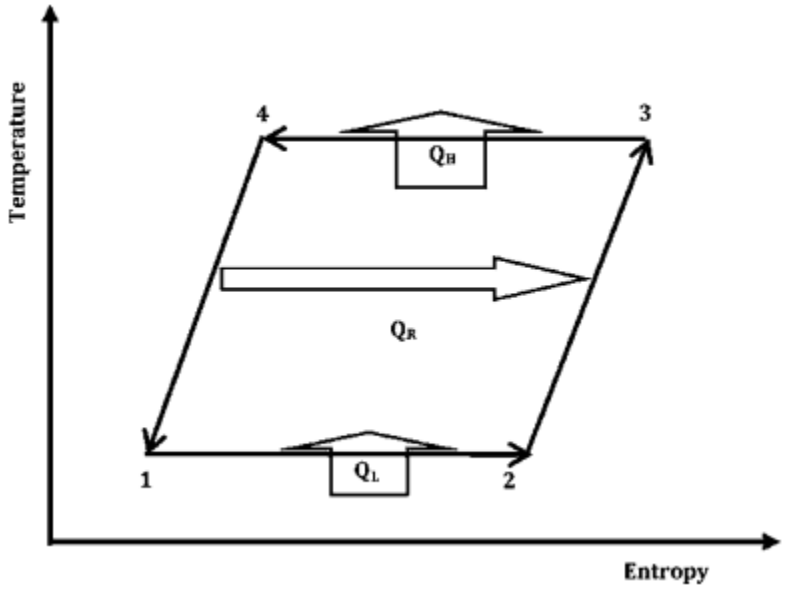

Fig. 1.15. *T-s* diagram of ideal Ericsson heat pump cycle (Kaushik and et al., 2002a).

For steady-state operation (negligible kinetic and potential energies), the heat transfer to and from the cycle can be given as below (Kaushik and et al., 2002a):

$$Q_L = nR\ln\lambda_r T_L = \Delta S T_L \text{ and } Q_H = nR\ln\lambda_r T_H = \Delta S T_H \tag{1.38}$$

where ΔS is the change in the entropy during isothermal heat addition and heat rejection processes of the cycle and λ_r is the volume ratio for Stirling and pressure ratio for the Ericsson cycle, respectively. Using the first law of thermodynamics, the work done on the cycle and the coefficient of performance (*COP*) are given as below (Kaushik and et al., 2002a):

$$W = Q_H - Q_L = \Delta S\left(T_H - T_L\right) \text{ and } COP_{HP} = \frac{Q_H}{W} = \frac{T_L}{T_H - T_L} \tag{1.39}$$

It is clear from **Eq. (1.39)** that the performance of reversible Ericsson/Stirling refrigeration cycle is similar to that of a reversed Carnot for the same set of operating conditions. However, in the actual cycles, there are number of irreversible processes such as compression, expansion, regeneration, heat addition, heat rejections, etc. So in general, the real processes are not ideal because there is some loss of the useful energy during the actual processes leading to loss of potential to do useful work.

1.2.4.4.3. Irreversible Stirling/Ericsson refrigeration cycle

The ideal cycle approximate the expansion stroke of real cycle as an isothermal process 1-2 with irreversible isothermal heat addition at temperature T_c from a heat source of finite heat capacity whose temperature varies from T_{L1} to T_{L2}. The heat addition to the working fluid from the regenerator is modeled as isobaric (in Ericsson cycle) or isochoric (in Stirling cycle) processes 2-

3 and 2-3s in real and ideal cycles, respectively. The compression stroke is modeled as an isothermal process 3-4 with irreversible heat rejection at temperature T_h to the heat sink of finite heat capacity whose temperature varies from T_{H1} to T_{H2}. Finally, the heat rejection to the regenerator is modeled as isothermal/isochoric processes 4-1 and 4-1s in real and ideal Ericsson/Stirling heat pump, respectively, completing the cycle. As mentioned earlier, the heat transfer processes 1-2 and 3-4 in real cycles must occur in finite time. This requires that these heat processes must proceed through a finite temperature difference and therefore, defined as being externally irreversible. Also the entropy change during process 3-4 is more than the entropy change during process 1-2 (Kaushik et al., 2002a). Thus, there is some net entropy generation per cycle and the ratio of entropy change in heat addition (expansion) to that of heat rejection (compression) is called internal irreversibility parameter (I) which also affects the performance of these cycles. There is also some heat loss through the regenerator, as an ideal regeneration requires infinite regeneration time or area, which is not the case in practice. Hence, it is desirable to consider a real regenerator. By considering all these factors, these heat pumps models become irreversible. The external irreversibility is due to finite temperature difference between the cycle and the external reservoirs and internal irreversibilities are due to regenerative loss and entropy generation.

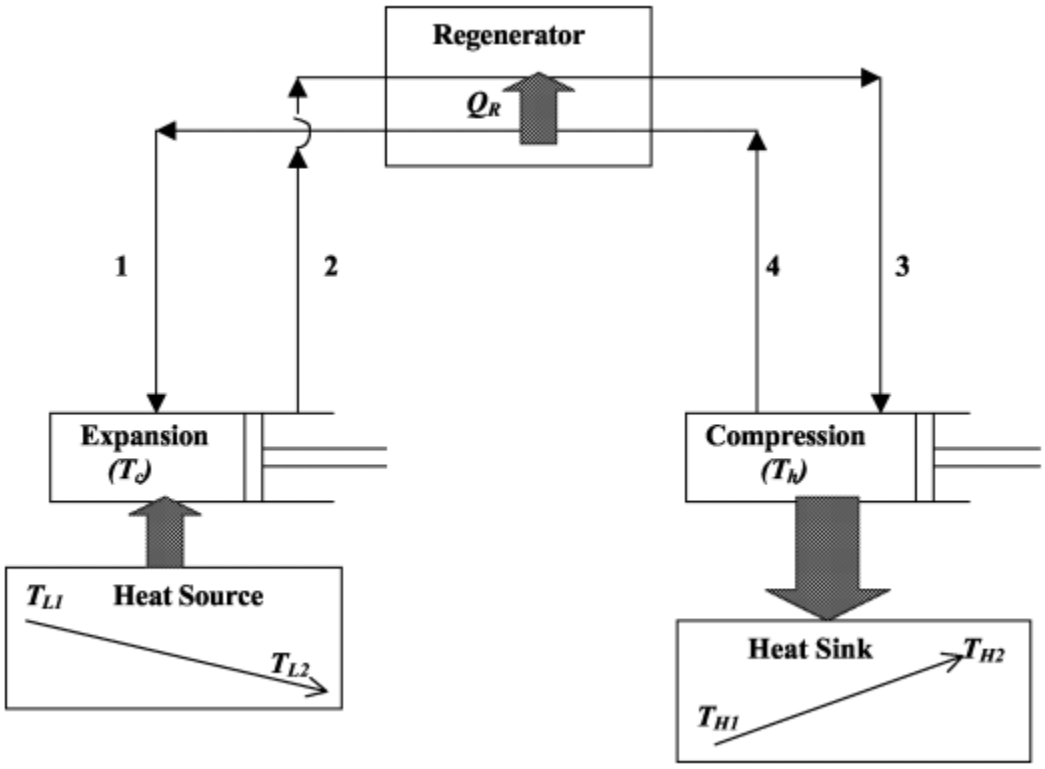

Fig. 1.16. Schematic of irreversible Stirling/Ericsson heat pump cycles. (Kaushik et al., 2002a).

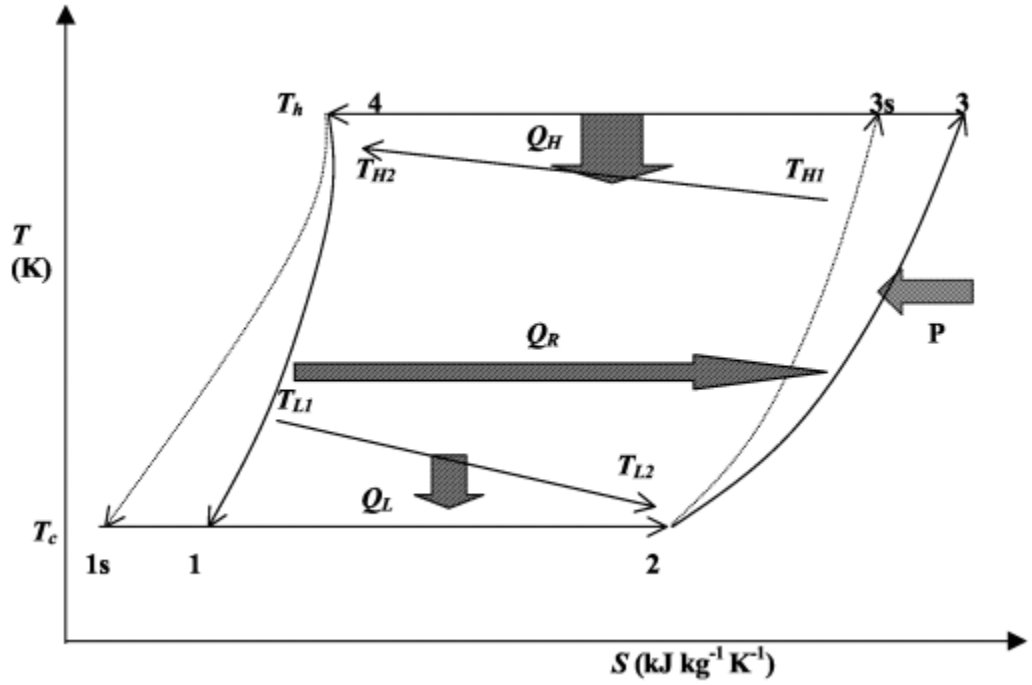

Fig. 1.17. *T-s* diagram of irreversible Stirling heat pump cycle (Kaushik et al., 2002a).

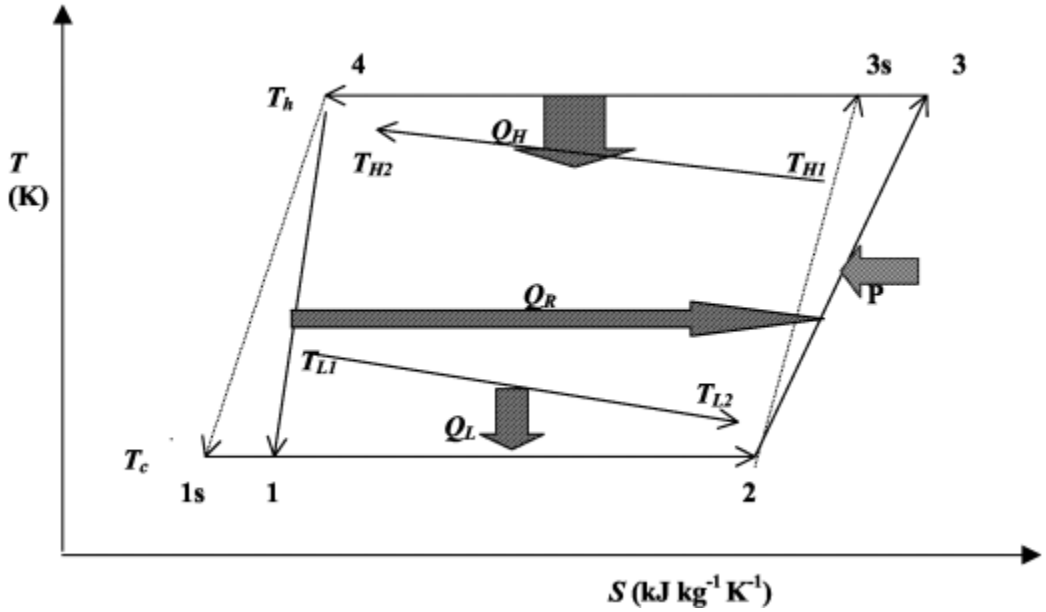

Fig. 1.18. *T-s* diagram of irreversible Ericsson heat pump cycle (Kaushik et al., 2002a).

Let Q_c be the amount of heat absorbed from the source at temperature T_c and Q_h be the amount of heat release to the sink at temperature T_h then (Kaushik et al., 2002a):

$$Q_h = T_h\left(S_3 - S_4\right) = T_h nR\ln\left(\lambda_1\right) = C_H\left(T_{H2} - T_{H1}\right)t_H$$

and $$Q_c = T_c\left(S_2 - S_1\right) = T_c nR\ln\left(\lambda_2\right) = C_L\left(T_{L1} - T_{L2}\right)t_L \qquad (1.40)$$

where λ_1 and λ_2 are the volume (for Stirling cycle) and pressure (for Ericsson cycle) ratios for the sink and source side in both the cycles, respectively, n is the number of moles for the working

fluid and R is the universal gas constant. C_H, C_L and t_H, t_L are the heat capacitance rates of source/sink reservoirs and heat addition/rejection times, respectively. Also from the heat transfer theory, the heat Q_h and Q_c will be proportional to the Log Mean Temperature Difference $(LMTD)$ (Kaushik and Kumar, 2000a, 2000b, 2001; Kaushik et al., 2002a, 2002b), i.e.,

$$Q_h = U_H A_H \left(LMTD\right)_H t_H \text{ and } Q_c = U_L A_L \left(LMTD\right)_L t_L \tag{1.41}$$

where $U_H A_H$ and $U_L A_L$ are the overall heat transfer coefficient-area products and $\left(LMTD\right)_H$ and $\left(LMTD\right)_L$ are the Log Mean Temperature Difference on sink and source side, respectively, and defined as:

$$\left(LMTD\right)_H = U_H A_H \left(\frac{\left(T_h - T_{H1}\right) - \left(T_h - T_{H2}\right)}{\ln\left(T_h - T_{H1}\right) / \left(T_h - T_{H2}\right)} \right) \quad \text{and} \quad \left(LMTD\right)_L = U_L A_L \left(\frac{\left(T_{L1} - T_c\right) - \left(T_{L2} - T_c\right)}{\ln\left(T_{L1} - T_c\right) / \left(T_{L2} - T_c\right)} \right)$$

(1.42)

Considering the finite heat transfer in the regeneration processes, it should be noted that these cycles do not have the perfect regeneration condition. Thus, it is assumed reasonably that the regenerator loss per cycle is proportional to the temperature difference of the two processes, i.e.,

$$\Delta Q_R = nC_f \left(1 - \varepsilon_R\right)\left(T_h - T_c\right) \tag{1.43}$$

where C_f is the specific heat of the working fluid ($C_f = C_v$ for Stirling cycle and $C_f = C_p$ for Ericsson cycle) and ε_R is the effectiveness of the regenerator.

The influence of irreversibility of finite heat transfer, the regenerative time should be finite as compared to the two isothermal processes, as given by authors Chen et al. (1998a, 1998b, 1998c), Chen (1998) and Ni et al. (1999);

$$t_R = t_3 + t_4 = 2\alpha\left(T_h - T_c\right) \text{ and } t_{cycle} = \left(T_H + T_L + T_R\right) \tag{1.44}$$

where α is the proportionality constant which is independent of the temperature difference but depends on the property of the regenerative material, and t_{cycle} is the total cycle time.

Considering the external irreversibilities, the net amount of heat released to the sink and absorbed from the source are given by:

$$Q_H = Q_h - \Delta Q_R \text{ and } Q_L = Q_c - \Delta Q_R \tag{1.45}$$

Also, using the **Eqs. (1.44) and (1.45)**, the objective functions such as power input, heating load and *COP* are as follows:

$$P=\frac{Q_H-Q_L}{t_{cycle}}=\frac{Q_h-Q_c}{T_H+T_L+T_R},\qquad R_H=\frac{Q_H}{t_{cycle}}=\frac{Q_H}{T_H+T_L+T_R}\qquad\text{and}\qquad COP_{HP}=\frac{R_H}{P}=\frac{Q_H}{Q_h-Q_c}$$

(1.46)

and the second law of thermodynamics for irreversible cycle gives:

$$\left(Q_c/T_c\right)-\left(Q_h/T_h\right)<0\ \text{ or }\left(Q_c/T_c\right)=I\left(Q_h/T_h\right)\tag{1.47}$$

with I the internal irreversibility parameter and less than unity for real cycle.

$$P=\frac{x-I}{\frac{x}{k_1\left(xy-T_{H1}\right)}+\frac{I}{k_2\left(T_{L1}-y\right)}+b_1\left(x-1\right)},\qquad R_H=\frac{x-a_1\left(x-1\right)}{\frac{x}{k_1\left(xy-T_{H1}\right)}+\frac{I}{k_2\left(T_{L1}-y\right)}+b_1\left(x-1\right)}\qquad\text{and}$$

$$COP_{HP}=\frac{x-a_1\left(x-1\right)}{x-I}\tag{1.48}$$

where $k_1=\varepsilon_H C_H$, $k_2=\varepsilon_L C_L$, $x=T_h/T_c$, $y=T_c$, $b_1=2/\left(\alpha nR\ln\lambda_1\right)$ and $a_1=C_f\left(1-\varepsilon_R\right)/R\ln\lambda_1$.

The purpose of any heat pump is to reject as much heat as possible to the sink (space to be heated) with the expenditure of as little work as possible. This implies that we should do our best to minimize the power input for a given heating load or maximize the heating load for a given power input. For this end, we introduce the Lagrangian

$$L=R_H+\lambda P=\frac{\left(x-a_1\left(x-1\right)\right)+\lambda\left(x-I\right)}{\frac{x}{k_1\left(xy-T_{H1}\right)}+\frac{I}{k_2\left(T_{L1}-y\right)}+b_1\left(x-1\right)}\tag{1.49}$$

where λ is Lagrangian multiplier. From Euler-Lagrange equation:

$\partial L/\partial y=0$ and we find the optimal relation $x\left(T_{L1}-y\right)=\sqrt{\frac{Ik_1}{k_2}}\left(xy-T_{H1}\right)$ (1.50)

It is found that from the optimal analytical relations of the objective functions, the effectiveness of each heat exchanger, the source side external inlet temperature of the fluids, the heat capacitance rate on sink side external fluid and the irreversibility parameter should be higher enough while the sink side inlet temperature of the fluids and the heat capacitance rates on source side should be lower for better performance of both of the heat pumps. Since, the larger heat capacitance allows the fluid to reject the heat at lower temperature thus it is desirable to have higher capacitance rate on sink side in comparison to that on source side (i.e., $C_H>C_L$) for better performance of both the cycles.

1.3. Analysis by heating load, cooling load and coefficient of performance as performance criteria

1.3.1. Optimization by using coefficient of performance and heating load criteria

Cooling systems, air conditioning, heat pumps and heat engines were once analyzed and optimized using the coefficient of performance, cooling load, heating load and mechanical power respectively. This is for endoreversible and irreversible thermodynamic cycles with the finite-time thermodynamics approach. Therefore, Goktun (1998) evaluated the performance of cogeneration heat pump by coupling a Carnot absorption heat pump (Carnot AHP) for heating and a Carnot heat engine to produce the work, using as criterion of performance the COP under the effects of thermal resistances and internal irreversibilities. Chen et al. (1997, 1999b, 1999c) analyzed the effect of heat transfer on the performance of two-heat-reservoir HP by maximizing the specific heating load for internal and external reversibilities and irreversibilities, the endoreversible HP with three-heat-reservoir and the irreversible Brayton HP from the COP and the heating load respectively. However, for irreversible Brayton HP they found the optimal matching between the different heat exchangers and the working fluid in the heat reservoirs under the effects of irreversible losses by heat transfer, non-isentropic expansion, compression losses in the compressor and expander and pressure drop loss in the piping. Afterwards, Bi et al. (2008) and Chen et al. (2008) viewed on a two-heat-reservoir HP, air reversible and two-stage irreversible thermoelectric respectively, using in addition to the COP and the heating load, the heating load density as a performance criteria; Chen et al. (2005a), Huang et al. (2008), Xiling et al. (2011), Kato et al. (2005) and Xia et al. (2007) worked on the performance of a four-heat-reservoir AHP, with internal irreversibility, two internal irreversibilities and endoreversible chemical heat pumps respectively, this successively by the COP, the specific heating load and the rate of energy pumping; Chen (1999), Qin et al. (2006, 2007, 2015) on AHP and Wei et al. (2011) on magnetic Ericsson HP, obtained the optimal value of the heating load corresponding to the maximum value of the *COP* then they obtained the optimal value of the *COP* corresponding to the maximum value of the heating load by using heat exchanges, the laws of thermodynamics with heat resistances, finite heat capacity, heat leakages and irreversibilities by dissipation or friction.

On the other hand, Qin et al. (2004a, 2004b, 2008) and Chen et al. (2007a) on AHT, used the heating load and the *COP* as objective functions.

This being the case, we expose some studies carried out by different authors, in particular for two-heat-reservoir cycle (Carnot cycle), for three-heat-reservoir cycle and for four-heat reservoir cycle. Chen et al. (1997) with two heat reservoirs revealed an HP cycle operating with

four different processes which are the foundation on which future research on thermodynamic analysis of thermodynamic cycle devices will be based. The first process is reversible HP (external and internal reversibilities), i.e. the ideal Carnot cycle with two isothermal and two adiabatic alternately (**Fig. 1.19** and **Fig. 1.20**). Here the objective functions, *COP* (β) and specific heating load q are obtained with the following relationships:

$$\beta = T_H/(T_H - T_L) = 1/(1 - T_L/T_H) \text{ and } q_H = Q_H/(A_H - A_L) \tag{1.51}$$

where T_H and A_H are the temperature and the heat transfer surface area for heat sink reservoir T_L and A_L are the temperature and the heat transfer surface area for heat source reservoir.

The second process is endoreversible HP (external irreversibility and internal reversibility), that is to say the modified Carnot cycle which takes heat resistances into account. The heat exchange rates $Q_L = U_L A_L (T_L - T_C)$ and $Q_H = U_H A_H (T_W - T_H)$ (1.52)

the first and second law of thermodynamics give $p = Q_H - Q_L$ and $Q_H/T_W - Q_L/T_C = 0$ (1.53)

By combining **Eqs. (1.52)** and **(1.53)** we have

$$\beta = Q_H/P = \left(1 - T_L/\left(T_H + q_H (A_H + A_L)\left((U_H A_H)^{-1} + (U_L A_L)^{-1}\right)\right)\right)^{-1}$$

$$q_H = Q_H/(A_H + A_L) = \left(T_L/\left(1 - \beta^{-1}\right) - T_H\right)/\left((A_H + A_L)\left((U_H A_H)^{-1} + (U_L A_L)^{-1}\right)\right) \tag{1.54}$$

By maximizing the *COP* and the specific heating load we obtain the optimal relationship

$$A_H/A_L = (U_L/U_H)^{1/2} \tag{1.55}$$

The third process is exoreversible HP (external reversibility and internal irreversibility), of which the ideal thermoelectric HP is a typical case. The heat exchange rates

$$Q_L = \alpha T_C I - 0.5 I^2 R - K(T_W - T_C) \text{ and } Q_H = \alpha T_W I - 0.5 I^2 R - K(T_W - T_C) \tag{1.56}$$

and the first law becomes $P = I^2 R + \alpha I (T_W - T_C)$ (1.57)

where $I^2 R$ represents the Joulean loss generates an internal heat, R is the total internal electrical resistance of the semiconductor couple, I is the electrical current flowing through the couple, $K(T_W - T_C)$ the conduction heat loss, K the thermal conductance of the semiconductor couple and α is the Seebeck coefficient. To find the maximum *COP*, taking the derivative of β with respect to I and setting it equal to zero gives the optimal values

$$I_{op} = \alpha (T_W - T_C)/((M - 1)R)$$

and $\left(Q_H\right)_{op} = \alpha\left(T_W - T_C\right) M\left(MT_W - T_C\right)\alpha^2 \Big/ \left(R\left(M+1\right)\left(M-1\right)^2\right)$ (1.58)

also, the maximal value of the *COP*, $\beta_m = \left(\beta_{carnot}\right)_{ideal}\left(M - T_C/T_W\right)\Big/\left(M+1\right)$ (1.59)

where $M = \left(1 + Z\left(T_W + T_C\right)/2\right)^{1/2}$. The heating load versus *COP* characteristic curve of the exoreversible thermoelectric heat pump, shows a bell curve in **Fig. 1.21**, with $T_H = T_W = 294.6\text{K}$; $T_L = T_C = 262.1\text{K}$; $\alpha = 4\times10^{-4}\ \text{V/K}$; $Z = 0.0019$ and $\left(\beta_{carnot}\right)_{ideal} = 9.06$.

The last process is irreversible HP (external and internal irreversibilities), which is the combination of the second and third process. These are the effects of friction, finite-rate heat transfer, heat leaks, free expansion, mixing and pressure drop. Consequently, in practice for reasons of efficiency, the real HP must operate with a maximum specific heating load. The results obtained show that engineers must design new heat pumps by taking them into account while working towards a COP Carnot ideal.

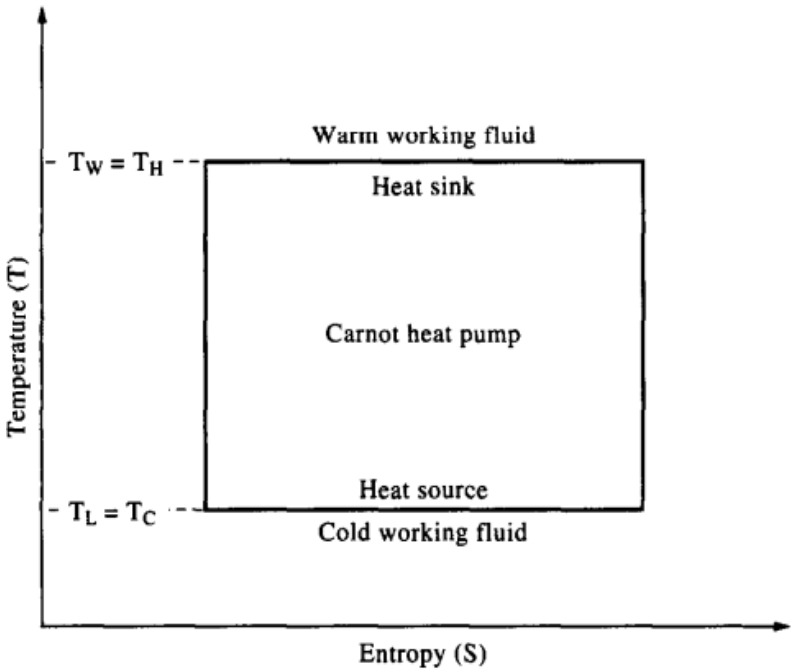

Fig. 1.19. Heat pump Diagram $T-s$ (Chen et al., 1997).

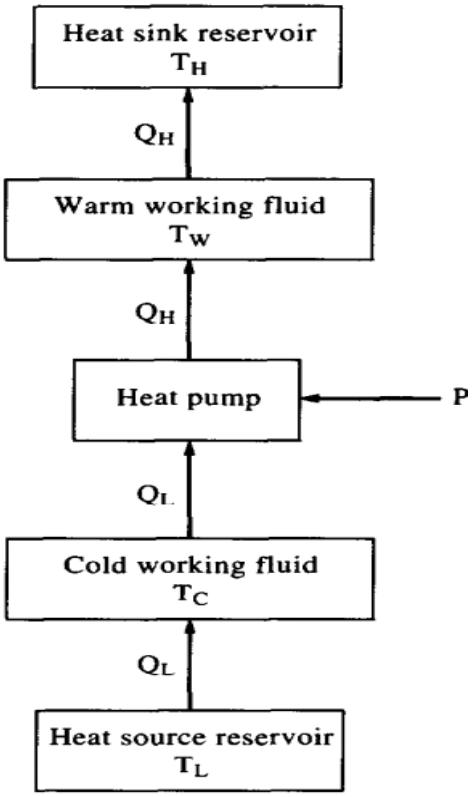

Fig. 1.20. Schematic diagram two-heat-reservoir (Carnot cycle) (Chen et al., 1997).

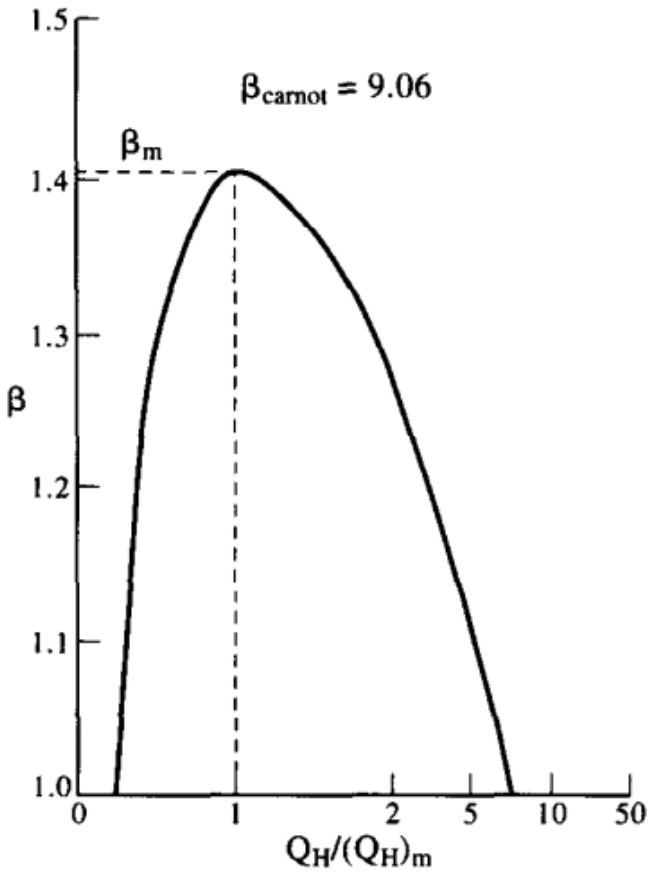

Fig. 1.21. Heating load vs *COP* characteristic of exoreversible thermoelectric heat pump (Chen et al., 1997).

Chen et al. (1999b), considered three heat reservoirs at temperatures T_H, T_P and T_O as shown in **Fig. 1.22**, representing the heat source, the heating space and the ambient atmosphere. The temperatures of the working fluid in the corresponding heat exchangers T_1, T_2 and T_3. The general heat transfer law is following

$$Q_H = \alpha\left(T_H{}^n - T_1^n\right)t_1;\ Q_P = \beta\left(T_2{}^n - T_P{}^n\right)t_2 \text{ and } Q_O = \gamma\left(T_O{}^n - T_3^n\right)t_3 \tag{1.60}$$

where n is the heat-transfer exponent coefficient in the general heat transfer law. If $n=1$, the general law becomes the linear Newton's law. If $n=-1$, the general law becomes the linear phenomenological law in irreversible thermodynamics. Notice that, are heat conductance, have negative values when $n=-1$. The period time of the cycle, $\tau = t_1 + t_2 + t_3$, where t_1, t_2 and t_3 are the times required for the heat pump working fluid in the three heat exchangers.

The *COP* (ψ) of the heat pump cycle is

$$\psi = Q_P / Q_H = \left(T_3^{-1} - T_1^{-1}\right)/\left(T_3^{-1} - T_2^{-1}\right) \tag{1.61}$$

and $$\psi_R = \eta_H / \eta_P = \left(T_H - T_O\right)T_P / \left(T_P - T_O\right)T_H \tag{1.62}$$

where $\eta_H = 1 - T_O/T_H$ and $\eta_P = 1 - T_O/T_P$ are Carnot coefficient of heat source and cooling space; ψ_R is the reversible *COP* bound of the three-heat-reservoir heat pump. The relationships among the reversible *COP* bound, the *COP* bound at maximum heating load and the *COP* bound at maximum profit have been optimized and analyzed.

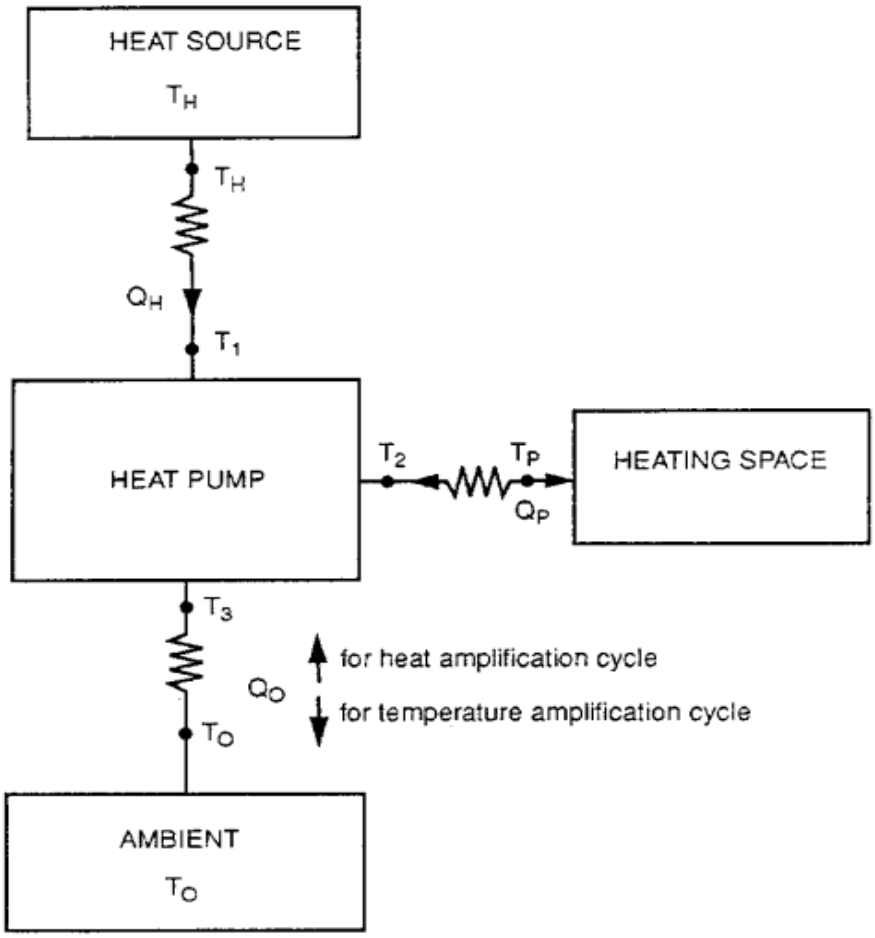

Fig.1.22. Three heat-heat-reservoir endoreversible heat pump (Chen et al. 1999b).

Chen et al. (2005a) and Xiling et al. (2011) on four temperature levels used two different approaches to heat transfer with FTT. This is done for the flow of the working substance exchanges heat with the heat reservoirs at temperatures T_g, T_a, T_c and T_e in the generator, absorber, condenser and evaporator, respectively, during the time τ. The corresponding temperatures of the working substance in the generator, absorber, condenser and evaporator are T_1, T_2, T_3 and T_4, respectively as shown in **Fig. 1.23** (Chen et al., 2005a). However, **Fig. 1.24** allows to write Newton's law of heat-transfer between the working fluid and the external heat-reservoir in heat exchangers is carried out under a finite temperature-difference

$$Q_1 = U_1 A_1 (T_g - T_1)\tau,\ Q_2 = U_2 A_2 (T_2 - T_a)\tau,\ Q_3 = U_3 A_3 (T_3 - T_c)\tau \text{ and } Q_4 = U_4 A_4 (T_e - T_4)\tau \quad (1.63)$$

and heat leaks between the heated space and the environment reservoir

$$Q_L = K_L\left(T_a - T_e + T_c - T_e\right)\tau \tag{1.64}$$

In addition, the first and second laws of thermodynamics make it possible to write respectively:

$$Q_1 + Q_2 + Q_3 + Q_4 = 0 \text{ and } I = \left(Q_3/T_3 + Q_4/T_4\right)/\left(Q_1/T_1 + Q_2/T_2\right) \geq 1 \tag{1.65}$$

where I characterizes the irreversibility due to the internal dissipations of the working fluid. Also according to **Eq. (1.65)**, when $I = 1$, the cycle is said to be endoreversible and when $I > 1$ the cycle is said to be irreversible.

The objective functions of performance *COP* (ψ) and the heating load π are given

$$\psi = \frac{Q_2 + Q_3 - Q_L}{Q_1} = \frac{Q_2 + Q_3}{Q_1}\left(1 - \frac{Q_L}{Q_2 + Q_3}\right) = \frac{(1+a)\left(T_1^{-1} - T_4^{-1}\right)}{\left(IT_2\right)^{-1} + a\left(IT_3\right)^{-1} - (1+a)T_4^{-1}}\left(1 - \frac{q_L}{q_L + \pi}\right)$$

and

$$\pi = \frac{Q_2 + Q_3 - Q_L}{\tau} = A(1+a)\left(\begin{array}{l}\dfrac{\left(IT_2\right)^{-1} + a\left(IT_3\right)^{-1} - (1+a)T_4}{U_1\left(T_1^{-1} - T_4^{-1}\right)\left(T_g - T_1\right)} + \\ \dfrac{1}{U_2\left(T_2 - T_a\right)} + \dfrac{a}{U_3\left(T_3 - T_c\right)} + \dfrac{(1+a)T_1^{-1} - a\left(IT_2\right)^{-1} - a\left(IT_3\right)^{-1}}{U_4\left(T_1^{-1} - T_4^{-1}\right)\left(T_e - T_4\right)}\end{array}\right)^{-1} - q_L \tag{1.66}$$

where $A = A_1 + A_2 + A_3 + A_4$ represents the total heat-transfer surface area and $q_L = Q_L/\tau$, is the heat-leak rate.

By maximizing the *COP* and π from the Lagrangian functions,

$$L_1 = \psi + \lambda_1\pi \text{ and } L_2 = \psi + \lambda_2\pi \tag{1.67}$$

under the extremal conditions, $\partial L_1/\partial x = 0$, $\partial L_1/\partial y = 0$, $\partial L_1/\partial z = 0$, $\partial L_1/\partial T_4 = 0$, $\partial L_2/\partial x = 0$, $\partial L_2/\partial y = 0$, $\partial L_2/\partial z = 0$ and $\partial L_2/\partial T_4 = 0$. (1.68)

we obtain the general relation

$$\sqrt{U_1}\left(T_g x - T_4\right) = \sqrt{U_2^*}\left(T_4 - T_a^* y\right) = \sqrt{U_3^*}\left(T_4 - T_c^* z\right) = \sqrt{U_4}\left(T_e - T_4\right) \tag{1.69}$$

where $T_a^* = IT_a$, $T_c^* = IT_c$, $U_2^* = U_2/I$, $U_3^* = U_3/I$, $x = T_4/T_1$, $y = T_4/I\,T_2$ and $z = T_4/I\,T_3$ (1.70)

Which gives **Eqs. (1.68)** and **(1.69)**, the optimal value of $\pi\left(\pi_\psi\right)$ corresponding to the maximum value of the $COP\left(\psi_{\max}\right)$ and the optimal value of the $COP\left(\psi_\pi\right)$ corresponding to the maximum value of $\pi\left(\pi_{\max}\right)$.

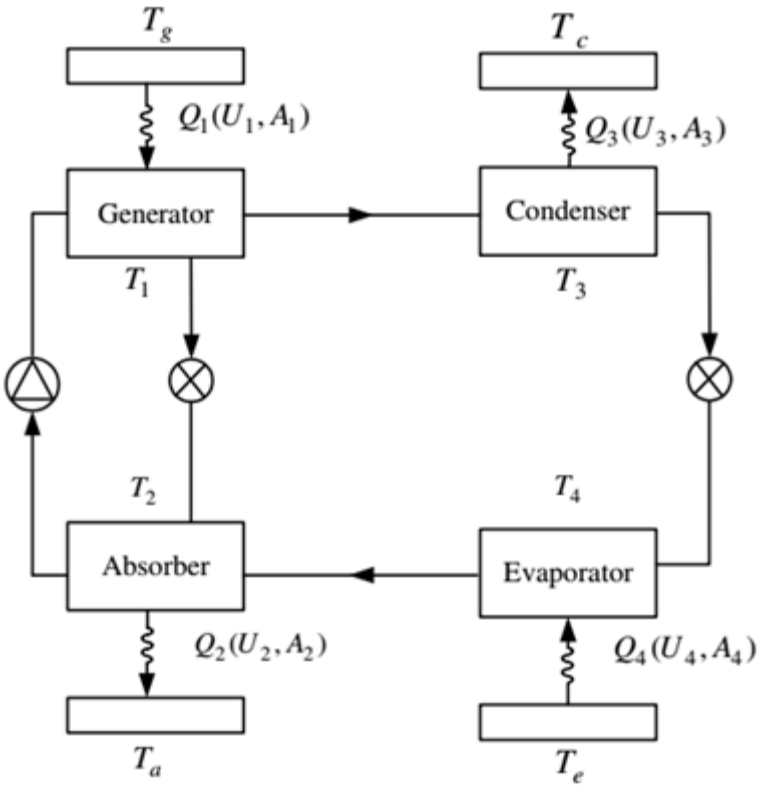

Fig. 1.23. Symbolic diagram of an absorption heat pump (Chen et al., 2005a).

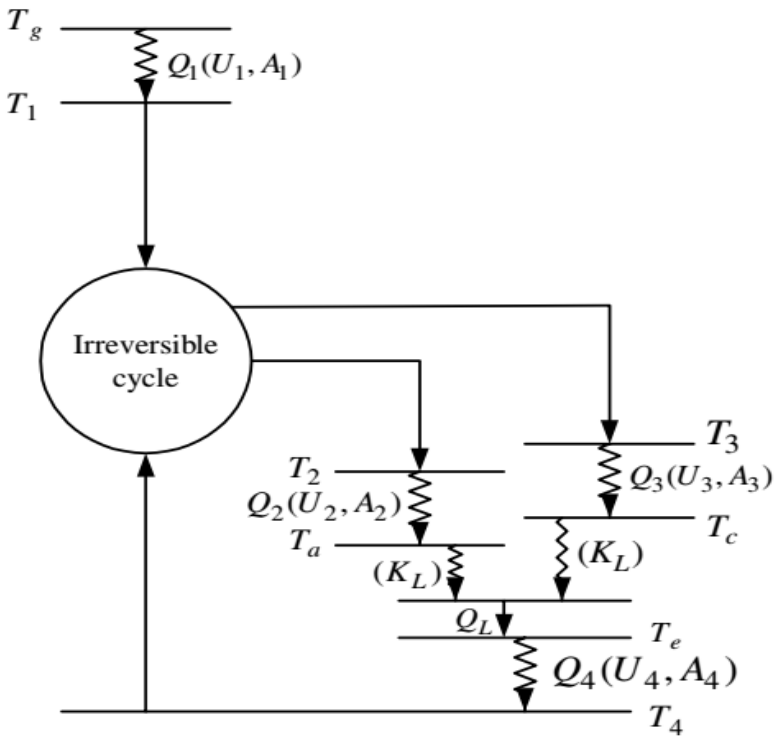

Fig. 1.24. An irreversible four-heat-reservoir absorption heat pump cycle (Chen et al., 2005a).

Fig. 1.25 explore this configuration with the characteristic curve $\pi - \psi$, taking as numerical examples $A = 5\text{m}^2$; $U_1 = U_2 = U_3 = U_4 = 0.5\,\text{kW/km}^2$; $a = 1$; $T_g = 403\text{K}$; $T_a = 313\text{K}$; $T_c = 333\text{K}$ and $T_e = 293\text{K}$. Curve 'a' represents the $\pi - \psi$ characteristics of a reversible absorption heat-pump with $K_L = 0$ and $I = 1.00$; curve 'b' represents the $\pi - \psi$ characteristics of an exoreversible absorption heat-pump with internal irreversibility where $K_L = 0$ and $I = 1.02$; curve 'c' represents the $\pi - \psi$ characteristics of an endoreversible absorption heat-pump with heat resistance and heat leak with $K_L = 0.02\,\text{kW/K}$ and $I = 1.00$; and curve 'd' represents the $\pi - \psi$ characteristics of a generalized irreversible absorption heat-pump with $K_L = 0.02\,\text{kW/K}$ and $I = 1.02$. Observations and analyzes lead to the fact that the optimal heating load decreases when the *COP* increases until reaching a certain value (case of the Curves 'c' and 'd' in **Fig. 1.25**). Also, as the heat leakage and dissipation losses increase, the maximum value of the COP decreases as long as the corresponding value of the optimal heating load increases.

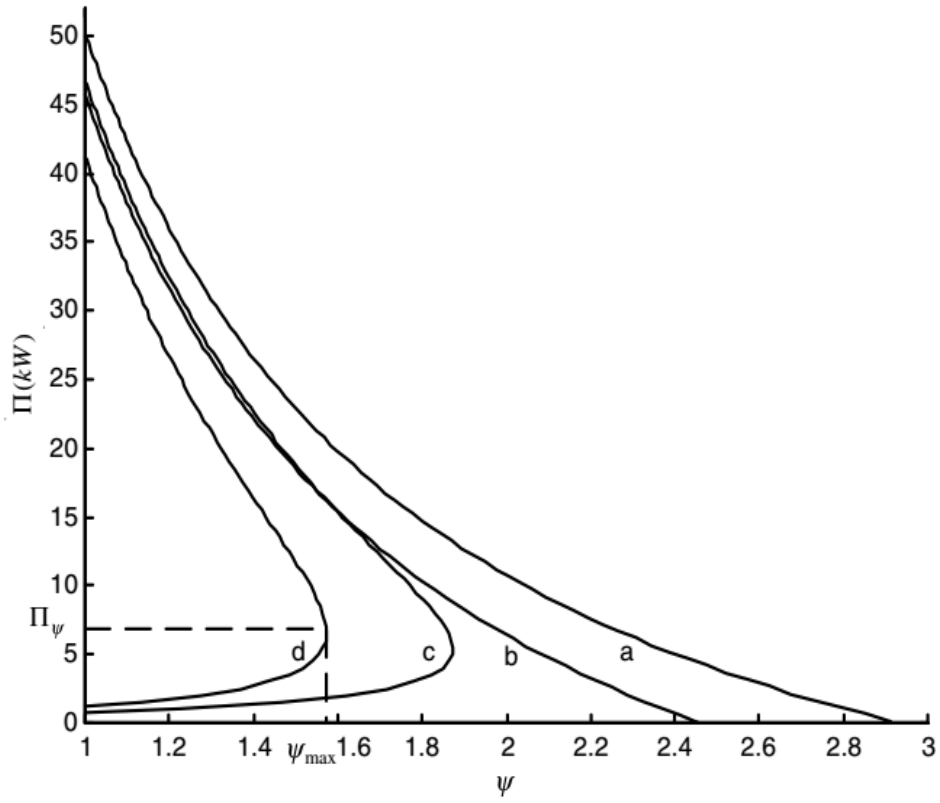

Fig. 1.25. The optimal heating load (π) versus the *COP* (ψ) (Chen et al. 2005a)

Xiling et al. (2011) unlike Chen et al. (2005a), considered heat leaks between the surroundings at temperature T_S and each heat exchanger (**Fig. 1.26**) and are given by:

$$Q_g^l = K_g^l\left(T_g^{in} - T_S\right),\ Q_a^l = K_a^l\left(T_a^{in} - T_S\right),\ Q_c^l = K_c^l\left(T_c^{in} - T_S\right) \text{ and } Q_e^l = K_e^l\left(T_S - T_e^{in}\right) \tag{1.71}$$

The inlet temperature of the heat reservoirs are T_g^{in}, T_a^{in}, T_c^{in} and T_e^{in}. The heat transfer in the generator, absorber, condenser and evaporator are

$$Q_g^{'} = C_g\varepsilon_g\left(T_g^{in} - T_g\right),\ Q_a^{'} = -C_a\varepsilon_a\left(T_a^{in} - T_a\right),\ Q_c^{'} = -C_c\varepsilon_c\left(T_c^{in} - T_c\right) \text{ and } Q_e^{'} = C_e\varepsilon_e\left(T_e^{in} - T_e\right) \tag{1.72}$$

and the efficiency of each heat exchanger, which could be written as,

$$\varepsilon_g = 1-\exp\left(\frac{-H_gF_g}{C_g}\right),\ \varepsilon_a = 1-\exp\left(\frac{-H_aF_a}{C_a}\right),\ \varepsilon_c = 1-\exp\left(\frac{-H_cF_c}{C_c}\right) \text{ and } \varepsilon_e = 1-\exp\left(\frac{-H_eF_e}{C_e}\right) \tag{1.73}$$

where K_g^l, K_a^l, K_c^l and K_e^l are the heat leak coefficient of different components; C_g, C_a, C_c and C_e are the thermal capacity (products of mass flow rate and specific heat capacity); H_g, H_a, H_c and H_e are the heat-transfer coefficient and F_g, F_a, F_c and F_e, are the heat-transfer surface areas of generator, absorber, condenser and evaporator, respectively.

They got the heat supplied by high grade heat source, Q_g, the heat supplied by absorber, Q_a, the heat supplied by condenser, Q_c, the heat supplied by low grade heat source, Q_e, yields following

$$Q_g = Q_g^{'} + Q_g^l,\ Q_a = Q_a^{'} - Q_a^l,\ Q_c = Q_c^{'} - Q_c^l \text{ and } Q_e = Q_e^{'} - Q_e^l \tag{1.74}$$

According the first and second laws of thermodynamics respectively, we have

$$Q_g^{'} + Q_e^{'} - Q_a^{'} - Q_c^{'} = 0$$

$$I_{he} = \left(Q_g^{'}/T_g\right)/\left(Q_a^{'}/T_a\right)\ \left(0 < I_{he} \le 1\right)$$

$$I_{re} = \left(Q_e^{'}/T_e\right)/\left(Q_c^{'}/T_c\right)\ \left(0 < I_{re} \le 1\right) \tag{1.75}$$

The heating ability and the coefficient of performance of AHP are defined as

$$R = Q_a + Q_c \text{ and } COP = \left(Q_a + Q_c\right)/Q_g \tag{1.76}$$

According to **Eqs. (1.72), (1.74)-(1.76)**, the temperature of working substance to generator and evaporator could be given by

$$T_g = T_g^{in} - \frac{\left(\frac{R}{COP} - Q_g^l\right)}{C_g\varepsilon_g}$$

$$T_e = T_e^{in} - \frac{\left(\left(1-\frac{1}{COP}\right)R + Q_{acg}^l\right)}{C_e\varepsilon_e}$$

$$T_a = T_a^{in}\frac{\left(C_g\varepsilon_g T_g^{in} - \left(\frac{R}{COP} - Q_g^l\right)\right)}{\left(C_g\varepsilon_g T_g^{in} - \left(1+\frac{C_g\varepsilon_g}{C_a\varepsilon_a I_{he}}\right)\left(\frac{R}{COP} - Q_g^l\right)\right)}$$

$$T_c = T_c^{in}\frac{\left(C_e\varepsilon_e T_e^{in} - \left(\left(1-\frac{1}{COP}\right)R + Q_{acg}^l\right)\right)}{\left(C_e\varepsilon_e T_e^{in} - \left(1+\frac{C_e\varepsilon_e}{C_c\varepsilon_c I_{re}}\right)\left(\left(1-\frac{1}{COP}\right)R + Q_{acg}^l\right)\right)} \tag{1.77}$$

Using **Eqs. (1.72) and (1.77)**, the base correlation of AHP could be given,

$$\frac{T_c^{in}\left(\left(1-\frac{1}{COP}\right)R + Q_{acg}^l\right)}{\left(I_{he}T_e^{in} - \left(\left(1-\frac{1}{COP}\right)R + Q_{acg}^l\right)\left(\frac{I_{re}}{C_e\varepsilon_e} + \frac{1}{C_c\varepsilon_c}\right)\right)\left(R + Q_{acg}^l\right)} + \frac{T_a^{in}\left(\frac{R}{COP} - Q_g^l\right)}{\left(I_{he}T_g^{in} - \left(\frac{R}{COP} - Q_g^l\right)\left(\frac{I_{he}}{C_g\varepsilon_g} + \frac{1}{C_a\varepsilon_a}\right)\right)\left(R + Q_{ac}^l\right)} = 1 \tag{1.78}$$

where, $Q_{ac}^l = Q_a^l + Q_c^l$ and $Q_{acg}^l = Q_a^l + Q_c^l + Q_g^l$.

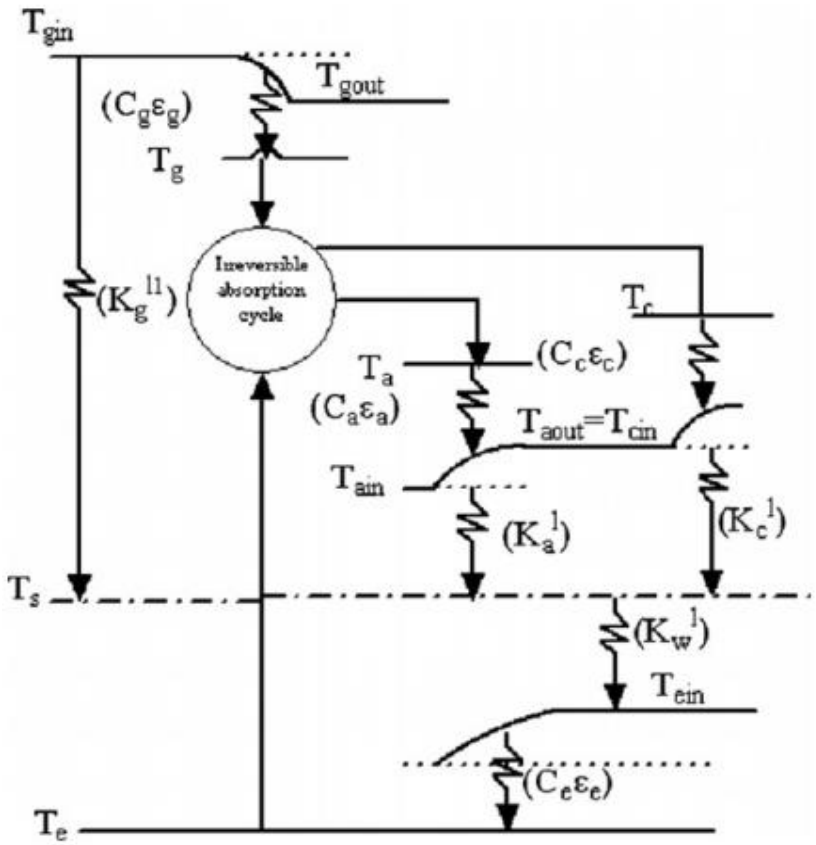

Fig. 1.26. Another irreversible FTL AHP model (Xiling et al., 2011).

The performance of AHP cycle could be analyzed by the physical model, the parameters are given as, $T_a^{in}=313\text{K}$; $T_c^{in}=316\text{K}$; $T_e^{in}=294\text{K}$; $T_g^{in}=803\text{K}$; $T_s=341\text{K}$; $C_g=5.544\,\text{kW/K}$; $C_a=C_c=18.6\,\text{kW/K}$; $C_e=11.6\,\text{kW/K}$; $K_g^l=0.02\text{kW/K}$; $K_a^l=0.05\text{kW/K}$; $K_c^l=K_e^l=0.04\text{kW/K}$; $H_g=0.06\text{kW}\left(\text{m}^2\text{K}\right)^{-1}$; $H_a=1.1\text{kW}\left(\text{m}^2\text{K}\right)^{-1}$; $H_c=5.5\text{kW}\left(\text{m}^2\text{K}\right)^{-1}$; $H_e=3.8\text{kW}\left(\text{m}^2\text{K}\right)^{-1}$; $I_{he}=0.9$; $I_{re}=0.9$; $F_g=34\text{m}^2$; $F_a=4.97\text{m}^2$; $F_c=0.74\text{m}^2$ and $F_e=1.25\text{m}^2$, the main results of which are noted in **Figs. 1.27-1.29**.

From **Fig. 1.27**, they showed on the one hand that the curves of the rate of heat transfer in the generator and the heating load decrease when the *COP* increases, until reaching a certain value corresponding to the maximum value of the *COP* $\left(COP_{\max}\right)$. On the other hand, they showed that the curve of the rate of heat transfer in the evaporator is a semi-parabola whose value corresponds to the maximum value of the *COP* $\left(COP_{\max}\right)$ and the maximum of the semi-parabola corresponds to the minimum value of the *COP* $\left(COP_{\min}\right)$. They have therefore obtained a region whose performance criteria are extreme. However, they showed in the curves of **Figs. 1.27 and 1.28**, the effects of internal and external irreversibilities respectively. The interpretation concedes to us that the internal dissipations resulting in the internal irreversibility factors I_{re} and I_{he} have more harmful impact in the evaporator-condenser assembly than in the generator-absorber assembly (**Fig. 1.27**) In addition, heat leaks (external irreversibilities) are greater in the generator than in the other components.

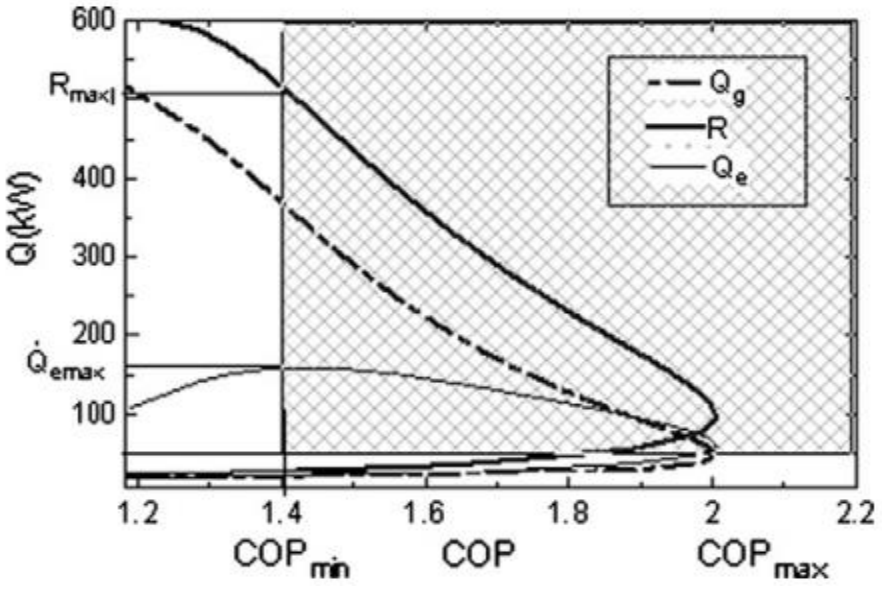

Fig. 1.27. *COP* with respect to the generator and evaporator heating rate of AHP cycle (Xiling et al., 2011).

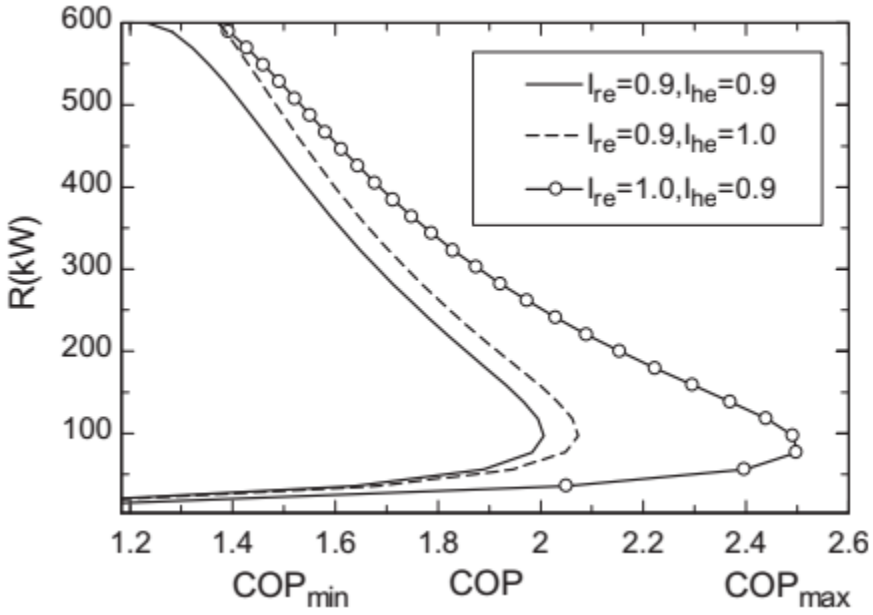

Fig. 1.28. Comparable of internal irreversibilities effects on the performance AHP cycle (Xiling et al., 2011).

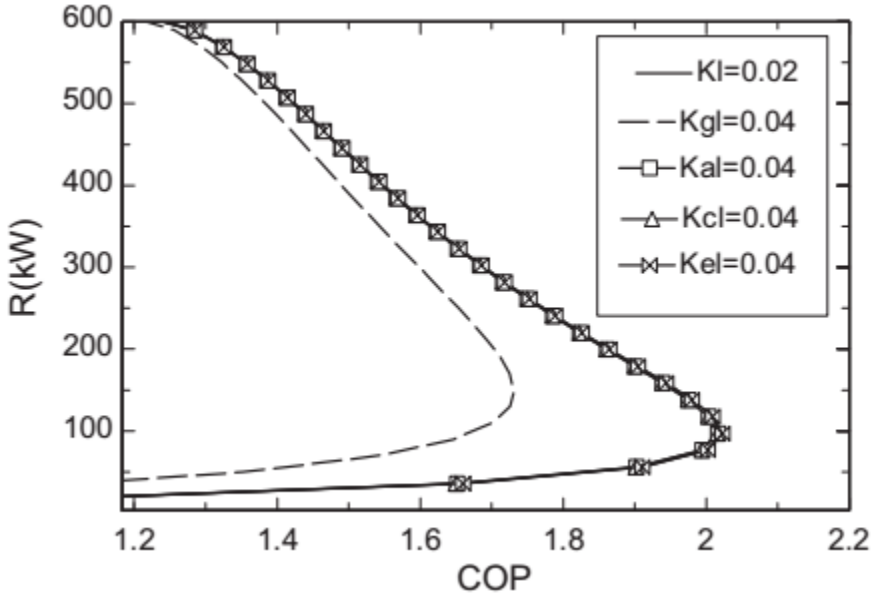

Fig. 1.29. Effects of heat leaks on the performance of AHP cycle (Xiling et al., 2011).

Besides, Qin et al. (2015) rather considered a variable-temperature heat reservoir AHP cycle, in which internal working substance is working in four temperature levels and all irreversibility factors are considered (**Fig. 1.31**).

However, the second law of thermodynamics taking into account an overall irreversibility gives:

$$I=\left(Q_a^{'}/T_a^{'}+Q_c^{'}/T_c^{'}\right)/\left(Q_g^{'}/T_g^{'}\,Q_e^{'}/T_e^{'}\right) \qquad \left(I\geq 1\right) \tag{1.79}$$

Substituting **Eqs. (1.72)** and **(1.77)** into **Eq. (1.79)** yields

$$\left(\frac{T_g^{in}}{\pi-K_g^l\left(T_g^{in}-T_s\right)\psi}-\frac{1}{C_gE_g\psi}\right)^{-1}+\left(\frac{T_e^{in}}{\left(\pi+K_a^l\left(T_a^{in}-T_s\right)+K_c^l\left(T_c^{in}-T_s\right)+K_g^l\left(T_g^{in}-T_s\right)\right)\psi-\pi}-\frac{1}{C_eE_e\psi}\right)^{-1}-$$
$$\frac{\psi}{I}\left(\left(\frac{T_a^{in}}{(1-a)\left(\pi+K_a^l\left(T_a^{in}-T_s\right)+K_c^l\left(T_c^{in}-T_s\right)\right)}+\frac{1}{C_aE_a}\right)^{-1}+\left(\frac{T_c^{in}}{a\left(\pi+K_a^l\left(T_a^{in}-T_s\right)+K_c^l\left(T_c^{in}-T_s\right)\right)}+\frac{1}{C_cE_c}\right)^{-1}\right)=0 \quad (1.80)$$

where, $a=Q_c^{'}/\left(Q_a^{'}+Q_c^{'}\right)$; $E_g=1-\exp\left(\frac{-U_gA_g}{C_g}\right)$; $E_a=1-\exp\left(\frac{-U_aA_a}{C_a}\right)$; $E_c=1-\exp\left(\frac{-U_cA_c}{C_c}\right)$ and $E_e=1-\exp\left(\frac{-U_eA_e}{C_e}\right)$.

They obtained a general equation **(Eq. 1.80)** including the *COP*, the heating load and some key irreversibility parameters of variable-temperature heat reservoir irreversible AHP coupled to a FTL cycle. This equation may be used directly to analyze the general characteristic and the effect of key irreversibility parameters on cycle characteristic of a practical AHP.

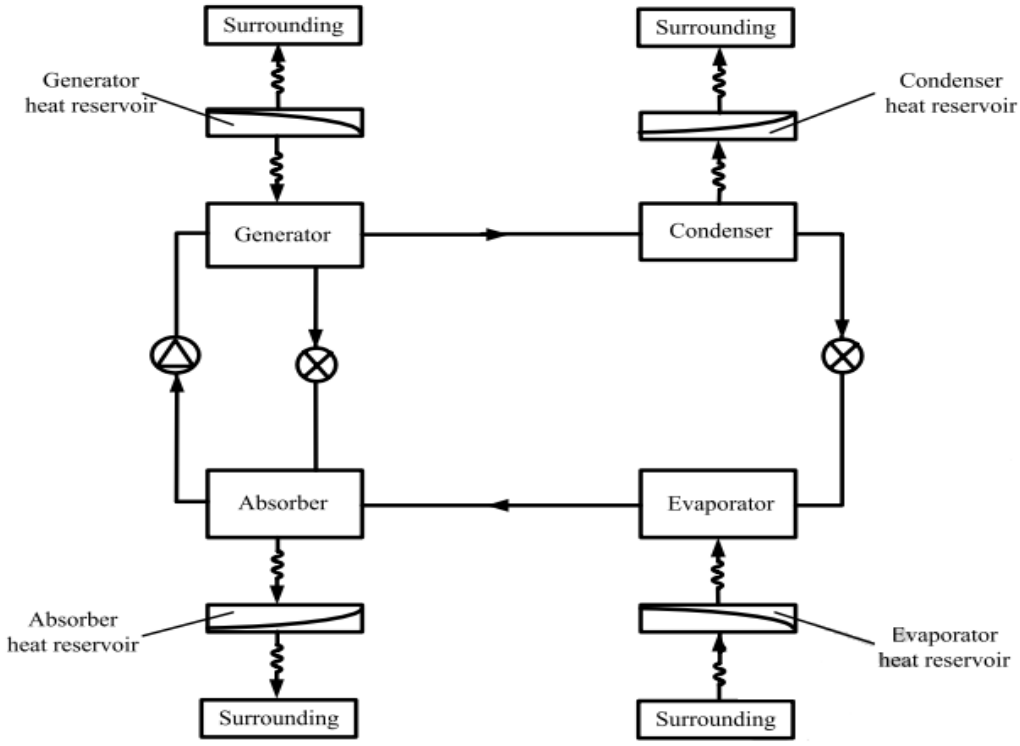

Fig. 1.30. Symbolic diagram of A variable-temperature heat reservoir irreversible AHP (Qin et al., 2015).

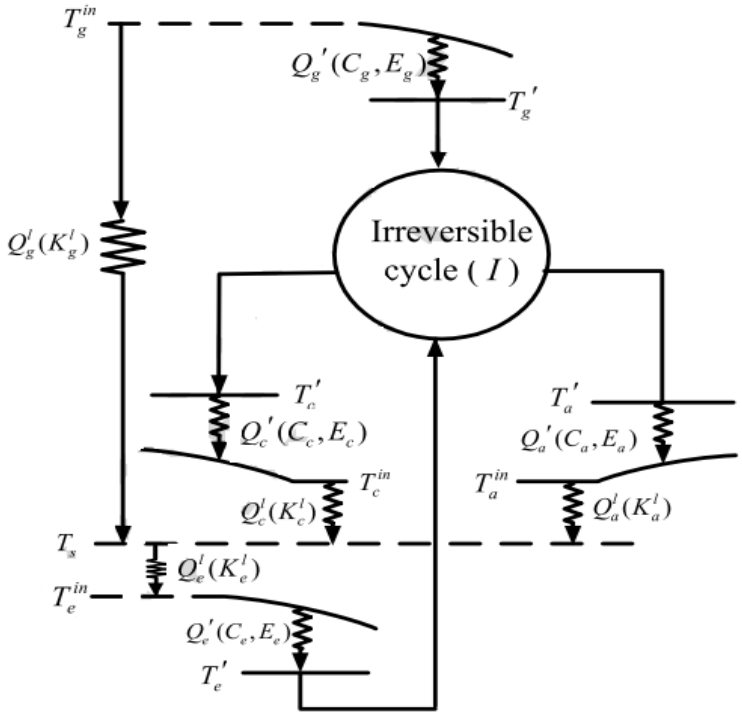

Fig. 1.31. A variable-temperature heat reservoir irreversible AHP model (Qin et al., 2015).

To analyze the performance of AHP, they assumed that $a = 0.45$, $T_a^{in} = 325\text{K}$, $T_c^{in} = 330\text{K}$, $T_e^{in} = 300\text{K}$, $T_g^{in} = 380\text{K}$, $T_s = 300\text{K}$, $C_a = C_c = C_e = C_g = 50.0\text{kWK}^{-1}$, $E_a = E_c = E_e = 0.6321$, $E_g = 0.6321$, $U_a = U_g = 0.5\text{kWm}^{-2}\text{K}^{-1}$, $U_c = U_e = 1.0\text{kWm}^{-2}\text{K}^{-1}$ and $A_a = A_c = A_e = A_g = 100\text{m}^2$, and obtained the characteristic curves among the heating load, the *COP* and some key irreversibility parameters shown in **Fig. 1.32**. When heat leakages and internal irreversibility are ignored, the characteristic is curve 1 in **Fig. 1.32**. When heat leakages are ignored, the characteristic is curve 2 in **Fig. 1.32**. When internal irreversibility is ignored, the characteristic is curve 3 in **Fig. 1.32**. When internal irreversibility and heat leakages with different values are considered, the characteristics are curves 4–6 in **Fig. 1.32**. We can see that the optimal heating load decreases when the *COP* increases until reaching a certain value (case of the Curves 4-6 in **Fig. 1.32**). Also, as the heat leakage and dissipation losses increase, the maximum value of the COP decreases as long as the corresponding value of the optimal heating load increases (**Fig. 1.33**).

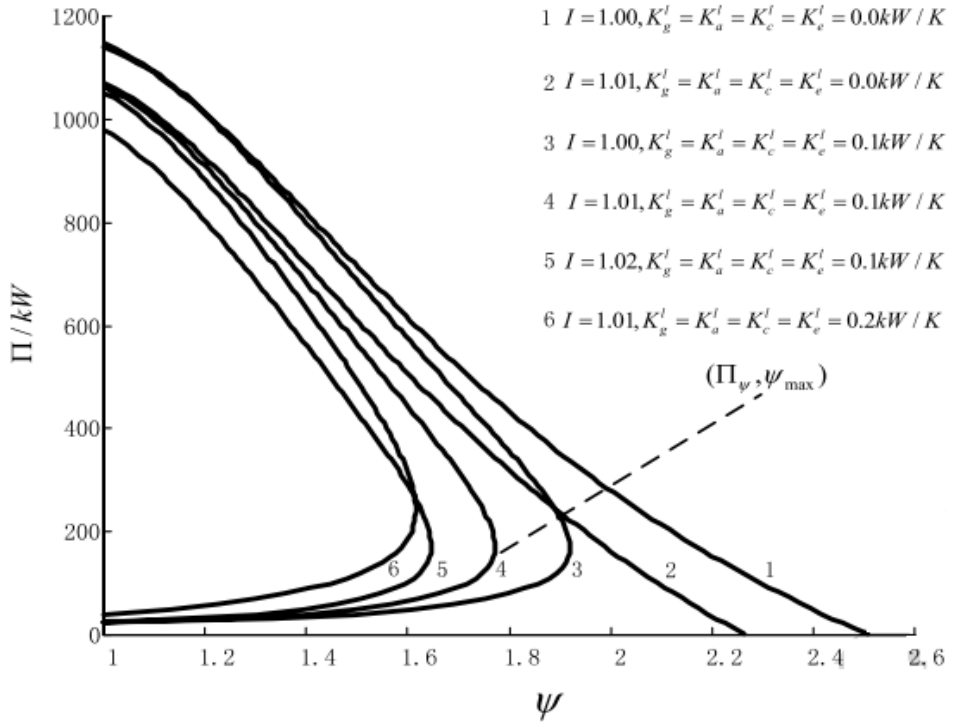

Fig. 1.32. The heating load, the *COP* and key irreversibility parameters characteristic curves (Qin et al., 2015).

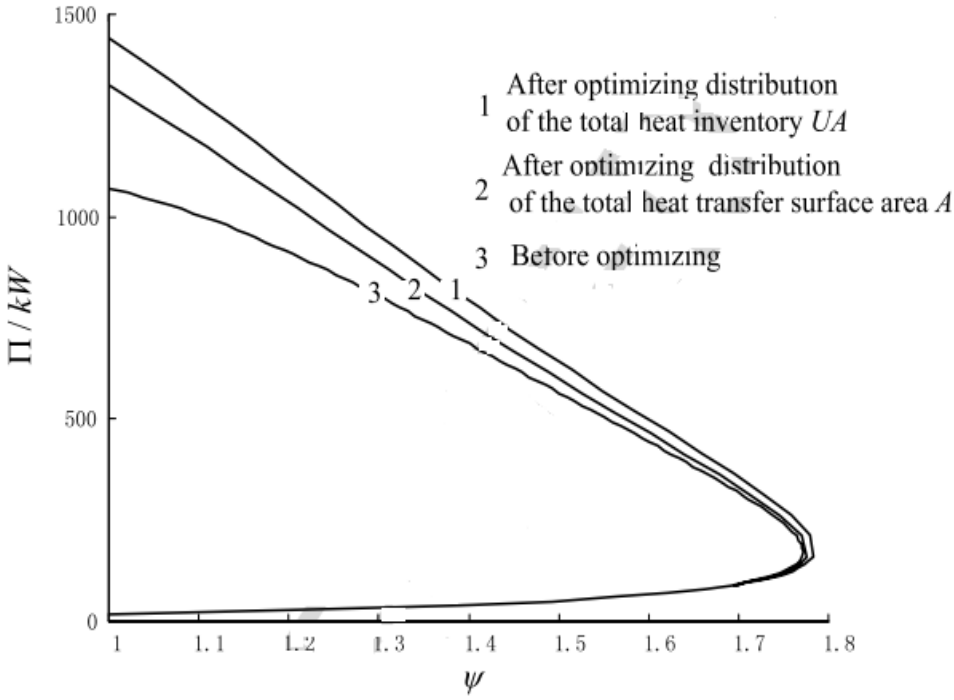

Fig. 1.33. Characteristic curves before and after optimizing *A* and *UA* (Qin et al., 2015).

1.3.2. Optimization by using coefficient of performance and cooling load criteria

Bhardwaj et al. (2003, 2005), Zheng et al. (2004), Chen et al. (2005b, 2006), Qin et al. (2010) and Kaushik et al. (2018) on AR, used the cooling load and the *COP* as decisive functions.

1.4. Analysis by thermo-economic criterion

The economic aspect is an important criterion for evaluating the performance of heat transformation and energy conversion devices. Better yet, it involves investment cost, energy consumed cost, maintenance cost and even the energy loss cost. This is why this criterion is used previously by scientists to analyze and optimize systems with thermodynamic processes such as compression and absorption refrigerators and heat pumps as well as in heat engines. However, Kodal et al. (2000a, 2000b, 2002, 2003a) are among the first to develop this approach on two-stage endoreversible HPs with two heat sources and HPs, on irreversible refrigerators with two heat sources and irreversible ARs and AHPs, respectively. They are followed by Silveira and Tuna (2003, 2004) on combined heat and power systems.

1.4.1. Thermo-economic approach on heat engine

Kodal and Sahin (2003b) and Chen et al (2005c) studied the thermoeconomics of irreversible heat engines and endoreversible heat engines on the basis of the linear phenomenological heat transfer law, respectively. Also, Sadatsakkak et al. (2015), worked on the irreversible regenerative cycles of closed Brayton with the thermo-economic function ($F = P/\left(C_i + C_f + C_{env} + C_{com}\right)$, with C_i, C_f, C_{env} and C_{com} are the investment cost, fuel cost, environmental cost and operation and maintenance cost, respectively. While Kaushik et al. (2016) worked on irreversible regenerative Brayton's cycles using the thermo-economic criterion ($F = P/(C_i + C_e + C_{cm})$, where C_i, C_e and C_{cm} are the annual investment cost, energy consumption cost and maintenance cost, respectively) described as the ratio of output power per unit of the sum of annual investment, energy consumption and maintenance cost. However, they considered the finite heat capacities, the external irreversibilities due to the finite temperature differences and the internal irreversibilities due to friction losses of the fluid in the compressor/turbine assembly, as well as regenerative heat losses and pressure drops. They were able to defend the hypothesis that the efficiency of the turbine has more effects on the performance of the model compared to the performance of the compressor under such conditions. Nevertheless, Ozel et al. (2016) carried out a comparative study between different thermo-economic criteria on the irreversible Carnot heat engine. There is the thermo-economic function ($F = \dot{W}/\left(C_1 m + C_2 \dot{Q}_H + C_3 \dot{E}X_D + C_4 \dot{W}\right)$, where $C_4 = C_5 + C_6$), the ecological-based thermoeconomic function ($F_E = E/\left(C_1 m + C_2 \dot{Q}_H + C_3 \dot{E}X_D + C_4 \dot{W}\right)$), the ecologico-economical function ($F_{EC} = C_5 \dot{W} - C_3 \dot{E}X_D$) and the exergoeconomic function ($F_{FTE} = C_7 \dot{W}_R - C_5 \dot{W}$, where C_1, C_2, C_3, C_4

, C_5, C_6 and C_7 are capital cost, fuel cost, environmental cost, sum capital recovery multiplied to the investment cost per unit power output, operation and maintenance cost and cost of reversible power output in ($ncu.kW^{-1}$), respectively). They were able to develop the fact that the ecological-based thermoeconomic function has better advantages in terms of exergy destruction rate and energy efficiency. Also, it is more advantageous in terms of output work.

1.4.2. Thermo-economic approach on refrigerators and heat pump

Kodal et al. (2000a) carried out their investigations on endoreversible two-stage HP with two heat sources, based on thermo-economic optimization. They maximized the thermo-economic criterion under the influence of design parameters such as economic and technical parameters. In fact, they obtained the corresponding optimum performance quantities such as the temperatures of the working fluid, the coefficient of performance, the heating load and the surface areas of the heat exchange. However, Kodal et al. (2000b) considered the influence of internal and external irreversibilities on heat pumps and refrigerators with two heat sources. They have shown that the optimal design parameters are obtained for a minimum of the total cost per unit of heating load or cooling load; this led Kodal et al. (2003a) to analyze the thermo-economic aspect on ARs and AHPs, and Durmayaz et al. (2004) to provide a review on irreversible and endoreversible thermal systems based on the thermo-economic criterion. Then, Misra et al. (2003, 2005, 2006) on single-effect, double-effect H_2O/LiBr and H_2O/NH_3 vapour-absorption refrigeration systems, respectively, Qin et al. (2005) on endoreversible ARs and Wu et al. (2005) on irreversible AHP. Zare et al. (2012) and Ahmadi et al. (2014a) conducting a thermo-economic and exergy study on an ammonia-water power/cooling cogeneration cycle and on irreversible four-temperature-level absorption refrigeration using the evolutionary genetic algorithm. Qureshi and Syed (2015) analyzed irreversible refrigeration and heat pump cycles with allocation of stocks of heat exchangers with finite heat capacities. They noted that it is preferable to measure the effects of internal dissipation by deriving exact mathematical expressions as the effect on some performance parameters could be lost due to the averaging effect of the internal irreversibility parameter. Furthermore, Xu et al. (2016) provided a theoretical overview of the optimal design of Ericsson magnetic refrigerator cycles. However, the thermo-economic function was obtained as a function of the high and low temperatures of the working fluid in the heat reservoirs with two isothermal processes and its maximum corresponding to an extremal cooling load for an appropriate high value of the temperature in the two isothermal processes. Xu (2016) studied the irreversible Stirling HP by considering the investment cost and the energy consumed cost in order to obtain more realistic results on the operating cost of such a device ($F = R_H/(C_i + C_e)$, where R_H is the heating

load, C_i the annual investment cost, $C_i = a_1(A_H + A_L)$ in $(\text{ncu.year}^{-1}.\text{m}^{-2})$ and C_e the energy consumption cost, $C_e = bP$ in $(\text{ncu.year}^{-1}.\text{kW}^{-1})$).

In **Fig. 1.34** (Kodal et al., 2003a), the liquid rich solution at state 1 is pressurized to state 1' with a pump. In the generator, the working fluid is concentrated to state 3 by evaporating the working medium by means of $\dot{Q}_H$ heat rate input. The weak solution at state 2 passes through the expansion valve into the absorber with a pressure reduction (2–2'). In the condenser, the working fluid at state 3 is condensed to state 4 by removing $\dot{Q}_C$ heat rate. The condensed working fluid at state 4 is then throttled by a valve and enters the evaporator at state 4'. The liquid working fluid is evaporated due to heat transfer rate $\dot{Q}_L$ from the cooling space to the working fluid (4'–5). Finally, the vaporized working fluid is absorbed by the weak solution in the absorber, and by means of $\dot{Q}_A$ heat rate release in the absorber, state 1 is reached.

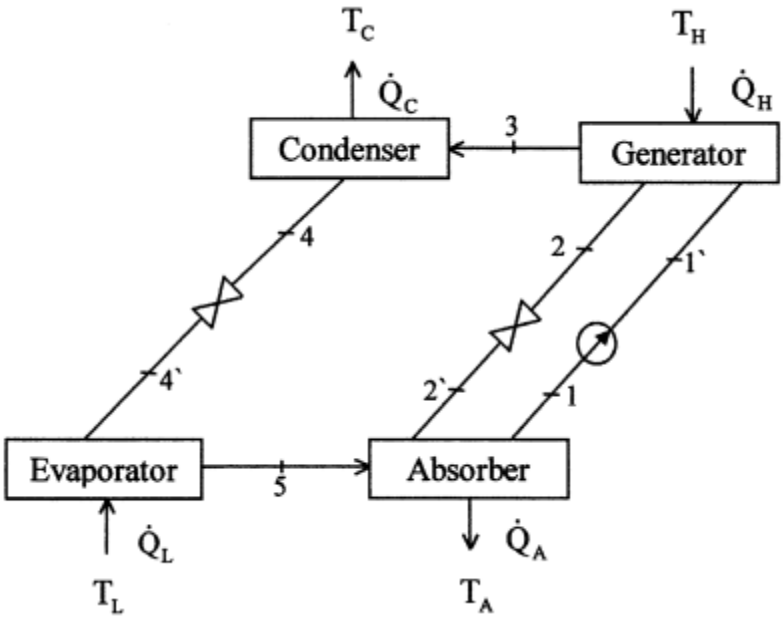

Fig. 1.34. Schematic diagram of AHP system (Kodal et al., 2003a).

However, the heat exchanges between the working fluid and heat reservoirs obeys a linear law so that one has

$\dot{Q}_L = U_L A_L (T_L - T_Y)$, $\dot{Q}_H = U_H A_H (T_H - T_X)$ and $\dot{Q}_K = U_K A_K (T_Z - T_K)$ with $\dot{Q}_K = \dot{Q}_A + \dot{Q}_C$ and

$T_K = T_A = T_C$ (1.81)

where U_L, U_H and U_K are, respectively, the heat transfer coefficients between the working fluid in $\left(\mathrm{kWm^{-2}K^{-1}}\right)$ and the heat reservoirs at temperatures T_L, T_H and T_K in (K), and A_L, A_H, and A_K are the corresponding heat transfer areas $\left(\mathrm{m^2}\right)$.

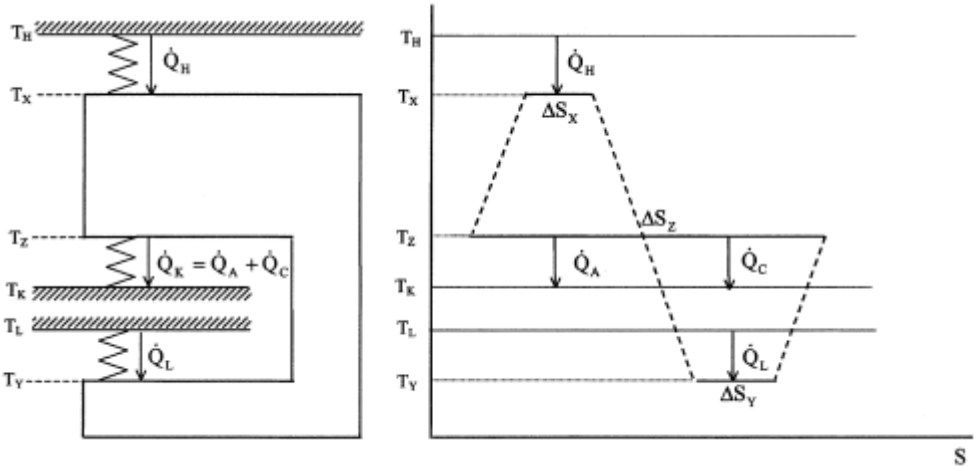

Fig. 1.35. Considered irreversible AHP model and its *T*-*s* diagram (Kodal et al., 2003a).

Also, the first law of thermodynamics deduced from **Fig. 1.35** and the second law of thermodynamics due to the external irreversibilities arise from the temperature differences between the working fluid and the heat sources, on the other hand, the internal irreversibilities result from friction, mass transfer and other working fluid dissipation requires

$$\dot{Q}_H+\dot{Q}_L-\dot{Q}_K=0 \tag{1.82}$$

$$\frac{\dot{Q}_K}{T_Z}-\frac{\dot{Q}_H}{T_X}-\frac{\dot{Q}_L}{T_Y}\geq 0 \tag{1.83}$$

Eq. (1.83) becomes, $\dfrac{\dot{Q}_K}{T_Z}-I\left(\dfrac{\dot{Q}_H}{T_X}+\dfrac{\dot{Q}_L}{T_Y}\right)=0$ because $I=\dfrac{\Delta S_Z}{\Delta S_X+\Delta S_Y}=\dfrac{\dot{Q}_K/T_Z}{\dot{Q}_H/T_X+\dot{Q}_L/T_Y}$ (1.84)

$\Delta S_Z > \Delta S_X + \Delta S_Y$ for an internally irreversible cycle, so that $I > 1$. If the internal irreversibility can be neglected, the cycle is endoreversible and so $I=1$.

From **Eqs. (1.81)–(1.84)**, they obtained the coefficient of performance (ε_{hp}) and the specific heating load ($\dot{q}_K$) of the absorption refrigerator cycle, respectively, as

$$\varepsilon_{hp}=\frac{\dot{Q}_K}{\dot{Q}_H}=\frac{IT_Z\left(T_Y-T_X\right)}{T_X\left(T_Y-IT_Z\right)} \tag{1.85}$$

$$\dot{q}_K=\frac{\dot{Q}_K}{A}=\left(\frac{T_X\left(IT_Z-T_Y\right)}{U_H\left(T_H-T_X\right)IT_Z\left(T_X-T_Y\right)}+\frac{1}{U_K\left(T_Z-T_K\right)}+\frac{T_Y\left(IT_Z-T_X\right)}{U_L\left(T_L-T_Y\right)IT_Z\left(T_Y-T_X\right)}\right)^{-1} \tag{1.86}$$

The thermo-economic objective function to be optimized for the heat pump is defined as the heating load per unit total cost, i.e.

$$F_{hp} = \dot{Q}_K \Big/ \left(C_i + C_e\right) = \dot{Q}_K \Big/ \left(a\left(A_H + A_L + A_K\right) + b\dot{Q}_H \right) \tag{1.87}$$

Using **Eqs. (1.81)–(1.84)**, in **Eq. (1.87)**

$$bF_{hp} = \frac{1}{\dfrac{T_X\left(T_Y - IT_Z\right)}{IT_Z\left(T_Y - T_X\right)}\left(1 + \dfrac{k}{U_H\left(T_H - T_X\right)}\right) + \dfrac{kT_Y\left(IT_Z - T_X\right)}{U_L\left(T_L - T_Y\right)IT_Z\left(T_Y - T_X\right)} + \dfrac{k}{U_k\left(T_Z - T_K\right)}} \tag{1.88}$$

where $k = a/b$ is the economical parameter.

By maximizing the thermo-economic objective function, they obtained the variations of this function with respect to the COP (ε_{hp}) and heating load rate, respectively under the influences of internal and external irreversibilities, respectively in order to obtain the optimal operating points (**Fig. 1.36** and **Fig. 1.37**).

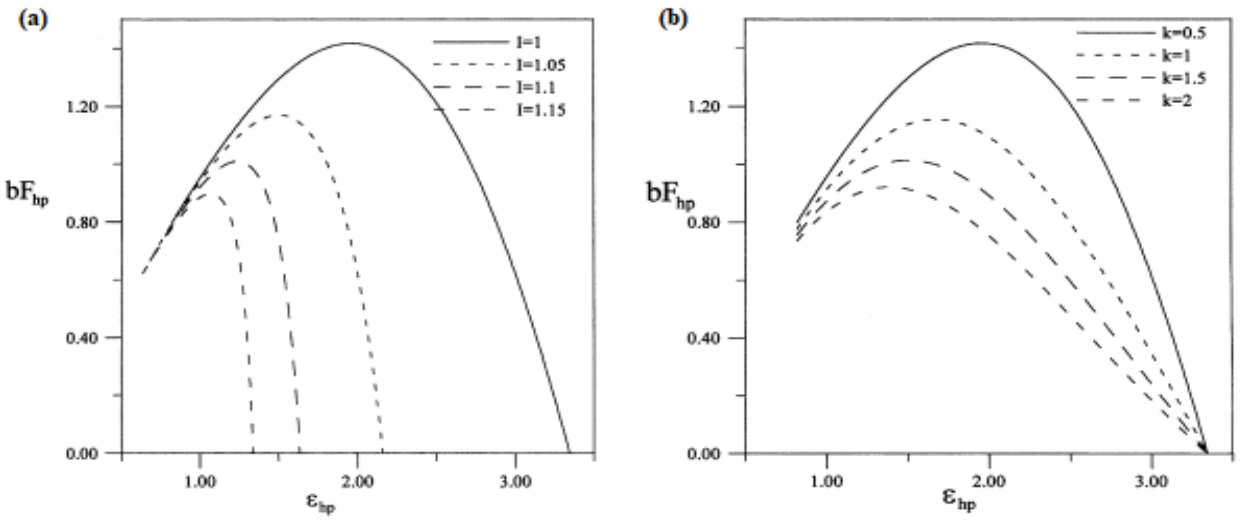

Fig. 1.36. Variations of the objective function for the heat pump with respect to the coefficient of performance, for various I values ($k = 0.5$) **(a)** and for various k values ($I = 1$) **(b)** ($T_H = 393\text{K}$, $T_L = 288\text{K}$, $T_K = 313\text{K}$, $U_H = U_L = U_K = 0.5\,\text{kWm}^{-2}\text{K}^{-1}$ (Kodal et al., 2003a).

As the internal irreversibility and the economical parameters increase the $F_{hp} \sim \varepsilon_{hp}$ characteristics and the optimal performance coefficient reduce significantly for the AHP. In addition, when $\varepsilon = \varepsilon_{\max}$, the objective function of the heat pump (F_{hp}) becomes zero, as shown in **Fig. 1.36**. It is also seen from **Fig. 1.36(a)** that very large differences exist between the optimal performance coefficient and the maximum performance coefficient. However, this difference reduces with

increased internal irreversibility but increases with increased economical parameter (**Fig. (1.36(a) and 1.36(b)**).

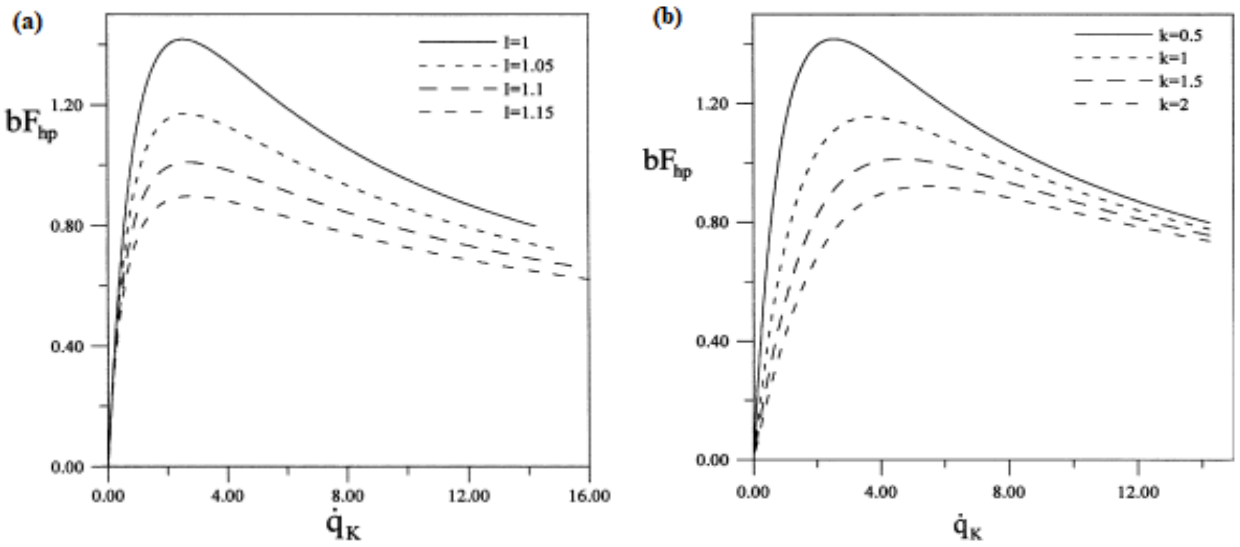

Fig. 1.37. Variations of the objective function for the heat pump with respect to the specific heating load, for various I values ($k = 0.5$) **(a)** and for various k values ($I = 1$) **(b)** ($T_H = 393\,\mathrm{K}$, $T_L = 288\,\mathrm{K}$, $T_K = 313\,\mathrm{K}$, $U_H = U_L = U_K = 0.5\,\mathrm{kWm^{-2}K^{-1}}$ (Kodal et al., 2003a).

Then, in **Fig. 1.37(a)** the maximum operating point of the thermo-economic objective function decreases as the corresponding optimal specific heating load decreases for increased values of internal irreversibility. Whereas, In **Fig. 1.37(b)** the maximum operating point of the thermo-economic objective function decreases as the corresponding optimal specific heating load increases for increased values of economic parameter.

In contrast, Wu et al. (2005) in addition to having considered three heat reservoirs, each heat exchanger experiences heat leakages as shown in **Fig. 1.38** ($\dot{Q}_H = \dot{Q}_1 + \dot{Q}_L$ and $\dot{Q}_C = \dot{Q}_3 - \dot{Q}_L$).

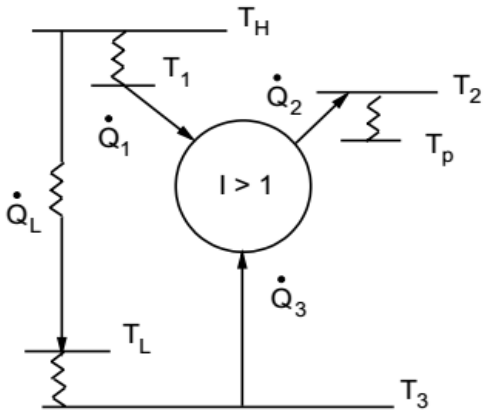

Fig. 1.38. The schematic diagram of an irreversible three-heat-source heat pump (Wu et al., 2005).

In this figure, the first law of thermodynamics gives

$$\dot{Q}_1 - \dot{Q}_2 + \dot{Q}_3 = 0 \tag{1.89}$$

Also, the law of heat transfer being considered linear, so

$$\dot{Q}_1 = U_1 A_1 (T_H - T_1);\ \dot{Q}_2 = U_2 A_2 (T_2 - T_P);\ \dot{Q}_3 = U_3 A_3 (T_L - T_3) \text{ and } \dot{Q}_L = \gamma (T_H - T_L) \tag{1.90}$$

where U_1, U_2, U_3 and A_1, A_2, A_3 are, respectively, the heat transfer coefficients and areas between the working fluid in $\left(\mathrm{kWm^{-2}K^{-1}}\right)$ and in $\left(\mathrm{m^2}\right)$, respectively, and the three external heat reservoirs at temperatures T_H, T_P and T_L in (K), and γ is the heat leak coefficient between the source at temperature T_H and sink at temperature T_L.

Besides the irreversibilities of finite-rate heat transfer and heat loss between the heat source and the heat sink, the internal dissipation resulting from the friction, eddy flow and other irreversible effects inside the cyclic working fluid is also one of the main irreversibilities of the heat pump. According to the second law of thermodynamics, we may introduce an irreversibility factor

$$I = \frac{\Delta S_2}{\Delta S_1 + \Delta S_3} = \frac{\dot{Q}_2 / T_2}{\dot{Q}_1 / T_1 + \dot{Q}_3 / T_3} \geq 1 \tag{1.91}$$

From the above equations they defined the coefficient of performance and specific heating load (**Eqs. 1.92** and **1.93,** respectively)

$$\psi = \frac{\dot{Q}_2}{\dot{Q}_H} = \frac{\dot{Q}_2}{\dot{Q}_1 + \dot{Q}_L} = \left(\frac{T_1 (IT_2 - T_3)}{IT_2 (T_1 - T_3)} \left(1 + \frac{C}{U_1 (T_H - T_1)} \right) + \frac{C}{U_2 (T_2 - T_P)} + \frac{C T_3 (T_1 - IT_2)}{U_3 IT_2 (T_L - T_3) IT_Z (T_1 - T_3)} \right)^{-1} \tag{1.92}$$

$$q_2 = \frac{\dot{Q}_2}{A} = \frac{\dot{Q}_2}{A_1 + A_2 + A_3} = \left(\frac{T_1 (IT_2 - T_3)}{IT_2 (T_1 - T_3) U_1 (T_H - T_1)} + \frac{1}{U_2 (T_2 - T_P)} + \frac{T_3 (T_1 - IT_2)}{U_3 IT_2 (T_L - T_3)(T_1 - T_3)} \right)^{-1} \tag{1.93}$$

where A is the total heat transfer area of the three heat exchangers in the cycle, and $C = \gamma (T_H - T_L)/A$. They thus introduced the thermo-economic objective function

$$F = \dot{Q}_2 / \left(C_i + C_e + C_y \right) = \dot{Q}_2 / \left(aA + b\dot{Q}_H + C_y \right) = \dot{Q}_2 / \left(a(A_1 + A_2 + A_3) + b\left(\dot{Q}_1 + \dot{Q}_L \right) + C_y \right)$$

(1.94)

where C_i and C_e refer to the average investment and energy consumption costs per unit time, respectively, C_y is the average maintenance cost per unit time and considered to be a constant for a given heat pump, a is the proportionality coefficient for the average investment cost of the system and is equal to the average investment cost per unit heat transfer area per unit time, and b is the proportionality coefficient and is equal to the price per unit energy.

Using **Eqs. (1.89)–(1.91)**, in **Eq. (1.94),** they obtained

$$bF=\left(\frac{T_1(IT_2-T_3)}{IT_2(T_1-T_3)}\left(1+\frac{B}{U_1(T_H-T_1)}\right)+\frac{B}{U_2(T_2-T_P)}+\frac{BT_3(T_1-IT_2)}{U_3IT_2(T_L-T_3)(T_1-T_3)}\right)^{-1} \tag{1.95}$$

where $B=C+k+C_Y/(bA)$ and $k=a/b$.

To determine the maximum thermo-economic objective function for a given specific heat load, they introduced the Lagrangian

$$L=bF+\lambda q_2 \tag{1.96}$$

where λ is the Lagrange multiplier. From the Euler-Lagrange equations

From the Euler-Lagrange equations, an important relationship with respect to the temperatures of the working fluid in the three isothermal processes is obtained

$$\partial L/\partial T_i=0 \quad (i=1,2,3) \;\Rightarrow\; \frac{T_1}{T_H-T_1}=\frac{T_2}{R_2(T_2-T_P)}=\frac{T_3}{R_1(T_L-T_3)} \tag{1.97}$$

where $R_1=\sqrt{U_3/U_1}$ and $R_2=\sqrt{U_2/(IU_1)}$.

By introducing **Eq. (1.97)** in the **Eqs. (1.92, 1.93 and 1.95)**, they easily generated the general performance characteristics curves of an irreversible heat pump as shown in **Figs. 1.39 and 1.40**.

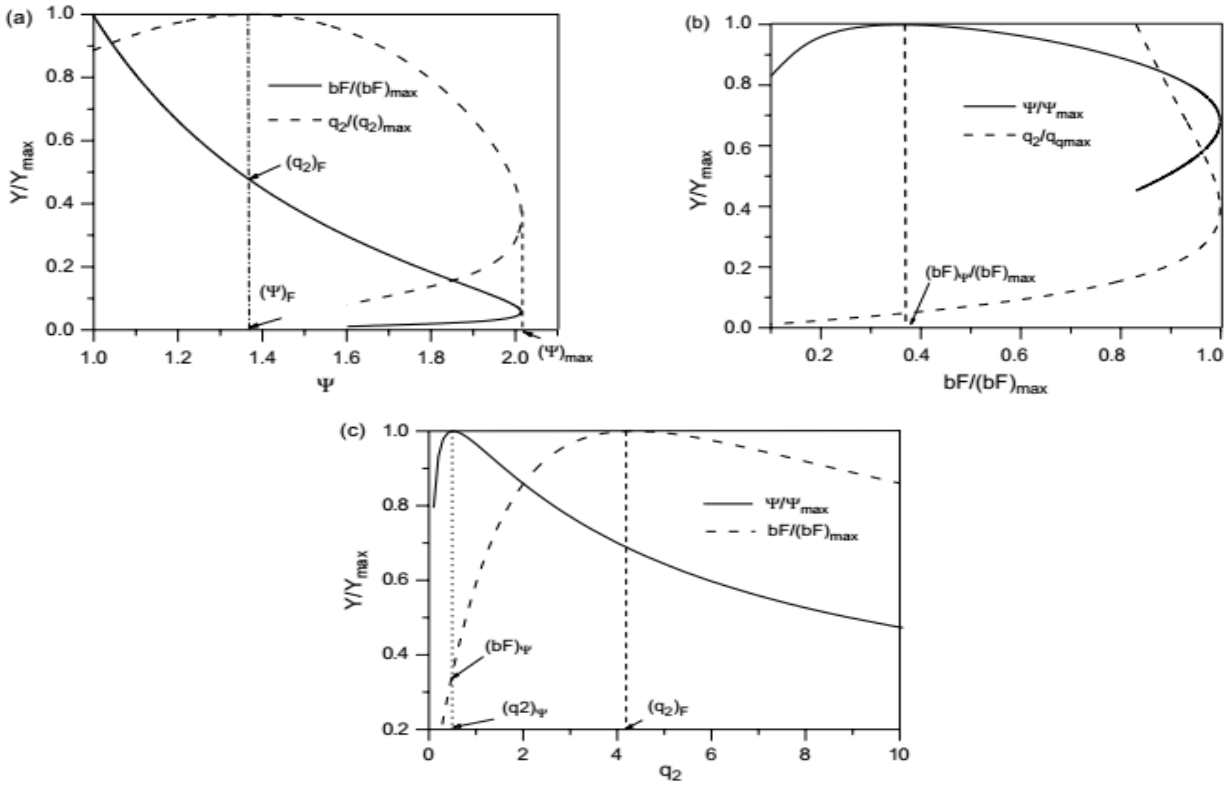

Fig. 1.39. Some optimum characteristic curves of an irreversible heat pump, where **(a)** the $Y/(Y)_{\max}\sim\Psi$ $(Y=bF,q_2)$ curves, **(b)** the $Y/(Y)_{\max}\sim bF$ $(Y=\Psi,q_2)$ curves, and **(c)** the $Y/(Y)_{\max}\sim q_2$ $(Y=bF,\Psi)$ curves. Curves are presented for $(T_H=393\,\mathrm{K}, T_P=303\,\mathrm{K}, T_L=280\,\mathrm{K}, I=1.01,$ $B=1.2\,\mathrm{kWm^{-2}K^{-2}}, \mathrm{C}=0.02\,\mathrm{kWm^{-2}K^{-2}}, U_1=U_2=U_3=0.5\,\mathrm{kWm^{-2}K^{-1}}$ (Wu et al., 2003).

It is seen from **Figs. 1.39 and 1.40** that there exist a maximum thermo-economic objective function and a maximum coefficient of performance. **Fig. 1.39** shows that when a heat pump is operated in the region of $q_2 > (q_2)_F$, not only the coefficient of performance but also the thermo-economic objective function will decrease as the specific heating load q_2 is increased. Thus, if there is not special requirement for the specific heating load, the heat pump should not be operated in the region larger than $(q_2)_F$, that is to say, the heat pump should be, in general, operated in the part of the $bF/(bF)_{\max} \sim \Psi$ curve with a negative slope. It is seen from **Fig. 1.40** that in the optimally operating regions, the thermo-economic objective function, coefficient of performance and specific heating load always decrease with an increase of the internal irreversibility factor.

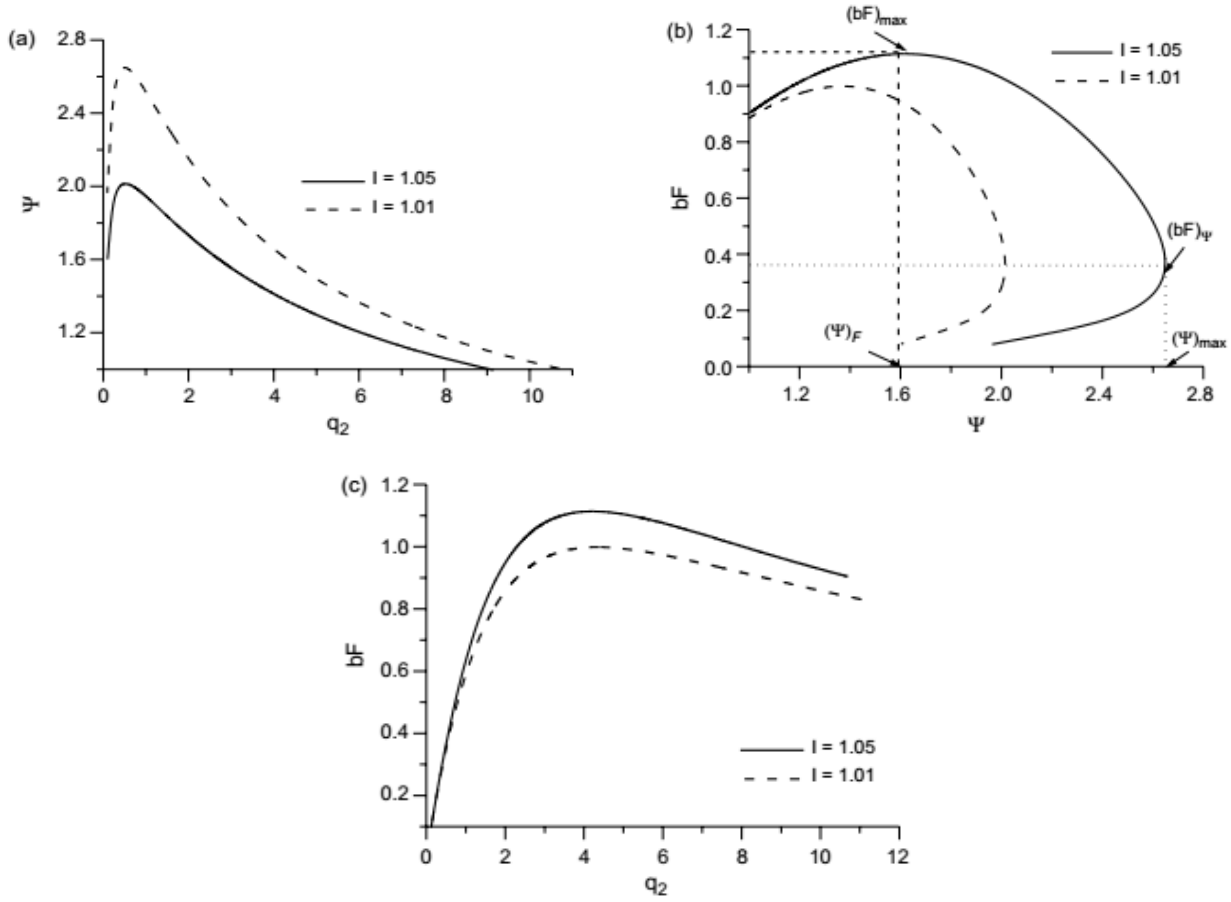

Fig. 1.40. The effect of the internal irreversibility factor I on **(a)** the $\Psi \sim q_2$ curves, **(b)** the $bF \sim \Psi$ curves, and **(c)** the $bF \sim q_2$ curves. Curves are presented for ($T_H = 393\,\mathrm{K}$, $T_P = 303\,\mathrm{K}$, $T_L = 280\,\mathrm{K}$, $I = 1.01$, $B = 1.2\,\mathrm{kWm^{-2}K^{-2}}$, $C = 0.02\,\mathrm{kWm^{-2}K^{-2}}$, $U_1 = U_2 = U_3 = 0.5\,\mathrm{kWm^{-2}K^{-1}}$ (Wu et al., 2003).

1.5. Analysis by thermo-ecological and ecological criteria

Although the economic criterion is a very important factor in the performance of thermodynamic systems and in particular AHPs, the ecological approach complements this consideration.

Angulo-Brown (1991) first developed the ecological approach on heat engine (HE) as the difference between the output power and the loss rate of availability ($E = P - T_0 \Delta S$; where P is the output power, T_0 is the ambient temperature and ΔS is the entropy generation rate), it is followed by Sun et al. (2005) on endoreversible AHT which described the ecological criterion as the difference between the heating load and the loss rate of availability. Later, Ust et al. (2006a, 2006b) that some of them first developed and stated a fundamental criterion to more effectively evaluate the irreversible Brayton HE and irreversible Brayton regenerative HE, respectively. This thermo-ecological criterion or also called ecological coefficient of performance defined as the output power per unit of the loss rate of availability ($ECOP = \dot{W} / T_0 \dot{S}_g$,where $\dot{W}$ is the output power, T_0 is the ambient temperature and $\dot{S}_g$ is the entropy generation rate) is taken up by Chen et al. (2007c) on the irreversible cycles of universal heat engine.

Chronologically, the heat losses caused by the pressure drops and the friction of the working fluid against the walls during the flow in the piping are characterized by an overall internal irreversibility factor which accounts for the second law of thermodynamics. Thus, Huang et al. (2008) studied the optimal performance of an irreversible AHP at four temperature levels (FTL), highlighting a general relationship between the heating load, the COP and the heat-transfer area. This relationship made it possible to optimize the system by first using the heat-transfer area of the heat exchangers as an objective function. Then to show that the minimum of the total heat-transfer area is described in terms of the entropy rate exchanged in the four reservoirs. On the other hand, the ecological criterion E ($E = q - \mu T_e \sigma$; where q is the heating load, T_e is the environment temperature, μ is the dissipation coefficient of the heating load and σ is the entropy generation) is proposed to complete the analysis by the COP, the heating load and the entropy generation rate. However, Chen et al. (2007b, 2019) worked on an irreversible Carnot HP and irreversible FTL AHPs, respectively, using the ecological criterion E ($E = \dot{E}_{out} / \tau - T_0 \Delta S / \tau$; τ is the cycle period), as long as Frikha and Abid (2016) worked on the irreversible Carnot refrigerators and Qin et al. (2017) on irreversible AHT. They found a better compromise between the exergy output rate and the exergy destruction rate, under the influence of overall internal irreversibility and heat leakage. In addition, Ngouateu Wouagfack and Tchinda (2012a, 2012b) using the first and second laws of thermodynamics studied irreversible AHPs operating between three heat sources and four temperature levels, respectively. The objective function used was the ecological performance coefficient (ECOP) described as the heating load per unit of loss rate of availability ($ECOP = qA / T_{env} \sigma$; where q is the specific heating load, A is the total heat-transfer area, T_{env} is the

environment temperature and σ is the entropy generation). This optimization criterion was maximized analytically as a function of the temperatures of the working fluid, while analyzing the performance parameters under the influence of the design parameters. This led to providing a general theoretical tool for the ecological design of absorption AHPs. Then Ahmadi et al. (2015) that in addition to this objective thermo-ecological function, they considered the specific heating load and the coefficient of performance (COP) as additional objective functions on irreversible AHPs with three heat sources. These three objective functions ECOP, COP and the specific heating load were optimized simultaneously using the multi-objective optimization of the NSGA II genetic algorithm. It appears that the best performances are obtained with a maximized ECOP and COP and a minimized specific heating load according to three methods, LINAMP, TOPSIS and FUSSY supplemented by sensitivity and error analyzes.

In a similar way as on irreversible AHP, Ngouateu Wouagfack and Tchinda (2011a, 2011b, 2014) undertook work on the thermo-ecological aspect of the performance of ARs with three heat sources, using the phenomenological linear law of transfer heat $Q \sim \left(\Delta T^{-1}\right)$ and ARs at four temperature levels, respectively. The major results have shown that under maximum ECOP conditions, the refrigeration cycle has a significant advantage in terms of the entropy generation rate and of COP compared to the maximum of ecological criterion *E* conditions and the maximum of the specific cooling load conditions. They are followed by Ahmadi and Ahmadi (2016) on irreversible ARs with three heat sources, Ahmadi et al. (2016) on irreversible HP working in the reverse Brayton cycle and Medjo Nouadje et al. (2014, 2016) on single effect ARs with two internal irreversibilities and double effect with parallel flow, respectively.

We can therefore show some results obtained by Ngouateu Wouagfack and Tchinda (2012b) on AHP at four temperature levels.

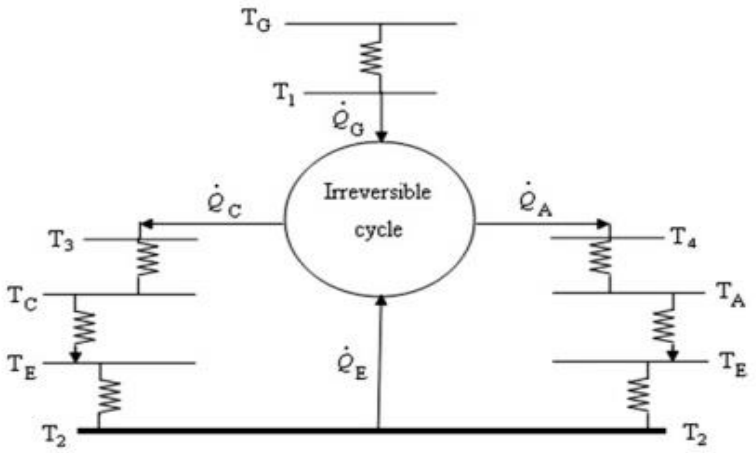

Fig. 1.41. A four-temperature-level irreversible absorption heat pump cycle model (Ngouateu Wouagfack and Tchinda, 2012b).

Fig. 1.41 gives the linear law of heat transfer between the working substance in the heat exchangers and the external heat reservoirs

$$\dot{Q}_G = U_G A_G \left(T_G - T_1\right), \quad \dot{Q}_E = U_E A_E \left(T_E - T_2\right), \quad \dot{Q}_C = U_C A_C \left(T_3 - T_C\right) \quad \text{and} \quad \dot{Q}_A = U_A A_A \left(T_4 - T_A\right) \tag{1.98}$$

and heat leakages due to heat exchanges between the space to be heated and the environment are given by

$$\dot{Q}_L = K_L \left(T_A - T_E + T_C - T_E\right) \tag{1.99}$$

The total area of the heat exchangers, $A = A_G + A_E + A_C + A_A$ (1.100)

The first and second law of thermodynamics in the consideration of an overall internal irreversibility are obtained

$$\dot{Q}_G + \dot{Q}_E - \dot{Q}_C - \dot{Q}_A = 0 \text{ and } I = \left(\dot{Q}_C \big/ T_3 + \dot{Q}_A \big/ T_4\right) \Big/ \left(\dot{Q}_G \big/ T_1 + \dot{Q}_E \big/ T_2\right) \geq 1 \tag{1.101}$$

From equations **Eqs. (1.98-1.101)** they obtained the performance parameters such as the coefficient of performance, the specific heating load and the entropy generation rate

$$COP = \frac{\dot{Q}_A + \dot{Q}_C - \dot{Q}_L}{\dot{Q}_G} = \frac{T_1^{-1} - T_2^{-1}}{\left(IT_3\right)^{-1} + m\left(IT_4\right)^{-1} - \left(1+m\right)T_2^{-1}} \left(1 + m - C_1 \left(\frac{1}{U_C\left(T_3 - T_C\right)} + \frac{m}{U_A\left(T_4 - T_A\right)} + \frac{\left(IT_3\right)^{-1} + m\left(IT_4\right)^{-1} - \left(1+m\right)T_2^{-1}}{U_G\left(T_G - T_1\right)\left(T_1^{-1} - T_2^{-1}\right)} + \frac{\left(IT_3\right)^{-1} + m\left(IT_4\right)^{-1} - \left(1+m\right)T_1^{-1}}{U_E\left(T_E - T_2\right)\left(T_2^{-1} - T_1^{-1}\right)}\right)\right) \tag{1.102}$$

$$q = \frac{\dot{Q}_A + \dot{Q}_C - \dot{Q}_L}{A} = \left(1+m\right)\left(\frac{1}{U_C\left(T_3 - T_C\right)} + \frac{m}{U_A\left(T_4 - T_A\right)} + \frac{\left(IT_3\right)^{-1} + m\left(IT_4\right)^{-1} - \left(1+m\right)T_2^{-1}}{U_G\left(T_G - T_1\right)\left(T_1^{-1} - T_2^{-1}\right)} + \frac{\left(IT_3\right)^{-1} + m\left(IT_4\right)^{-1} - \left(1+m\right)T_1^{-1}}{U_E\left(T_E - T_2\right)\left(T_2^{-1} - T_1^{-1}\right)}\right)^{-1} - C_1 \tag{1.103}$$

$$S = \frac{1}{A}\left(\frac{\dot{Q}_C - K_L\left(T_C - T_E\right)}{T_C} + \frac{\dot{Q}_A - K_L\left(T_A - T_E\right)}{T_A} - \frac{\dot{Q}_G}{T_G} - \frac{\dot{Q}_E - K_L\left(T_A - T_E + T_C - T_E\right)}{T_E}\right)$$

$$= C_4 + C_5 \frac{\left(IT_3\right)^{-1} + m\left(IT_4\right)^{-1} - \left(1+m\right)T_2^{-1}}{T_1^{-1} - T_2^{-1}} + \left(C_2 + C_3 \frac{\left(IT_3\right)^{-1} + m\left(IT_4\right)^{-1} - \left(1+m\right)T_2^{-1}}{T_1^{-1} - T_2^{-1}}\right) \tag{1.104}$$

$$\left(\left(1+m\right)\left(\frac{1}{U_C\left(T_3 - T_C\right)} + \frac{m}{U_A\left(T_4 - T_A\right)} + \frac{\left(IT_3\right)^{-1} + m\left(IT_4\right)^{-1} - \left(1+m\right)T_2^{-1}}{U_G\left(T_G - T_1\right)\left(T_1^{-1} - T_2^{-1}\right)} + \frac{\left(IT_3\right)^{-1} + m\left(IT_4\right)^{-1} - \left(1+m\right)T_1^{-1}}{U_E\left(T_E - T_2\right)\left(T_2^{-1} - T_1^{-1}\right)}\right)^{-1} - C_1\right)$$

and the ecological coefficient of performance objective function.

$$ECOP = \frac{\dot{Q}_A + \dot{Q}_C - \dot{Q}_L}{T_{env}\,\dot{\sigma}} = \frac{1}{T_{env}}\left[\left(C_2 + C_3\frac{(IT_3)^{-1} + m(IT_4)^{-1} - (1+m)T_2^{-1}}{T_1^{-1} - T_2^{-1}} + \left(C_4 + C_5\frac{(IT_3)^{-1} + m(IT_4)^{-1} - (1+m)T_2^{-1}}{T_1^{-1} - T_2^{-1}}\right)\right.\right.$$
$$\left.\left.\left((1+m)\left(\frac{1}{U_C(T_3 - T_C)} + \frac{m}{U_A(T_4 - T_A)} + \frac{(IT_3)^{-1} + m(IT_4)^{-1} - (1+m)T_2^{-1}}{U_G(T_G - T_1)(T_1^{-1} - T_2^{-1})} + \frac{(IT_3)^{-1} + m(IT_4)^{-1} - (1+m)T_1^{-1}}{U_E(T_E - T_2)(T_2^{-1} - T_1^{-1})}\right)^{-1} - C_1\right)^{-1}\right] \quad (1.105)$$

where, $C_1 = \xi\left(T_A - T_E + T_C - T_E\right)$, $C_2 = \dfrac{1}{1+m}\left(\dfrac{1}{T_C} + \dfrac{m}{T_A}\right) - \dfrac{1}{T_E}$, $C_3 = \dfrac{1}{1+m}\left(\dfrac{1}{T_E} - \dfrac{1}{T_G}\right)$,

$$C_4 = \xi\left(T_A - T_E + T_C - T_E\right)\left(\frac{1}{1+m}\left(\frac{1}{T_C} + \frac{m}{T_A}\right) - \frac{1}{T_E}\right) + \xi\left(\frac{T_A}{T_E} + \frac{T_E}{T_A} + \frac{T_C}{T_E} + \frac{T_E}{T_C} - 4\right),$$

$$C_5 = \frac{\xi\left(T_A - T_E + T_C - T_E\right)}{1+m}\left(\frac{1}{T_E} - \frac{1}{T_G}\right),\ \xi = K_L/A \text{ and } m = \dot{Q}_A\big/\dot{Q}_C .$$

By making the variable changes below they were able to derive the thermo-ecological criterion with respect to the temperatures of the working substance in the heat reservoirs

$$b_1 = \left(IT_3\right)^{-1},\ b_2 = \left(1+m\right)T_1^{-1},\ b_3 = \left(1+m\right)T_2^{-1} \text{ and } b_4 = m\left(IT_4\right)^{-1} \quad (1.106)$$

$$\partial ECOP/\partial b_i = 0 \quad (i = 1,2,3,4) \quad (1.107)$$

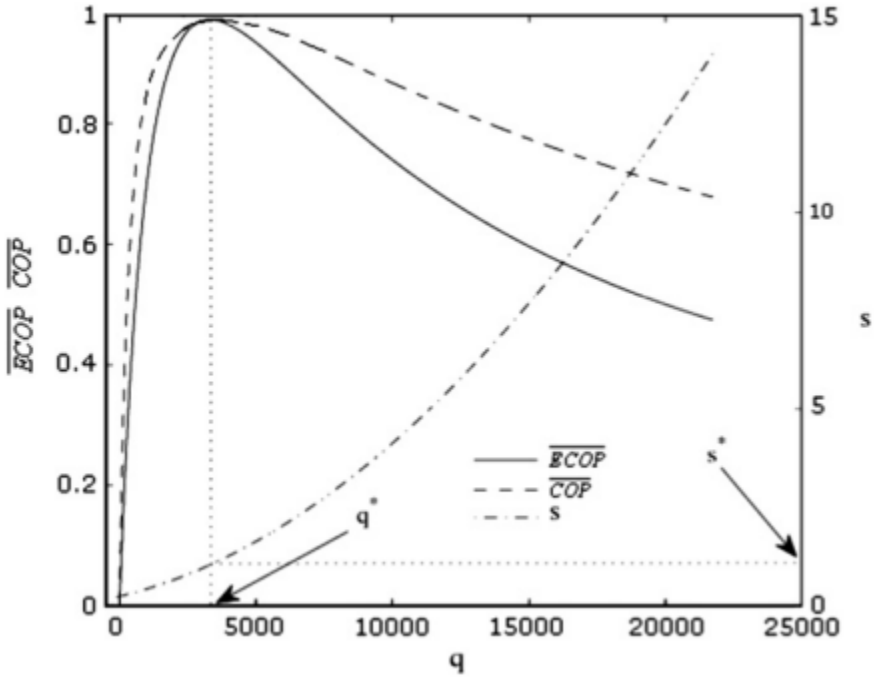

Fig. 1.42. Variations of the normalized *ECOP* ($\overline{ECOP}$), normalized *COP* ($\overline{COP}$) and the specific entropy generation rate with respect to the specific heating load ($T_G = 413\,\mathrm{K}$, $T_E = 283\,\mathrm{K}$, $T_C = 333\,\mathrm{K}$, $T_A = 313\,\mathrm{K}$, $T_{env} = 290\,\mathrm{K}$, $U_G = 1163\,\mathrm{WK^{-1}m^{-2}}$, $U_E = 2326\,\mathrm{WK^{-1}m^{-2}}$, $U_C = 4650\,\mathrm{WK^{-1}m^{-2}}$, $U_A = 1153\,\mathrm{WK^{-1}m^{-2}}$, $m = 1.3$, $I = 1.05$ and $\xi = 5$) (Ngouateu Wouagfack and Tchinda, 2012b).

They have shown in summary in **Fig. 1.42**, variations of the normalized *ECOP* ($\overline{ECOP} = ECOP/ECOP_{\max}$), normalized *COP* ($\overline{COP} = COP/COP_{\max}$) and the entropy generation rate (s) with respect to the specific heating load (q). One interesting observation from this figure is that maximum of the ECOP and COP coincides although their functional forms are different: the coefficient of performance gives information about the necessary heat rate input in order to produce certain amount of heating load and the ecological coefficient of performance gives information about the entropy generation rate or loss rate of availability in order to produce certain amount of heating load. They also showed that the temperatures, the specific heating load, the entropy generate rate and the optimal heat exchange areas corresponding to the maximum of the *ECOP* and the *COP* are the same. Getting the same optimal conditions at the maxima of the *ECOP* and *COP* is a normal result. Since, for a certain heating load, the maximum *COP* results from minimum heat consumption so that minimum environmental pollution. The minimum environmental pollution is also achieved by maximizing the *ECOP*.

Furthermore, considering the temperature of the absorber T_A and the condenser T_C identical, we obtain an absorption heat pump with three heat reservoirs (Ngouateu Wouagfack and Tchinda 2012a, Ahmadi et al. 2015) as in **Fig. 1.43** for an overall internal irreversibility.

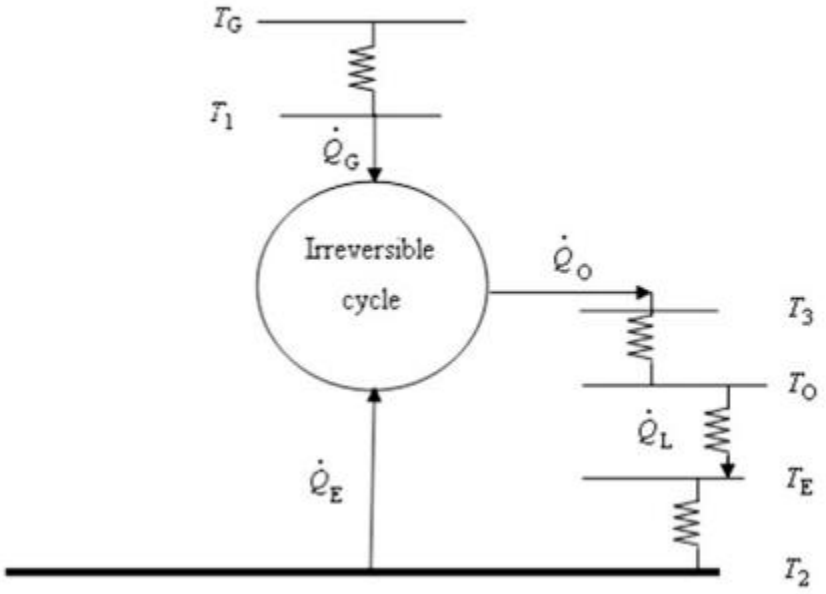

Fig. 1.43. The irreversible cycle model of a three-heat-source absorption heat pump (Ngouateu Wouagfack and Tchinda, 2012a).

Ngouateu Wouagfack and Tchinda (2012a) therefore obtained in **Fig. 1.44** variations of the normalized *ECOP*, normalized *COP* and the specific entropy generation rate (*s*) with respect to the specific heating load (*q*) for three heat reservoirs. The maximum of the *ECOP* and the maximum of the *COP* always coincide for the same reasons as above (**Fig. 1.42**). In addition, the performance of systems with three heat reservoirs admits a lower production of optimal entropy for a lower production of heating load than systems with four temperature levels each corresponding to the maximum of the *ECOP*.

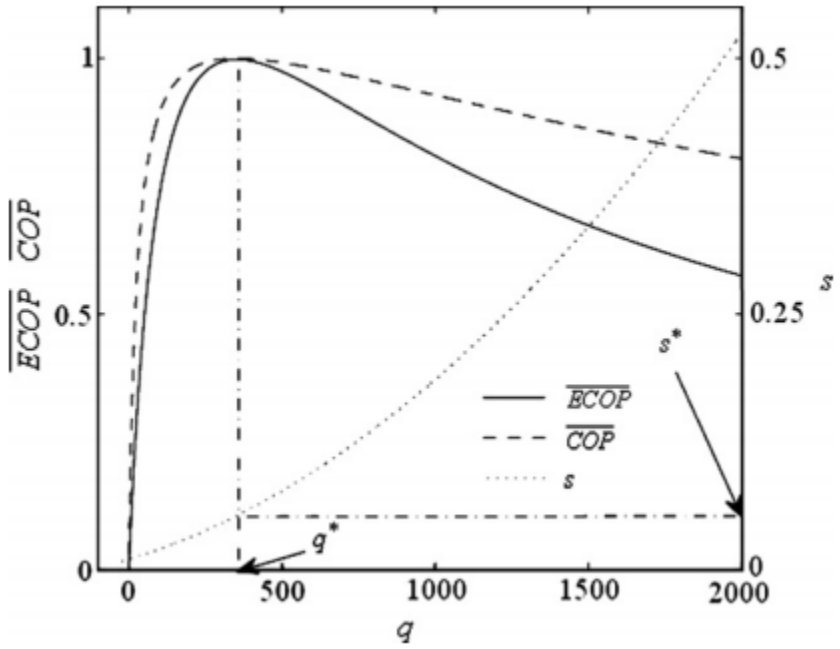

Fig. 1.44. Variations of the normalized *ECOP*, normalized *COP* and the specific entropy generation rate with respect to the specific heating load ($T_G = 393\,\mathrm{K}$, $T_E = 288\,\mathrm{K}$, $T_O = 313\,\mathrm{K}$, $T_{env} = 290\,\mathrm{K}$, $U_G = U_E = U_O = 500\,\mathrm{WK^{-1}m^{-2}}$, $I = 1.025$, $\xi = 1.082$) (Ngouateu Wouagfack and Tchinda, 2012a).

Under the constraints of the conditions that must be met by the temperatures T_1, T_2 and T_3 ($380 \le T_1 \le 390$, $270 \le T_2 \le 282$ and $320 \le T_3 \le 370$) of the working fluid in the generator, the evaporator and the absorber-condenser assembly respectively, Ahmadi et al. (2015) obtained **Fig. 1.45**. The *ECOP* and *COP* are maximized simultaneously and the specific heating load (*q*) is minimalized counter-currently via the multi-objective optimizing scheme which performs on the basis of the NSGA-II method. Also, obtained optimal solutions of TOPSIS and LINMAP and FUZZY methods exhibited in **Fig. 1.45**.

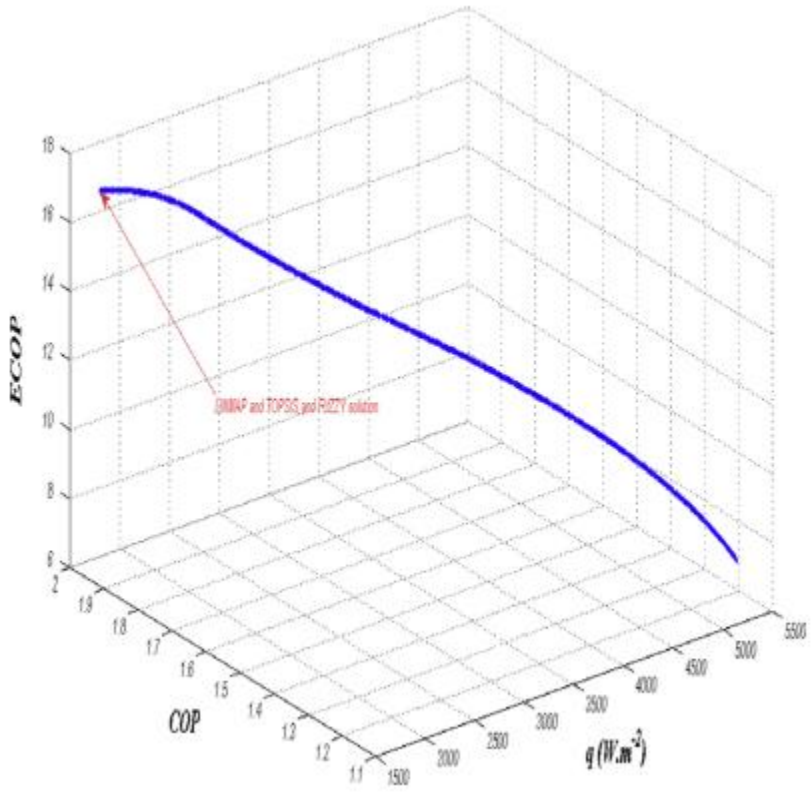

Fig.1.45. Pareto frontier (Pareto optimal solutions) using NSGA-II ($T_G = 393\,\mathrm{K}$, $T_E = 288\,\mathrm{K}$, $T_O = 303\,\mathrm{K}$, $T_{env} = 290\,\mathrm{K}$, $U_G = U_E = U_O = 500\,\mathrm{WK^{-1}m^{-2}}$, $I = 1.025$, $\xi = 1.082$) (Ahmadi et al., 2015).

Regarding the ecological criterion, Chen et al. (2019) have carried out work on irreversible FTL AHP by integrating heat resistances and heat leaks with each component, as well as an overall internal irreversibility. Irreversible FTL AHP cycle model is shown in **Fig. 1.46**. The solution pump work input required is negligible, because it is relative little to the whole energy input. It is supposed that the heat transfer processes in four heat exchangers are according to Newtonian heat transfer law, and the heat transfer equations are

$$Q_g^{'} = U_g A_g \left(T_g - T_g^{'}\right),\ Q_a^{'} = U_a A_a \left(T_a^{'} - T_a\right),\ Q_c^{'} = U_c A_c \left(T_c^{'} - T_c\right) \text{ and } Q_e^{'} = U_e A_e \left(T_e - T_e^{'}\right) \quad (1.108)$$

There exist heat exchanges between surrounding and heat reservoir, named heat leakage. Supposing that heat leakage processes are according to Newtonian heat transfer law, too, heat leakage equations are

$$Q_g^{l} = K_g^{l}\left(T_g - T_s\right),\ Q_a^{l} = K_a^{l}\left(T_a - T_s\right),\ Q_c^{l} = K_c^{l}\left(T_c - T_s\right) \text{ and } Q_e^{l} = K_e^{l}\left(T_s - T_e\right) \quad (1.109)$$

There also exists internal dissipation of working fluid, named internal irreversibility. As shown in **Fig. 1.46**, a factor 1 is imported to represent internal irreversibility

$$I = \left(Q_a^{'}/T_a^{'} + Q_c^{'}/T_c^{'}\right)\Big/\left(Q_g^{'}/T_g^{'} + Q_e^{'}/T_e^{'}\right) \geq 1 \quad (1.110)$$

The energy conservation law or first law of thermodynamics gives

$$Q_c^{'} + Q_a^{'} = Q_e^{'} + Q_g^{'} \tag{1.111}$$

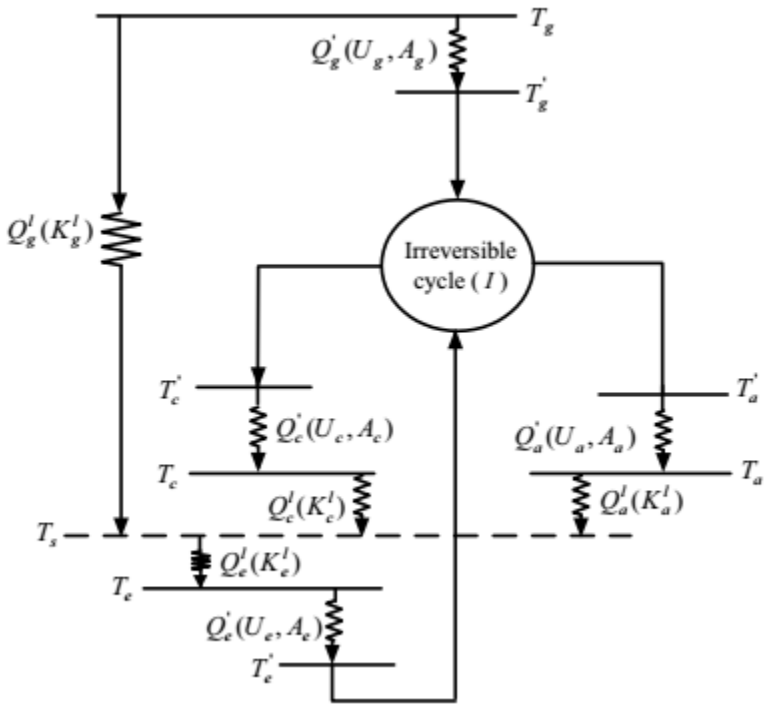

Fig. 1.46. An irreversible FTL AHP cycle model (Chen et al., 2019).

The performance parameters *COP*(ψ) and heating load (Π) of the cycle can be written as

$$\psi = \left(Q_a + Q_c\right)/Q_g = \left(Q_a^{'} + Q_c^{'} - Q_a^{I} - Q_c^{I}\right)/\left(Q_g^{I} + Q_g^{I}\right) \tag{1.112}$$

$$\Pi = Q_a + Q_c = Q_a^{'} + Q_c^{'} - Q_a^{I} - Q_c^{I} \tag{1.113}$$

The general equation among *COP*, heating load, irreversibility factor, heat leakages and heat transfer irreversibility of a FTL AHP cycle can be derived as follows

$$\begin{aligned} &\left(\frac{T_g}{\Pi - Q_g^{I}\psi} - \frac{1}{U_g A_g \psi}\right)^{-1} + \left(\frac{T_e}{\left(\Pi - Q_a^{I} + Q_c^{I} + Q_g^{I}\right)\psi - \Pi} - \frac{1}{U_e A_e \psi}\right)^{-1} - \\ &\frac{\psi}{I}\left(\left(\frac{T_a}{(1-a)\left(\Pi + Q_a^{I} + Q_c^{I}\right)} + \frac{1}{U_a A_a}\right)^{-1} + \left(\frac{T_c}{a\left(\Pi + Q_a^{I} + Q_c^{I}\right)} + \frac{1}{U_c A_c}\right)^{-1}\right) = 0 \end{aligned} \tag{1.114}$$

where $a = Q_c^{'}/\left(Q_a^{'} + Q_c^{'}\right)$ represents the allocation ratio of released heat from cycle fluid.

They established the expression of ecological function as follows

$$E = EX - T_s\sigma = EX_a + EX_c - EX_e - T_s\sigma \tag{1.115}$$

where $EX_a = Q_a\left(1-T_s/T_a\right)$ is exergy output rate of absorber, $EX_c = Q_c\left(1-T_s/T_c\right)$ is exergy output rate of condenser and $EX_e = Q_e\left(1-T_s/T_e\right)$ is evaporator exergy output rate.

$$Q_g = \Pi/\psi,\ Q_a = \left(1-a\right)\left(\Pi + Q_a^{\,l} + Q_c^{\,l}\right) - Q_c^{\,l} \text{ and } Q_e = \Pi\left(\psi-1\right)/\psi + Q_a^{\,l} + Q_c^{\,l} + Q_g^{\,l} - Q_e^{\,l} \quad (1.116)$$

The entropy production rate (σ) can be written as

$$\sigma = \frac{Q_a}{T_a} + \frac{Q_c}{T_c} + \frac{Q_a^{\,l} + Q_c^{\,l} + Q_g^{\,l} - Q_e^{\,l}}{T_s} - \frac{Q_g}{T_g} - \frac{Q_e}{T_e} \quad (1.117)$$

substituting Eq. (1.116) into Eq. (1.117) yields

$$\begin{aligned}\sigma = \Pi\left(\frac{1-a}{T_a} + \frac{a}{T_c} - \frac{1}{T_e} + \left(\frac{1}{T_e} - \frac{1}{T_g}\right)\frac{1}{\psi}\right) - Q_a^{\,l}T_s\left(\frac{1}{T_e} - \frac{1}{T_s} + a\left(\frac{1}{T_a} - \frac{1}{T_c}\right)\right) - \\ Q_c^{\,l}T_s\left(\frac{1}{T_e} - \frac{1}{T_s} + \left(1-a\right)\left(\frac{1}{T_c} - \frac{1}{T_a}\right)\right) + \left(Q_g^{\,l} - Q_e^{\,l}\right)\frac{1}{T_s}\end{aligned} \quad (1.118)$$

Substituting **Eqs. (1.116)** and **(1.118)** into **Eq. (1.115)** yields

$$\begin{aligned}E = \Pi T_s\left(2\left(\frac{1}{T_e} - \frac{1-a}{T_a} - \frac{a}{T_c}\right) + \left(\frac{1}{T_g} + \frac{1}{T_s} - \frac{2}{T_e}\right)\frac{1}{\psi}\right) - 2Q_a^{\,l}T_s\left(\frac{1}{T_s} - \frac{1}{T_e} - a\left(\frac{1}{T_a} - \frac{1}{T_c}\right)\right) - \\ 2Q_c^{\,l}T_s\left(\frac{1}{T_s} - \frac{1}{T_e} - \left(1-a\right)\left(\frac{1}{T_c} - \frac{1}{T_a}\right)\right) - \left(Q_g^{\,l} - Q_e^{\,l}\right)T_s\left(\frac{2}{T_s} - \frac{1}{T_e}\right)\end{aligned} \quad (1.119)$$

Numerical calculations: $T_g = 378\,\mathrm{K}$, $T_a = 327\,\mathrm{K}$, $T_c = 332\,\mathrm{K}$, $T_e = 298\,\mathrm{K}$, $T_s = 300\,\mathrm{K}$, $A_g = A_a = A_c = A_e = 100\,\mathrm{m^2}$, $U_g = U_a = 500\,\mathrm{Wm^{-2}K^{-1}}$, $U_c = U_e = 1000\,\mathrm{Wm^{-2}K}$, $I = 1.01$, $K_g^{\,l} = K_a^{\,l} = K_c^{\,l} = K_e^{\,l} = 100\,\mathrm{WK^{-1}}$ and $a = 0.45$.

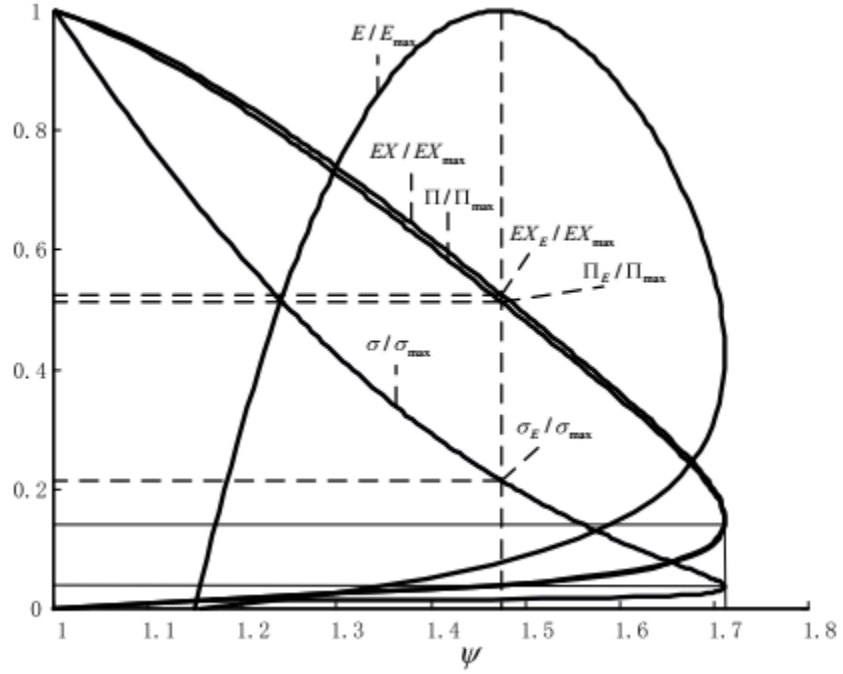

Fig. 1.47. Ecological function, entropy generation rate, exergy output rate and heating load versus *COP* relationship (Chen et al., 2019).

The relations between $E/E_{\max}$ and ψ, $EX/EX_{\max}$ and ψ, and $\sigma/\sigma_{\max}$ and ψ of irreversible AHP cycles are shown in **Fig. 1.47**. $E/E_{\max}$ denotes the dimensionless exergy output rate, which are defined as ratio of ecological function (E) to maximum ecological function ($E_{\max}$). The definitions of $EX/EX_{\max}$ and $\sigma/\sigma_{\max}$ are similar to $E/E_{\max}$. Using numerical example mentioned above, they were able to get that $\psi_E = 1.48$, $\Pi_E/\Pi_{\max} = 0.51$, $EX_E/EX_{\max} = 0.52$ and $\sigma_E/\sigma_{\max}$ at the $E_{\max}$ point. Comparing the $E_{\max}$ point with the $\Pi/\Pi_{\max} = 1$ point, one can find that the $E_{\max}$ point makes ψ increase about 48% and $EX/EX_{\max}$ decreases about 48%, but $\sigma/\sigma_{\max}$ decreases about 79%. Comparing the Emax point with the $\psi_{\max}$ ($\psi_{\max} = 1.71$) point, they found that the $E_{\max}$ point makes ψ decreases about 13% and $\sigma/\sigma_{\max}$ increases about 16%, but $EX/EX_{\max}$ increases about 37% and $\Pi/\Pi_{\max}$ increases about 36%. We can be seen that the $E_{\max}$ point makes the heating load (compared to the $\psi_{\max}$ point) increase with a little increase of $\sigma/\sigma_{\max}$, and the *COP* (compared to the $\Pi_{\max}$ point) increase with a little decrease of $EX/EX_{\max}$. Therefore, the ecological objective function of AHP cycles has a certain reference value, which attains a compromise in inter restricted relations of *COP* and heating load, and of exergy output and entropy generation.

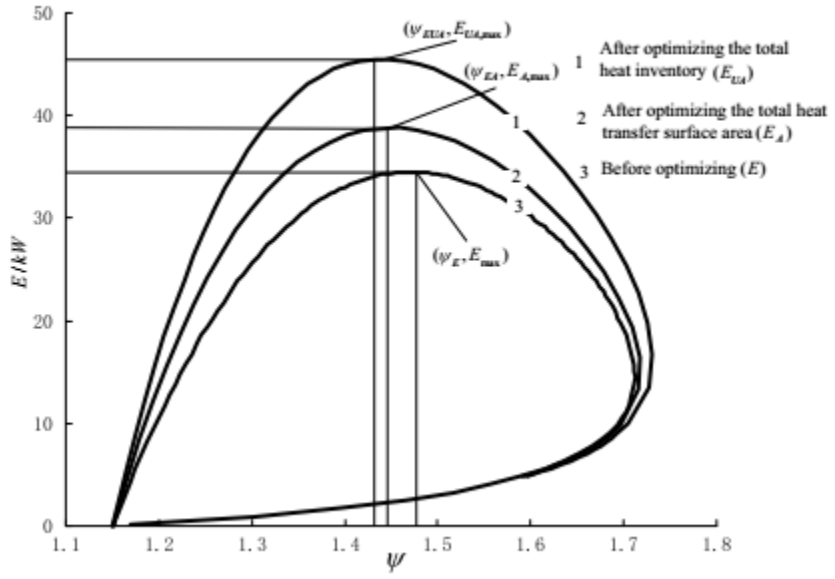

Fig. 1.48. Ecological function versus *COP* relationship before and after optimizing (Chen et al., 2019).

Fig. 1.48 shows the relations between E_A and ψ_A, and E_{UA} and ψ_{UA} of irreversible AHP cycles before and after optimizing distributions of *A* and *UA*. One can see that optimizing distribution of *A* and *UA* changes ecological function versus *COP* relationships quantitatively, ecological function performances are improved after optimizing distribution of *A* and *UA*, and ψ_{EUA} and ψ_{EA} (*COP* at maximum ecological function ($E_{A,\max}$ and $E_{UA,\max}$) after optimizing) are smaller than ψ_E (*COP* at maximum ecological function ($E_{\max}$) before optimizing).

All previous ecological analyzes and observations have been carried out in the study of systems under to the influence of overall internal irreversibility. However, they do not make it possible to understand from the second law of thermodynamics in which compartments of heat exchangers the quality of the energy produced is deteriorated.

1.6. Analysis by exergetic criterion

For most researchers and engineers, the energy analysis and optimization on thermodynamic systems (heat engines, refrigerators, air conditioners, heat pumps, etc.) using finite time thermodynamics is of great importance and allows a synthesis between economic and ecological approaches. However, it is interesting to evaluate for these systems the exergy destruction, the exergy output and the exergy input by taking into account the surface areas of heat exchange in the various heat exchangers and design factors such as heat leakage, heat loss and heat resistance.

Talbi and Agnew (2000) developed a computer program on an AR using the pair of working fluid H2O/LiBr, to identify the least efficient components of the system. Then Kilic and

Kaynakli (2007) and Kaynakli and Kilic (2007) on the same system showed using an exergetic analysis that the losses were greater in the generator and the absorber. Then Sarkar et al. (2005) presented the analysis and optimization of a transcritical carbon dioxide HP cycle for simultaneous heating and cooling applications. The effects of heat transfer and fluid flow in the analysis led to the evaluation of the optimal COP and the exergetic efficiency of the system. These two objective functions have been shown to be functions of the compressor speed, the ambient temperature and the temperature of the secondary working fluid at the evaporator and gas cooler inlets and the discharge pressure of the compressor. This allowed them to present various measures to improve performance with gains by reducing the irreversibilities of the components. Also, Farshi et al. (2013), worked double-effect AR with the exergoeconomic approach and Ahmadi et al. (2016) carried out a multi-objective optimization of an irreversible HP working on a reverse Brayton cycle using the exergetic efficiency among the criteria studied according to three methods, LINAMP, TOPSIS and FUSSY.

This being so, several researchers will characterize the exergetic analysis with a criterion called the exergetic performance coefficient (EPC). This is the case of Ust et al. (2007) who established on an irreversible dual cycle cogeneration system the optimization EPC criterion. This objective function is described as the ratio of total exergy output to the loss rate of availability (exergy destruction rate). This approach is an improvement of the endoreversible system of a cogeneration cycle proposed by Sahin et al. (1997). Ust and Karakurt (2014) have taken up this objective function on cascade refrigeration systems using different pairs of refrigerants. They have shown that the R23-R717 pair has better performances in terms of EPC and COP compared to the R23-R290, R23-R404A, R23-R507A and R23-R717 refrigerant pairs. Lostec et al. (2010) investigated single-stage absorption systems operating with an ammonia-water mixture under steady state conditions. They showed the existence of three optimal COP values: the first minimizes the total thermal conductance, the second minimizes the overall irreversibility of the system and the third maximizes the exergetic efficiency. Moreover, these three optimal COP values are lower than the maximum COP which corresponds to the convergence of internal and external temperatures towards an average value. Later, Liu et al. (2017) presented an exergetic study on a combined absorption heat pump transformer system operating with the pair of water/lithium bromide working fluid driven by waste heat at medium temperature to provide two types of useful heat. On the basis of the law of energy conservation and mass and of phase equilibrium, a calculation model is developed in Engineering Equation Solver to study the performance of this system compared to the different temperatures of the components, efficiency of the solution heat exchanger, flow ratio and gross temperature rise. The results showed that the

efficiency of the system is close to 100% and the exergetic performance coefficient (EPC) is 71.1%, which are respectively 33.2% and 33.1% higher than those of the reference system. This made it possible to quantify the rate of irreversibility of each component at a certain pressure.

Açikkalp and Ahmadi (2018) have used previous research on heat engines by evaluating the energy source or exergy fuel converted into output power.

From the exergetic analysis of an ammonia-water FTL AHP, Lostec et al (2010), using **Fig. 1.49** and a computer program, they developed **Table 1.1**. This gives the balance of heat exchange and destruction exergy in each component. It appears that the losses are greater in the absorber and the generator.

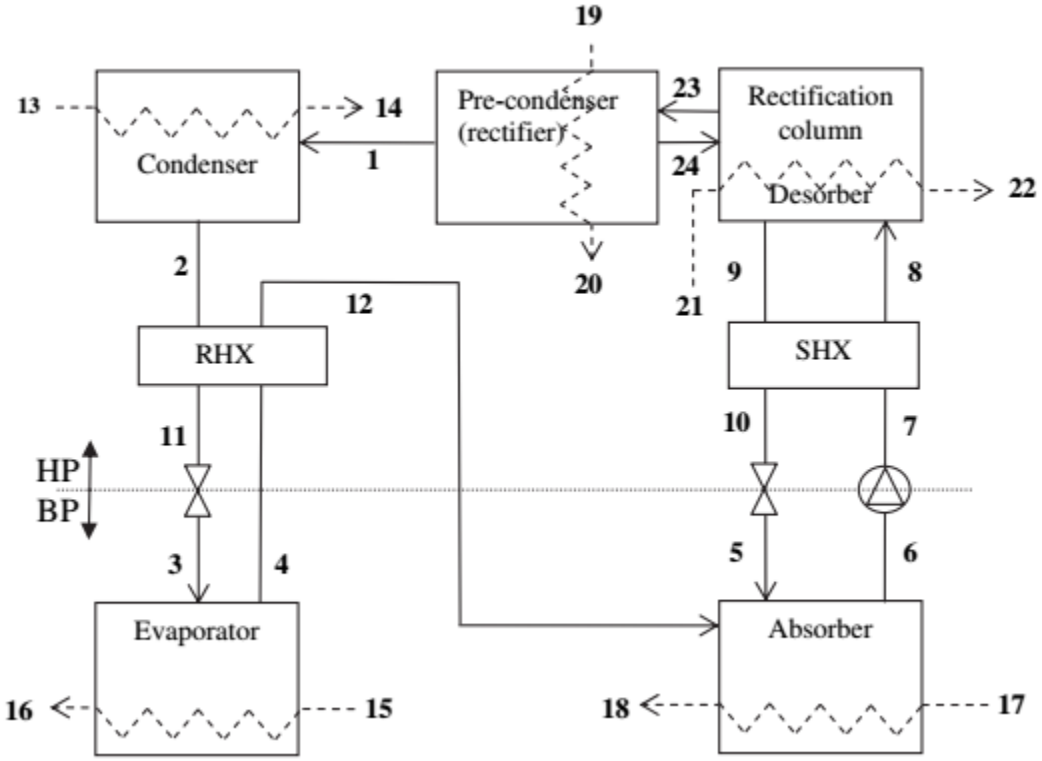

Fig. 1.49. Schematic representation of the system (Lostec et al., 2010).

Table 1.1. Energy fluxes and rate of exergy destruction for operation at maximum exergetic efficiency (Lostec et al., 2010).

Component	Heat transfer (internal) (W)	Exergy destroyed (external and internal) (W)	
Evaporator	3000	−33.44	5.81%
Condenser	−2945	−45.73	7.95%
Absorber	−4066	−190.00	33.03%
Desorber	4341	−195.99	34.07%
Heat exchanger (7–8)	1544	−73.16	12.72%
Heat exchanger (9–10)	−1544		
Pump	7	−0.62	0.11%
Expansion valve (11–3)	0	−8.27	1.44%
Expansion valve (10–5)	0	−17.33	3.01%
Heat exchanger (4–12)	132	−5.41	0.94%
Heat exchanger (2–11)	−132		
Pre-condenser	−338	−5.24	0.91%
Total	0	−575.20	100.00%

However, Ahmadi et al. (2016) on irreversible heat pump working on reversed Brayton cycle, established from the following equations a Pareto optimal frontier. The finite heat transfer law

$$Q_L = \frac{U_L\left(T_2 - T_1\right)}{\ln\left(\frac{T_L - T_1}{T_L - T_2}\right)} \text{ and } Q_H = \frac{U_H\left(T_3 - T_4\right)}{\ln\left(\frac{T_3 - T_H}{T_4 - T_H}\right)} \tag{1.120}$$

The entropy production rate, the input exergy and the output exergy are given by **eqs. (1.121)** and **(1.122)**.

$$S = \frac{Q_H}{T_H} - \frac{Q_L}{T_L} \tag{1.121}$$

$$E_{in} = Q_H - Q_L,\ E_{out} = \left(1 - \frac{T_O}{T_H}\right)Q_H - \left(1 - \frac{T_O}{T_L}\right)Q_L \text{ and } E_{out} = E_{in} - E_d \tag{1.122}$$

This makes it possible to establish the expressions for the coefficient of performance, the ecological coefficient of performance and the exergetic efficiency, respectively.

$$COP = \frac{Q_H}{Q_H - Q_L},\ ECOP = \frac{Q_H}{T_O S} \text{ and } \eta_{ex} = \frac{E_{out}}{E_{in}} = \frac{\left(1 - \frac{T_O}{T_H}\right)Q_H - \left(1 - \frac{T_O}{T_L}\right)Q_L}{Q_H - Q_L} \tag{1.123}$$

Pareto optimal frontier for three objective functions, objective function associated to the *COP* and *ECOP* and the exergetic efficiency of the irreversible Brayton heat pump are represented in **Fig. 1.50**. Moreover, the outcomes of each decision maker are marked in this Figure.

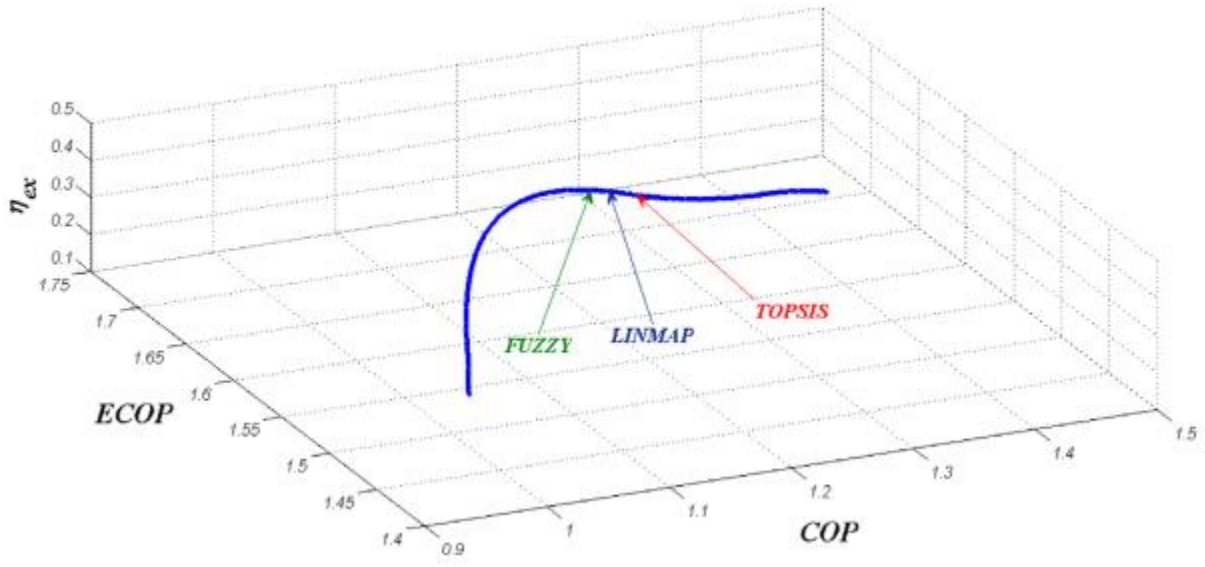

Fig. 1.50. Pareto optimal frontier in the objectives' space for first scenario

1.7. New trends

Growing concerns about energy conservation and conversion as well as environmental protection have led research to develop heating and cooling driven by renewable energy sources of which absorption machines are a natural model. The most widespread source being the solar thermal source.

Mention is made of authors such as Mortazavi et al. (2017) who studied the AHP driven by solar collectors and the waste heat operating with a new design of compact plate-and-frame generator as shown in **Fig. 1.51** and **Fig. 1.52**. Aguilar-Jiménez et al. (2020) presented the simulation study of a solar absorption air-conditioning LiBr-H_2O system installed in an isolated primary school in Mexico.

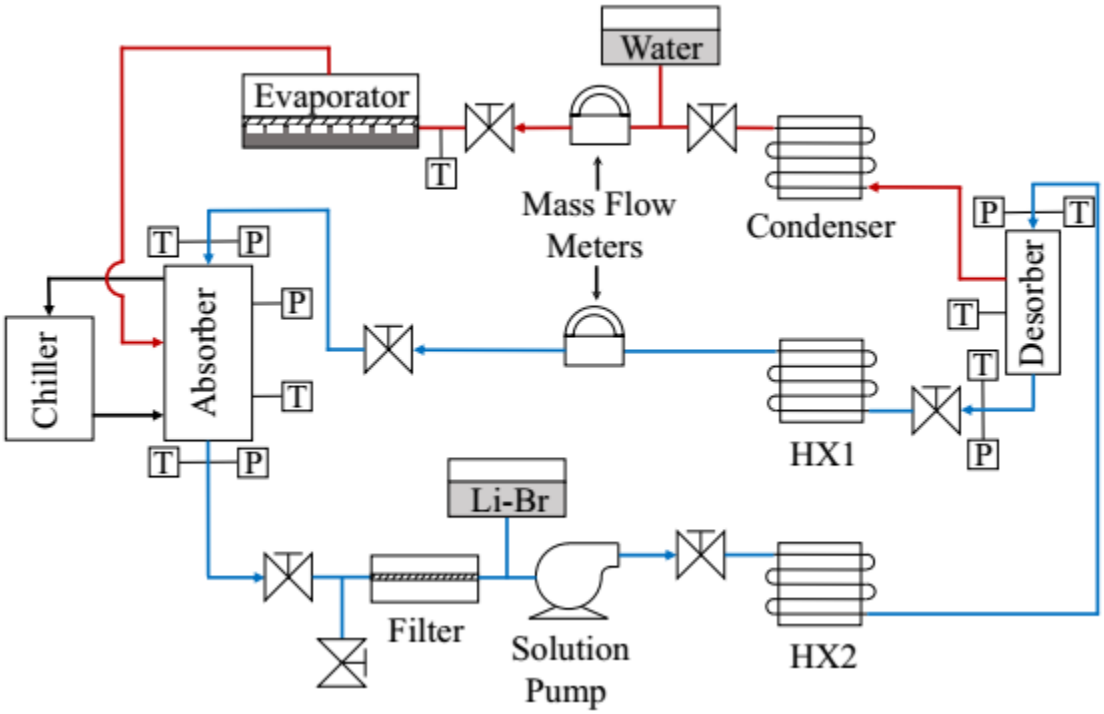

Fig. 1.51 A schematic diagram of the experimental setup (Mortazavi et al. 2017).

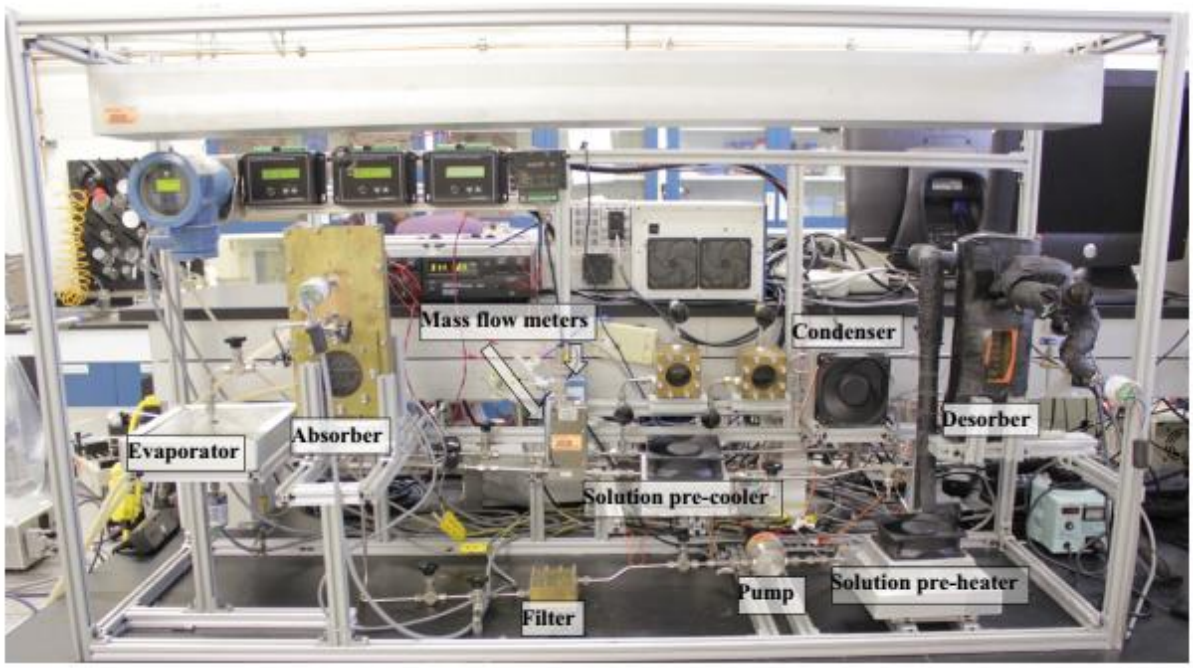

Fig. 1.52 A photograph of the experimental setup (Mortazavi et al. 2017).

Then, Zheng et al. (2019) who developed mathematical models from the FTT to evaluate the performance of solar heating and cooling absorption systems driven by a parabolic trough collectors and operating with the H_2O/LiBr pair, this in the use of office buildings . The energy generated by solar collectors was supplied to the absorption chiller during the cooling period, and

was directly used for space heating with the integration of plate heat exchanger during the heating period. This system compared to a conventional gas-fired heating and cooling system over a year shows a consumption of 21.3% of primary energy and an 18.8% reduction in CO_2 emissions. The solar collector loop mainly consists of PTC which generates and supplies thermal energy to the absorption chiller for cooling or provides heating via PHE. The load loop comprises the double-effect absorption chiller loop and the PHE loop, which cover the building loads with the circuits of chilled water and hot water through the evaporator and the PHE respectively. The gas burner equipped in high pressure generator is used as a backup heater in case of solar energy shortage. The schematic diagram of the SHC system is illustrated in **Fig. 1.53**. During the cooling period, valve V1, valve V2, valve V3 are opened and valve V6 is closed. The heat-transfer oil in PTC can be heated to 100–250 °C. With the high pressure generator branch opened by three-way valve V5, the thermal energy generated by PTC can be supplied to the absorption chiller, thus refrigerant vapor could be boiled off from weak solution. During the early period of system operation, the heat-transfer oil is circulated in the collectors and heated by solar radiation with valve V4 closed. The high pressure generator branch will be opened after the temperature of heat-transfer oil meet the absorption chiller driven requirement. Under the priority of using solar power, the double-effect refrigeration system can be powered by solar thermal and gas fired independently or simultaneously, depending on the intensity of the solar radiation. During the heating period, valve V1, valve V2, valve V3 are closed. The heat-transfer oil in PTC is heated to low temperature (< 100 °C). The thermal energy derived by PTC is directly used for heating purpose coupled with PHE. Hot water can be supplied with the branch of PHE opened by three-way valve V5. Analogously, if the harvested solar energy is not adequate for building demand, the gas burner installed in generator will be activated. The heat- transfer oil is preheated in the collectors in the same way as cooling condition. Also, Wang et al. (2019) proposed a solar-assisted hybrid combined cooling, heating and power (CCHP) system that consists of an internal combustion engine, solar heat collectors, an absorption heat pump, a heat exchanger, and a thermal storage tank. They showed on the basis of a thermodynamic model using the exergetic, economic and environmental criteria that compared to the conventional CCHP system, without solar energy, the hybrid system saves 11.3% of natural gas to reduce carbon dioxide emission and shortens the capital payback period by 1 year.

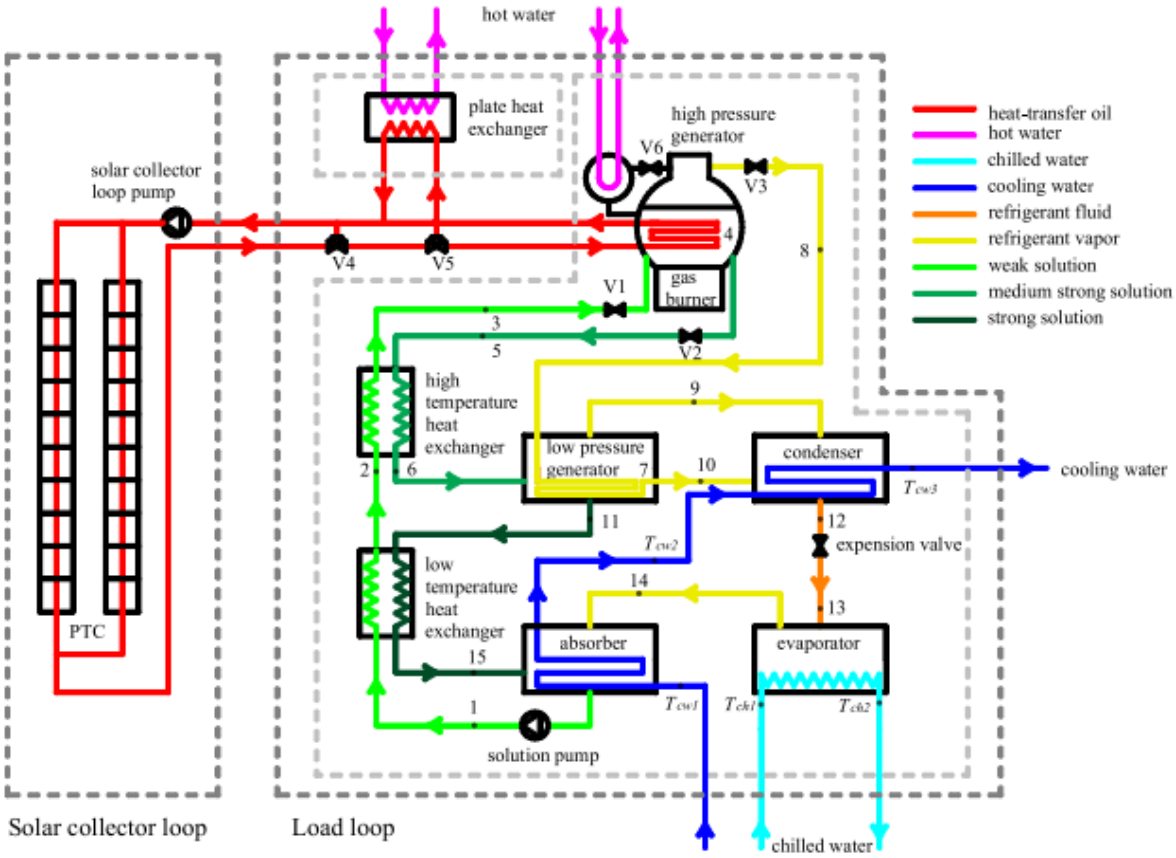

Fig. 1.53. Schematic diagram of the SHC system (Zheng et al., 2019).

However, Asadi et al. (2018) presented a combined thermo-economic analysis and multi-objective optimization of an ammonia-water single-effect solar absorption cooling system of a 10kW. Exergetic analyzes were performed using the FTT and they were able to compare the performance of solar collectors such as the flat plate, evacuated tube, compound parabolic and parabolic trough collectors at different ambient temperatures. Their results showed that the evacuated tube collector have a better economic profitability according to the installation cost and the area occupied by the collectors, while the parabolic trough collectors have an exergetic efficiency which is reached at high ambient temperature and at a low evaporator temperature. The symbolic device for the flow of the NH_3-H_2O pair is presented in **Fig. 1.54**. Many other authors such as Figaj et al. (2019) presented the results of experiments conducted with a hybrid solar system integrating a concentrator, and computer simulations of a hybrid solar cooling system incorporating flat plate collectors and a concentrator. Xu et al. (2018) to give the best absorption cycle options under different conditions, chose five absorption refrigeration cycles suitable for air cooled solar cooling including three double lift absorption cycles and two semi-GAX (generator-absorber heat exchange) absorption cycles were compared. So say that Yu et al. (2019) have shown that the solar absorption-subcooled compression hybrid cooling system is to be the economically feasible solution for the high-rise building.

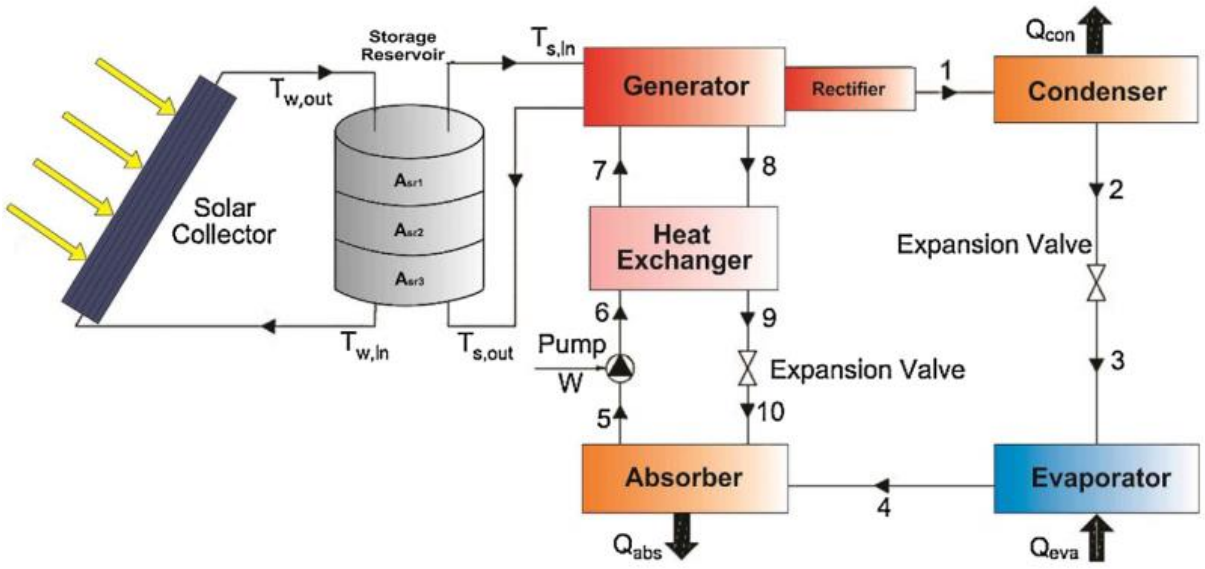

Fig. 1.54. Schematic diagram of a solar absorption cooling system (Asadi et al. 2018).

Therefore, the solar heating and cooling system has a promising, application prospect in sustainable development in view of its considerable energy saving benefits, potential economic viability and environmental friendly characteristics.

1.8. Conclusion

This review summarizes in detail the foundations of finite time thermodynamics (FTT) and its various applications. We have shown the importance of this approach in the theoretical analysis of the performance of real thermodynamic processes, that is to say finite time processes in absorption cycles with the notion of irreversibility. Nevertheless, the FTT is also a powerful tool in the development of experimental protocols for absorption heating and cooling systems driven by a heat source which can be either waste heat from industry or a renewable energy source such as thermal solar. This being so, three basic criteria have been defined, including the economic, ecological and exergetic criteria in order to optimize the efficiency of said systems in order to be able to compete with the conventional systems most used today.

In the rest of this work, we will analyze and optimize using FTT, absorption heat pump systems subjected to several irreversibility factors.

CHAPTER 2: OPTIMIZATION OF AN IRREVERSIBLE ABSORPTION HEAT PUMP

2.1. Introduction

Finite time thermodynamics is a powerful tool for advanced analysis and optimization of thermodynamic systems. However, the optimization of thermodynamic systems such as vapor compression cycles, thermal engines and recently absorption systems was until then based on the first law of thermodynamics. The performance criteria evaluated in this case were the coefficient of performance and the cooling load for refrigerators and air conditioning (Bhardwaj et al., 2001, 2003b, 2005; Zheng et al., 2004; Qin et al., 2010), the energy efficiency and the power supplied for the thermal engines (Curzon et Ahlborn, 1975; Kaushik and Kumar, 2000a, 2001; Kaushik and Tyagi, 2002). Also, the coefficient of performance and the heating load for HP (Chen et al., 1999b, 1999c, 2005a; Bi et al., 2008; Xiling et al. 2011; Wei et al., 2011; Qin et al., 2007, 2015). In addition, the use of vapor compression systems, although having a high coefficient of performance, consumes large amounts of electricity and uses still polluting refrigerants. However, absorption systems can use residual heat from industry or even free renewable energy. Better still they use

environmentally friendly working fluids although despite their coefficient of performance enough low.

Moreover, the second law of thermodynamics bringing out internal irreversibilities during real processes, it is crucial to take this aspect into consideration. The new performance criteria take into account real operating considerations, i.e. external irreversibilities and internal irreversibilities.

In this chapter, we will use the FTT, the Maple software (Maple 13) and a flowchart algorithm, analytically establish the expressions of the objective functions, determine their maximum values and obtain the corresponding optimal performance parameters, respectively.

2.2. Presentation of the software used

2.2.1. Maple software

Maple is a symbolic and numeric computing environment as well as a multi-paradigm programming language. This software covers several areas of technical computing, such as symbolic mathematics, numerical analysis, data processing, visualization, and others. A toolbox, adds functionality for multidomain physical modeling and code generation. Maple's capacity for symbolic computing include those of a general-purpose computer algebra system. For instance, it can manipulate mathematical expressions and find symbolic solutions to certain problems, such as those arising from ordinary and partial differential equations. The latest version is from 2020.

In our work, we used Maple 2013 to perform symbolic operations.

2.2.2. MATLAB software

MATLAB “Matrix Laboratory” is a scripting language emulated by a development environment of the same name; it is used for numerical calculation purposes. Developed by The MathWorks, MATLAB allows you to manipulate matrices, display curves and data, implement algorithms, create user interfaces, and can interface with other languages such as C, C ++, Java, and Fortran. MATLAB users are from very different backgrounds such as engineering, science and economics in an industrial as well as research context. Matlab can be used alone or with toolbox. A command line interface, which is part of the MATLAB desktop, allows you to execute simple commands. Sequences of commands can be saved in a text file, typically with the MATLAB editor, in the form of a "script" or encapsulated in a function.

We got our results and displayed the curves from MATLAB software R2014a.

2.3. Thermodynamic analysis of an irreversible absorption heat pump with three-heat-reservoir

2.3.1. Application of the first law of thermodynamics and Newton's law of heat-transfer

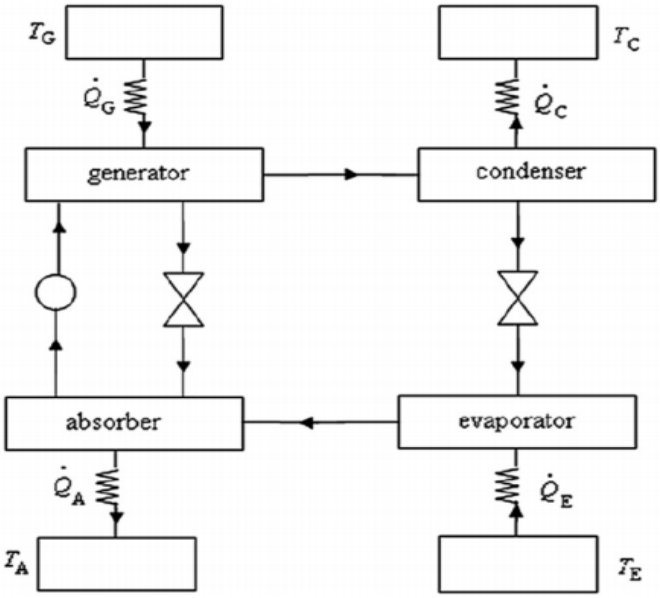

Fig.2.1. Symbolic diagram of an AHP (Medjo Nouadje et al., 2014).

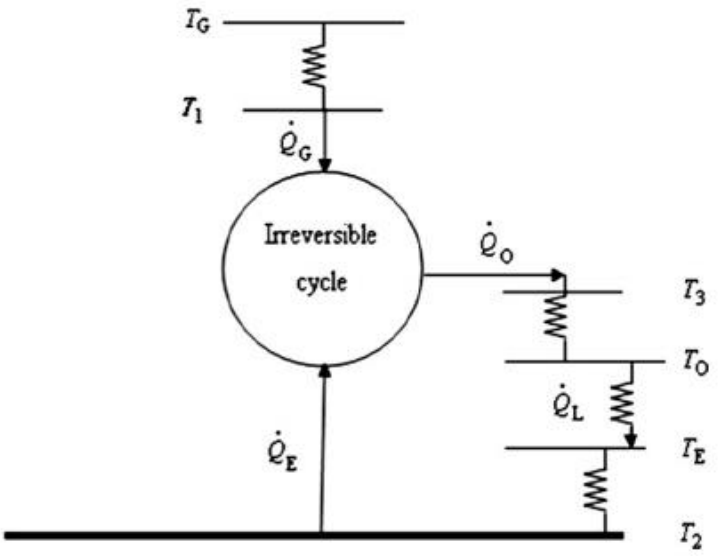

Fig. 2.2. The irreversible cycle model of a three-heat-reservoir AHP (Ahmadi et al., 2015).

The symbolic diagram giving the operation of the AHP is shown in **Fig. 2.1**. The liquid rich solution mixture coming from the absorber following an exothermic reaction of a heat rate $\dot{Q}_A$ is compressed by a pump, then evaporated in the generator by supplying a heat input rate $\dot{Q}_G$ coming from a heat source (renewable or non-renewable), this to separate the refrigerant from the

absorbent. Then the high pressure working fluid is condensed due to a discharge of a heat rate $\dot{Q}_C$ and the following liquid is sub-cooled. Finally, the liquid obtained is expanded and then evaporated in the evaporator by extracting a heat rate $\dot{Q}_E$ from the environment (heat sink). The vapour that emanates is super-heated and absorbed in a weak absorbent-refrigerant mixture. The weak solution goes from the generator to the absorber to be able to absorb the refrigerant and thus complete the cycle. Thoughts taken into account are intended to approximate the study to real operating conditions. First thought is the influences of internal dissipations during the flow of the absorbent-refrigerant mixture, from the absorber to the generator under a high pressure and during the flow of the refrigerant, from the condenser to the evaporator under a low pressure expansion. Second thought is the influences of external irreversibilities and finite heat resistances caused by finite temperature differences between the condenser, absorber and the evaporator which is in a heat sink (environment) at temperature T_{env} as shown in **Fig. 2.2**.

The first law of thermodynamics can be written from **Fig. 2.2** using the Refs. Ngouateu Wouagfack and Tchinda (2011a, 2011b, 2012a, 2012b, 2014), Medjo Nouadje et al. (2014, 2016) and Ahmadi et al. (2015, 2016).

$$\dot{Q}_G + \dot{Q}_E - \dot{Q}_C - \dot{Q}_A = 0 \tag{2.1}$$

By considering $\dot{Q}_O = \dot{Q}_C + \dot{Q}_A$, Eq. (2.1) becomes:

$$\dot{Q}_G + \dot{Q}_E - \dot{Q}_O = 0 \tag{2.2}$$

The Newton's law of heat transfer states that the heat exchanged between a wall of heat-transfer area S of a solid body at the temperature T and the surrounding fluid are deduced from Refs. Chen et al. (2005a), Ahmadi et al. (2014a), Huang et al. (2008), Ngouateu Wougfack and Tchinda (2011a, 2012a, 2012b, 2014), Medjo Nouadje et al. (2014, 2016), Ahmadi et al. (2015) and Ahmadi and Ahmadi (2016).

$$\dot{Q} = hS\Delta T \tag{2.3}$$

We deduce the finite heat-transfer law in the different components:

$$\dot{Q}_G = U_G A_G \left(T_G - T_1\right) \tag{2.4}$$

$$\dot{Q}_E = U_E A_E \left(T_E - T_2\right) \tag{2.5}$$

$$\dot{Q}_O = U_O A_O \left(T_3 - T_O\right) \tag{2.6}$$

with $A_O = A_A + A_C$ and $T_O = T_A = T_C$ (2.7)

The heat loss due to the influence of the surrounding environment thanks to the convective exchange of the heat resistances (Ngouateu Wouagfack and Tchinda, 2012a) are evaluated between the absorber-condenser assembly and the evaporator:

$$\dot{Q}_L = K_L \left(T_O - T_E\right) \tag{2.8}$$

A_G, A_E, A_A, A_C and A_O are the heat-transfer areas of the heat exchangers in the generator, the evaporator, the absorber, the condenser and the absorber-condenser assembly respectively and are expressed in $\left(\mathrm{m}^2\right)$. U_G, U_E and U_O are the coefficients of heat transfer by convection in $\left(\mathrm{Wm}^{-2}\mathrm{K}^{-1}\right)$ respectively of the generator, the evaporator and the absorber-condenser assembly. $\dot{Q}_L$ in $\left(\mathrm{W}\right)$ and K_L the thermal conductivity of the heat leakage in $\left(\mathrm{WK}^{-1}\right)$.

Moreover the total heat-transfer area of the heat exchangers is evaluated by the relation (2.9):

$$A = A_G + A_E + A_O \tag{2.9}$$

2.3.2. Application of the second law of thermodynamics

Historically, the irreversibility of certain phenomena gave rise to the second law of thermodynamics. As a result, when there is degradation of energy at the time of a transformation, it is known as irreversible thus the importance and utility of the extensive size entropy. The application of the second law of thermodynamics to the system is due to actual operating considerations of AHP. These considerations lead to two internal irreversibility factors I_1 and I_2 which represent the heat loss rate generated during the passage of the working fluid respectively between the absorber and the generator and between the condenser and the evaporator. By applying the second law of thermodynamics still called Clausius inequality as in the Refs. Ngouateu Wougfack and Tchinda (2011a, 2011b, 2012a), Medjo Nouadje et al. (2014) and Ahmadi and Ahmadi (2016), we obtain:

$$\oint \frac{\delta \dot{Q}}{T} = \frac{\dot{Q}_G}{T_1} + \frac{\dot{Q}_E}{T_2} - \frac{\dot{Q}_O}{T_3} < 0 \tag{2.10}$$

where T_1, T_2 and T_3 are the temperatures of the working liquid respectively in the generator, the evaporator and the absorber-condenser assembly in $\left(\mathrm{K}\right)$.

By introducing the two internal irreversibilities into **Eq. (2.10)**, we obtain a quantitative and qualitative entropy relation assessment which will enable us to minimize the degradation of energy and the influences of the irreversibilities in our system. We obtain:

$$\frac{\dot{Q}_G}{T_1}=\frac{\dot{Q}_A}{I_1T_3}\quad (I_1\geq 1)$$

$$\frac{\dot{Q}_E}{T_2}=\frac{\dot{Q}_C}{I_2T_3}\quad (I_2\geq 1) \tag{2.11}$$

Considering the **Eqs. (2.10)** and **(2.11)**, we obtain for an irreversible system ($I_1 > 1$ and $I_2 > 1$) :

$$\frac{\dot{Q}_G}{T_1}+\frac{\dot{Q}_E}{T_2}-\frac{\dot{Q}_A}{I_1T_3}-\frac{\dot{Q}_C}{I_2T_3}=0 \tag{2.12}$$

For a system with an internal irreversibility used in the Refs. Ngouateu Wouagfack and Tchinda (2011a, 2012a) and Ahmadi and Ahmadi (2016), **Eq. (2.12)** becomes:

$$\frac{\dot{Q}_G}{T_1}+\frac{\dot{Q}_E}{T_2}-\frac{\dot{Q}_O}{IT_3}=0 \tag{2.13}$$

While for an endoreversible system ($I_1=I_2=1$), **Eq. (2.12)** becomes:

$$\frac{\dot{Q}_G}{T_1}+\frac{\dot{Q}_E}{T_2}-\frac{\dot{Q}_O}{T_3}=0 \tag{2.14}$$

2.3.3. Thermo-ecological analysis

2.3.3.1. Performance parameters

By using the **Eqs. (2.2)**, **(2.4)-(2.9)** and **(2.12)**, the coefficient of performance of an irreversible AHP is following:

$$COP=\frac{\dot{Q}_O-\dot{Q}_L}{\dot{Q}_G}=\frac{\dot{Q}_O}{\dot{Q}_G}\left(1-\frac{\dot{Q}_L}{\dot{Q}_O}\right)=\frac{T_3\left(I_1T_2-I_2T_1\right)}{T_1\left(T_2-I_2T_3\right)}$$
$$\left(1-\xi\left(T_O-T_E\right)\left(\frac{T_3\left(T_2-I_2T_3\right)}{U_G\left(T_G-T_1\right)T_3\left(I_1T_2-I_2T_1\right)}+\frac{T_2\left(I_1T_3-T_1\right)}{U_E\left(T_E-T_2\right)T_3\left(I_1T_2-I_2T_1\right)}+\frac{1}{U_O\left(T_3-T_O\right)}\right)\right) \tag{2.15}$$

where $\xi=K_L/A$ is a heat leakage coefficient by the system and is expressed in $\left(\mathrm{WK^{-1}m^{-2}}\right)$.

The Specific heating load is obtained from the Eqs. (2.4)-(2.9) :

$$q=\frac{\dot{Q}_O-\dot{Q}_L}{A}=\left(\frac{T_3\left(T_2-I_2T_3\right)}{U_G\left(T_G-T_1\right)T_3\left(I_1T_2-I_2T_1\right)}+\frac{T_2\left(I_1T_3-T_1\right)}{U_E\left(T_E-T_2\right)T_3\left(I_1T_2-I_2T_1\right)}+\frac{1}{U_O\left(T_3-T_O\right)}\right)^{-1}-\xi\left(T_O-T_E\right) \tag{2.16}$$

The specific entropy generation rate is the entropy produced per unit of heat-transfer area generated by the system. The specific entropy generation rate is as follows of the **Eqs. (2.4)-(2.8)** and **(2.12)**:

$$S=\frac{\dot{\sigma}}{A}=\frac{\frac{\dot{Q}_O-\dot{Q}_L}{T_O}-\frac{\dot{Q}_G}{T_G}-\frac{\dot{Q}_E-\dot{Q}_L}{T_E}}{A}=$$
$$\left(\frac{1}{T_E}-\frac{1}{T_O}\right)\left(\begin{array}{l}\xi\left(T_O-T_E\right)+\left(\zeta_r\frac{T_1\left(T_2-I_2T_3\right)}{T_3\left(I_1T_2-I_2T_1\right)}-1\right)\\ \left(\frac{T_3\left(T_2-I_2T_3\right)}{U_G\left(T_G-T_1\right)T_3\left(I_1T_2-I_2T_1\right)}+\frac{T_2\left(I_1T_3-T_1\right)}{U_E\left(T_E-T_2\right)T_3\left(I_1T_2-I_2T_1\right)}+\frac{1}{U_O\left(T_3-T_O\right)}\right)^{-1}\end{array}\right) \quad (2.17)$$

Where $\zeta_r=\left(1-\frac{T_E}{T_G}\right)\Big/\left(1-\frac{T_E}{T_O}\right)$ is the coefficient of performance of a heat pump ideal cycle with three-heat-reservoir.

$\dot{\sigma}$ being the entropy generated by the system described in **Fig. 2.2** and is expressed in $\left(\mathrm{WK}^{-1}\right)$ and S in $\left(\mathrm{WK}^{-1}\mathrm{m}^{-2}\right)$.

Exergy-based ecological function (Angulo-Brown, 1991; Sun et al., 2005; Chen et al., 2007b, 2019; Qin et al., 2017 and Frikha and Abid, 2016) is given by **Eqs. (2.2, 2.4-2.9, 2.12)** and **(2.17)**:

$$E=\left(\dot{Q}_O-\dot{Q}_L\right)\left(1-\frac{T_{env}}{T_0}\right)-T_{env}\dot{\sigma}=$$
$$A\left(\begin{array}{l}\xi\left(T_0-T_E\right)\left(\frac{2T_{env}}{T_0}-\frac{T_{env}}{T_0}-1\right)+\left(1-\frac{T_{env}}{T_0}-T_{env}\left(\frac{1}{T_E}-\frac{1}{T_O}\right)\left(\zeta_r\frac{T_1\left(T_2-I_2T_3\right)}{T_3\left(I_1T_2-I_2T_1\right)}-1\right)\right)\\ \left(\frac{T_1\left(T_2-I_2T_3\right)}{U_G\left(T_G-T_1\right)T_3\left(I_1T_2-I_2T_1\right)}+\frac{T_2\left(I_1T_3-T_1\right)}{U_E\left(T_E-T_2\right)T_3\left(I_1T_2-I_2T_1\right)}+\frac{1}{U_O\left(T_3-T_O\right)}\right)^{-1}\end{array}\right) \quad (2.18)$$

Where the term $\left(\dot{Q}_O-\dot{Q}_L\right)\left(1-\frac{T_{env}}{T_0}\right)$ represents the output exergy of the THR AHP cycle and $T_{env}\dot{\sigma}$ is the exergy destroyed or the loss rate of availability.

The ecological coefficient of performance given by Refs. Chen et al. (2007a), Ngouateu Wouagfack and Tchinda (2011a, 2011b, 2014), Medjo Nouadje et al. (2014, 2016), Ahmadi et al. (2015) and Ahmadi and Ahmadi (2016).of an irreversible THR AHP is the ratio between the specific heating load and the exergy loss (product of the entropy generation rate and the

temperature of the environment). The *ECOP* characterizes the impact of energy lost on the environment.

$$ECOP = \frac{\dot{Q}_O - \dot{Q}_L}{T_{env}\dot{\sigma}} = \frac{1}{T_{env}\left(\frac{1}{T_E} - \frac{1}{T_O}\right)} \left(\frac{\zeta_r \frac{T_1(T_2 - I_2T_3)}{T_3(I_1T_2 - I_2T_1)} - 1}{1 - \xi(T_O - T_E)\left(\frac{T_3(T_2 - I_2T_3)}{U_G(T_G - T_1)T_3(I_1T_2 - I_2T_1)} + \frac{T_2(I_1T_3 - T_1)}{U_E(T_E - T_2)T_3(I_1T_2 - I_2T_1)} + \frac{1}{U_O(T_3 - T_O)} \right)} - 1 \right)^{-1} \quad (2.19)$$

When $I_1 = I_2 = I$ we find the results of Ngouateu Wouagfack and Tchinda (2012a).

2.3.3.2. Optimization of an absorption heat pump with multi-irreversibilities: Maximum ecological coefficient of performance (ECOP) and maximum Exergy-based ecological criterion (E)

$$\text{Let, } a = \frac{I_1T_3}{T_1} \text{ ; } b = \frac{I_2T_3}{T_2} \text{ and } c = T_3 \quad (2.20)$$

we can rewrite in a simpler way $ECOP$ objective function of performance.

$$ECOP = \frac{1}{T_{env}\left(\frac{1}{T_E} - \frac{1}{T_O}\right)} \left(\frac{\zeta_r\left(\frac{1-b}{a-b}\right)}{1 - \frac{\xi(T_O - T_E)}{b-a}\left(\frac{a(b-1)}{U_G(aT_G - I_1c)} + \frac{b(1-a)}{U_E(bT_E - I_2c)} + \frac{b-a}{U_O(c - T_O)} \right)} - 1 \right)^{-1} \quad (2.21)$$

The optimization of the system must reach the maximum values of $ECOP$ objective function, which implies that one must determine the optimal temperatures up stream T_{1op}, T_{2op} and T_{3op}. $ECOP_{\max}$ corresponds to the maximum of $ECOP$ objective function obtained by solving the first order partial differentials equations to the variables a, b and c.

$$\frac{\partial ECOP}{\partial a} = 0 \text{ ; } \frac{\partial ECOP}{\partial b} = 0 \text{ and } \frac{\partial ECOP}{\partial c} = 0 \quad (2.22)$$

However, the optimization of the system using exergy-based ecological objective function makes it possible to obtain the corresponding optimal performance parameters. At the maximum criterion E that is $E_{\max,E}$ we have T_1^*, T_2^*, T_3^*, COP^*, S^* and q^*. $E_{\max,E}$ is obtained by solving the partial differential equation.

$$\frac{\partial E}{\partial a} = 0 \text{ ; } \frac{\partial E}{\partial b} = 0 \text{ and } \frac{\partial E}{\partial c} = 0 \quad (2.23)$$

By solving the **Eqs. (2.22**, **2.23)** and substituting their values of the variables a , b and c into **Eq. (2.20)**, we obtain the following double equality:

$$\sqrt{I_1 U_G}\left(\frac{T_G}{T_1}-1\right)=\sqrt{I_2 U_E}\left(\frac{T_E}{T_2}-1\right)=\sqrt{U_O}\left(1-\frac{T_O}{T_3}\right) \tag{2.24}$$

Using the relationships **(2.22)** and **(2.24)**, optimal temperatures at maximum $ECOP$ are obtained;

$$T_{1op}=\frac{I_1 T_G}{b_1\left(1-\frac{T_O}{D}\right)+I_1}$$

$$T_{2op}=\frac{I_2 T_E}{b_2\left(1-\frac{T_O}{D}\right)+I_2}$$

$$T_{3op}=D \tag{2.25}$$

where $D=\dfrac{\left(I_2 U_O T_E-\xi\left(T_O-T_E\right)\left(b_2+I_2\right)b_2\right)T_O+\sqrt{\left(I_2 U_O\left(I_2 T_O-T_E\right)+\xi\left(T_O-T_E\right)\left(b_2+I_2\right)^2\right)I_2\left(T_O-T_E\right)T_E T_O \xi}}{I_2 U_O T_E-\xi\left(T_O-T_E\right)\left(b_2+I_2\right)^2}$

and $b_1=\sqrt{\dfrac{I_1 U_O}{U_G}}$, $b_2=\sqrt{\dfrac{I_2 U_O}{U_E}}$ (2.26)

Substituting **Eqs. (2.25)** into **Eqs. (2.15)-(2.19)** yields the maximum *ECOP*:

$$ECOP_{\max}=\frac{1}{T_{env}\left(\frac{1}{T_E}-\frac{1}{T_O}\right)}\left(\frac{\zeta_r T_G\left(T_E-b_2\left(D-T_O\right)-I_2 D\right)U_O\left(D-T_O\right)}{\left(\begin{array}{l}U_O\left(D-T_O\right)\left(\left(D-T_O\right)\left(T_E b_1-T_G b_2\right)+D\left(I_1 T_E-I_2 T_G\right)\right)-\\ \xi\left(T_O-T_E\right)\left(\beta U_O+\left(D-T_O\right)\left(T_E b_1-T_G b_2\right)+D\left(I_1 T_E-I_2 T_G\right)\right)\end{array}\right)-1\right)^{-1} \tag{2.27}$$

and the optimal coefficient of performance $\left(COP_{op}\right)$, the optimal specific heating load $\left(q_{op}\right)$ and the optimal specific entropy generation rate $\left(S_{op}\right)$ at the maximum **ECOP** conditions, respectively, as :

$$COP_{op}=\frac{U_O\left(D-T_O\right)\left(\left(D-T_O\right)\left(T_E b_1-T_G b_2\right)+D\left(I_1 T_E-I_2 T_G\right)\right)-\xi\left(T_O-T_E\right)\left(\beta U_0+\left(D-T_O\right)\left(T_E b_1-T_G b_2\right)+D\left(I_1 T_E-I_2 T_G\right)\right)}{T_G\left(T_E-b_2\left(D-T_O\right)-I_2 D\right)U_O\left(D-T_O\right)} \tag{2.28}$$

$$q_{op}=\frac{U_O\left(D-T_O\right)\left(\left(D-T_O\right)\left(T_E b_1-T_G b_2\right)+D\left(I_1 T_E-I_2 T_G\right)\right)}{\beta U_0+\left(D-T_O\right)\left(T_E b_1-T_G b_2\right)+D\left(I_1 T_E-I_2 T_G\right)}-\xi\left(T_O-T_E\right) \tag{2.29}$$

$$S_{op}=\left(\frac{1}{T_E}-\frac{1}{T_O}\right)\left(\xi\left(T_O-T_E\right)+\frac{\left(\zeta_r T_G\left(T_E-b_2\left(D-T_O\right)-I_2 D\right)-\left(D-T_O\right)\left(T_E b_1-T_G b_2\right)-D\left(I_1 T_E-I_2 T_G\right)\right)U_O\left(D-T_O\right)}{\beta U_0+\left(D-T_O\right)\left(T_E b_1-T_G b_2\right)+D\left(I_1 T_E-I_2 T_G\right)}\right) \tag{2.30}$$

with

$$\beta=\frac{U_E b_2\left(b_1\left(D-T_O\right)+I_1 D\right)\left(T_E-b_2\left(D-T_O\right)-I_2 D\right)+U_G b_1\left(b_2\left(D-T_O\right)+I_2 D\right)\left(b_1\left(D-T_O\right)+I_1 D-T_G\right)}{U_G U_E b_1 b_2} \quad (2.31)$$

From **Eqs. (2.2)**, **(2.4)-(2.6)**, **(2.9) and (2.25)** we find that, when THR AHP is operated in the state of maximum *ECOP*, the relations between the heat-transfer areas of the heat exchangers and the total heat-transfer area are determined by:

$$\frac{\left(A_G\right)_{op}}{A}=\frac{U_E U_O b_2\left(b_1\left(D-T_O\right)+I_1 D\right)\left(b_2\left(D-T_O\right)+I_2 D-T_E\right)}{\left(\begin{array}{l}U_E U_O b_2\left(b_1\left(D-T_O\right) I_1 D\right)\left(b_2\left(D-T_O\right)+I_2 D-T_E\right)+U_G U_E b_1 b_2 U_G b_1\left(T_G\left(b_2\left(D-T_O\right)+I_2 D\right)-T_E\left(b_1\left(D-T_O\right)+I_1 D\right)\right)+\\ U_G U_O b_1\left(b_2\left(D-T_O\right)+I_2 D\right)\left(T_G-b_1\left(D-T_O\right)-I_1 D\right)\end{array}\right)} \quad (2.32)$$

$$\frac{\left(A_E\right)_{op}}{A}=\frac{U_G U_O b_1\left(b_1\left(D-T_O\right)+I_2 D\right)\left(b_1\left(D-T_O\right)+I_1 D-T_G\right)}{\left(\begin{array}{l}U_G U_O b_1\left(b_2\left(D-T_O\right)+I_2 D\right)\left(b_1\left(D-T_O\right)+I_1 D-T_G\right)+U_G U_E b_1 b_2\left(T_E\left(b_1\left(D-T_O\right)+I_1 D\right)-T_G\left(b_2\left(D-T_O\right)+I_2 D\right)\right)-\\ U_E U_O b_2\left(b_1\left(D-T_O\right)+I_1 D\right)\left(b_2\left(D-T_O\right)+I_1 D-T_G\right)\end{array}\right)} \quad (2.33)$$

$$\frac{\left(A_E\right)_{op}}{A}=\frac{U_G U_E b_1 b_2\left(T_G\left(b_2\left(D-T_O\right)+I_2 D\right)-T_E\left(b_1\left(D-T_O\right)+I_1 D\right)\right)}{\left(\begin{array}{l}U_G U_E b_1 b_2\left(T_G\left(b_2\left(D-T_O\right)+I_2 D\right)-T_E\left(b_1\left(D-T_O\right)+I_1 D\right)\right)+U_E U_O b_2\left(b_1\left(D-T_O\right)+I_1 D\right)\left(b_2\left(D-T_O\right)+I_2 D-T_E\right)-\\ U_G U_O b_1\left(b_2\left(D-T_O\right)+I_2 D\right)\left(b_1\left(D-T_O\right)+I_1 D-T_G\right)\end{array}\right)} \quad (2.34)$$

2.3.4. Exergetic coefficient of performance, Exergy-based ecololgical and thermo-economic criteria

2.3.4.1. Characteristics parameters

The coefficient of performance (*COP*) and the specific heating load are obtained for THR AHP $\psi=\pi\Big/\dot{Q}_G=\left(\dot{Q}_O-\dot{Q}_L\right)\Big/\dot{Q}_G$ and $q=\pi/A=\left(\dot{Q}_O-\dot{Q}_L\right)\Big/A$ (2.35)

The **Eqs. (2.1)** and **(2.35)** of the AHP cycle provide the heat-transfer rates derived from the coefficient of performance and the heating load

$$\dot{Q}_G=\pi/\psi$$

$$\dot{Q}_E=\pi\left(1-\frac{1}{\psi}\right)+\dot{Q}_L$$

$$\dot{Q}_O=\pi+\dot{Q}_L \quad (2.36)$$

and **Eqs. (2.4-2.6)** and **(2.36)** the temperatures of the working fluid yields

$$T_1=T_G-\frac{\pi}{U_G A_G \psi}$$

$$T_2 = T_E - \frac{\pi\left(1-\frac{1}{\psi}\right)+\dot{Q}_L}{U_E A_E}$$

$$T_3 = T_O + \frac{\pi+\dot{Q}_L}{U_O A_O} \tag{2.37}$$

Substituting **Eqs. (2.36)** and **(2.37)** into **Eq. (2.12)** we obtain another expression of the second law of thermodynamics deriving from the heating load, coefficient of performance, two internal irreversibility factors, heat leakage, heat-transfer areas of heat exchangers and convective heat exchange coefficients in the different components. This expression is obtained from that of Qin et al. (2007) and Chen et al. (2005a, 2019) who established an expression between the heating load and the coefficient of performance by considering an overall internal irreversibility in FTL AHP and Qin et al. (2017) in turn established a similar expression in FTL AHT always with an overall internal irreversibility.

$$\psi\left(\frac{T_O}{\pi+\dot{Q}_L}+\frac{1}{U_O A_O}\right)^{-1} - I_1\left(\frac{T_G}{\pi}-\frac{1}{U_G A_G \psi}\right)^{-1} - I_2\left(\frac{T_E}{\pi(\psi-1)+\dot{Q}_L\psi}-\frac{1}{U_E A_E \psi}\right)^{-1} = 0 \tag{2.38}$$

2.3.4.2. Performance analysis

2.3.4.2.1. Exergetic coefficient of performance and exergy-based ecological criterion

The output exergy of the system THR AHP cycle is as follows

$$\dot{EX}_{out} = \left(\dot{Q}_O - \dot{Q}_L\right)\left(1-\frac{T_{env}}{T_O}\right) = \pi\left(1-\frac{T_{env}}{T_O}\right) \tag{2.39}$$

the input exergy of the system THR AHP cycle

$$\dot{EX}_{in} = \dot{Q}_G = \frac{\pi}{\psi} \tag{2.40}$$

and the exergy destroyed or the loss rate of availability

$$\dot{EX}_D = T_{env}\dot{\sigma} = T_{env}\left(\frac{\dot{Q}_O-\dot{Q}_L}{T_O}-\frac{\dot{Q}_G}{T_G}-\frac{\dot{Q}_E-\dot{Q}_L}{T_E}\right) = T_{env}\pi\left(\frac{1}{T_O}-\frac{T_E+(\psi-1)T_G}{T_E\psi}\right) \tag{2.41}$$

where $\dot{\sigma}$ is the entropy production rate is expressed in $\left(\mathrm{WK}^{-1}\right)$

As a result, exergy-based ecological function and previously used by Huang et al. (2008), Chen et al. (2007, 2019), Frikha et al. (2016) and Qin et al. (2017) on absorption system

$$E = \dot{EX}_{out} - \dot{EX}_D = T_{env}\pi\left(\frac{1}{T_{env}} - \frac{2}{T_O} + \frac{T_E + (\psi - 1)T_G}{T_E\psi}\right) \tag{2.42}$$

We can define the exergetic efficiency which is the ratio between output exergy and input exergy. Previously, authors such as Ust et al. (2007), Kilic and Kaynakli (2007), Kaushik and Arora (2009) and Liu et al. (2017) used and analyzed the thermal systems with this criterion. by the way, using the **Eqs. (2.39)** and **(2.40)** we have

$$ex = \frac{\dot{EX}_{out}}{\dot{EX}_{in}} = \psi\left(1 - \frac{T_{env}}{T_O}\right) \tag{2.43}$$

Also, the exergetic performance coefficient (EPC) used by Ust et al. (2007) is established as the ratio of output exergy to the loss rate of availability (entropy production rate) and allows a careful measurement of the energy required, added to the impact on the environment . Using **Eqs. (2.39) and (2.41)**, we obtain:

$$EPC = \frac{\dot{EX}_{out}}{\dot{EX}_D} = \frac{1 - \frac{T_{env}}{T_O}}{\frac{1}{T_O} - \frac{T_E + (\psi - 1)T_G}{T_G T_E \psi}} \tag{2.44}$$

2.3.4.2.2. Thermo-economic criterion

The thermo-economic criterion stated by Kodal et al. (2000a, 200b, 2002, 2003) and followed by Ahmadi et al. (2014a, 2014b), is the heating load per unit sum of the cost on the investment and the cost of the energy consumed. It takes into account the location of the system and the load to be provided by it.

$$f = \frac{\pi}{C_i + C_e} \tag{2.45}$$

where, $C_i = k_1 A$ and $C_e = k_2 \dot{Q}_G$ (2.46)

C_i is the cost of the investment in AHP and depends proportionally on the total heat exchange area. C_e is the cost of energy consumed and is proportionally dependent on the heat input rate. Again, k_1 and k_2 the capital cost for the unit heat-transfer area and the unit cost of energy. Considering $k = k_1/k_2$ as a thermo-economic parameter of dimension $\left(\mathrm{Wm^{-2}}\right)$, and substituting **Eq. (2.46)** into **Eq. (2.45)** we obtain

$$F = k_2 f = \frac{1}{\frac{k}{q} + \frac{1}{\psi}} \tag{2.47}$$

2.3.4.3. Optimization

2.3.4.3.1. Special cases

Eq. (2.38) can be written in many other forms neglecting internal and external irreversibility factors.

In the first case, where the heat resistances and the heat leakages which represent the flow of heat leaving the medium to be heated for the environment during the thermodynamic cycle are neglected. It follow that the heat leakage coefficient nullifies for an exoreversible system $\left(K_L = 0 \Rightarrow K_L / A = \xi = 0\right)$, **Eq. (2.38)** becomes

$$\psi\left(\frac{T_O}{\pi}+\frac{1}{U_O A_O}\right)^{-1}-I_1\left(\frac{T_G}{\pi}-\frac{1}{U_G A_G \psi}\right)^{-1}-I_2\left(\frac{T_E}{\pi(\psi-1)}-\frac{1}{U_E A_E \psi}\right)^{-1}=0 \tag{2.48}$$

The second case, where the heat losses are neglected: $\left(I_1 = I_2 = 1\right)$ that is to say for an endoreversible system, **Eq. (2.38)** becomes

$$\psi\left(\frac{T_O}{\pi+\dot{Q}_L}+\frac{1}{U_O A_O}\right)^{-1}-\left[\left(\frac{T_G}{\pi}-\frac{1}{U_G A_G \psi}\right)^{-1}+\left(\frac{T_E}{\pi(\psi-1)+\dot{Q}_L \psi}-\frac{1}{U_E A_E \psi}\right)^{-1}\right]=0 \tag{2.49}$$

The third case, where the heat resistances, the heat leakages and the heat losses are neglected ($K_L = 0 \Rightarrow K_L / A = \xi = 0$ and $I_1 = I_2 = 1$) that is to say for a reversible system, **Eq. (2.38)** becomes

$$\psi\left(\frac{T_O}{\pi}+\frac{1}{U_O A_O}\right)^{-1}-\left[\left(\frac{T_G}{\pi}-\frac{1}{U_G A_G \psi}\right)^{-1}+\left(\frac{T_E}{\pi(\psi-1)}-\frac{1}{U_E A_E \psi}\right)^{-1}\right]=0 \tag{2.50}$$

2.3.4.3.2. Flowchart optimization

The three decisive objective functions taken into consideration for our work are the thermo-economic criterion (F), the exergy-based ecological function (E) and the exergetic performance criterion (EPC). The maximum values of each objective function *EPC*, *E*, and *F* can be evaluated using the flowchart optimization algorithm (**Fig. 2.3**) thus used by the Refs. Su et al. (2017) and Chen et al. (2019). We obtain the maximum value of the exergetic performance criterion $EPC_{\max}$ which corresponds to the optimal values ψ_{EPC}, A_{EPC}, q_{EPC}, $\dot{EX}_{out-EPC}$ and $\dot{EX}_{D-EPC}$. Then we determine the maximum value of the exergy-based ecological criterion $E_{\max}$ which corresponds to the optimal values ψ_E, A_E, q_E, $\dot{EX}_{out-E}$ and $\dot{EX}_{D-E}$. Finally, in the same way, we obtain the maximum values of the thermo-economic criterion $F_{\max}$ to which corresponds the optimal values ψ_F, A_F, q_F, $\dot{EX}_{out-F}$ and $\dot{EX}_{D-F}$.

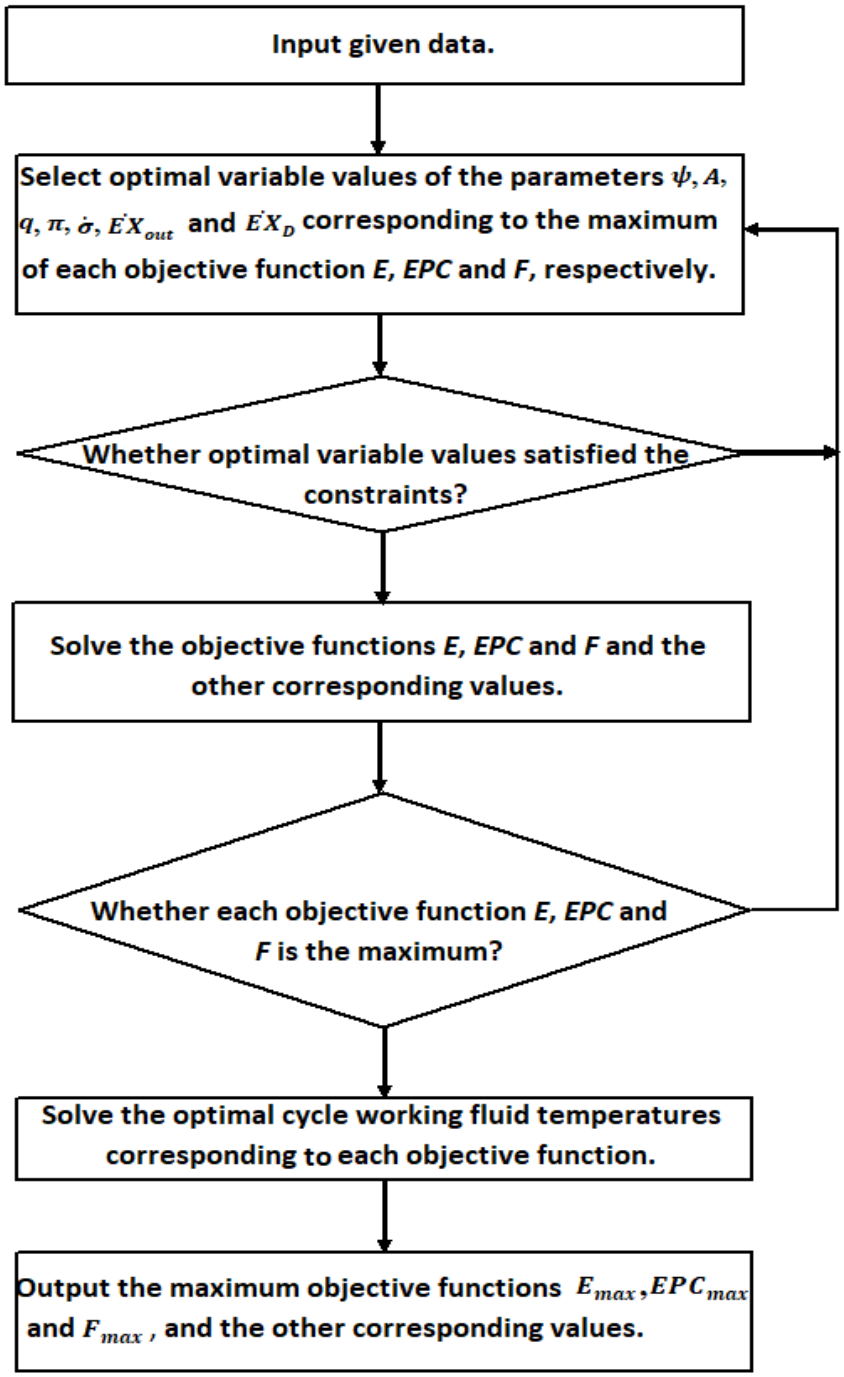

Fig. 2.3. The optimization flowchart.

2.4. Irreversible four-temperature-level absorption heat pump cycle model single effect

2.4.1. Finite time thermodynamics

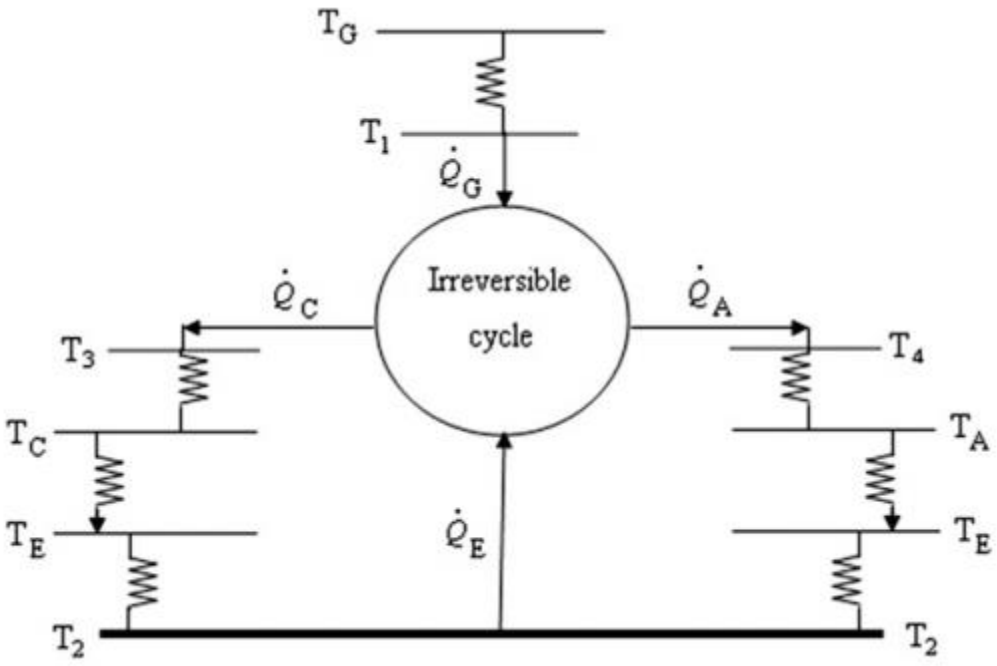

Fig. 2.4. The irreversible cycle model of a FTL AHP (Ngouateu Wouagfack and Tchinda, 2012).

The real operating conditions of the AHP in **Fig. 2.1** take into consideration the heat resistances, the heat leakages and the heat losses represented by two internal irreversibility factors. The irreversible cycle of FTL AHP as shown in **Fig. 2.4** allows us to write the first law of finite time thermodynamics (FTT). Nevertheless, the localized finite heat resistances and heat leakages in the absorber, condenser and evaporator heat exchangers makes it possible to model a cycle by relying on the refs. Ngouateu Wouagfack and Tchinda (2011a, 2011b, 2012a, 2012b, 2014), Medjo Nouadje et al. (2014, 2016) and Ahmadi et al. (2015, 2016).

This being so, the heat-exchange rates between the working fluid and the external heat reservoirs in the heat exchangers are obtained under the finite temperature difference, from Newton's law of heat-transfer.

$$\dot{Q}_G = U_G A_G \left(T_G - T_1\right)$$

$$\dot{Q}_E = U_E A_E \left(T_E - T_2\right)$$

$$\dot{Q}_C = U_C A_C \left(T_3 - T_C\right)$$

$$\dot{Q}_A = U_A A_A \left(T_4 - T_A\right) \tag{2.51}$$

Besides, the external irreversibilities or heat leakage between the space to be heated and the environment are reflected (Ngouateu Wouagfack and Tchinda, 2012b, 2014):

$$\dot{Q}_L = \dot{Q}_{L1} + \dot{Q}_{L2} = K_L\left(T_C - T_E\right) + K_L\left(T_A - T_E\right) \tag{2.52}$$

$\dot{Q}_L$ in (W), is the heat leakage from the heat sink to the cooled space, $\dot{Q}_{L1}$ and $\dot{Q}_{L2}$ are the heat leakages from the heat sink to the cooled space between the condenser and the evaporator and between the absorber and the evaporator respectively. K_L is the thermal conductivity due to heat leakage in $\left(\mathrm{WK}^{-1}\right)$. Also, the total of heat-transfer surfaces area in the external heat reservoirs of components such as generator, evaporator, absorber and condenser.

$$A = A_G + A_E + A_A + A_C \tag{2.53}$$

Furthermore, internal dissipations or heat losses reflecting the entropy generation rate lead to exploit the second law of thermodynamics. This law illustrates the irreversibility process of the thermodynamic cycle and is written

$$\Delta S_A + \Delta S_C - \Delta S_G - \Delta S_E > 0, \text{ where, } \Delta S_A = \dot{Q}_A/T_4 \text{ ; } \Delta S_C = \dot{Q}_C/T_3 \text{ ; } \Delta S_E = \dot{Q}_E/T_2 \text{ and } \Delta S_G = \dot{Q}_G/T_1 . \tag{2.54}$$

with T_1, T_2, T_3 and T_4 are expressed in (K) and represent the working fluid temperatures in the external heat transfer reservoirs such as the generator, evaporator, condenser and absorber, respectively. Then, we insert the two internal irreversibility factors caused by pressure drops and friction between the fluid particles and between the working fluid and the walls. This during the process of heat transfer between the external heat reservoirs of the heat exchangers and the working fluid in the absorber-generator connection (I_1) and in the condenser-evaporator connection (I_2). Xiling et al. (2011)], did so in the FTL AHPs and Medjo Nouadje et al. (2014) is done in THR ARs; so we have

$$I_1 = \Delta S_A/\Delta S_G \ \ (I_1 \geq 1) \text{ and } I_2 = \Delta S_C/\Delta S_E \ \ (I_2 \geq 1) \tag{2.55}$$

Substituting Eq. (2.55) into Eq. (2.54) we obtain

$$\Delta S_A + \Delta S_C - I_1\Delta S_G - I_2\Delta S_E = 0 \tag{2.56}$$

2.4.2.. Performance analysis

The performance analysis system at four-temperature-levels allows us to determine the coefficient of performance (*COP*), the specific heating load (*q*), the entropy generation rate (*S*) and the ecological coefficient of performance (*ECOP*). For this, taking into account the **Eqs. (2.1)**, **(2.51-2.56)** these performance criteria are written in this order according to **Eqs. (2.57)**, **(2.59)**, **(2.61)** and **(2.63)**.

The *COP* is the ratio between the heating load and the rate of heat transfer in the generator

$$COP=\frac{\pi}{\dot{Q}_G}=\frac{\dot{Q}_A+\dot{Q}_C-\dot{Q}_L}{\dot{Q}_G}=\frac{\dot{Q}_C}{\dot{Q}_G}\left(1+\frac{\dot{Q}_A}{\dot{Q}_C}-\frac{\dot{Q}_L}{\dot{Q}_C}\right)=\frac{T_1^{-1}-T_2^{-1}}{(I_2T_3)^{-1}+m(I_1T_4)^{-1}-(1+m)T_2^{-1}}$$
$$\left(1+m-C_1\left(\frac{1}{U_C(T_3-T_C)}+\frac{m}{U_A(T_4-T_A)}+\frac{(I_2T_3)^{-1}+m(I_1T_4)^{-1}-(1+m)T_2^{-1}}{U_G(T_G-T_1)(T_1^{-1}-T_2^{-1})}+\frac{(I_2T_3)^{-1}+m(I_1T_4)^{-1}-(1+m)T_1^{-1}}{U_E(T_E-T_2)(T_2^{-1}-T_1^{-1})}\right)\right) \quad (2.57)$$

Where $m=\dot{Q}_A/\dot{Q}_C$; $C_1=\xi(T_A-T_E+T_C-T_E)$ and $\xi=K_L/A$. (2.58)

m being the ratio of the rejected heat between the absorber and the condenser and ξ the set of external irreversibilities, also called coefficient of heat loss, is expressed in $\left(\mathrm{Wm^{-2}K^{-1}}\right)$.

The expression of the specific heating load is as follows;

$$q=\frac{\pi}{A}=\frac{\dot{Q}_A+\dot{Q}_C-\dot{Q}_L}{A}=(1+m)\left(\begin{array}{l}\dfrac{1}{U_C(T_3-T_C)}+\dfrac{m}{U_A(T_4-T_A)}+\\ \dfrac{(I_2T_3)^{-1}+m(I_1T_4)^{-1}-(1+m)T_2^{-1}}{U_G(T_G-T_1)(T_1^{-1}-T_2^{-1})}+\dfrac{(I_2T_3)^{-1}+m(I_1T_4)^{-1}-(1+m)T_1^{-1}}{U_E(T_E-T_2)(T_2^{-1}-T_1^{-1})}\end{array}\right)-C_1 \quad (2.59)$$

We get the specific entropy generation rate at the same time

$$S=\frac{\dot{\sigma}}{A}=\frac{\dfrac{\dot{Q}_A-K_L(T_A-T_E)}{T_A}+\dfrac{\dot{Q}_C-K_L(T_C-T_E)}{T_C}-\dfrac{\dot{Q}_G}{T_G}-\dfrac{\dot{Q}_E-K_L(T_A-T_E+T_C-T_E)}{T_E}}{A} \quad (2.60)$$

Substituting the **Eqs. (2.1)**, **(2.51-2.54)** and **(2.56)** into the **Eq. (2.60)** we finally obtain:

$$S=C_4+C_5\frac{(I_2T_3)^{-1}+m(I_1T_4)^{-1}-(1+m)T_2^{-1}}{T_1^{-1}-T_2^{-1}}+\left(C_2+C_3\frac{(I_2T_3)^{-1}+m(I_1T_4)^{-1}-(1+m)T_2^{-1}}{T_1^{-1}-T_2^{-1}}\right)$$
$$\left(\frac{1+m}{\dfrac{1}{U_C(T_3-T_C)}+\dfrac{m}{U_A(T_4-T_A)}+\dfrac{(I_2T_3)^{-1}+m(I_1T_4)^{-1}-(1+m)T_2^{-1}}{U_G(T_G-T_1)(T_1^{-1}-T_2^{-1})}+\dfrac{(I_2T_3)^{-1}+m(I_1T_4)^{-1}-(1+m)T_1^{-1}}{U_E(T_E-T_2)(T_2^{-1}-T_1^{-1})}}-C_1\right) \quad (2.61)$$

Where
$$C_2=\frac{1}{1+m}\left(\frac{1}{T_C}+\frac{m}{T_A}\right)-\frac{1}{T_E};C_3=\frac{1}{1+m}\left(\frac{1}{T_E}-\frac{1}{T_G}\right);$$
$$C_4=\xi(T_A-T_E+T_C-T_E)\left(\frac{1}{1+m}\left(\frac{1}{T_C}+\frac{m}{T_A}\right)-\frac{1}{T_E}\right)+\xi\left(\frac{T_E}{T_C}+\frac{T_E}{T_A}+\frac{T_A}{T_E}+\frac{T_C}{T_E}-4\right);$$
$$C_5=\frac{\xi(T_A-T_E+T_C-T_E)}{1+m}\left(\frac{1}{T_E}-\frac{1}{T_G}\right) \quad (2.62)$$

The ecological coefficient of performance (*ECOP*) given by the Refs. Ngouateu Wouagfack and Tchinda (2011a, 2011b, 2012a, 2012b, 2014), Medjo Nouadje et al. (2014, 2016), Ahmadi and Ahmadi (2016), Ahmadi et al. (2016) and Ust et al. (2017) of the real FTL AHP is

the ratio between the specific heating or cooling load and the exergy loss (product of the entropy generation rate by the temperature of environment). The *ECOP* characterizes the impact of energy lost in the environment.

$$ECOP = \frac{\pi}{T_{env}\dot{\sigma}} = \frac{1}{T_{env}}\left(C_2 + C_3\frac{\left(I_2T_3\right)^{-1} + m\left(I_1T_4\right)^{-1} - \left(1+m\right)T_2^{-1}}{T_1^{-1} - T_2^{-1}} + \left(C_4 + C_5\frac{\left(I_2T_3\right)^{-1} + m\left(I_1T_4\right)^{-1} - \left(1+m\right)T_2^{-1}}{T_1^{-1} - T_2^{-1}}\right)^{-1}\left(\frac{1+m}{\left(\frac{1}{U_C\left(T_3 - T_C\right)} + \frac{m}{U_A\left(T_4 - T_A\right)} + \frac{\left(I_2T_3\right)^{-1} + m\left(I_1T_4\right)^{-1} - \left(1+m\right)T_2^{-1}}{U_G\left(T_G - T_1\right)\left(T_1^{-1} - T_2^{-1}\right)} + \frac{\left(I_2T_3\right)^{-1} + m\left(I_1T_4\right)^{-1} - \left(1+m\right)T_1^{-1}}{U_E\left(T_E - T_2\right)\left(T_2^{-1} - T_1^{-1}\right)}\right)} - C_1\right)^{-1}\right)^{-1} \quad (2.63)$$

2.4.3. Exergetic analysis and optimization

2.4.3.1. Exergetic analysis

The output exergy is given by the relation:

$$EX_{out} = \left(\dot{Q}_C - \dot{Q}_{L1}\right)\left(1 - \frac{T_{env}}{T_C}\right) + \left(\dot{Q}_A - \dot{Q}_{L2}\right)\left(1 - \frac{T_{env}}{T_A}\right) \quad (2.64)$$

The input exergy is given by the relation:

$$EX_{in} = \dot{Q}_G \quad (2.65)$$

The exergy-based ecological criterion (Angulo-Brown, 1991; Sun et al., 2005; Chen et al., 2007, 2019; Ahmadi et al., 2016; Frikha and Abid, 2016 and Qin et al., 2017) is given by:

$$E = EX_{out} - T_{env}\dot{\sigma} \quad (2.66)$$

Where $T_{env}\dot{\sigma}$ is the exergy destruction rate or the loss rate of availability.

This makes it possible to define the exergetic efficiency which is the ratio between the output exergy and the input exergy. It had been previously written by the authors Ust et al. (2007), Kilic and Kaynakli (2007), Kaushik and Arora (2009) and Liu et al. (2017), so we have for the system using the **Eqs. (2.1)**, **(2.51)**, **(2.53)**, **(2.54)**, **(2.64)** and **(2.65)**:

$$ex = \frac{EX_{out}}{EX_{in}} = \left(\frac{T_1^{-1} - T_2^{-1}}{(I_2T_3)^{-1} + m(I_1T_4)^{-1} - (1+m)T_2^{-1}} \right)$$

$$\left(m\xi_1 + \xi_2 - C_6 \left(\frac{1}{U_C(T_3 - T_C)} + \frac{m}{U_A(T_4 - T_A)} + \frac{(I_2T_3)^{-1} + m(I_1T_4)^{-1} - (1+m)T_2^{-1}}{U_G(T_G - T_1)(T_1^{-1} - T_2^{-1})} + \frac{(I_2T_3)^{-1} + m(I_1T_4)^{-1} - (1+m)T_1^{-1}}{U_E(T_E - T_2)(T_2^{-1} - T_1^{-1})} \right) \right) \quad (2.67)$$

Where $C_6 = \xi\left[\xi_1(T_A - T_E) + \xi_2(T_C - T_E)\right]$ with $\xi_1 = 1 - T_{env}/T_A$ and $\xi_2 = 1 - T_{env}/T_C$

(2.68)

Furthermore, the exergetic performance coefficient (EPC) Ref. Ust et al. (2007) is defined as the ratio between the output exergy and the loss rate of availability (entropy production rate) and allows the necessary energy to be measured with care in addition to the impact in the environment. Using the **Eqs. (2.60)** and **(2.64)**, we obtain:

$$EPC = \frac{EX_{out}}{T_{env}\dot{\sigma}} =$$

$$\frac{1}{T_{env}} \left(C_7 + C_8 \frac{(I_2T_3)^{-1} + m(I_1T_4)^{-1} - (1+m)T_2^{-1}}{T_1^{-1} - T_2^{-1}} + \left(C_9 + C_{10} \frac{(I_2T_3)^{-1} + m(I_1T_4)^{-1} - (1+m)T_2^{-1}}{T_1^{-1} - T_2^{-1}} \right)^{-1} \left(\frac{\xi_2 + \xi_1 m}{\left(\frac{1}{U_C(T_3 - T_C)} + \frac{m}{U_A(T_4 - T_A)} + \frac{(I_2T_3)^{-1} + m(I_1T_4)^{-1} - (1+m)T_2^{-1}}{U_G(T_G - T_1)(T_1^{-1} - T_2^{-1})} + \frac{(I_2T_3)^{-1} + m(I_1T_4)^{-1} - (1+m)T_1^{-1}}{U_E(T_E - T_2)(T_2^{-1} - T_1^{-1})} \right)} - C_6 \right)^{-1} \right)^{-1} \quad (2.69)$$

In which,

$$C_7 = \frac{1}{\xi_2 + \xi_1 m}\left(\frac{1}{T_C} + \frac{m}{T_A} - \frac{1+m}{T_E}\right); C_8 = \frac{1}{\xi_2 + \xi_1 m}\left(\frac{1}{T_E} - \frac{1}{T_G}\right);$$

$$C_9 = \frac{\xi\left[\xi_1(T_A - T_E) + \xi_2(T_C - T_E)\right]}{\xi_2 + \xi_1 m}\left(\frac{1}{T_C} + \frac{m}{T_A} - \frac{1+m}{T_E}\right) + \xi\left(\frac{T_E}{T_C} + \frac{T_E}{T_A} + \frac{T_A}{T_E} + \frac{T_C}{T_E} - 4\right),$$

$$C_{10} = \frac{\xi\left[\xi_1(T_A - T_E) + \xi_2(T_C - T_E)\right]}{\xi_2 + \xi_1 m}\left(\frac{1}{T_E} - \frac{1}{T_G}\right) \quad (2.70)$$

2.4.3.2. Optimization by the exergetic performance coefficient (EPC)

By performing the variable change below, we obtain:

$$x=(1+m)T_1^{-1};\ y=(1+m)T_2^{-1};\ z=(I_2T_3)^{-1};\ t=m(I_1T_4)^{-1}. \tag{2.71}$$

And solving the partial differential equations

$$\partial EPC/\partial x=0;\partial EPC/\partial y=0;\partial EPC/\partial z=0;\partial EPC/\partial t=0 \tag{2.72}$$

Such as,

$$EPC=\frac{1}{T_{env}}\left(C_7+C_8\frac{(1+m)(z+t-y)}{x-y}+\left(C_9+C_{10}\frac{(1+m)(z+t-y)}{x-y}\right)\left(\frac{\xi_2+\xi_1 m}{\left(\begin{array}{l}\frac{I_2z}{U_C(1-I_2T_Cz)}+\frac{mI_1t}{U_A(m-I_1T_At)}+\\ \frac{x(1+m)(z+t-y)}{U_G(T_Gx-1-m)(x-y)}+\frac{y(1+m)(z+t-x)}{U_E(T_Ey-1-m)(y-x)}\end{array}\right)}-C_6\right)^{-1}\right)^{-1} \tag{2.73}$$

Which makes it possible to find the optimal temperatures of the working fluid in each component:

$$T_{1op}=\frac{T_G}{1+\frac{\alpha}{\sqrt{I_2}}(1-I_2T_CZ)}$$

$$T_{2op}=\frac{T_E}{1+\frac{\beta}{\sqrt{I_2}}(1-I_2T_CZ)}$$

$$T_{3op}=1/I_2Z$$

$$T_{4op}=\frac{T_A}{1-\gamma\sqrt{\frac{I_1}{I_2}}(1-I_2T_CZ)} \tag{2.74}$$

with $\alpha=\sqrt{U_C/U_G};\beta=\sqrt{U_C/U_E};\gamma=\sqrt{U_C/U_A}$;

$$Z=\frac{(1+m)\alpha-\frac{(1+m)\beta(1+\beta)}{T_E}-\frac{m\gamma(1-\gamma)}{I_1T_A}+\sqrt{\left(-(1+m)\alpha+\frac{(1+m)\beta(1+\beta)}{T_E}+\frac{m\gamma(1-\gamma)}{I_1T_A}\right)^2-\left((1+m)\alpha-\frac{(1+m)\beta^2}{T_E}+\frac{m\gamma^2}{I_1T_A}-(I_2T_C)^{-1}\right)\left((1+m)\alpha-\frac{(1+m)\beta(\beta+2)}{T_E}+\frac{m\gamma(\gamma-2)}{I_1T_A}\right)}}{I_2T_C\left((1+m)\alpha-\frac{(1+m)\beta^2}{T_E}+\frac{m\gamma^2}{I_1T_A}\right)-1} \quad (2.75)$$

2.4.4. Characteristics parameters and optimization by the flowchart optimization algorithm

2.4.4.1. Characteristics parameters

The COP which represents the amount of heat supplied to the surrounding to be heated compared to the amount of heat input, and the heating load are shown as follows

$$\psi=\pi\Big/\dot{Q}_G=\left(\dot{Q}_C+\dot{Q}_A-\dot{Q}_L\right)\Big/\dot{Q}_G \text{ and } q=\pi/A=\left(\dot{Q}_C+\dot{Q}_A-\dot{Q}_L\right)\Big/A \quad (2.76)$$

The **Eqs. (2.1)** and **(2.76)** of the AHP cycle provide the heat-transfer rates derived from the coefficient of performance and the heating load

$$\dot{Q}_G=\pi/\psi$$

$$\dot{Q}_E=\pi\left(1-\frac{1}{\psi}\right)+\dot{Q}_L$$

$$\dot{Q}_C=\left(\pi+\dot{Q}_L\right)\Big/(m+1)$$

$$\dot{Q}_A=m\left(\pi+\dot{Q}_L\right)\Big/(m+1) \quad (2.77)$$

where $m=\dot{Q}_A\Big/\dot{Q}_C$ being the ratio of the rejected heat between the absorber and the condenser, and **Eqs. (2.51)** and **(2.58)** the temperatures of the working fluid yields

$$T_1=T_G-\frac{\pi}{U_GA_G\psi}$$

$$T_2=T_E-\frac{\pi\left(1-\frac{1}{\psi}\right)+\dot{Q}_L}{U_EA_E}$$

$$T_3=T_C+\frac{\pi+\dot{Q}_L}{U_CA_C(m+1)}$$

$$T_4 = T_A + \frac{m\left(\pi + \dot{Q}_L\right)}{U_A A_A (m+1)} \tag{2.78}$$

An optimal generalized expression between the design indicators and the performance parameters (COP and heating load), integrating the two laws of thermodynamics is obtained. Previously, Qin et al. (2007) and Chen et al. (2005a, 2019) established a similar expression on FTL AHPs and Qin et al. (2017) on FTL AHTs. However, by replacing the **Eqs. (2.77)** and **(2.78)** into **Eq. (2.56)** this time we obtain in these works, an optimal relation for an FTL AHP cycle linking all the design indicators (the two internal dissipations in the absorber-generator connection and the condenser-evaporator connection, the heat leaks, the coefficients of heat exchange in the heat exchangers and the ratio of the heat rejected between the absorber and the condenser), and the performance parameters.

$$\left(\frac{1}{U_C A_C} + \frac{T_C(1+m)}{\pi + \dot{Q}_L}\right)^{-1} + \left(\frac{1}{U_A A_A} + \frac{T_A(1+m)}{m\left(\pi + \dot{Q}_L\right)}\right)^{-1} + I_1\left(\frac{1}{U_G A_G} - \frac{T_G \psi}{\pi}\right)^{-1} + I_2\left(\frac{1}{U_E A_E} - \frac{T_E}{\pi\left(1 - \frac{1}{\psi}\right) + \dot{Q}_L}\right)^{-1} = 0 \tag{2.79}$$

2.4.4.2. Performance analysis

2.4.4.2.1. Ecological criterion

The output exergy rate of the system FTL AHP cycle is as follows

$$\dot{EX}_{out} = \left(\dot{Q}_C - \dot{Q}_{L1}\right)\left(1 - \frac{T_{env}}{T_C}\right) + \left(\dot{Q}_A - \dot{Q}_{L2}\right)\left(1 - \frac{T_{env}}{T_A}\right) =$$
$$\pi\left(1 - \frac{T_{env}}{m+1}\left(\frac{1}{T_C} + \frac{m}{T_A}\right)\right) + \frac{K_L T_{env}}{m+1}\left(T_A - mT_C + (m-1)T_E\right)\left(\frac{1}{T_A} - \frac{1}{T_C}\right) \tag{2.80}$$

the input exergy rate of the system FTL AHP cycle

$$\dot{EX}_{in} = \dot{Q}_G = \frac{\pi}{\psi} \tag{2.81}$$

and the exergy destroyed rate or the loss rate of availability

$$\dot{EX}_D = T_{env}\dot{\sigma} = T_{env}\left(\frac{\dot{Q}_C - \dot{Q}_{L1}}{T_C} + \frac{\dot{Q}_A - \dot{Q}_{L2}}{T_A} - \frac{\dot{Q}_G}{T_G} - \frac{\dot{Q}_E - \dot{Q}_L}{T_E}\right)$$
$$= \frac{T_{env}}{m+1}\left(\pi\left(\frac{1}{T_C} + \frac{m}{T_A} - \frac{m+1}{\psi T_G} + \frac{m+1}{T_E}\left(\frac{1}{\psi} - 1\right)\right) - K_L\left(T_A - mT_C + (m-1)T_E\right)\left(\frac{1}{T_A} - \frac{1}{T_C}\right)\right) \tag{2.82}$$

where $\dot{\sigma}$ is the entropy production rate is expressed in $\left(\mathrm{WK}^{-1}\right)$

As a result, exergy-based ecological function and previously used by Huang et al. (2008), Chen et al. (2007, 2019), Frikha et al. (2016); Ahmadi et al. (2016) and Qin et al. (2017) on absorption system

$$E = \dot{EX}_{out} - \dot{EX}_D = \pi\left(1 - T_{env}\left(2\left(\frac{1}{T_C} + \frac{m}{T_A}\right) - \frac{1}{\psi T_G} + \frac{1}{T_E}\left(\frac{1}{\psi} - 1\right)\right)\right) + \frac{2K_L T_{env}}{m+1}\left(T_A - mT_C + (m-1)T_E\right)\left(\frac{1}{T_A} - \frac{1}{T_C}\right) \quad (2.83)$$

2.4.4.2.2. Thermo-economic criterion

The thermo-economic criterion stated by Kodal et al. (2000, 2002, 2003), and followed by Ahmadi et al. (2014a, 2014b) is the ratio of the heating load by the sum of the cost on the investment and the cost of the energy consumed. It takes into account the location of the system and the load to be provided by it.

$$f = \frac{\pi}{C_i + C_e} \quad (2.84)$$

where, $C_i = k_1 A$ and $C_e = k_2 \dot{Q}_G$ (2.85)

C_i is the cost of the investment in AHP and depends proportionally on the total heat exchange area. C_e is the cost of energy consumed and is proportionally dependent on the heat input rate. Again, k_1 and k_2 the capital cost for the unit heat-transfer area and the unit cost of energy. Considering $k = k_1/k_2$ as a thermo-economic parameter of dimension $\left(\mathrm{Wm^{-2}}\right)$, and substituting **Eq. (2.85)** into **Eq. (2.84)** we obtain

$$F = k_2 f = \frac{1}{\frac{k}{q} + \frac{1}{\psi}} \quad (2.86)$$

2.4.4.2.3. Exergetic performance criterion

Using **Eqs. (2.80) and (2.82)**, we obtain:

$$EPC = \frac{\dot{EX}_{out}}{\dot{EX}_D} = \frac{\pi\left(1 - \frac{T_{env}}{m+1}\left(\frac{1}{T_C} + \frac{m}{T_A}\right)\right) + \frac{K_L T_{env}}{m+1}\left(T_A - mT_C + (m-1)T_E\right)\left(\frac{1}{T_A} - \frac{1}{T_C}\right)}{\frac{T_{env}}{m+1}\left(\pi\left(\frac{1}{T_C} + \frac{m}{T_A} - \frac{m+1}{\psi T_G} + \frac{m+1}{T_E}\left(\frac{1}{\psi} - 1\right)\right) - K_L\left(T_A - mT_C + (m-1)T_E\right)\left(\frac{1}{T_A} - \frac{1}{T_C}\right)\right)} \quad (2.87)$$

2.4.4.3. Optimization

2.4.4.3.1. Exception examples

Heat loss and leakage being real considerations for an FTL AHP cycle, from **Eq. (2.79)** we can therefore obtain the following configurations.

Eventuality 1: $m=1$ ($\dot{Q}_C=\dot{Q}_A$), $I_1\neq 1$, $I_2\neq 1$ and $K_L\neq 0$

$$\left(\frac{1}{U_C A_C}+\frac{2T_C}{\pi+\dot{Q}_L}\right)^{-1}+\left(\frac{1}{U_A A_A}+\frac{2T_A}{\left(\pi+\dot{Q}_L\right)}\right)^{-1}+I_1\left(\frac{1}{U_G A_G}-\frac{T_G\psi}{\pi}\right)^{-1}+I_2\left(\frac{1}{U_E A_E}-\frac{T_E}{\pi\left(1-\frac{1}{\psi}\right)+\dot{Q}_L}\right)^{-1}=0 \quad (2.88)$$

Eventuality 2, an exoreversible FTL system where $K_L=0$, $I_1\neq 1$, $I_2\neq 1$ and $m\neq 1$

$$\left(\frac{1}{U_C A_C}+\frac{T_C(1+m)}{\pi}\right)^{-1}+\left(\frac{1}{U_A A_A}+\frac{T_A(1+m)}{m\pi}\right)^{-1}+I_1\left(\frac{1}{U_G A_G}-\frac{T_G\psi}{\pi}\right)^{-1}+I_2\left(\frac{1}{U_E A_E}-\frac{T_E}{\pi\left(1-\frac{1}{\psi}\right)}\right)^{-1}=0 \quad (2.89)$$

Eventuality 3, a reversible FTL cycle ($K_L=0$, $I_1=I_2=1$ and $m\neq 1$)

$$\left(\frac{1}{U_C A_C}+\frac{T_C(1+m)}{\pi}\right)^{-1}+\left(\frac{1}{U_A A_A}+\frac{T_A(1+m)}{m\pi}\right)^{-1}+\left(\frac{1}{U_G A_G}-\frac{T_G\psi}{\pi}\right)^{-1}+\left(\frac{1}{U_E A_E}-\frac{T_E}{\pi\left(1-\frac{1}{\psi}\right)}\right)^{-1}=0 \quad (2.90)$$

Eventuality 4, an endoreversible FTL device where ($K_L\neq 0$, $I_1=I_2=1$ and $m\neq 1$)

$$\left(\frac{1}{U_C A_C}+\frac{T_C(1+m)}{\pi+\dot{Q}_L}\right)^{-1}+\left(\frac{1}{U_A A_A}+\frac{T_A(1+m)}{m\left(\pi+\dot{Q}_L\right)}\right)^{-1}+\left(\frac{1}{U_G A_G}-\frac{T_G\psi}{\pi}\right)^{-1}+\left(\frac{1}{U_E A_E}-\frac{T_E}{\pi\left(1-\frac{1}{\psi}\right)+\dot{Q}_L}\right)^{-1}=0 \quad (2.91)$$

2.4.4.3.2. Flowchart optimization

By considering the ecological (*E*), exergetic (*EPC*) and thermo-economic (*F*) objective functions, we can obtain the maximum values of each of these functions using the Flowchart algorithm (**Fig. 2.3**). Recently, this algorithm was used by Su et al. (2016) to optimize an irreversible Carnot refrigerator, followed by Chen et al. (2019) to optimize a FTL AHP using the exergy-based ecological function.

2.5. Conclusion

In this chapter, we carried out a theoretical analysis using finite time thermodynamics or non-equilibrium thermodynamics. In addition, we used as a tool the Maple software which allowed us to analytically solve the symbolic equations which resulted in obtaining the maximum values

of the ECOP and E criteria for the THR cycles and the EPC and E criteria for the TFL cycles. However, the flowchart algorithm allowed us to obtain the maxima of the three objective functions E, EPC and F under certain operating conditions, which led to an optimal comparative study of system performance in the following.

CHAPTER 3: RESULTS AND DISCUSSION

3.1. Introduction

In the previous chapter, we established an analytical study based on finite time thermodynamics. Through a flowchart algorithm, we obtained the optimal parameters corresponding to the maximum of each objective function studied. However, in this chapter it is a question of understanding and determining the optimal operating ranges of a THR AHP and FTL AHP single effect system by considering real hypotheses. This being so, we will in the following plot the curves of the objective functions *ECOP* for the THR cycle and *EPC* for a FTL cycle with respect to the temperatures of the working fluid and the heat exchange surfaces areas in the various components, coefficient of performance, specific heating load and entropy generation rate. Then we will make a comparative study of the ecological, exergy and economic criteria for the THR and FTL cycles compared to performance indices such as the coefficient of performance, exergy output rate and exergy destruction rate. Finally we will discuss these results in order to find a suitable compromise.

3.2. Numerical applications for the THR AHP

The numerical values below allowed to perform numerical analyzes and to plot the curves of the variations of the different objective functions. This is under the influences of the dissipation effects, heat resistances and internal and external irreversibility factors. In a general framework, these values are taken from the Ref. literature (Ngouateu Wouagfack and Tchinda., 2012a and Ahmadi et al., 2015) and are the following: $T_G = 393\text{K}$; $T_E = 288\text{K}$; $T_A = 313\text{K}$; $T_C = 313\text{K}$; $A = 100\text{m}^2$; $U_G = U_E = U_O = 500\text{WK}^{-1}\text{m}^{-2}$; $\xi = K_L / A = 1.082\text{Wm}^{-2}\text{K}^{-1}$. In addition, in **Figs. 3.15-3.18, 3.25-3.27**, $k = 5$.

3.3. Effects of temperatures of the working fluid in the different components for the THR AHP

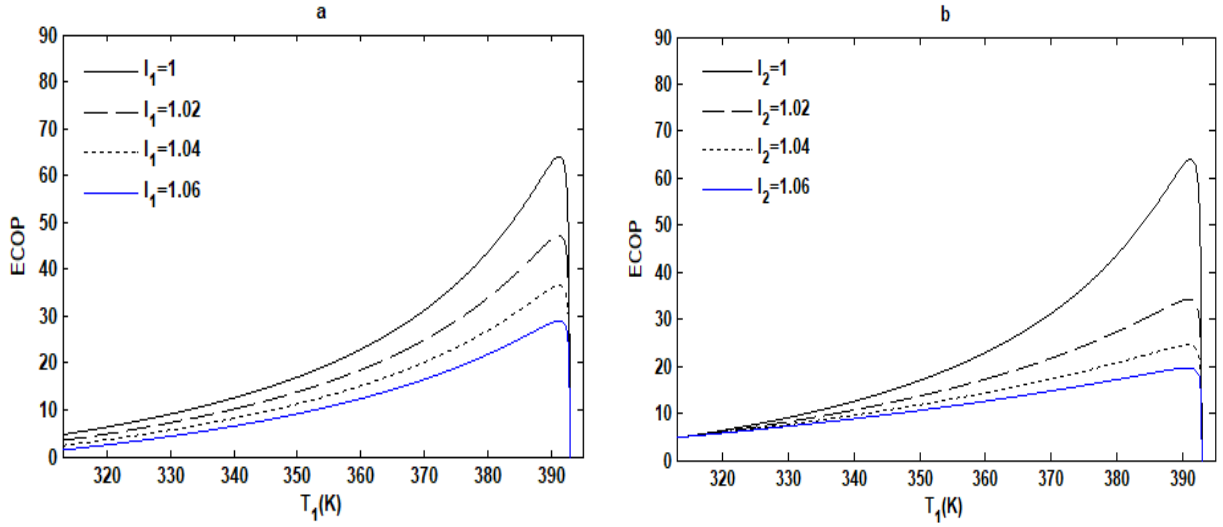

Fig. 3.1. Variation of *ECOP* objective function with respect to the temperature T_1 of the working fluid in the generator when $I_2 = 1$ for various I_1 (a); when $I_1 = 1$ for various I_2 (b).

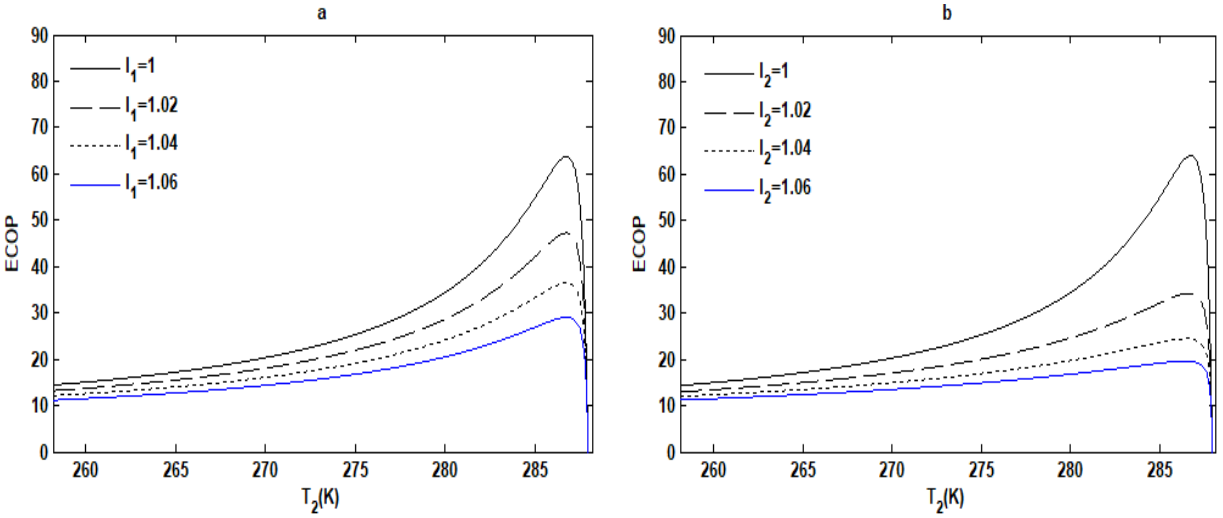

Fig. 3.2. Variation of *ECOP* objective function with respect to the temperature T_2 of the working fluid in the evaporator when $I_2 = 1$ for various I_1 (a); when $I_1 = 1$ for various I_2 (b).

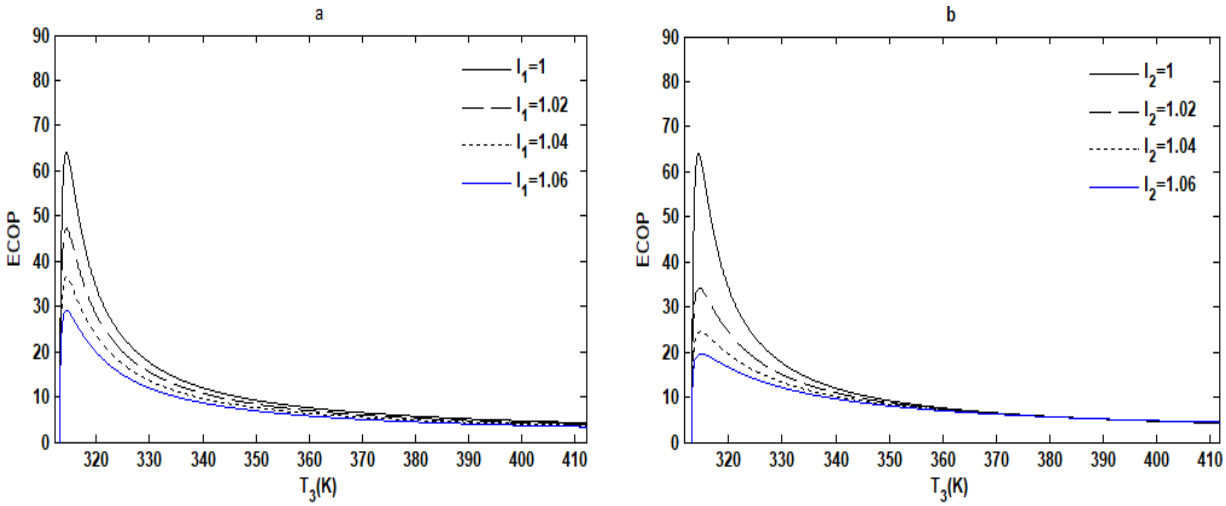

Fig. 3.3. Variation of $ECOP$ objective function with respect to the temperature T_3 of the working fluid in the absorber and the condenser assembly when $I_2 = 1$ for various I_1 (a); when $I_1 = 1$ for various I_2 (b).

Figs. 3.1-3.3 show the variations of the $ECOP$ objective function with respect to the temperatures T_1, T_2 and T_3 which respectively represent the temperatures of working fluid in the generator, the evaporator and the absorber-condenser assembly. In **Figs. 3.1(a), 3.2(a)** and **3.3(a)** I_2 is set $(I_2 = 1)$ for different values of I_1 and in **Figs. 3.1(b), 3.2(b)** and **3.3(b)** I_1 is set ($I_1 = 1$) for different values of I_2. The $ECOP$ gradually increases with increase in the temperatures T_1 and T_2 before reaching its maximum in **Figs. 3.1** and **3.2**. However $ECOP$ decreases abruptly after reaching its maximum value when T_3 increases in **Fig. 3.3**. As a result, when $T_1 < T_{1op}$, $T_2 < T_{2op}$ and $T_3 > T_{3op}$ the system is less ecological and losses are more accentuated and more when $T_1 > T_{1op}$, $T_2 > T_{2op}$ and $T_3 < T_{3op}$, the system is unstable. However, the $ECOP_{\max}$ is more affected in the system for the same values of the optimum temperatures in the condenser-evaporator assembly by the irreversibility factor I_2 than in the absorber-generator by the irreversibility factor I_1.

3.4. Influences of design parameters for the THR AHP

3.4.1. The two internal irreversibilities I_1 and I_2

3.4.1.1. On the ECOP criterion

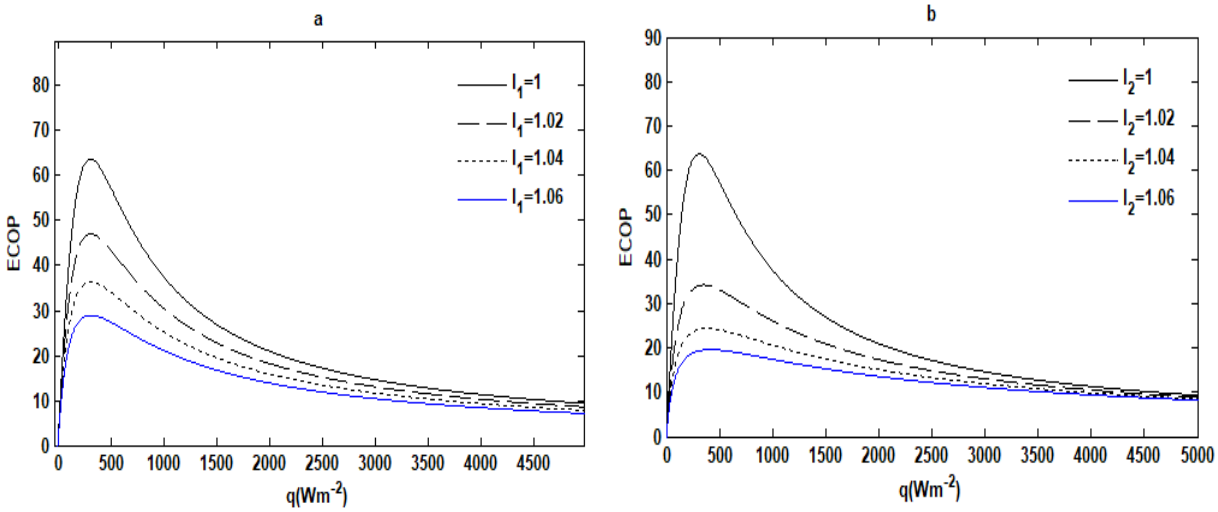

Fig. 3.4. Effects of internal irreversibility I_1 (a) of the generator-absorber assembly and of the internal irreversibility I_2 (b) of the evaporator-condenser assembly on the *ECOP* objective function with respect to the q objective function.

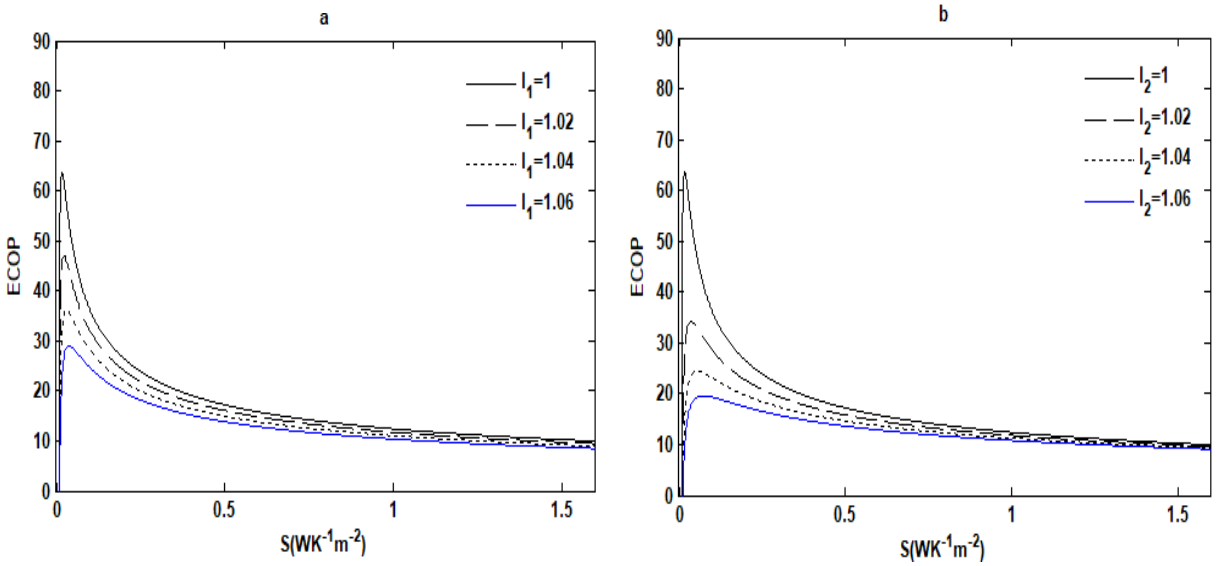

Fig. 3.5. Effects of internal irreversibility I_1 (a) of the generator-absorber assembly and of the internal irreversibility I_2 (b) of the evaporator-condenser assembly on the *ECOP* objective function with respect to the S objective function.

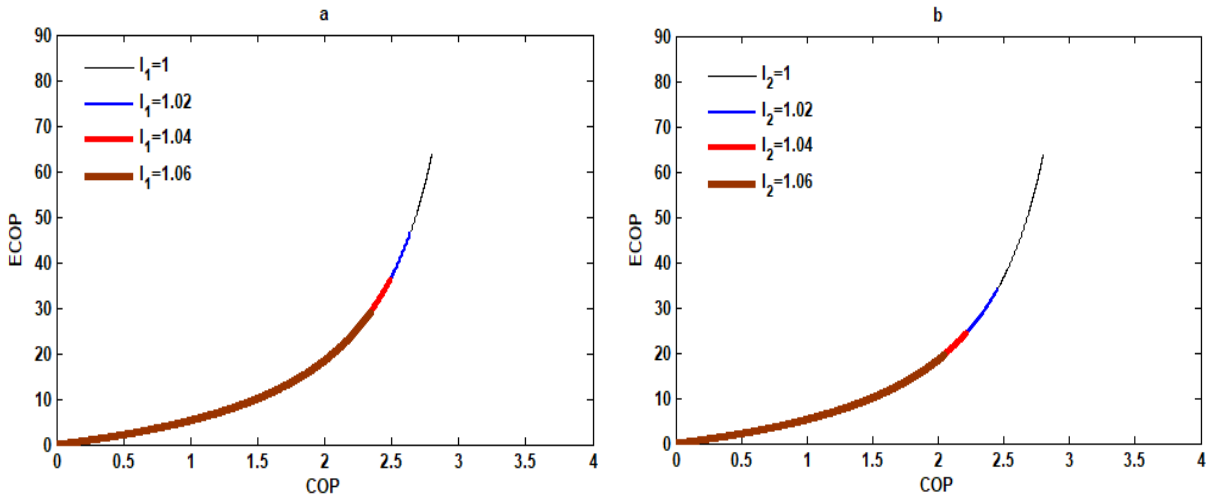

Fig. 3.6. Effects of internal irreversibility I_1 (a) of the generator-absorber assembly and of the internal irreversibility I_2 (b) of the evaporator-condenser assembly on the $ECOP$ objective function with respect to the COP objective function.

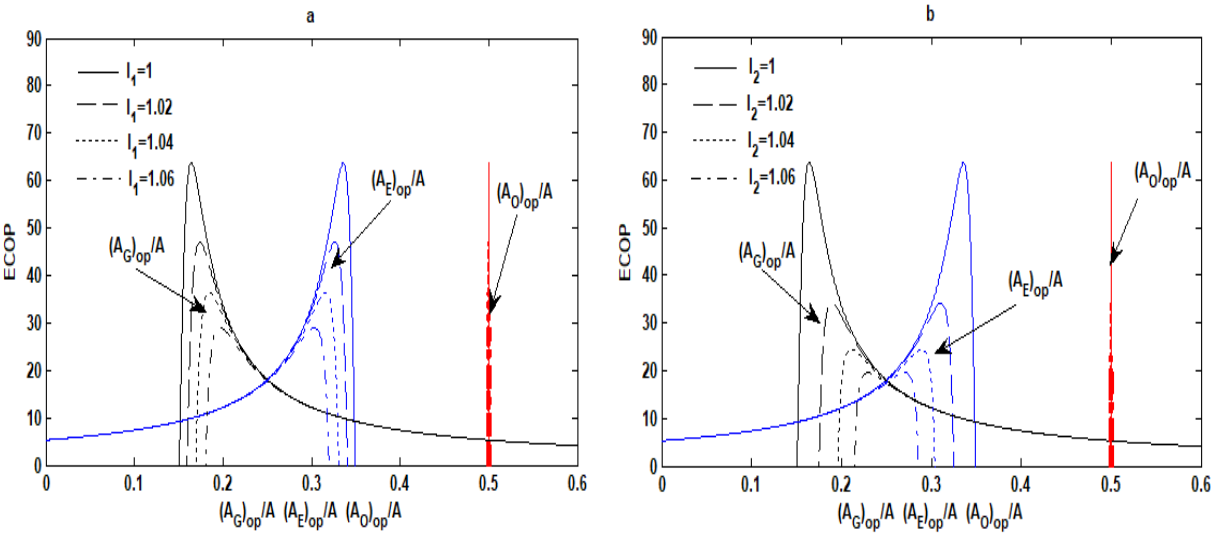

Fig. 3.7. Effects of internal irreversibility I_1 (a) of the generator-absorber assembly and of the internal irreversibility I_2 (b) of the evaporator-condenser assembly on the $ECOP$ objective function with respect to the heat-transfer areas of the heat exchangers $\left(A_O\right)_{op}/A$, $\left(A_G\right)_{op}/A$ and $\left(A_E\right)_{op}/A$ objective functions.

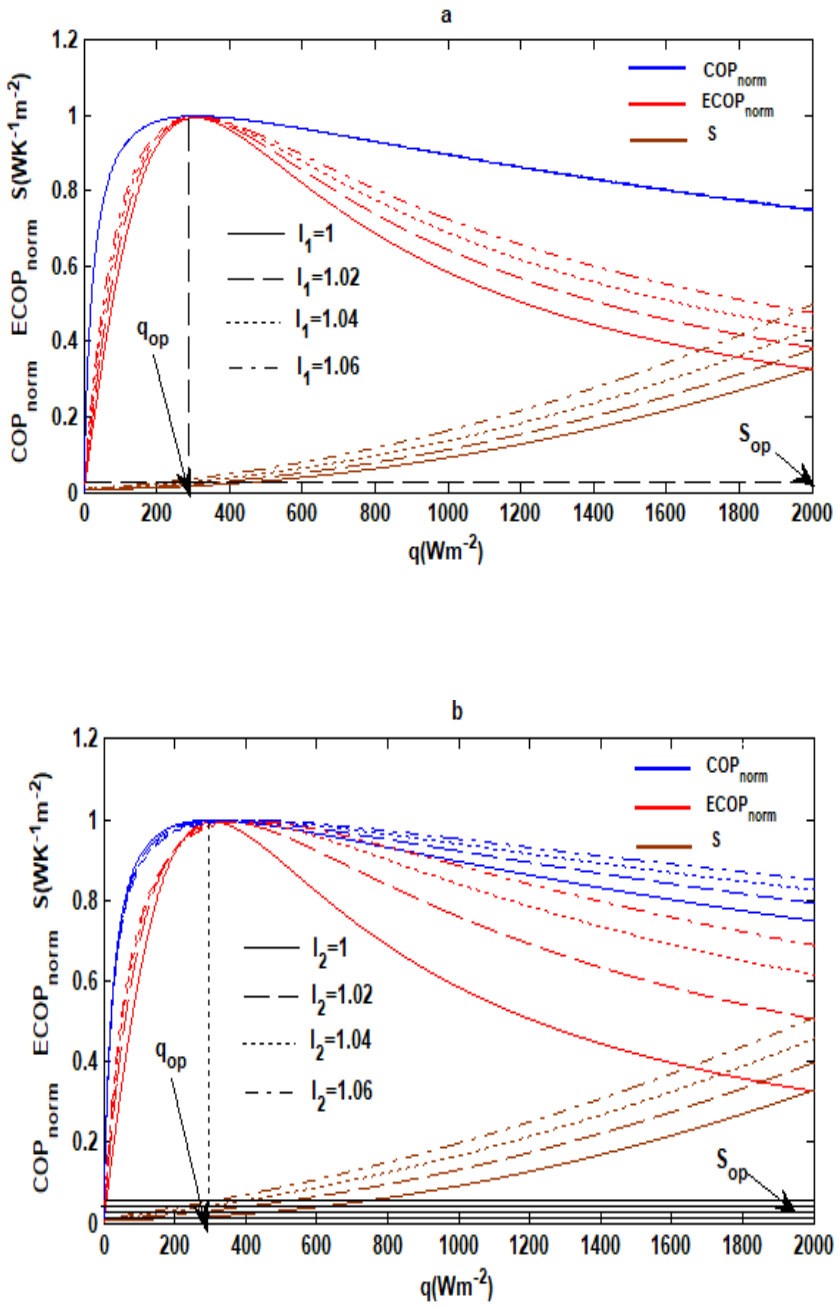

Fig. 3.8. Variation of the non-dimensional *ECOP* objective function, the non-dimensional *COP* objective function and entropy generation rate according to the specific heating load : (a) $I_2 = 1$ when I_1 varies and (b) $I_1 = 1$ when I_2 varies.

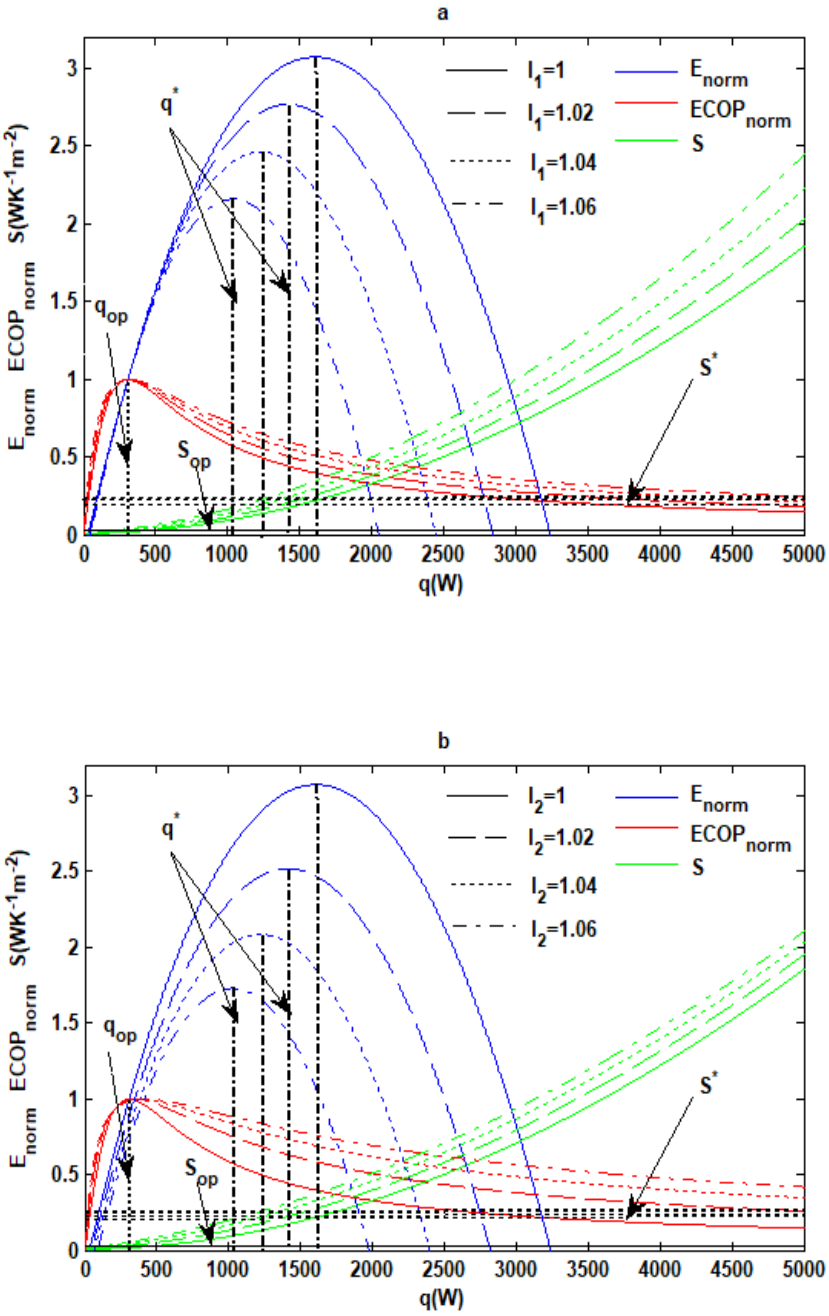

Fig. 3.9. Variation of the non-dimensional *ECOP* objective function, the non-dimensional *E* objective function and entropy generation rate according to the specific heating load : (a) $I_2 = 1$ when I_1 varies and (b) $I_1 = 1$ when I_2 varies.

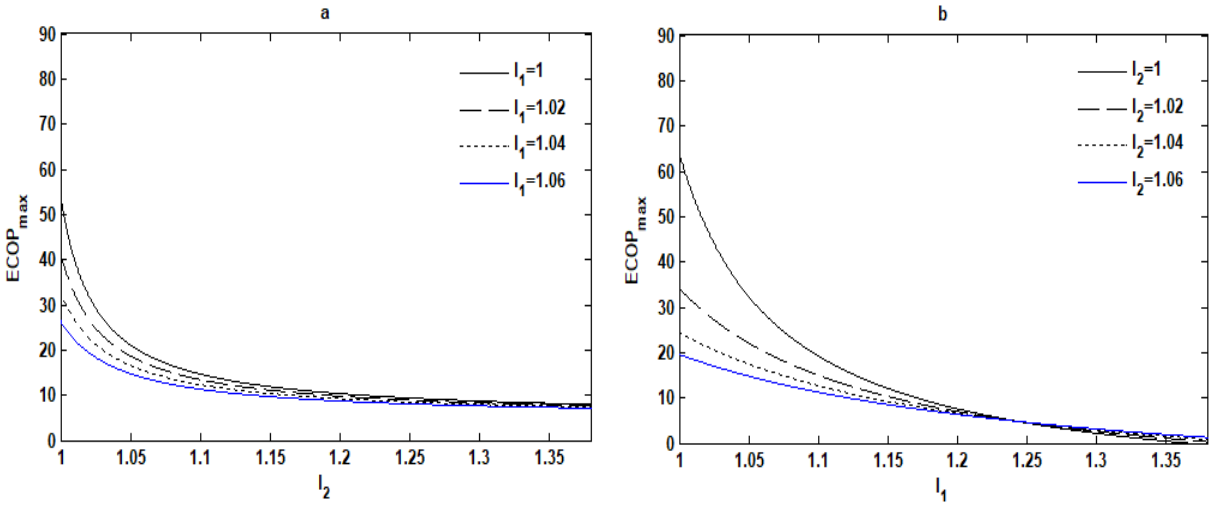

Fig. 3.10. Effects of internal irreversibility I_2 (a) of the generator-absorber assembly and of the internal irreversibility I_1 (b) of the evaporator-condenser assembly on the $ECOP_{\max}$ maximal objective function respectively for certain values of I_1 (a) and I_2 (b).

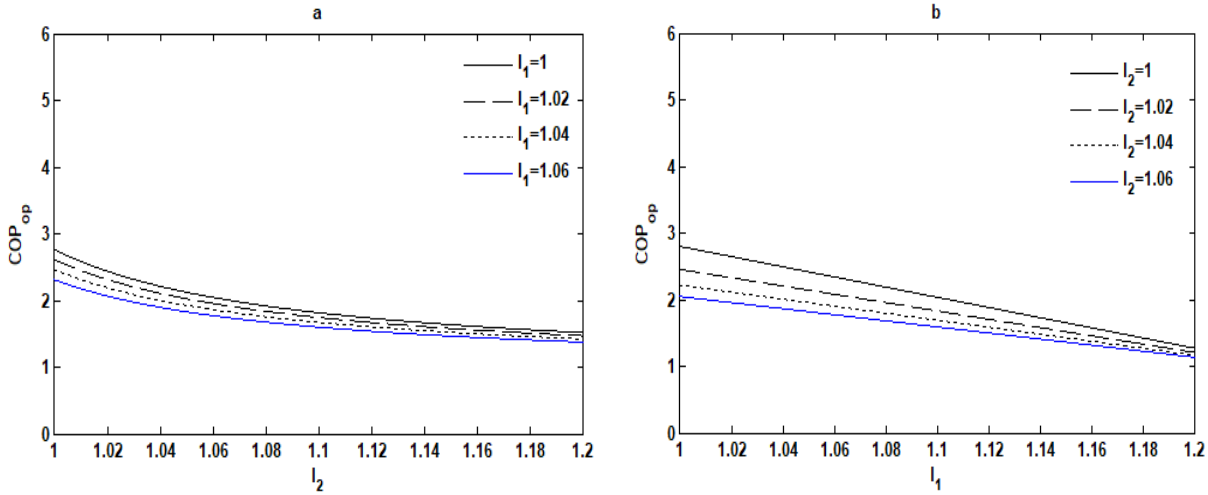

Fig. 3.11. Effects of internal irreversibility I_2 (a) of the generator-absorber assembly and of the internal irreversibility I_1 (b) of the evaporator-condenser assembly on the COP_{op} optimal objective function respectively for certain values of I_1 (a) and I_2 (b).

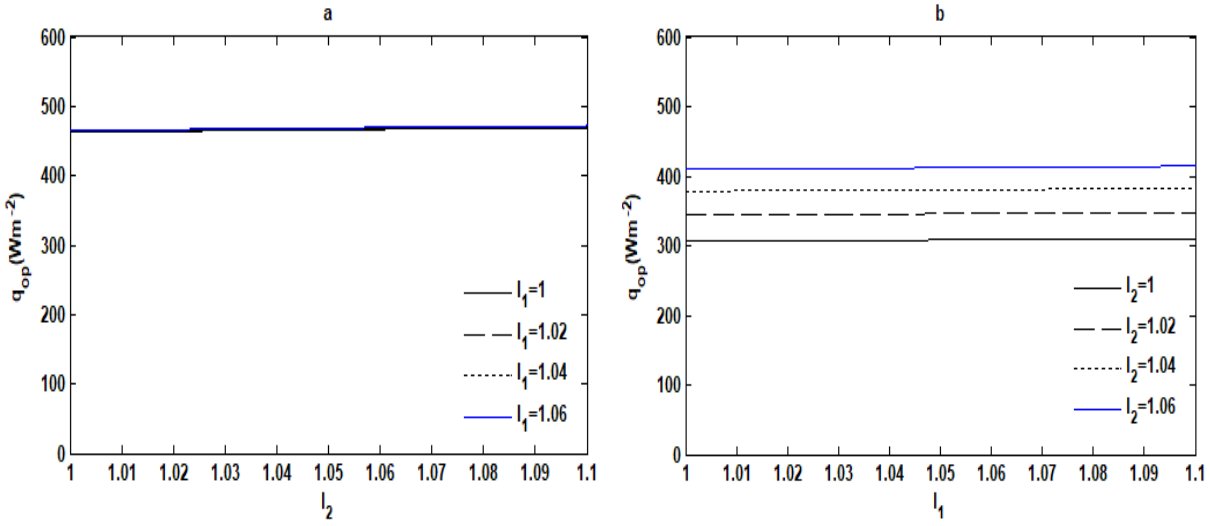

Fig. 3.12. Effects of internal irreversibility I_2 (a) of the generator-absorber assembly and of the internal irreversibility I_1 (b) of the evaporator-condenser assembly on the q_{op} optimal objective function respectively for certain values of I_1 (a) and I_2 (b).

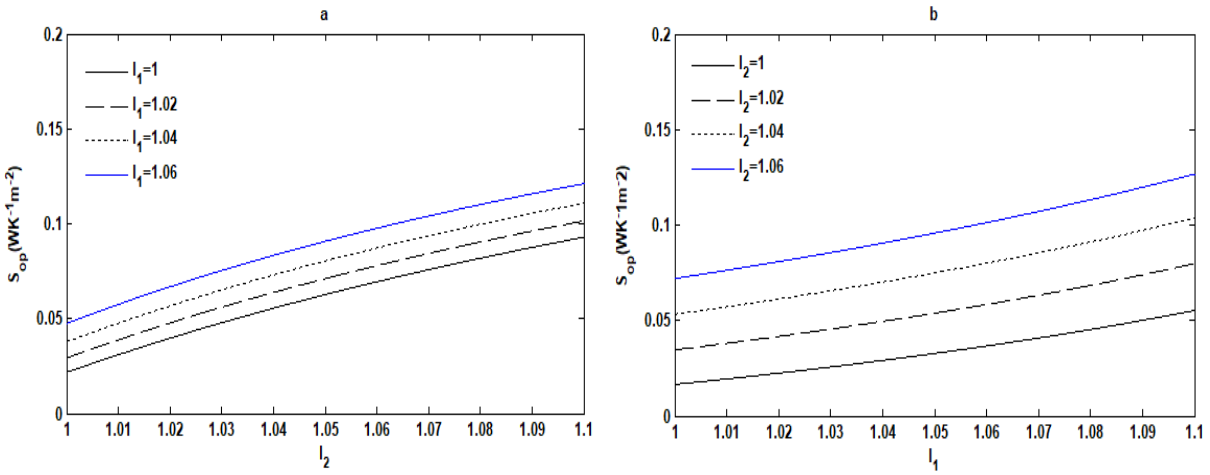

Fig. 3.13. Effects of internal irreversibility I_2 (a) of the generator-absorber assembly and of the internal irreversibility I_1 (b) of the evaporator-condenser assembly on the S_{op} optimal objective function respectively for certain values of I_1 (a) and I_2 (b).

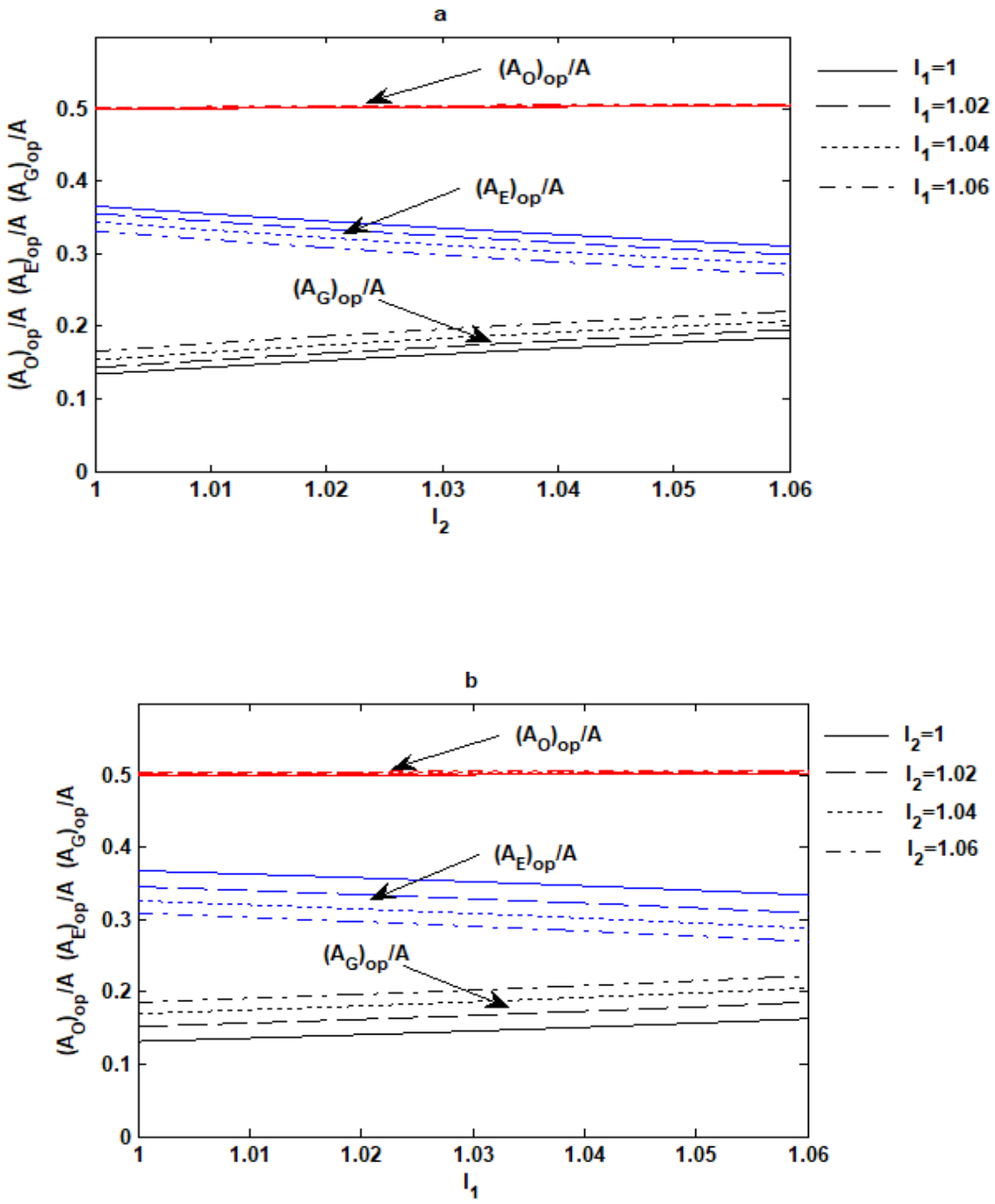

Fig. 3.14. Effects of internal irreversibility I_2 (a) of the generator-absorber assembly and of the internal irreversibility I_1 (b) of the evaporator-condenser assembly on the $(A_O)_{op}/A$, $(A_G)_{op}/A$ and $(A_E)_{op}/A$ optimal objective functions respectively for certain values of I_1 (a) and I_2 (b).

The effects of internal irreversibilities I_1 and I_2 on the $ECOP$ objective function with respect to the specific heating load, the specific entropy generation rate, the coefficient of performance (COP) and heat-transfer areas of the heat exchangers are shown respectively in **Figs. 3.4-3.7**. For progressively large values of I_1 and I_2, we make the following observations. In **Figs.**

3.4 and **3.5**, we observe that the maximum of the objective function $ECOP$ is reached for a certain value of the specific heating load (q) **Fig. 3.4** and a minimum of the specific entropy generation rate (S) **Fig 3.5**. This $ECOP$ objective function decreases gradually when the internal irreversibility parameters I_1 and I_2 increase. Moreover, from the definition of COP and $ECOP$ in **Eqs. (2.15)** and **(2.19)** respectively, we obtain a relation between these two objective functions $ECOP = \dfrac{COP}{T_{env}\left(\left(\dfrac{1}{T_O}-\dfrac{1}{T_E}\right)COP-\left(\dfrac{1}{T_G}-\dfrac{1}{T_E}\right)\right)}$. This equation makes it possible to obtain **Fig. 3.6** and shows that the $ECOP$ increases as COP also increases. The analysis of the performance of the AHP shows that the objective function COP is always such that $COP < 3$ for any maximum value of the objective function $ECOP$ which corresponds to an optimal system. Among others, **Fig. 3.7** shows that the maximum of the objective function $ECOP$ varies symmetrically with respect to the optimum heat transfer areas $(A_G)_{op}$ of the generator and $(A_E)_{op}$ of the evaporator. This means that the $ECOP_{\max}$ values decrease when the $(A_G)_{op}$ values increase while the $(A_E)_{op}$ values decrease. However, the $ECOP_{\max}$ values decrease always leaving the optimal values of $(A_O)_{op}$ constant of the absorber-condenser assembly. **Fig. 3.8** shows variations of the normalized $ECOP$ $\left(ECOP_{norm} = ECOP/ECOP_{\max}\right)$, normalized COP $\left(COP_{norm} = COP/COP_{\max}\right)$, and S with respect to the q for different values of I_1 and I_2. It is observed that at the point of optimal functioning of the system, the optimal values of COP_{op}, q_{op}, S_{op}, T_{1op}, T_{2op}, T_{3op}, $(A_G)_{op}$, $(A_E)_{op}$ and $(A_O)_{op}$, the maximum values of $ECOP$ and COP coincide. Yet these last two objective functions have a different physical meaning. Ngouateu Wouagfack and Tchinda (2011a, 2012a, 2012b, 2014) made this observation between $ECOP$ and COP for AR and AHP having three and four heat reservoirs with internal irreversibility. Same for Medjo Nouadje et al. (2014) for THR AR and two internal irreversibilities. Also, the maximum of the $ECOP$ and COP objective functions correspond to a certain value of q for minimum value of S according to the variations of I_1 and I_2. However, **Fig. 3.9** shows variations of the normalized $ECOP$ $\left(ECOP_{norm} = ECOP/ECOP_{\max}\right)$, normalized E $\left(E_{norm} = E/E_{\max,E}\right)$, and S with respect to the q for different values of I_1 and I_2. It is observed that when the THR cycle operates under the maximum $ECOP$ values conditions $\left(ECOP_{\max}\right)$ on the one hand and maximum E values on the

other hand $(E_{\max})$, $q_{op} < q^*$ and $S_{op} < S^*$. q_{op} and q^* being the optimal specific heating load at $ECOP_{\max}$ and $E_{\max,E}$ respectively and S_{op} and S^* being the optimal specific entropy generation rate at $ECOP_{\max}$ and $E_{\max,E}$ respectively. The results show that the system operating under maximum $ECOP$ conditions has a significant advantage over the maximum E conditions in terms of specific entropy generation rate. Otherwise, under maximum E conditions has a significant advantage over the maximum $ECOP$ conditions in terms of specific heating load. The results obtained by Ngouateu Wouagfack and Tchinda (2011b) show that the THR cycle operating at maximum $ECOP$ values conditions has a significant advantage over the maximum E values and maximum specific cooling load values conditions concerning the specific entropy generation rate and coefficient of performance. **Figs. 3.10-3.14** show variations of the $ECOP_{\max}$ maximal objective function and the COP_{op}, q_{op}, S_{op}, $(A_G)_{op}$, $(A_E)_{op}$ and $(A_O)_{op}$ optimal objective functions corresponding to the maximum of $ECOP$. These variations with respect to I_2 for different values of I_1 on the one hand **Figs. 3.10(a)–3.14(a)** and I_1 for different values of I_2 on the other hand **Figs. 3.10(b)-3.14(b)**. $ECOP_{\max}$ decreases rapidly, COP_{op} and $(A_E)_{op}$ decreases gradually while S_{op} and $(A_G)_{op}$ increases, q_{op} and $(A_O)_{op}$ remains constant when the parameters I_1 and I_2 increase. As a result, $ECOP_{\max}$ and COP_{op} are better for values of I_1 and I_2 close to the unit corresponding to the endoreversible system with a specific entropy generation rate S_{op} minimum for a certain value of the specific heating load q_{op} and heat-transfer areas of heat exchangers $(A_G)_{op}$, $(A_E)_{op}$ and $(A_O)_{op}$.

Table 3.1. Real AHP maximum values from the ecological coefficient of performance ($ECOP_{\max}$) versus the endoreversible system ($I_1 = I_2 = 1$ and $\xi = 1.082$) for different values of I_1 and I_2.

Percentage (%) of $ECOP_{max}$	$I_1 = 1.00$	$I_1 = 1.02$	$I_1 = 1.04$	$I_1 = 1.06$	$I_1 = 1.08$
$I_2 = 1.00$	100.00	73.79	57.01	45.35	36.78
$I_2 = 1.02$	53.56	44.59	37.58	31.96	27.35
$I_2 = 1.04$	38.28	33.34	29.18	25.63	22.56
$I_2 = 1.06$	30.67	27.38	24.49	21.94	19.66
$I_2 = 1.08$	26.12	23.68	21.49	19.52	17.72

The preceding figures can be summarized in **Table 3.1**, which shows how the maximum ecological coefficient of performance varies according to the internal irreversibilities I_1 and I_2 respectively of the generator-absorber assembly and the evaporator-condenser assembly. We can

also deduce that the optimal functioning of a real AHP is less efficient than an endoreversible AHP. Which for an obtained $ECOP_{\max}$ ($I_1 = I_2 = 1$ and $\xi = 1.082\text{WK}^{-1}\text{m}^{-2}$) we have certain value of the specific heating load $q_{op} = 307\text{Wm}^{-2}$, a minimum entropy generation rate $S_{op} = 0.0165\text{WK}^{-1}\text{m}^{-2}$ and a maximum coefficient of performance $COP_{\max} = 2.8$ (According to **Eqs. 2.28-2.30**).

As a whole, **Figs. 1(a)-14(a)** and **Figs 1(b)-14(b)** show that the factor of internal irreversibility I_2 of the condenser-evaporator assembly characterized by the loss rate, the losses of heat resistance, the friction, the singularity points and the turbulence of the working fluid has a more unfavorable impact on the performance of the system.

3.4.1.2. On the EPC, E and F objective functions

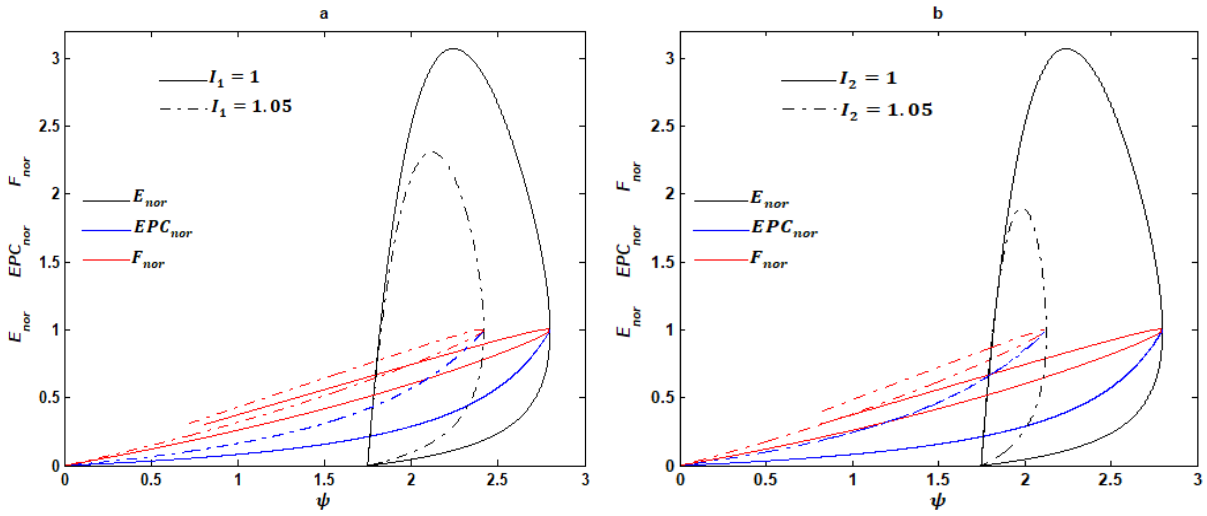

Fig. 3.15. Effects of internal irreversibility I_1 (a) of the generator-absorber assembly and of the internal irreversibility I_2 (b) of the evaporator-condenser assembly on the dimensionless E_{nor}, EPC_{nor} and F_{nor} with respect to the COP (ψ) objective function.

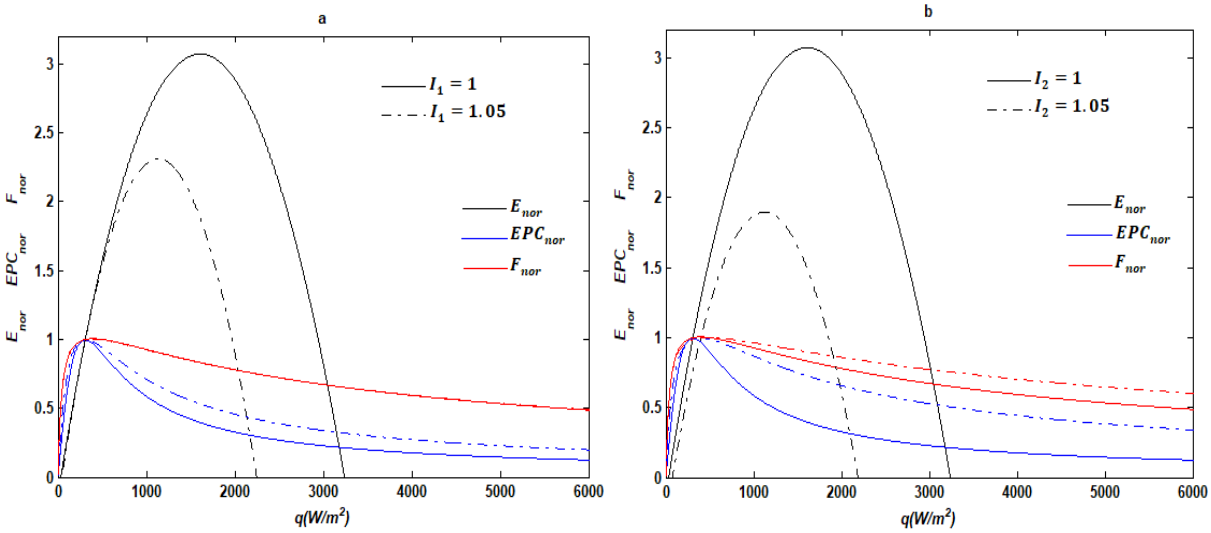

Fig. 3.16. Effects of internal irreversibility I_1 (a) of the generator-absorber assembly and of the internal irreversibility I_2 (b) of the evaporator-condenser assembly on the dimensionless E_{nor}, EPC_{nor} and F_{nor} with respect to the q objective function.

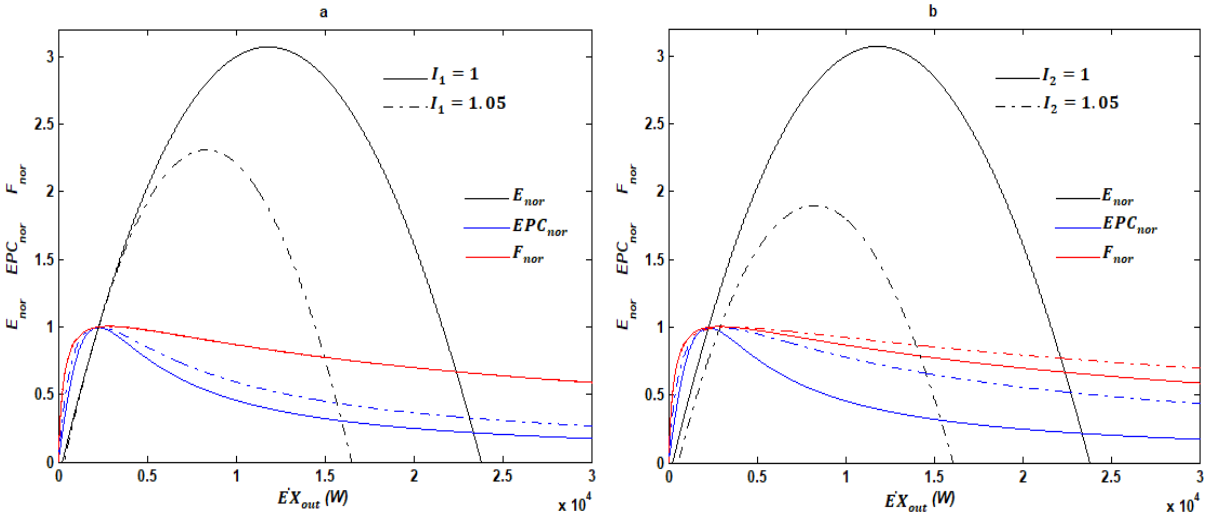

Fig. 3.17. Effects of internal irreversibility I_1 (a) of the generator-absorber assembly and of the internal irreversibility I_2 (b) of the evaporator-condenser assembly on the dimensionless E_{nor}, EPC_{nor} and F_{nor} with respect to the $\dot{E}X_{out}$ objective function.

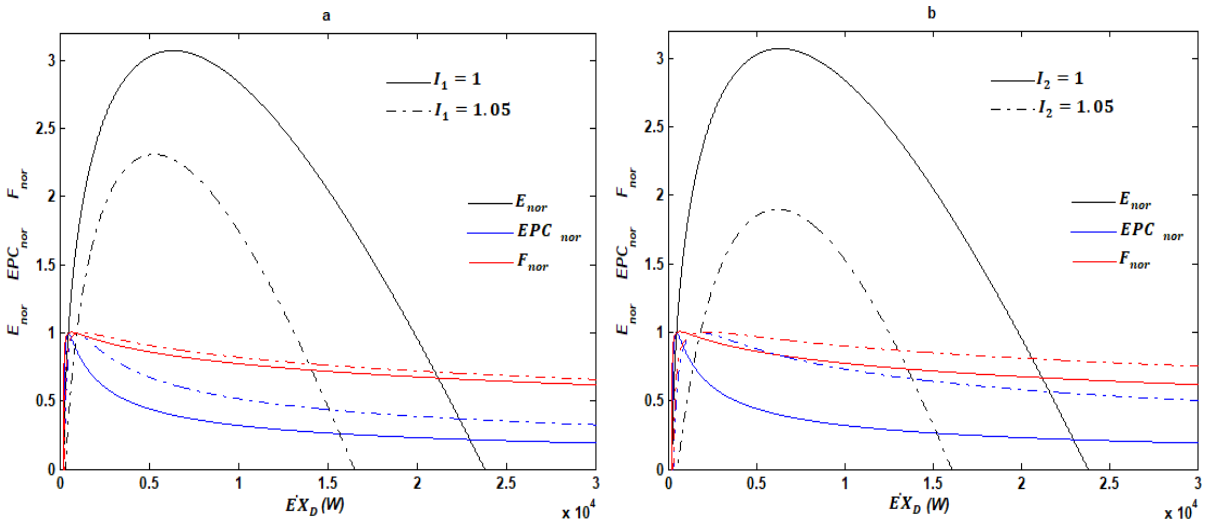

Fig. 3.18. Effects of internal irreversibility I_1 (a) of the generator-absorber assembly and of the internal irreversibility I_2 (b) of the evaporator-condenser assembly on the dimensionless E_{nor}, EPC_{nor} and F_{nor} with respect to the $\dot{E}X_D$ objective function.

In **Figs. 3.15-3.18**, the dimensionless or normalized values E_{nor} ($E_{nor} = E/E_{op}$ where E_{op} is the optimal value of E corresponding to the value of E when F and EPC are at their maximum values, and E varies to $E_{\max}$), EPC_{nor} ($EPC_{nor} = EPC/EPC_{\max}$) and F_{nor} ($F_{nor} = F/F_{\max}$) has a curve with respect to ψ, q, $\dot{E}X_{out}$ and $\dot{E}X_D$. These characterizes the influences of the two internal irreversibility factors I_1 and I_2 on the exergy-based ecological function E, exergetic performance coefficient EPC and thermo-economic function F criteria. Unlike the increase of k values, when the parameters I_1 and I_2 increase, then:

i) The maximum of each criterion F, E and EPC decreases with decreasing values of the corresponding optimal coefficient of performance ψ (**Fig. 3.15**).

ii) The maximum of each criterion F and E decreases with decreasing values of the corresponding optimum objective functions of performance q and $\dot{E}X_{out}$ (**Figs. 3.16** and **3.17** respectively). Whereas the maximum of the objective function EPC decreases with the gradual increasing values of the corresponding optimum objective functions of performance q and $\dot{E}X_{out}$ (**Figs. 3.16** and **3.17** respectively).

iii) The maximum of the objective function E decreases with the decreasing values of the corresponding optimal exergy destruction rate $\dot{E}X_D$ (**Fig. 3.18**). Whereas the maximum of each criterion F and EPC decreases with the abrupt increasing values of the corresponding optimal exergy destruction rate $\dot{E}X_D$ (**Fig. 3.18**).

Under optimal operating conditions, optimization parameters ψ , q , $\dot{EX}_{out}$ and $\dot{EX}_D$ related to the maximum of the exergy-based ecological function E and for an endoreversible system $(I_1 = I_2 = 1)$ are taken as references because they have the highest values: $\psi_{EPC} = \psi_F = 2.80$, $q_E = 1603 \text{Wm}^{-2}$, $\dot{EX}_{out-E} = 11779\text{W}$ and $\dot{EX}_{D-E} = 6324\text{W}$. Also, two cases are taken into account.

In the first case where $I_1 = 1.05$ and $I_2 = 1$, we make the following observations. ψ_F and ψ_{EPC} are both lower than the highest coefficient of performance value by 13.65%, whereas ψ_E is lower by a rate of 24.33%, in **Fig. 3.15(a)**. q_E, q_F and q_{EPC} are lower than the highest specific heating load value by rates of $29.60\%, 76.29\%$ and 80.85% respectively, in **Fig. 3.16(a)**. $\dot{EX}_{out-E}$, $\dot{EX}_{out-F}$ and $\dot{EX}_{out-EPC}$ are lower than the highest specific exergy output rate value which is itself proportional to the specific heating load by rates of $29.60\%, 76.29\%$ and 80.85% respectively, in **Fig. 3.17(a)**. On the other hand, $\dot{EX}_{D-EPC}$, $\dot{EX}_{D-F}$ and $\dot{EX}_{D-E}$ are lower than the highest exergy destruction rate value by rates of 85.01%, 81.20% and 16.90% respectively, in **Fig. 3.18(a)**.

In the second case where $I_1 = 1$ and $I_2 = 1.05$, we make the following observations. ψ_F and ψ_{EPC} are both lower than the highest coefficient of performance value by a rate of 24.22%, whereas ψ_E is lower by a rate of 29.08%, in **Fig. 3.15(b)**. q_E, q_F and q_{EPC} are lower than the highest specific heating load value by rates of 30.31%, 70.51% and 75.55% respectively, in **Fig. 3.16(b)**. $\dot{EX}_{out-E}$, $\dot{EX}_{out-F}$ and $\dot{EX}_{out-EPC}$ are lower than the highest specific exergy output rate value by rates of 30.31%, 70.51% and 75.55% respectively, in **Fig. 3.17(b)**. On the other hand, $\dot{EX}_{D-EPC}$, $\dot{EX}_{D-F}$ and $\dot{EX}_{D-E}$ are lower than the highest exergy destruction rate value by rates of 71.39%, 65.30% and 2.67% respectively, in **Fig. 3.18(b)**.

From this we deduce that, the impact of heat losses on system performance between the condenser and the evaporator characterized by the internal irreversibility factor I_2 is greater than that between the generator and the absorber characterized by the internal irreversibility factor I_1. This is manifested by highest maximum values of the objective functions F , EPC and E which correspond to the best optimal performance of the parameters ψ , q , $\dot{EX}_{out}$ and $\dot{EX}_D$, under the

influence of I_1. Furthermore, under the effects of the two internal irreversibility factors, THR AHP cycle has a significant advantage at the maxima of the F and the EPC criteria in terms of coefficient of performance. Nevertheless, the system has a significant advantage at the maximum of the EPC in terms of exergy destruction rate, and at the maximum of the E criterion in terms of specific heating load and exergy output rate.

3.4.2. Thermo-economic parameter (k) on the EPC, E and F objective functions

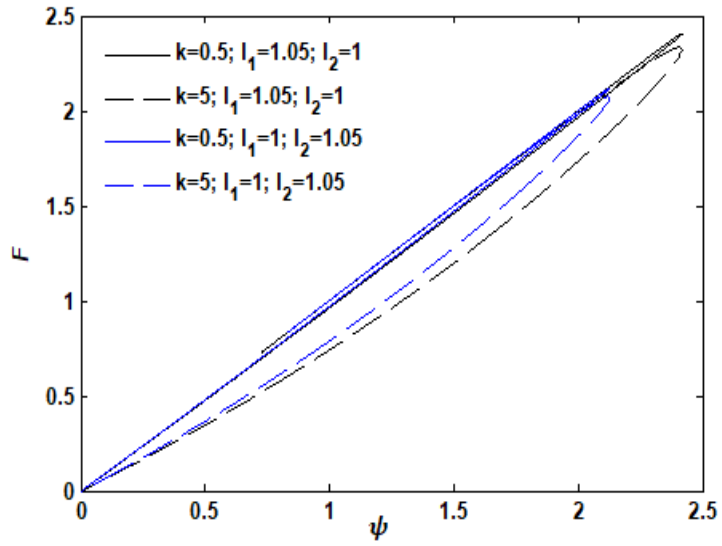

Fig. 3.19. Effects of thermo-economic factor on the *F* criterion with respect to the *COP* (ψ) objective function.

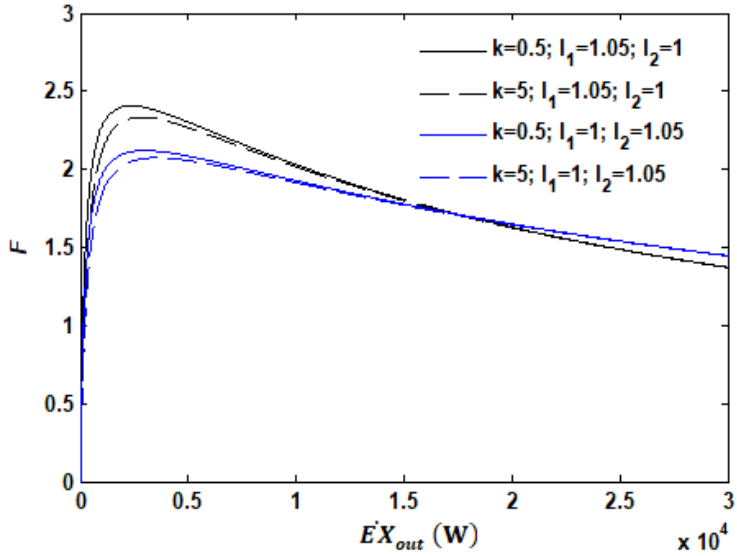

Fig. 3.20. Effects of thermo-economic factor on the *F* criterion with respect to the $\dot{E}X_{out}$ objective function.

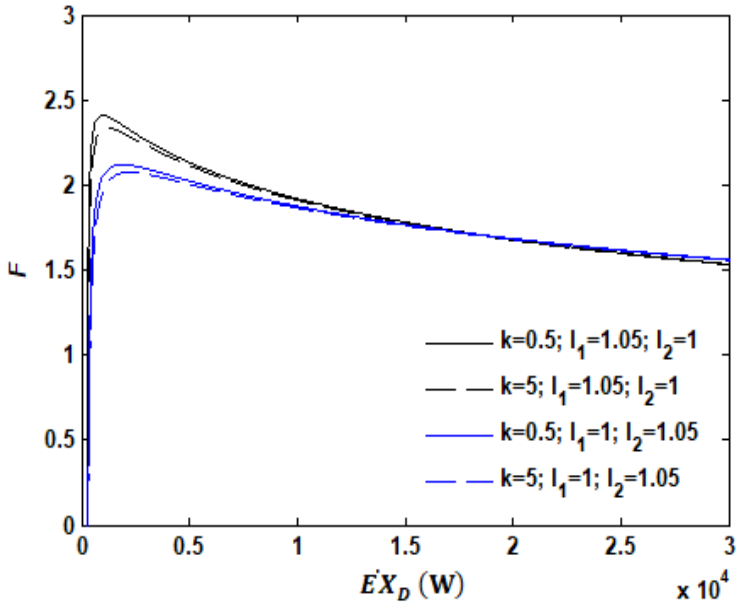

Fig. 3.21. Effects of thermo-economic factor on the *F* criterion with respect to the $\dot{E}X_D$ objective function.

Among the three decisive objective functions *F*, *E* and *EPC*, the thermo-economic parameter only affects the objective function *F*. Again, when the capital cost increases and the cost of the consumed energy decreases, thereafter thermo-economic parameter (*k*) increases while *F* decreases. The variations of the thermo-economic criterion (*F*) with respect to the coefficient of performance (ψ), the exergy output rate ($\dot{E}X_{out}$) and the exergy destruction rate ($\dot{E}X_D$) respectively were plotted under the influences of thermo-economic parameter (*k*) in **Figs. 19-21**. In **Fig. 3.19**, the thermo-economic *F* objective function increases as the *COP* increases and the curves obtained are loops passing through the origin which are less and less sharp when the thermo-economic parameter values (*k*) increase. So much so that in **Figs. 3.20** and **3.21**, the criterion *F* increases rapidly near its maximum before decreasing asymptotically thereafter, especially in **Fig. 3.21**, this when *k* increases. It is useful to observe that when *k* increases, the maximum of the objective function *F* is lower. Whereas the specific heating load, the exergy output rate and the exergy destruction rate have higher optimal corresponding values.

However, it is crucial in the optimization of the THR AHP by the objective function *F* that we have an important of maximum values *F*, corresponding to a minimum exergy destruction rate for certain values of the specific heating load and the exergy output rate.

3.4.3. Heat leakage and heat resistance

3.4.3.1. On the ECOP objective function

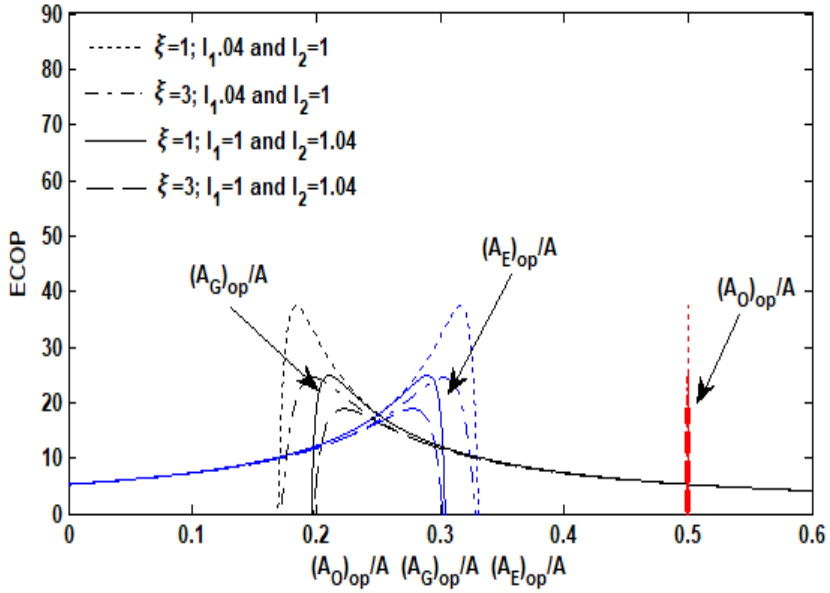

Fig. 3.22. Effects of heat leakage coefficient ξ on the *ECOP* objective function with respect to the $\left(A_O\right)_{op}/A$, $\left(A_G\right)_{op}/A$ and $\left(A_E\right)_{op}/A$ objective functions.

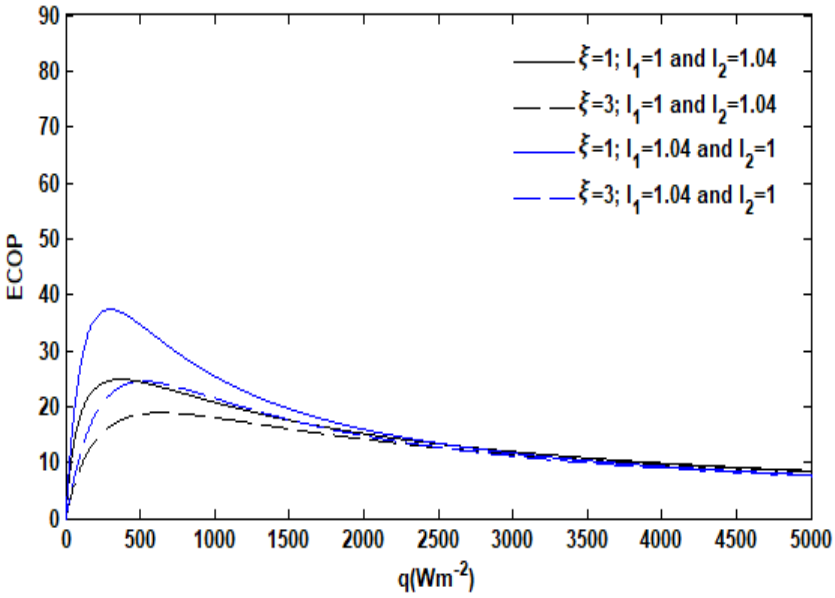

Fig. 3.23. Effects of heat leakage coefficient ξ on the *ECOP* objective function with respect to the q objective function.

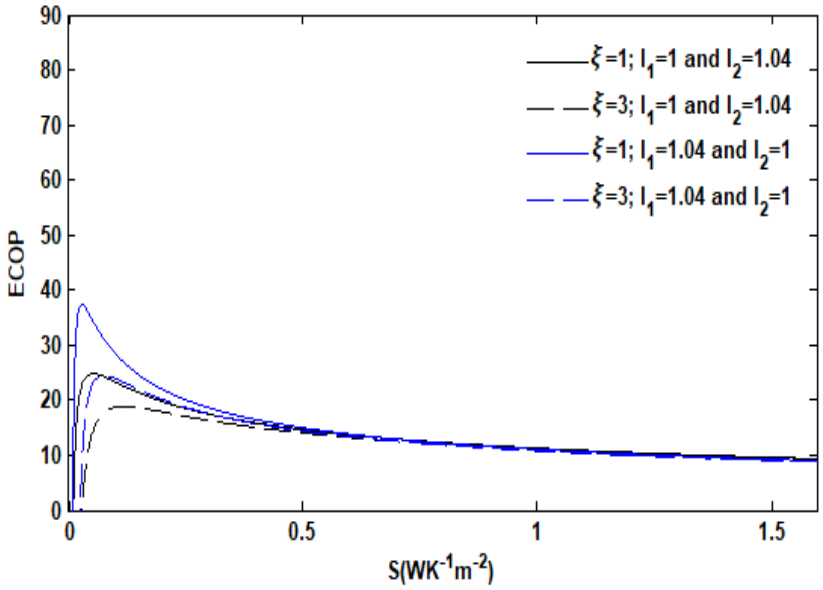

Fig. 3.24. Effects of heat leakage coefficient ξ on the *ECOP* objective function with respect to the S objective function.

Figs. 3.22-3.24 show the variations of the *ECOP* objective function respectively with respect to the specific entropy generation rate (S), the specific heating load (q) and the heat-transfer areas of the heat exchangers (A_G, A_E, A_O). These variations are presented under the effect of external irreversibility or heat leakage coefficient (ξ). External irreversibility affects the performance parameters of the AHP cycle the same way that the two internal irreversibilities factors affect these parameters, that is quantitatively and qualitatively. However, the effects of heat loss and internal irreversibility (I_2) of the condenser-evaporator assembly are greater.

3.4.3.2. On the EPC, E and F criteria

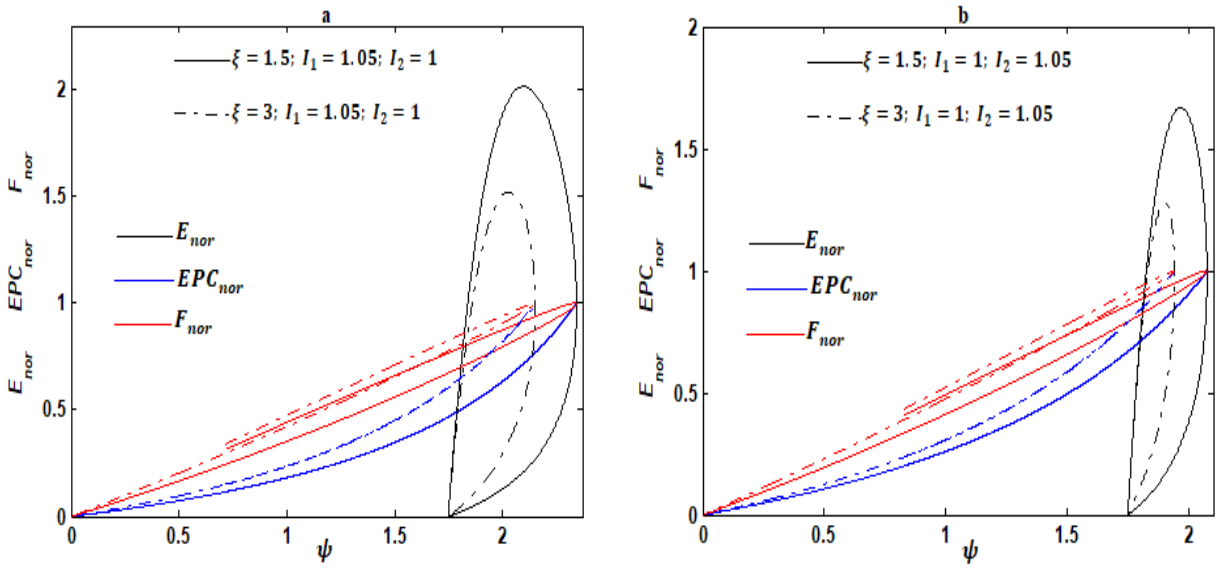

Fig. 3.25. Effects of heat leakage coefficient ξ on the dimensionless E_{nor}, EPC_{nor} and F_{nor} with respect to the COP (ψ) objective function.

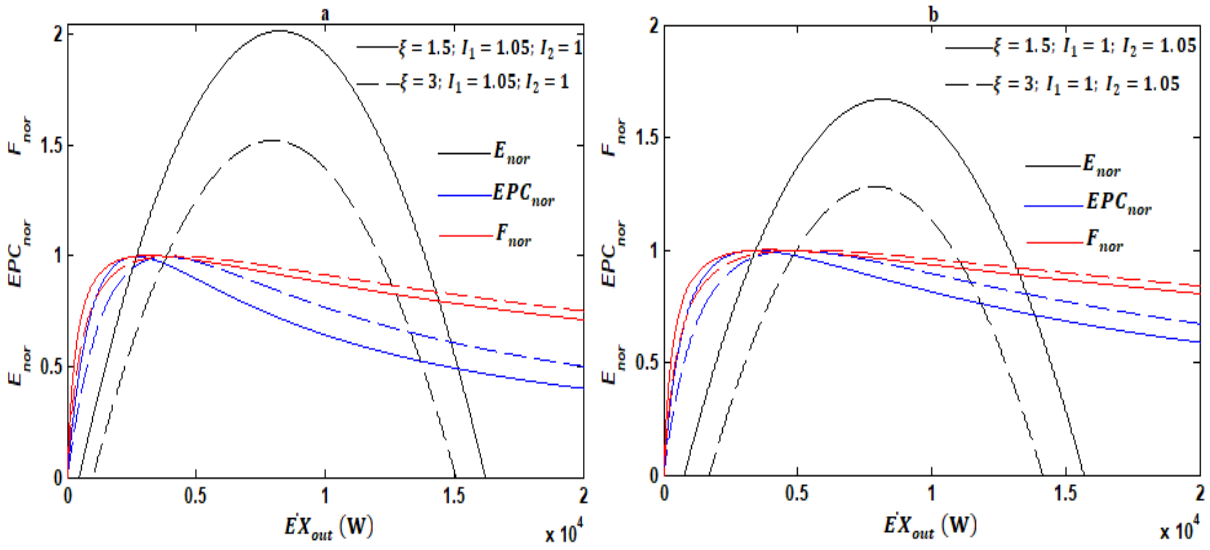

Fig. 3.26. Effects of heat leakage coefficient ξ on the dimensionless E_{nor}, EPC_{nor} and F_{nor} with respect to the $\dot{E}X_{out}$ objective function.

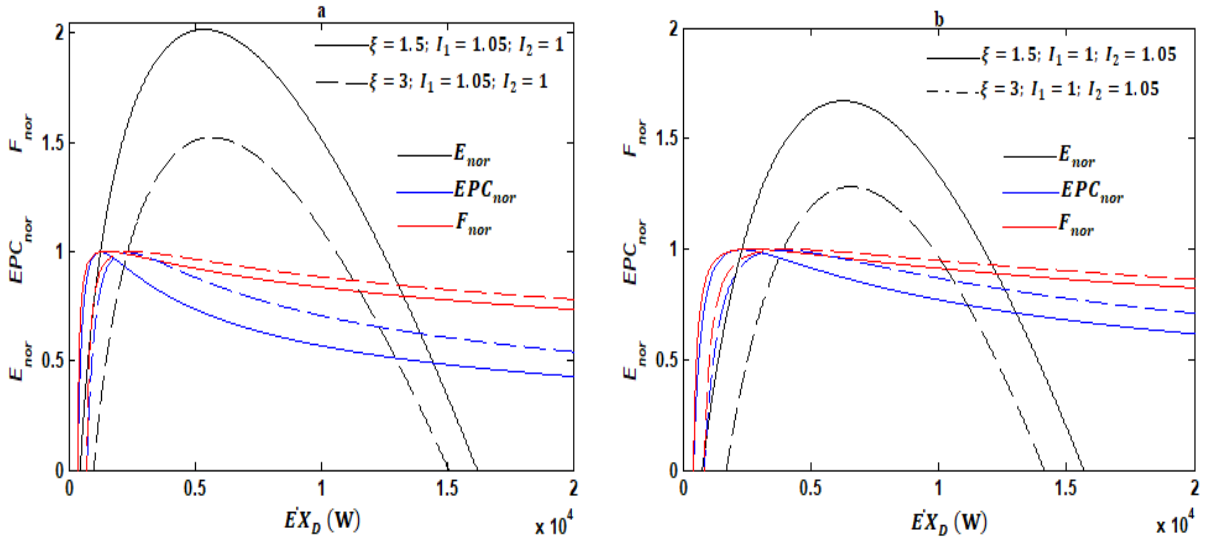

Fig. 3.27. Effects of heat leakage coefficient ξ on the dimensionless E_{nor}, EPC_{nor} and F_{nor} with respect to the $\dot{E}X_D$ objective function.

Figs. 3.25-3.27 show the variations of the dimensionless E_{nor}, EPC_{nor} and F_{nor} with respect to the objective functions of performance ψ, $\dot{E}X_{out}$ and $\dot{E}X_D$ respectively. These characterizes the influences of the heat resistances and heat leakages on the exergy-based ecological function *E*, exergetic performance coefficient *EPC* and thermo-economic function *F* criteria. In these figures, when the parameter ξ increases with each time $I_1 = 1.05$ when $I_2 = 1$ and $I_1 = 1$ when $I_2 = 1.05$, then:

i) The maximum of each objective function F, E and EPC decreases with decreasing values of the corresponding optimal coefficient of performance ψ (**Fig. 3.25**).

ii) The maximum of each objective function F and EPC decreases with increasing values of the corresponding optimal exergy output rate $\dot{E}X_{out}$ (**Fig. 3.26**). Whereas the maximum of the objective function E decreases with the gradual decreasing values of the corresponding optimal exergy output rate $\dot{E}X_{out}$ (**Fig. 3.26**).

iii) The maximum of each objective functions F and EPC decreases with the abrupt increasing values of the corresponding optimal exergy destruction rate $\dot{E}X_D$ (**Fig. 3.27**), while the maximum of the objective function E decreases with the gradual increasing values of the corresponding optimal exergy destruction rate $\dot{E}X_D$ (**Fig. 3.27**).

To explore the effects of heat leakage and heat resistances, the optimal reference system is chosen according to whether $\xi = K_L = 0$ with in the first case $I_1 = 1.05$ when $I_2 = 1$ ($\psi_{EPC} = 2.88$

, $q_E = 1156 \mathrm{W m^{-2}}$, $\dot{EX}_{out-E} = 8492 \mathrm{W}$ and $\dot{EX}_{D-E} = 5038 \mathrm{W}$) and in the second case $I_2 = 1.05$ when $I_1 = 1$ ($\psi_{EPC} = 2.44$, $q_E = 1144 \mathrm{W m^{-2}}$, $\dot{EX}_{out-E} = 8408 \mathrm{W}$ and $\dot{EX}_{D-E} = 5938 \mathrm{W}$).

Firstly ($\xi = 1.5$, $I_1 = 1.05$ and $I_2 = 1$); ψ_F and ψ_{EPC} are both lower than the highest coefficient of performance value by 18.87%, whereas ψ_E is lower by a rate of 27.23%, in **Fig. 3.25**(a). $\dot{EX}_{out-E}$, $\dot{EX}_{out-F}$ and $\dot{EX}_{out-EPC}$ are lower than the highest exergy output rate value which is itself proportional to the specific heating load by rates of 3.25%, 63.09% and 68.63% respectively, in **Fig. 3.26(a)**. However, $\dot{EX}_{D-EPC}$ and $\dot{EX}_{D-F}$ are lower than the highest exergy destruction rate value by rates 75.22% and 70.62% respectively, in **Fig. 3.27(a)**. Whereas $\dot{EX}_{D-E}$ is greater than the highest exergy destruction rate value by a rate 6% in **Fig. 3.27(a)**.

On the other hand ($\xi = 1.5$, $I_1 = 1$ and $I_2 = 1.05$); ψ_F and ψ_{EPC} are both lower than the highest coefficient of performance value by 15.07%, whereas ψ_E is lower by a rate of 19.44%, in **Fig. 3.25(b)**. $\dot{EX}_{out-E}$, $\dot{EX}_{out-F}$ and $\dot{EX}_{out-EPC}$ are lower than the highest exergy output rate value which is itself proportional to the specific heating load by rates of 3.28%, 53.38% and 59.55% respectively, in **Fig. 3.26(b)**. However, $\dot{EX}_{D-EPC}$ and $\dot{EX}_{D-F}$ are lower than the highest exergy destruction rate value by rates of 61.58% and 70.62% respectively, in **Fig. 3.27(b)**. Whereas $\dot{EX}_{D-E}$ is greater than the highest exergy destruction rate value by rate 5.08% in **Fig. 3.27(b)**.

We deduce that under the effects of the heat leakages and heat resistances, the THR AHP cycle has a significant advantage at the maxima of the *F* and the EPC criteria in terms of coefficient of performance. Nevertheless, the THR AHP cycle has a significant advantage at the maximum of the EPC, in terms of exergy destruction rate. Also, the system has a significant advantage at the maximum of the *E*, in terms of specific heating load and exergy output rate. Moreover, the effects of heat resistances and heat leakages are more pronounced than the effects of internal irreversibility factors, on the performance of THR AHP.

3.5. Numerical applications for the FTL AHP single effect

The optimization of the AHP by considering the *EPC* objective function is necessary because this criterion of optimization takes into account the quality and the quantity of the energy produced in the medium to be heated. Its mathematical expression implies that, it takes into

account the specific entropy generation rate (S), the specific heating load (q), the exergy output rate, the exergy destruction rate and the influence of the surrounding medium at temperature T_{env}. We have considered the numerical values given in **table 3.2** for conformity with the literature.

Table 3.2. Parameters used in the model of the FTL AHP multi irreversible.

parameter	value
Temperature in generator, evaporator, condenser and absorber, respectively, T (K)	413, 283, 333, 313 (Bi et al., 2008; Ngouateu Wouagfack and Tchinda, 2012b)
Heat-transfer coefficient of generator, evaporator, condenser and absorber, U ($\mathrm{WK^{-1}m^{-2}}$)	1163, 2326, 4650, (Bi et al., 2008; Ngouateu Wouagfack and Tchinda, 2012b)
Distribution of the total rejected heat rate between the absorber and the condenser, m (-)	1.3 (Bi et al., 2008; Ngouateu Wouagfack and Tchinda, 2012b)
Total heat-transfer area of the external heat reservoirs in the heat exchangers, A ($\mathrm{m^2}$)	100 (Fossi Nemogne et al., 2020)
Thermal conductivity linked to heat leaks, K_L ($\mathrm{WK^{-1}}$)	300
Heat leakage coefficient, ξ ($\mathrm{WK^{-1}m^{-2}}$)	3 (Bi et al., 2008; Ngouateu Wouagfack and Tchinda, 2012b)
Thermo-economic parameter, k (-)	5

3.6. Effects of temperatures of the working fluid in the different components for the FTL AHP

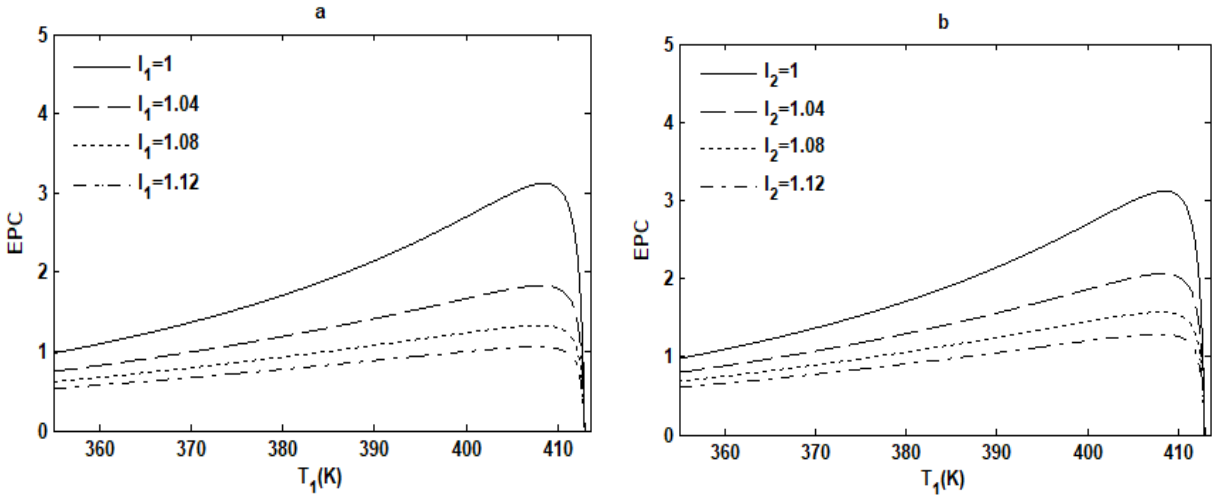

Fig. 3.28. Variation of *EPC* objective function with respect to the temperature T_1 of the working fluid in the generator when $I_2 = 1$ for various I_1 (a); when $I_1 = 1$ for various I_2 (b).

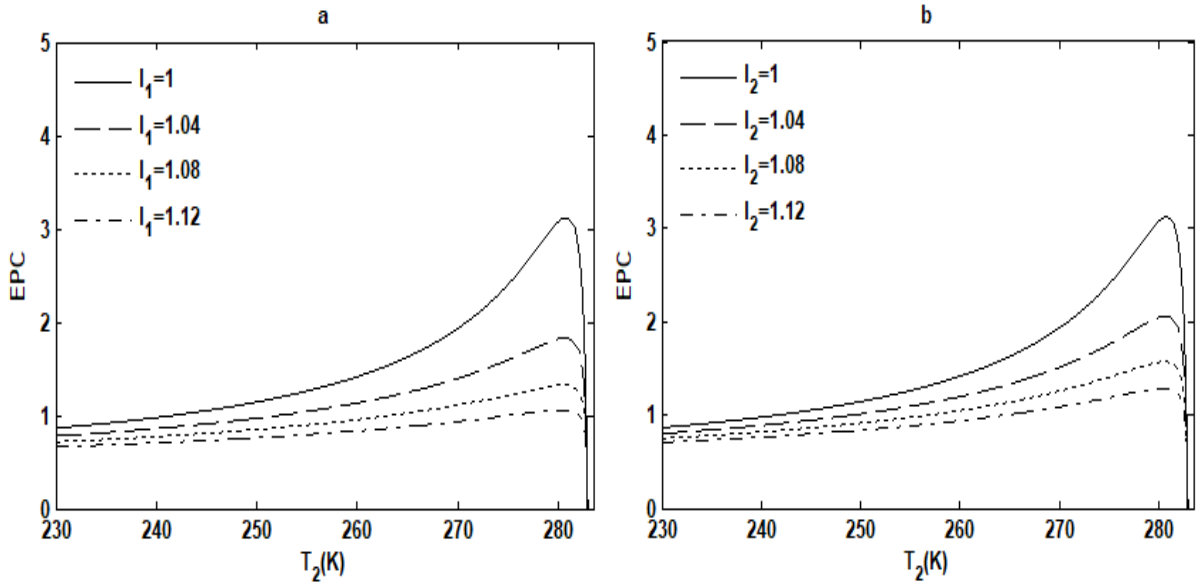

Fig. 3.29. Variation of *EPC* objective function with respect to the temperature T_2 of the working fluid in the evaporator when $I_2 = 1$ for various I_1 (a); when $I_1 = 1$ for various I_2 (b).

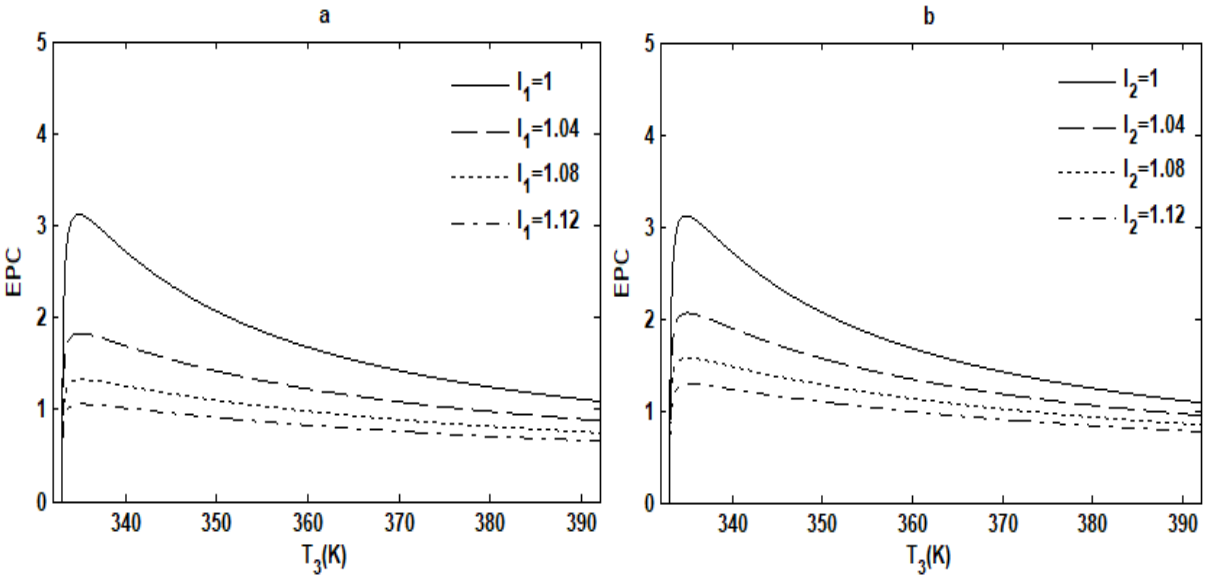

Fig. 3.30. Variation of *EPC* objective function with respect to the temperature T_3 of the working fluid in the condenser when $I_2 = 1$ for various I_1 (a); when $I_1 = 1$ for various I_2 (b).

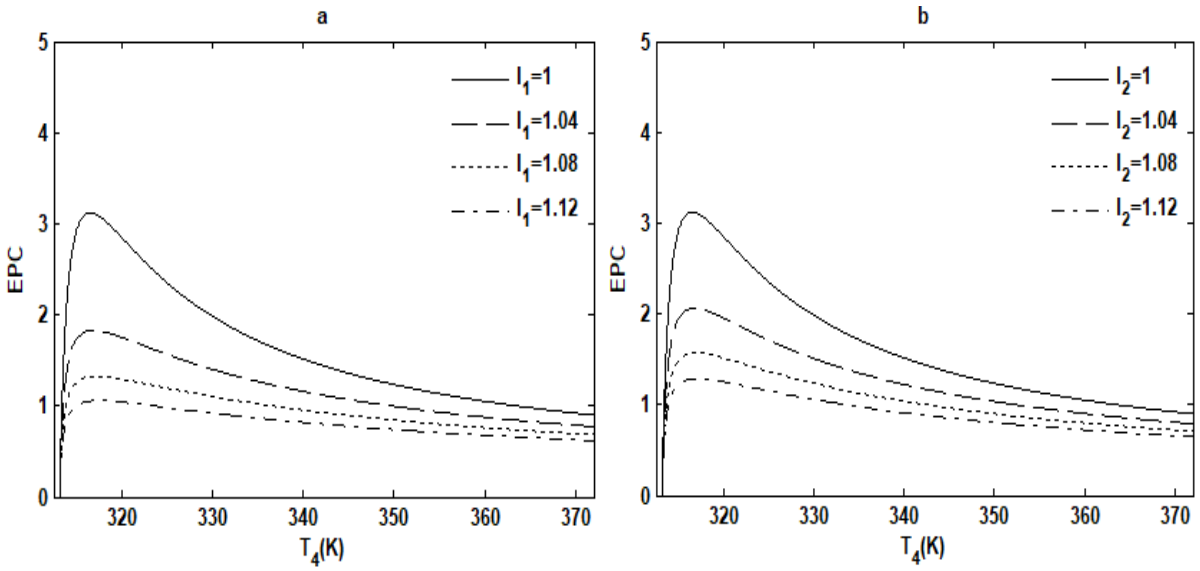

Fig. 3.31. Variation of *EPC* objective function with respect to the temperature T_4 of the working fluid in the absorber when $I_2 = 1$ for various I_1 (a); when $I_1 = 1$ for various I_2 (b).

Figs. 3.28-3.31 show the variations of the EPC objective function with respect to the temperatures T_1, T_2, T_3 and T_4 which respectively represent the temperatures of working fluid in the generator, the evaporator, the condenser and the absorber. In **Figs. 3.28(a)**, **3.29(a)**, **3.30(a)** and **3.31(a)** I_2 is set $(I_2 = 1)$ for different values of I_1 and in **Figs. 3.28(b)**, **3.29(b)**, **3.30(b)** and **3.31(b)** I_1 is set $(I_1 = 1)$ for different values of I_2. The EPC gradually increases with increase in the temperatures T_1 and T_2 before reaching its maximum in **Figs. 3.28** and **3.29**. However EPC decreases after reaching its maximum values when T_3 and T_4 increase in **Figs. 3.30** and **3.31**. As a result, when $T_1 < T_{1op}$, $T_2 < T_{2op}$, $T_3 > T_{3op}$ and $T_4 > T_{4op}$ the system is less ecological because the heat losses are greater, and when $T_1 > T_{1op}$, $T_2 > T_{2op}$, $T_3 < T_{3op}$ and $T_4 < T_{4op}$ the system is unstable. However, the $ECOP_{\max}$ is more affected in the system for the same values of the optimum temperatures in the absorber-generator assembly by the irreversibility factor I_1 than in the condenser-evaporator by the irreversibility factor I_2.

3.7. Effects of design parameters for the FTL AHP

3.7.1. Influences of two internal irreversibilities I_1 and I_2

3.7.1.1. On the EPC criterion

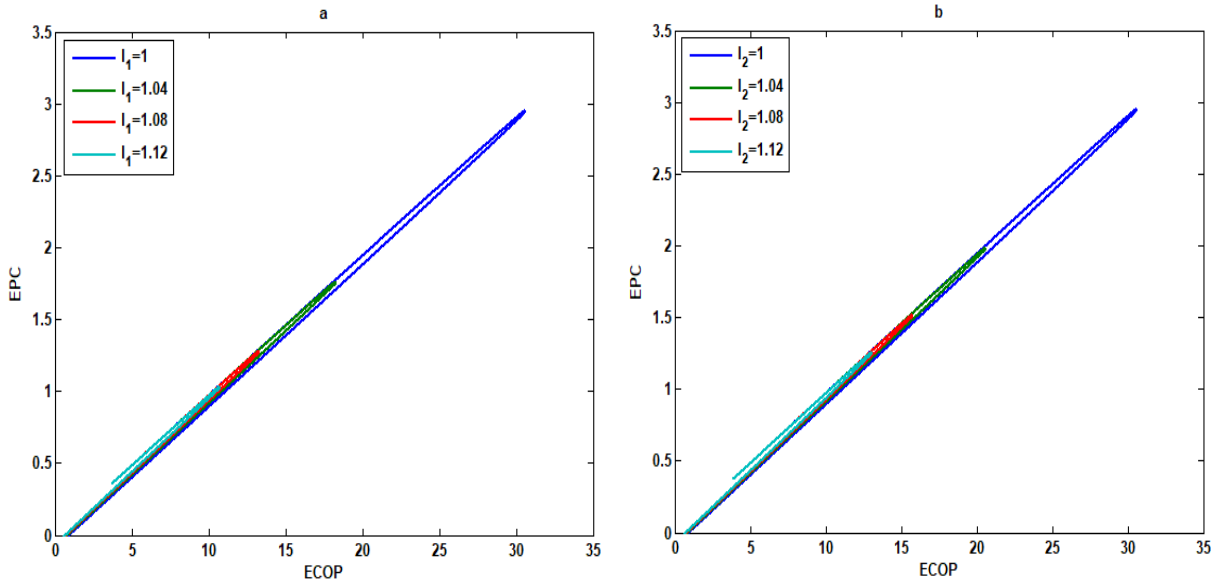

Fig. 3.32. Effects of internal irreversibility I_1 (a) ($I_2 = 1$) of the generator-absorber assembly and of the internal irreversibility I_2 (b) ($I_1 = 1$) of the evaporator-condenser assembly on the *EPC* objective function with respect to the *ECOP* objective function.

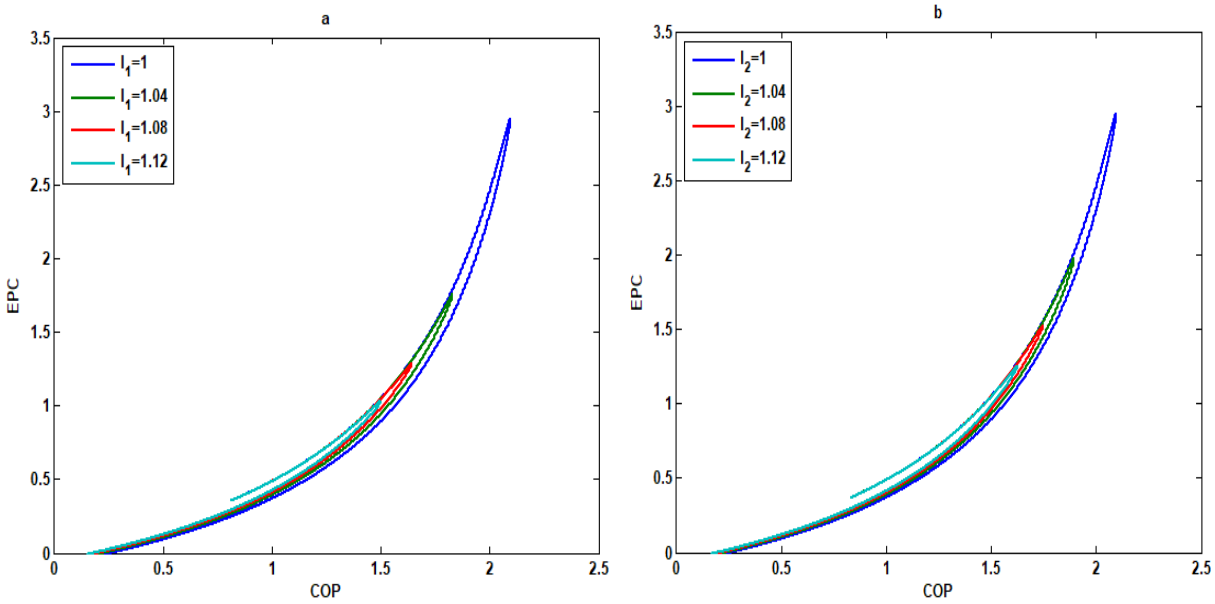

Fig. 3.33. Effects of internal irreversibility I_1 (a) ($I_2 = 1$) of the generator-absorber assembly and of the internal irreversibility I_2 (b) ($I_1 = 1$) of the evaporator-condenser assembly on the *EPC* objective function with respect to the *COP* objective function.

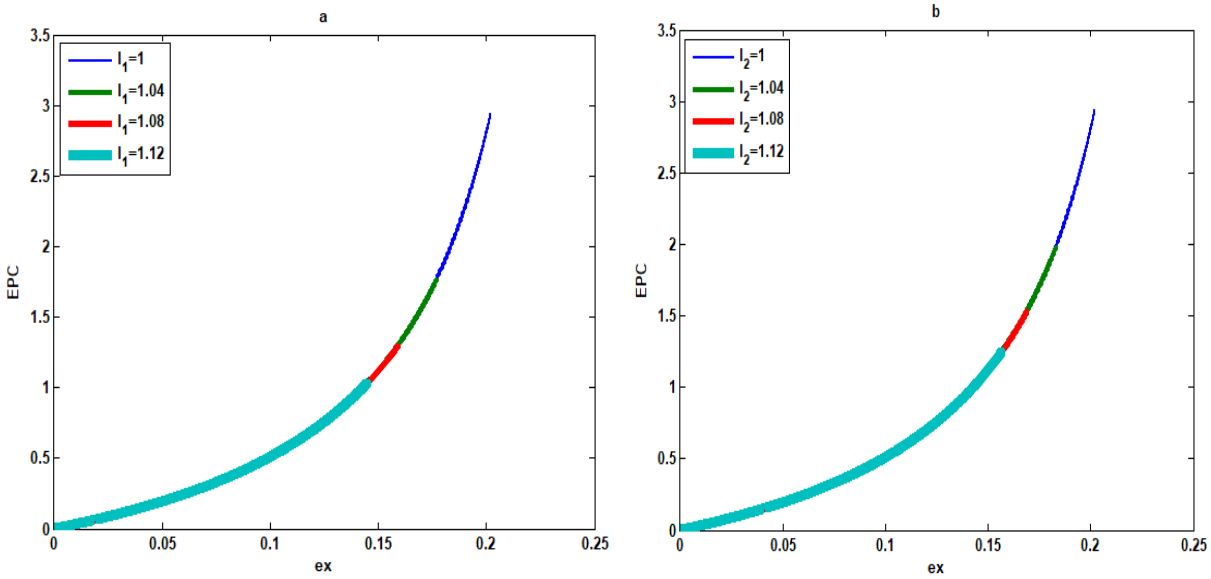

Fig. 3.34. Effects of internal irreversibility I_1 (a) ($I_2 = 1$) of the generator-absorber assembly and of the internal irreversibility I_2 (b) ($I_1 = 1$) of the evaporator-condenser assembly on the *EPC* objective function with respect to the *ex* objective function.

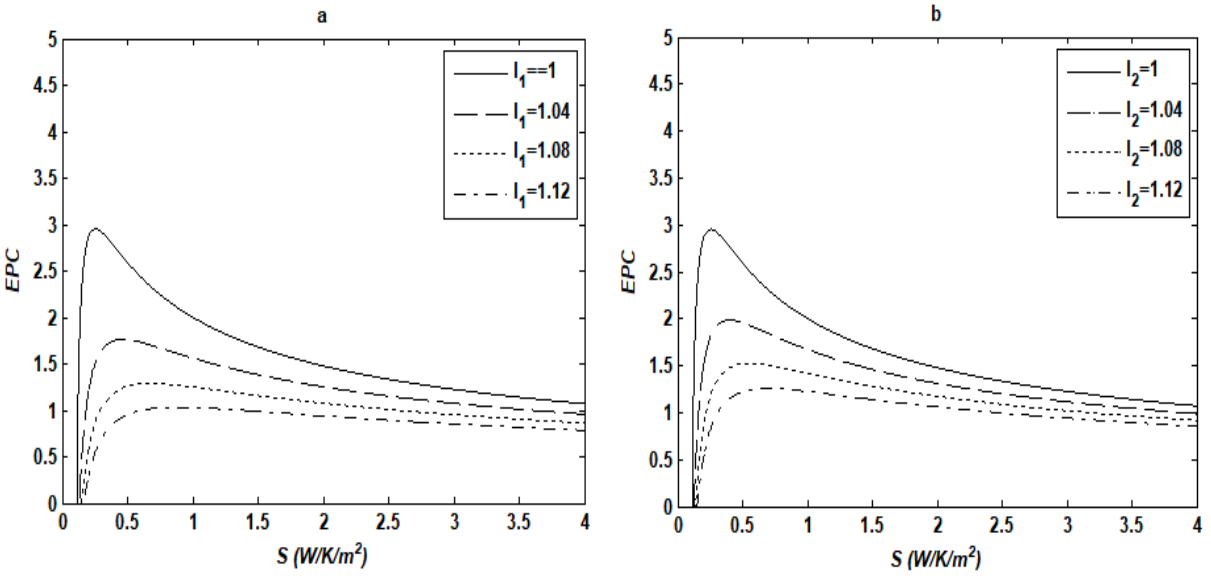

Fig. 3.35. Effects of internal irreversibility I_1 (a) ($I_2 = 1$) of the generator-absorber assembly and of the internal irreversibility I_2 (b) ($I_1 = 1$) of the evaporator-condenser assembly on the *EPC* objective function with respect to the *S* objective function.

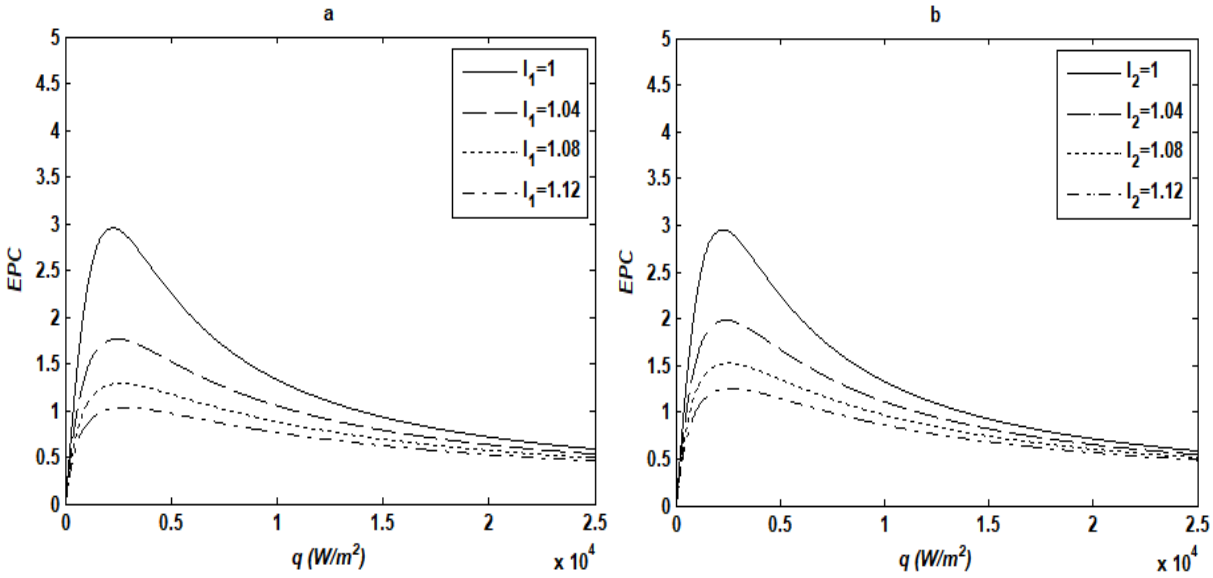

Fig. 3.36. Effects of internal irreversibility I_1 (a) ($I_2 = 1$) of the generator-absorber assembly and of the internal irreversibility I_2 (b) ($I_1 = 1$) of the evaporator-condenser assembly on the *EPC* objective function with respect to the *q* objective function.

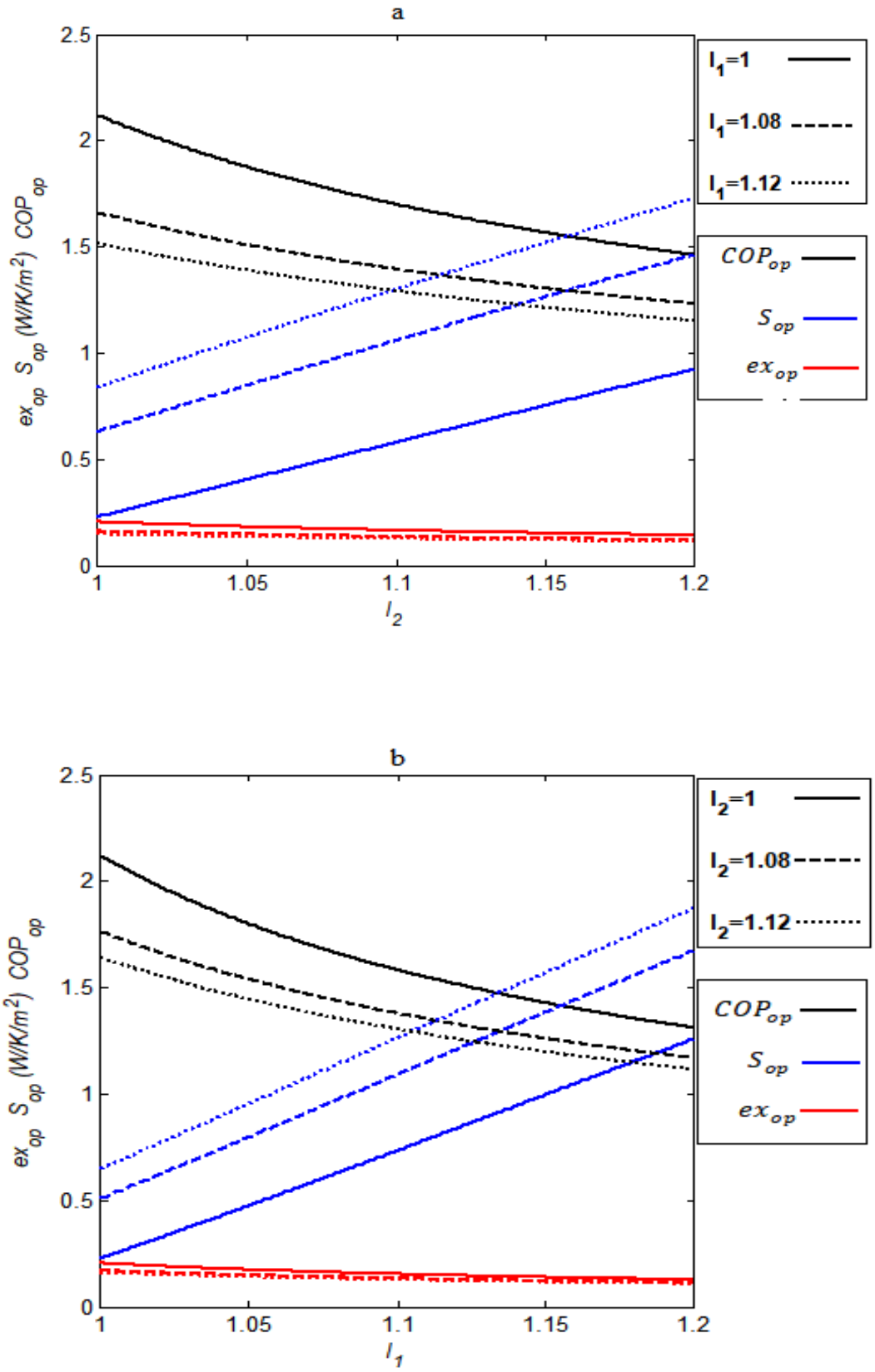

Fig. 3.37. Effects of internal irreversibility I_2 (a) of the evaporator-condenser assembly and of the internal irreversibility I_1 (b) of the generator-absorber assembly on the ex_{op}, S_{op} and COP_{op} optimal objective functions for certain values of I_1 and I_2 respectively.

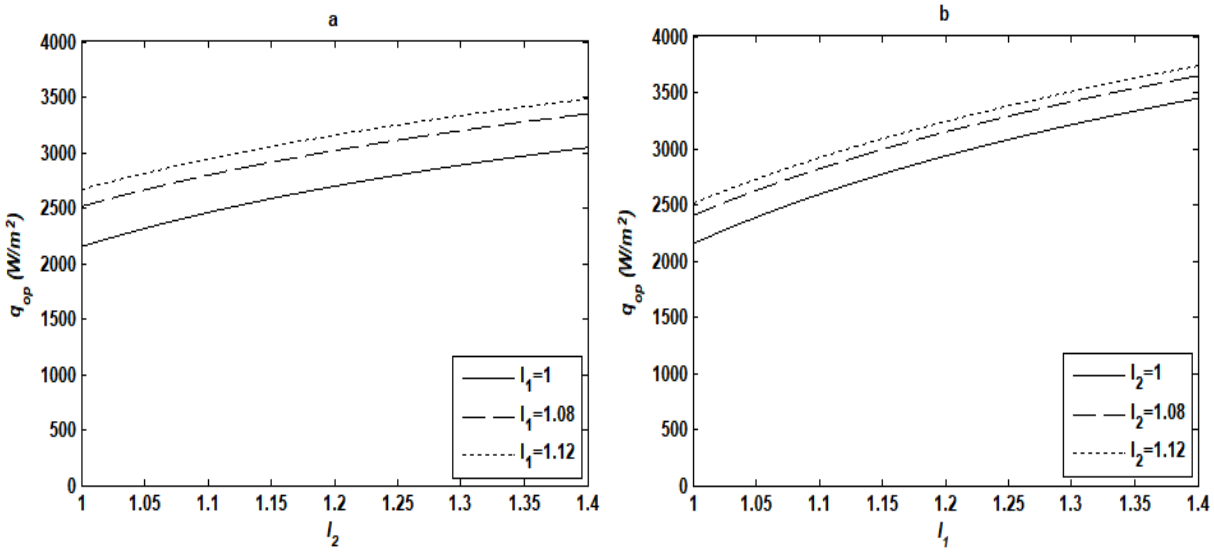

Fig. 3.38. Effects of internal irreversibility I_2 (a) of the evaporator-condenser assembly and of the internal irreversibility I_1 (b) of the generator-absorber assembly on the q_{op} optimal objective function for certain values of I_1 and I_2 respectively.

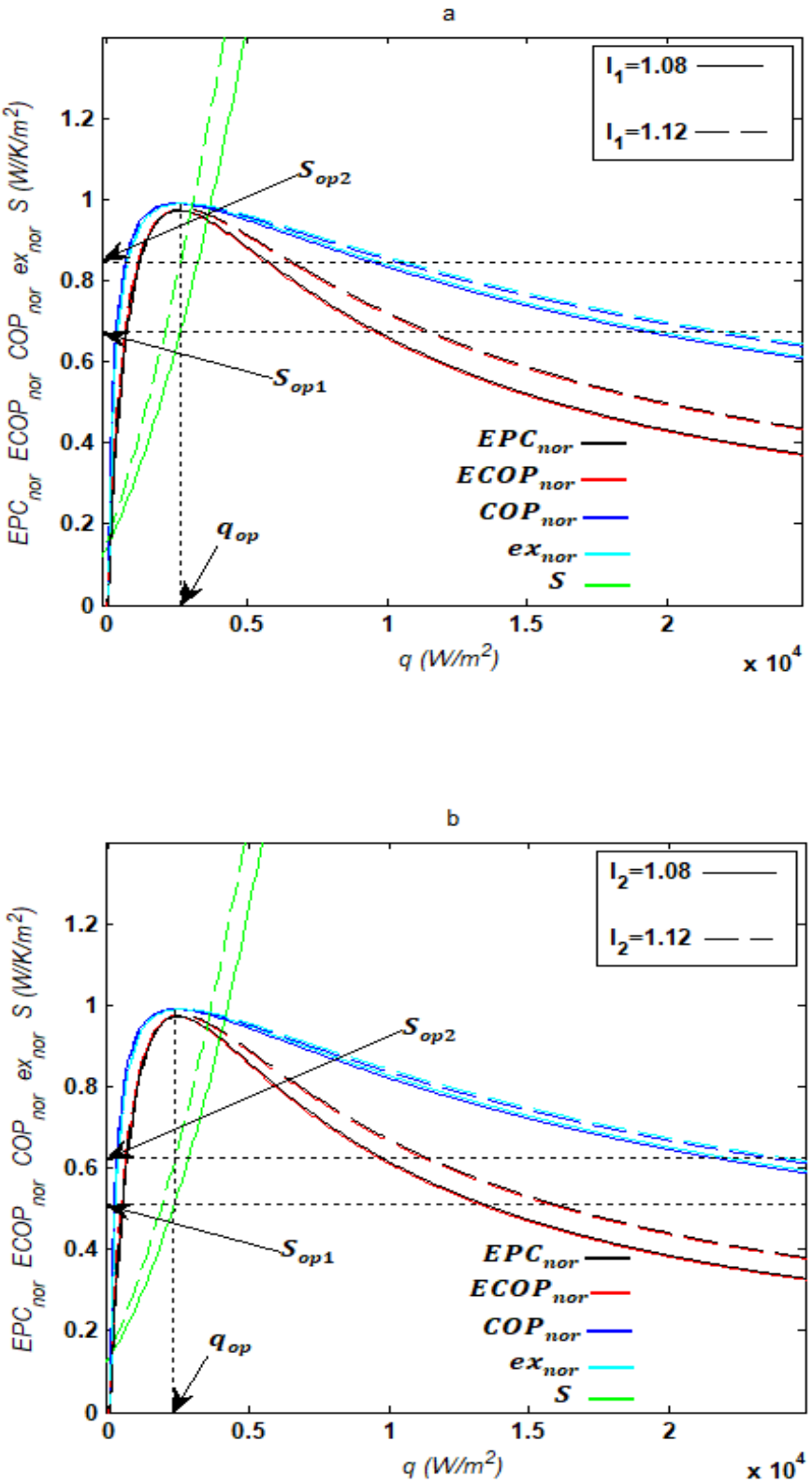

Fig. 3.39. Variations of the non-dimensional *EPC*, the non-dimensional *ECOP*, the non-dimensional *COP*, the non-dimensional *ex* and the specific entropy generation rate with respect to the specific heating load for certain values of I_1 (a) when $I_2 = 1$ and for certain values of I_2 (b) when $I_1 = 1$.

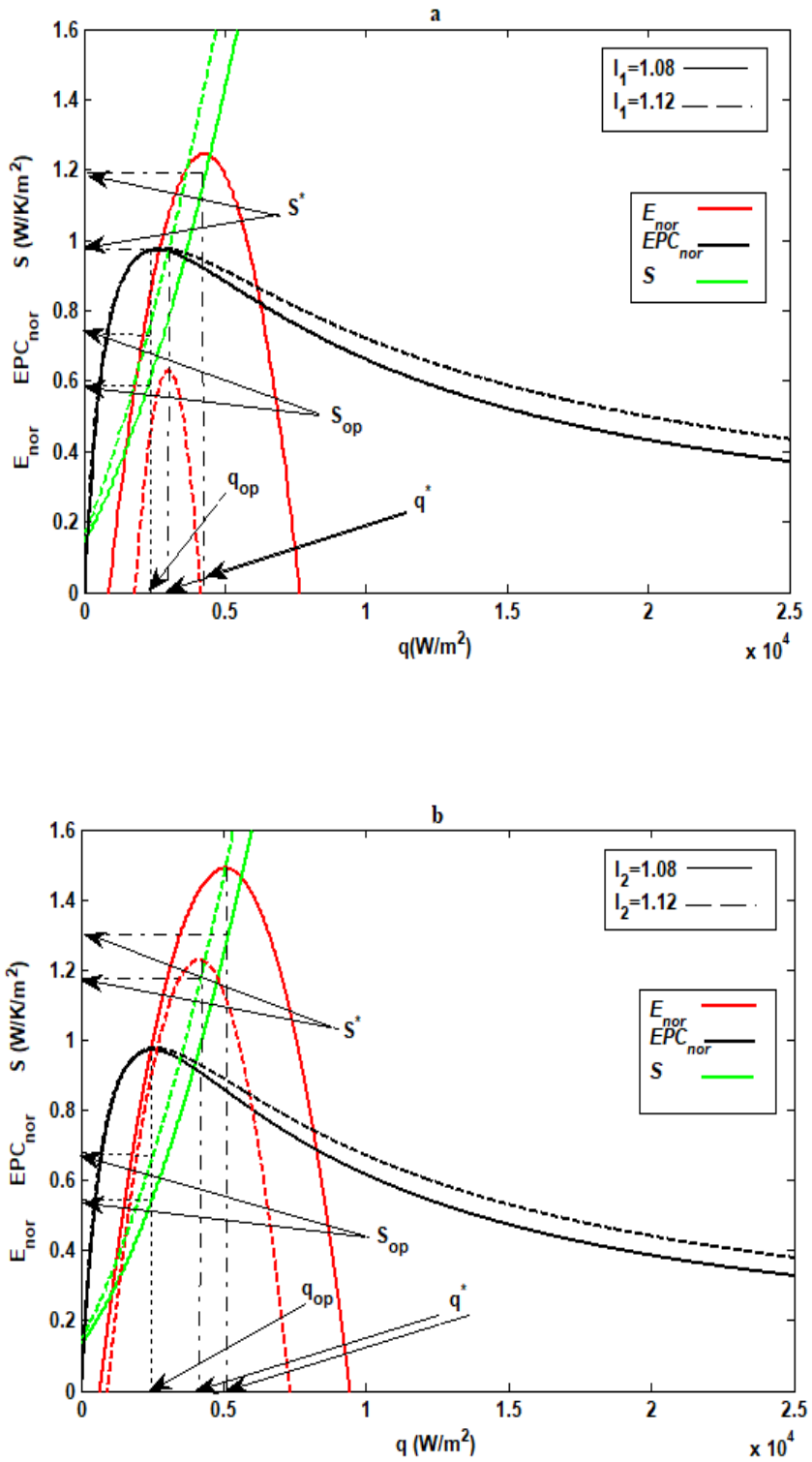

Fig. 3.40. Variations of the non-dimensional *EPC* objective function, the non-dimensional *E* function and specific entropy generation rate with respect to the specific heating load for certain values of I_1 (a) when $I_2 = 1$ and for certain values of I_2 (b) when $I_1 = 1$.

Figs. 3.32-3.38 show how the friction, the singularity points and the turbulence of the working fluid modeled by the two internal irreversibility factors, influence the performance parameters of the FTL AHP. It follows that in **Figs. 3.32-3.34**, the EPC objective function increases with increasing *ECOP* values, the *COP* and the exergetic efficiency (*ex*). Specifically, the linear

growth of the *EPC* objective function with the *ECOP* objective function (**Fig. 3.32**) shows the proportionality between the *EPC* and *ECOP* objective functions. **Figs. 3.35** and **3.36** show the variation of *EPC* with respect to *S* and *q* values respectively under the influence of I_1 on the one hand when $I_2 = 1$ (**Figs. 3.35(a)** and **3.36(a)**) and under the influence of I_2 on the other hand when $I_1 = 1$ (**Figs. 3.35(b)** and **3.36(b)**). We observe that the *EPC* increases abruptly before reaching its maximum then decreases asymptotically (**Figs. 3.35** and **3.36**). In addition, the maximum of the *EPC* values decrease when the optimal values corresponding of the specific entropy generation rate (*S*) and the specific heating load (*q*) increase, for increasing values of I_1 on the one hand (**Figs. 3.35(a)** and **3.36(a)**) and I_2 on the other hand (**Figs. 3.35(b)** and **3.36(b)**). **Figs. 3.37** and **3.38** show variations of the ex_{op}, S_{op}, COP_{op} and q_{op} optimal objective functions corresponding to the maximum of *EPC* with respect to I_2 for different values of I_1 (**Figs. 3.37(a) and 3.38(a)**) on the one hand and I_1 for different values of I_2 (**Figs. 3.37(b)** and **3.38(b)**) on the other hand. COP_{op} and ex_{op} values decrease when I_1 and I_2 increase (**Figs. 3.37(a)**, **(b)**), as S_{op} and q_{op} values increase when I_1 and I_2 increase (**Figs. 37(a)**, **(b)** and **38(a)**, **(b)**).

As a result, the COP_{op} and the ex_{op} values are better for values of I_1 and I_2 close to the unit corresponding to the endoreversible FTL AHP because the optimal specific entropy generation rate is minimal for certain values of the optimal specific heating load.

Table 3.3. FTL AHP loss rate from the exergetic performance criterion (*EPC*) versus the endoreversible system ($I_1 = I_2 = 1$, $m = 1.3$ and $\xi = 3$) for different values of I_1 and I_2.

Percentage (%) loss rate of *EPC*	$I_1 = 1.00$	$I_1 = 1.03$	$I_1 = 1.06$	$I_1 = 1.09$	$I_1 = 1.12$
$I_2 = 1.00$	0	34.81	50.84	60.07	66.07
$I_2 = 1.03$	27.99	47.92	58.65	65.36	69.95
$I_2 = 1.06$	42.98	56.20	64.02	69.20	72.87
$I_2 = 1.09$	52.32	61.90	67.94	72.11	75.15
$I_2 = 1.12$	58.70	66.07	70.94	74.39	76.97

Table 3.3 summarizes the influence of the two parameters of internal irreversibility by showing the exergy loss rate of I_1 and I_2. The endoreversible FTL AHP is taken for reference because it is not affected by heat losses and its designed parameters are $I_1 = I_2 = 1$, $m = 1.3$ and $\xi = 3$. This table shows that the highest exergy loss rate are observed in the generator-absorber assembly, while the lowest exergy loss rate are observed in the evaporator-condenser assembly. This observation was confirmed rather in the AR by Talbi and Agnew (2000) who showed that the

exergy losses are greater in the generator and the absorber, due to the differences in temperature between the absorber and the environment and between the generator and the heat source.

Fig. 3.39 shows variations of the normalized *EPC* ($EPC_{nor} = EPC/EPC_{\max}$), normalized *ECOP* ($ECOP_{nor} = ECOP/ECOP_{\max}$), normalized *COP* ($COP_{nor} = COP/COP_{\max}$), normalized ($ex_{nor} = ex/ex_{\max}$), and *S* versus *q* for different values of I_1 and I_2. $ECOP_{op}$, COP_{op}, ex_{op}, S_{op} and q_{op} being each optimal objective functions corresponding to the maximum of the *EPC* criterion. It is important to observe that the maximum of these four objective functions (EPC_{nor}, $ECOP_{nor}$, COP_{nor} and ex_{nor}) coincide, yet they each have a different physical meaning by definition. Ngouateu Wouagfack and Tchinda (2011a, 2011b, 2012a, 2012b, 2014) made this observation between *ECOP* and *COP* for AR and AHP having three and four heat sources with internal irreversibility. Same for Medjo Nouadje et al. (2014) for AR with three-heat-source and two internal irreversibilities.

Also, At the maximum of each *EPC*, *ECOP*, *COP* and *ex* objective function corresponds each time the same value of the optimal specific heating load q_{op} and the increasing optimal values of the specific entropy generation rate, according to the increasing values of the parameters I_1 and I_2.

However, **Fig. 3.40** shows the variations of the normalized *EPC* ($EPC_{nor} = EPC/EPC_{\max}$), normalized *E* ($E_{nor} = E/E_{op,E}$), and S with respect to the q for different values of I_1 and I_2. It is observed that when the FTL cycle operates in optimal conditions to the maximum values of the ecological criterion *E*, $q_{op} < q^*$ and $S_{op} < S^*$. Here q^* and S^* are the values of the optimal objective functions corresponding to the maximum of the ecological criterion *E*.

In other words, the results obtained in **Figs. 3.39** and **3.40** show that:

i) At the maximum of the *EPC* and *ECOP* objectives functions, a low specific entropy generation rate and a better *COP* compared to the maximum of *E* objective function are obtained.

ii) At the maximum of the *E* objective, a higher specific heating load has been found than the maximum of the *EPC* and *ECOP* objectives functions. In addition, the optimal functions of performance at the maximum *E* criterion are higher under the influence of the internal irreversibility factor I_2.

3.7.1.2. On the E, EPC and F criteria

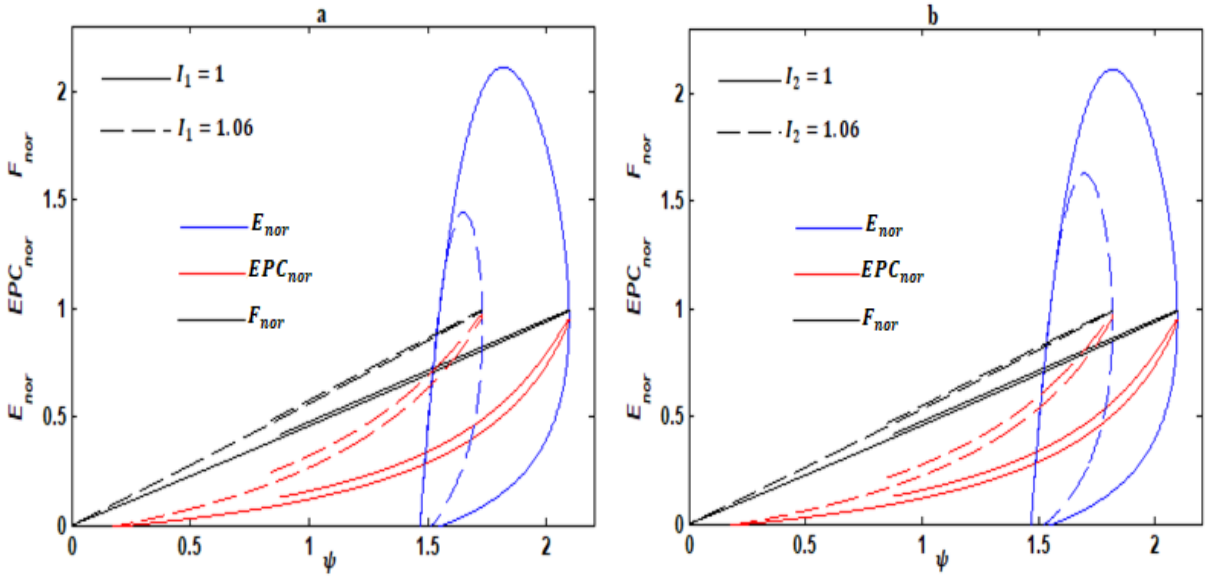

Fig. 3.41. Effects of internal irreversibility I_1 (a) of the generator-absorber assembly and of the internal irreversibility I_2 (b) of the evaporator-condenser assembly on the dimensionless E_{nor}, EPC_{nor} and F_{nor} with respect to the *COP* (ψ) objective function.

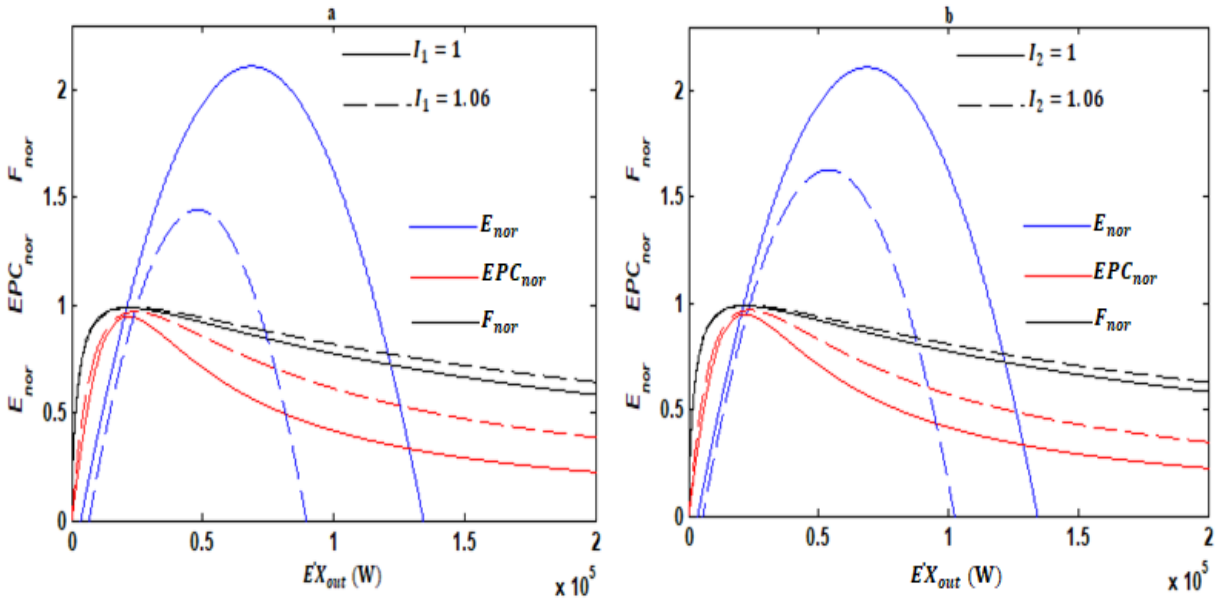

Fig. 3.42. Effects of internal irreversibility I_1 (a) of the generator-absorber assembly and of the internal irreversibility I_2 (b) of the evaporator-condenser assembly on the dimensionless E_{nor}, EPC_{nor} and F_{nor} with respect to the $\dot{E}X_{out}$ objective function.

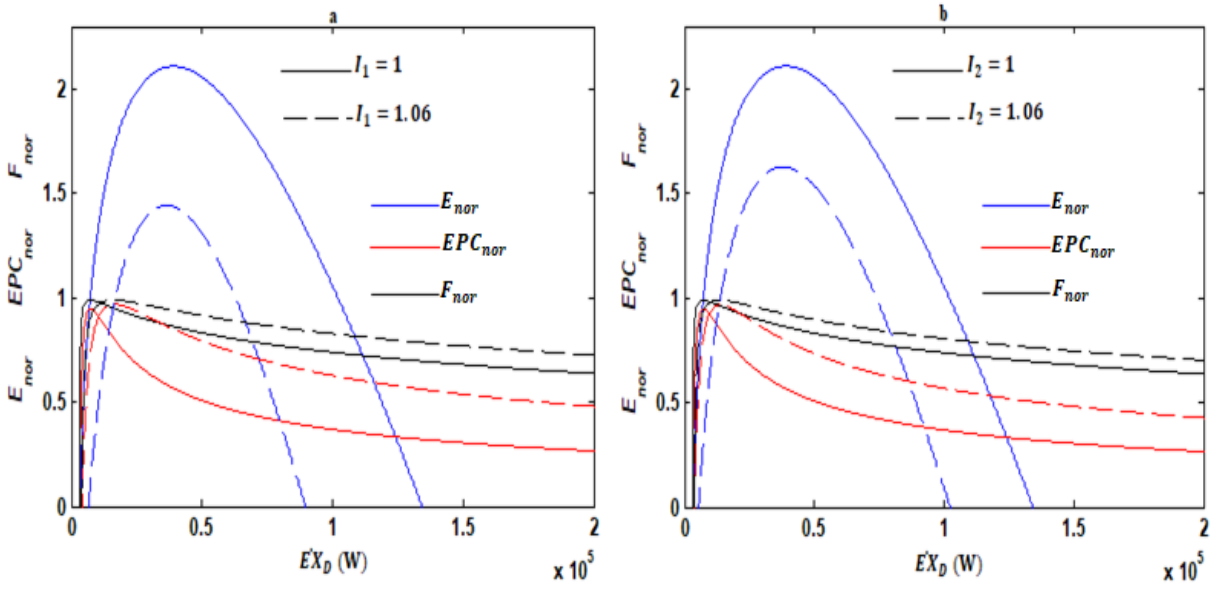

Fig. 3.43. Effects of internal irreversibility I_1 (a) of the generator-absorber assembly and of the internal irreversibility I_2 (b) of the evaporator-condenser assembly on the dimensionless E_{nor}, EPC_{nor} and F_{nor} with respect to the $\dot{E}X_D$ objective function.

The curves of the normalized values E_{nor} ($E_{nor} = E/E_{op}$ where E_{op} is the optimal value of E corresponding to the value of E when F and EPC are at their maximum values, and E varies to $E_{\max}$), EPC_{nor} ($EPC_{nor} = EPC/EPC_{\max}$) and F_{nor} ($F_{nor} = F/F_{\max}$) with respect the functions such as: coefficient of performance ψ, exergy output rate $\dot{E}X_{out}$ and exergy destruction rate $\dot{E}X_D$ are shown in **Figs 3.41-3.43**. **Table 3.4** illustrates the numerical results obtained from **Figs 3.41(a)-3.43(a)** under the influence of I_1 and **Figs 3.41(b)-3.43(b)** under the influence of I_2.

The previous analyzes allow us to draw the following conclusions, under the effects of heat losses between the generator and the absorber characterized by the irreversibility I_1 and between the condenser and the evaporator characterized by the irreversibility I_2. The FTL AHP has the same significant benefit at the maxima of the F and EPC criteria in terms of coefficient of performance. Similarly, it has a significant benefit in order, at the maxima of the F, then EPC criteria in terms of exergy destruction rate. However, it is much more efficient at the maximum of E criterion in terms of exergy output rate. Even more, the harmful impact of internal irreversibility I_1 on the system performance is greater than that of I_2 on E, EPC and F criteria in terms of coefficient of performance; on E criterion in terms of exergy output rate and on EPC and F criteria in terms of exergy destruction rate, unlike a THR AHP cycle.

Table 3.4. Comparative evaluation with criteria *E*, *EPC* and *F* criteria of the heat losses rates in the generator-absorber assembly and in the evaporator-condenser assembly (the reference is set for an endoreversible system $I_1 = I_2 = 1$ $K_L = 300\,\mathrm{WK}^{-1}$ and $\psi_{EPC} = \psi_F = 2.095$, $\dot{EX}_{out-E} = 68500\,\mathrm{W}$, $\dot{EX}_{D-F} = 7062\,\mathrm{W}$).

	Parameters of performance	Losses rates corresponding to the $E_{\max}$ (%)	Losses rates corresponding to the $EPC_{\max}$ (%)	Losses rates corresponding to the $F_{\max}$ (%)
$I_1 = 1.06$; $I_2 = 1$	ψ	21.13	17.42	17.42
	$\dot{EX}_{out}$	30.08	64.76	65.93
	$\dot{EX}_D$	411.7	130.13	122.6
$I_1 = 1$; $I_2 = 1.06$	ψ	18.95	13.27	13.27
	$\dot{EX}_{out}$	21.69	65.85	66.93
	$\dot{EX}_D$	431.35	92.58	86.52

3.7.2. Influences of external irreversibilities (ξ) on the EPC criterion

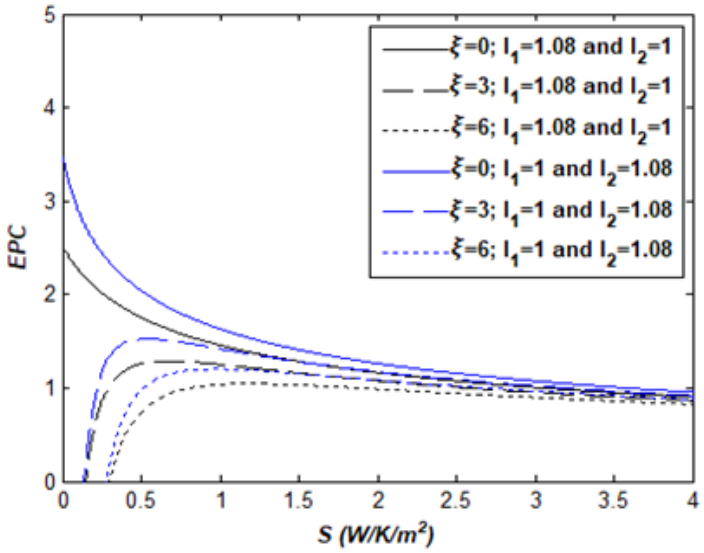

Fig. 3.44. Effects of heat leakage coefficient ξ on the *EPC* objective function with respect to the *S* objective function.

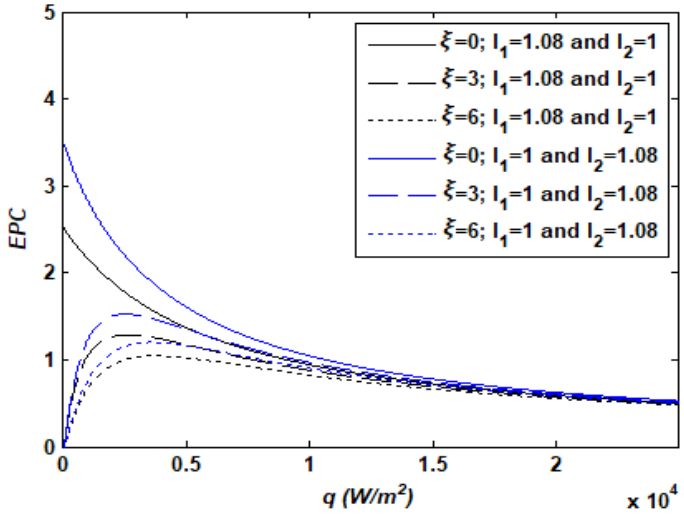

Fig. 3.45. Effects of heat leakage coefficient ξ on the *EPC* objective function with respect to the *q* objective function.

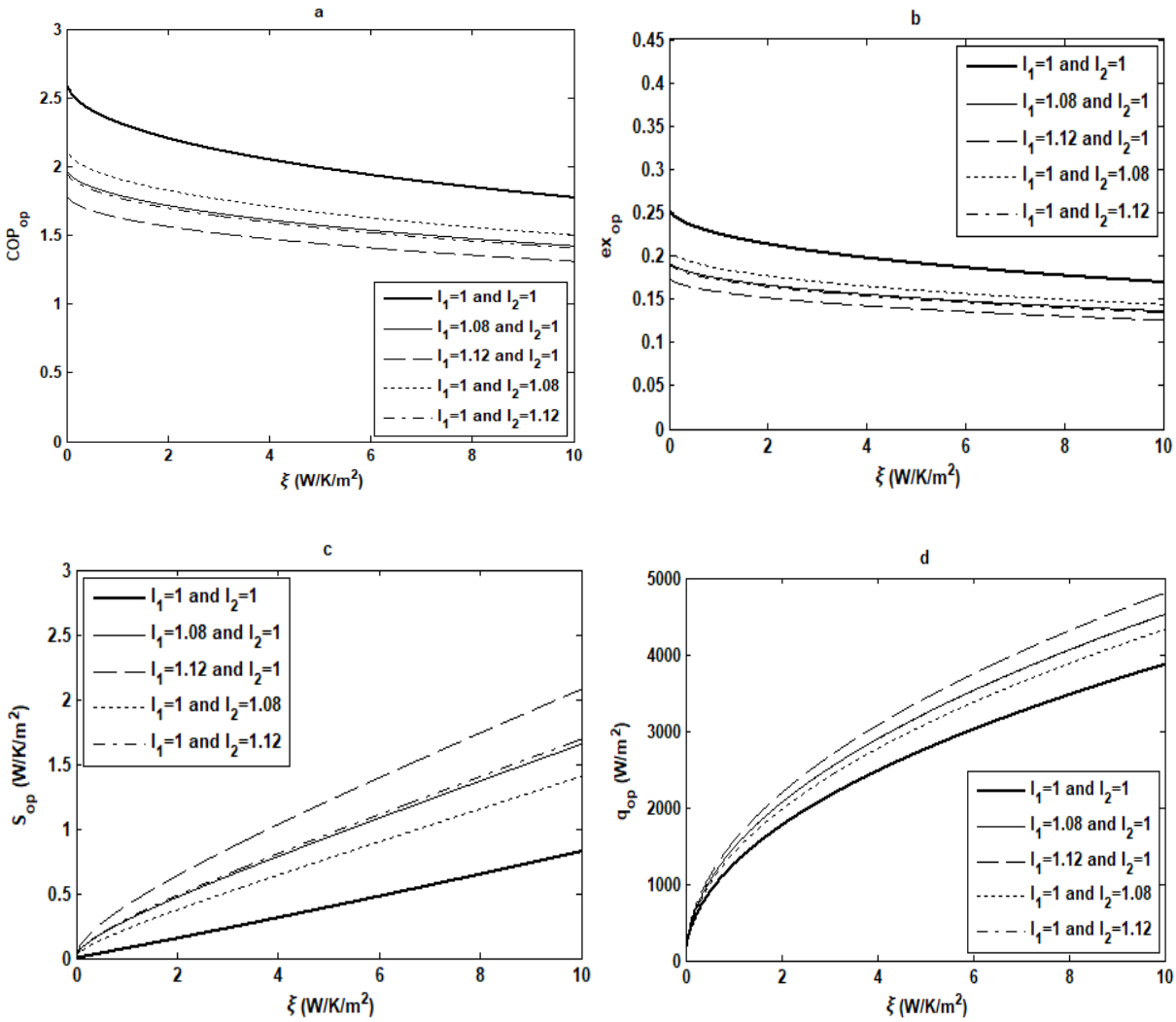

Fig. 3.46. Effects of heat leakage coefficient ξ on the COP_{op} (a), ex_{op} (b), S_{op} (c) and q_{op} (d) optimal objective functions respectively for certain values of I_1 and I_2.

In **Figs. 3.44** and **3.45** the *EPC* objective function varies with respect to the specific entropy generation rate (*S*) and the specific heating load (*q*) respectively, under the influence of ξ. It is observed that the *EPC* objective function is highest when $\xi = 0$ because heat leakage no longer exists. For $\xi > 0$, the *EPC* objective function increases abruptly before decreasing asymptotically towards a limit value. Moreover, the maxima obtained by the *EPC* objective function are lower when ξ increases, for increasing optimal values corresponding of *S* (**Fig.3.44**) and *q* (**Fig.3.45**).

Fig. 3.46 shows the variations of ex_{op}, S_{op}, COP_{op} and q_{op} with respect to the heat leakage coefficient (ξ) according to the values of I_1 and I_2. It can be seen that COP_{op} and ex_{op} decrease while S_{op} and q_{op} increase. Also, the optimal values COP_{op}, ex_{op} and S_{op} of the objective functions are better when $I_1 < I_2$ then the optimal value q_{op} of the objective function is better for $I_1 > I_2$.

Table 3.5. FTL AHP loss rate from the exergetic performance criterion (*EPC*) versus the endoreversible system ($\boldsymbol{I_1 = I_2 = 1}$ and $m = 1.3$) for different values of ξ.

$\boldsymbol{\xi}$ $\mathbf{(W/K/m^2)}$	**3**	**6**	**9**	**12**	**15**
Percentage (%) loss rate of EPC for $\boldsymbol{I_1 = 1.08}$ and $\boldsymbol{I_2 = 1}$	57.46	65.27	69.82	72.97	75.34
Percentage (%) loss rate of EPC for $\boldsymbol{I_1 = 1}$ and $\boldsymbol{I_2 = 1.08}$	49.62	60.08	65.91	69.85	72.75

However, **Table 3.5** illustrates the exergy loss rate caused by the effect of heat leakage and heat resistance characterized by the heat leakage coefficient (ξ). It follows that the exergetic losses increase when ξ increases and are smaller when $I_1 < I_2$. Kilic and Kaynakli (2007) and Kaushik and Arora (2009) showed these results on the water-lithium bromide absorption refrigeration.

3.7.3. Influences of the distribution of the total rate of rejected heat between the absorber and the condenser (*m*)

3.7.3.1. On the EPC criterion

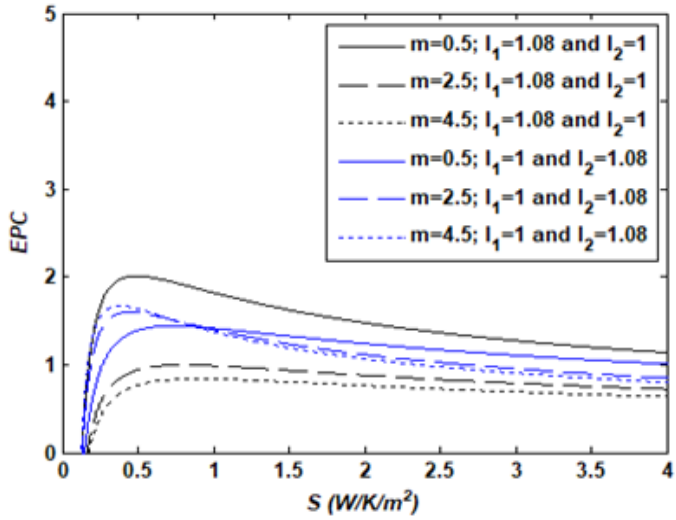

Fig. 3.47. Effects of the ratio of the rejected heat of the absorber to the condenser *m* on the *EPC* objective function with respect to the *S* objective function.

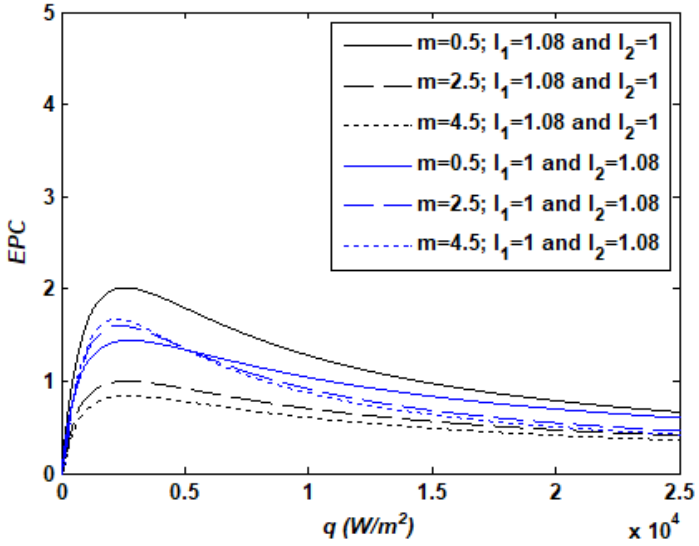

Fig. 3.48. Effects of the ratio of the rejected heat of the absorber to the condenser *m* on the *EPC* objective function with respect to the *q* objective function.

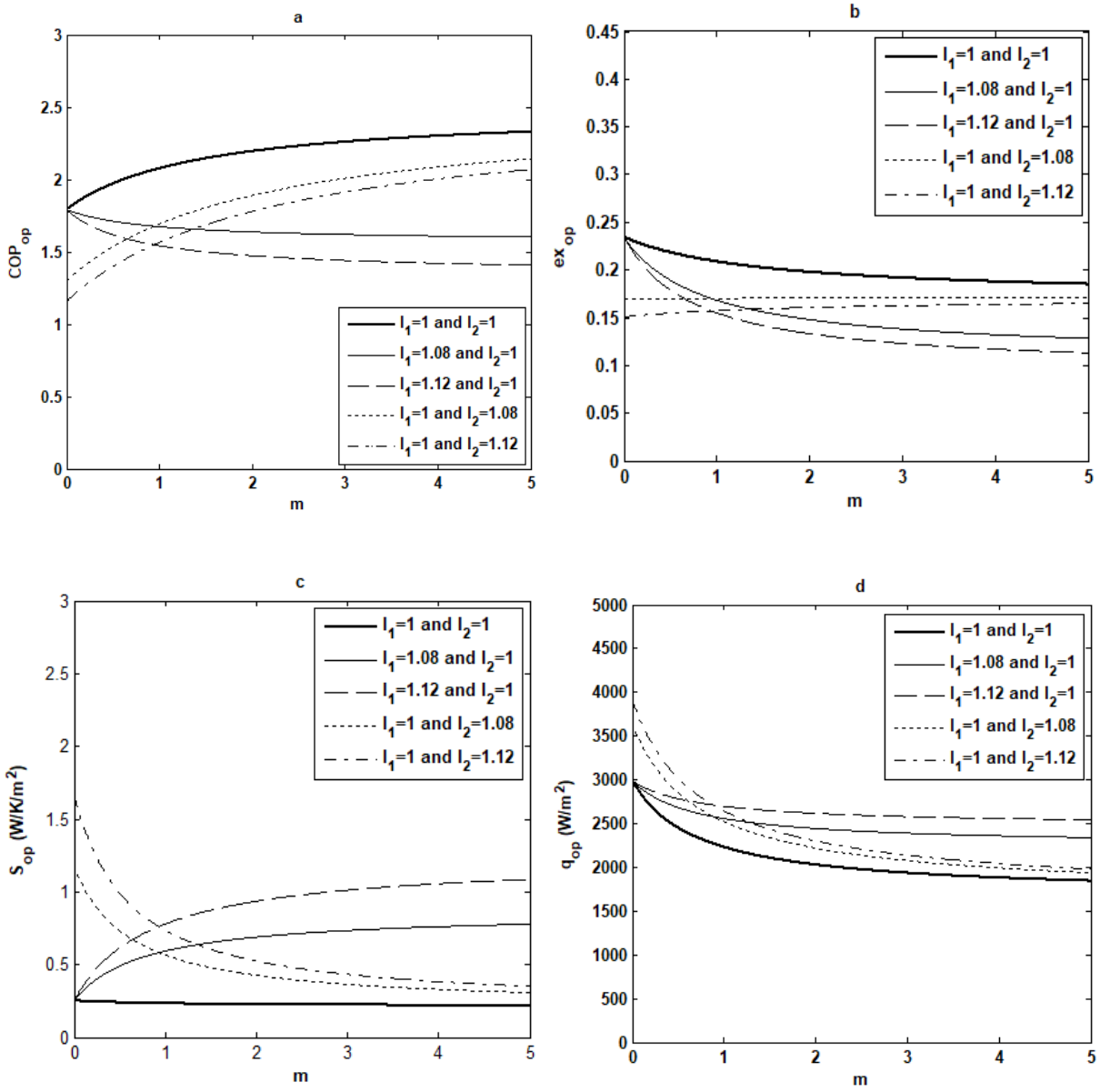

Fig. 3.49. Effects of the ratio of the rejected heat of the absorber to the condenser *m* on the COP_{op} (a), ex_{op} (b), S_{op} (c) and q_{op} (d) optimal objective functions respectively for certain values of I_1 and I_2.

Figs. 3.47 and **3.48** show the variations of the *EPC* objective function under the influence of the distribution of the total rate of rejected heat between the absorber and the condenser (*m*) with respect to *S* and *q* respectively. The maximum values of the *EPC* criterion decrease as *m* increases ($I_1 > I_2$) and increase as *m* increases ($I_1 < I_2$).

On the other hand, **Fig. 3.49** shows the effects of the ratio of the rejected heat of the absorber to that of the condenser (*m*) on the COP_{op} (**Fig. 3.49(a)**) ex_{op} (**Fig. 3.49(b)**), S_{op} (Fig. **3.49**(c)) and q_{op} (**Fig. 3.49(d)**) optimal objective functions when I_1 and I_2 take certain values. The optimal values COP_{op} and ex_{op} decrease when *m* increases for $I_1 > I_2$ and increase when *m* increases

for $I_1 < I_2$. Whereas the optimal values S_{op} increases, q_{op} decreases when *m* increases for $I_1 > I_2$ and all decrease when *m* increases for $I_1 < I_2$.

Nevertheless, when:

(i) *m*<0.5 ($\dot{Q}_A < \dot{Q}_C/2$), the optimal values COP_{op}, ex_{op} and S_{op} are better for $I_1 > I_2$ while the optimal value q_{op} is better for $I_1 < I_2$.

(ii) $0.5 \leq m \leq 1$, the impact of the two internal irreversibility factors I_1 and I_2 is balanced.

(iii) $m > 1$ ($\dot{Q}_A > \dot{Q}_C$), the optimal values COP_{op}, ex_{op} and S_{op} are better for $I_1 < I_2$ while the optimal value q_{op} is better for $I_1 > I_2$.

Table 3.6. FTL AHP loss rate from the exergetic performance criterion (*EPC*) versus the endoreversible system ($I_1 = I_2 = 1$ and $\xi = 3$) for different values of *m*.

distribution of the total rate of rejected heat between the absorber and the condenser ($\boldsymbol{m}$)	**0.5**	**1.5**	**2.5**	**3.5**	**4.5**
Percentage (%) loss rate of EPC for $\boldsymbol{I_1 = 1.08}$ and $\boldsymbol{I_2 = 1}$	32.71	60.06	67.33	70.70	72.64
Percentage (%) loss rate of EPC for $\boldsymbol{I_1 = 1}$ and $\boldsymbol{I_2 = 1.08}$	52.39	49.11	47.20	45.95	45.06

Table 3.6 shows the exergy loss rate on the EPC_{max} of an endoreversible FTL cycle according to the values of the distribution of the total rate of heat-rejected between the absorber and the condenser. It summarizes the fact that the best satisfactory compromise of minimal exergetic losses and an optimal heating load is achieved for $0.5 \leq m \leq 1.5$.

3.7.3.2. On the E, EPC and F criteria

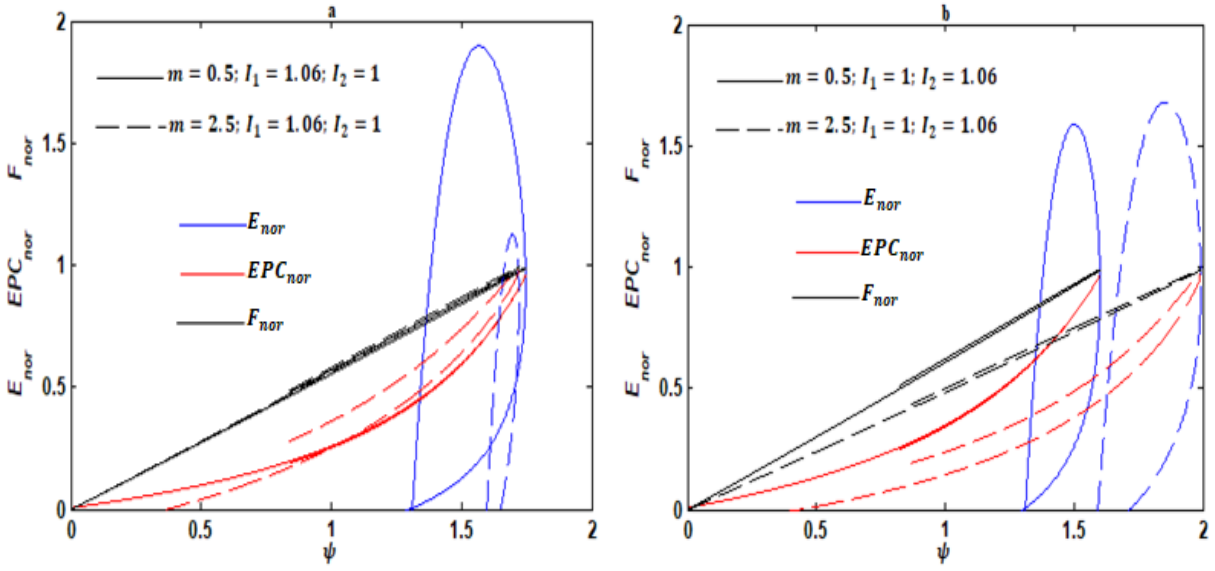

Fig. 3.50. Effects of the ratio of the rejected heat of the absorber to the condenser on the dimensionless E_{nor}, EPC_{nor} and F_{nor} with respect to the *COP* (ψ) objective function.

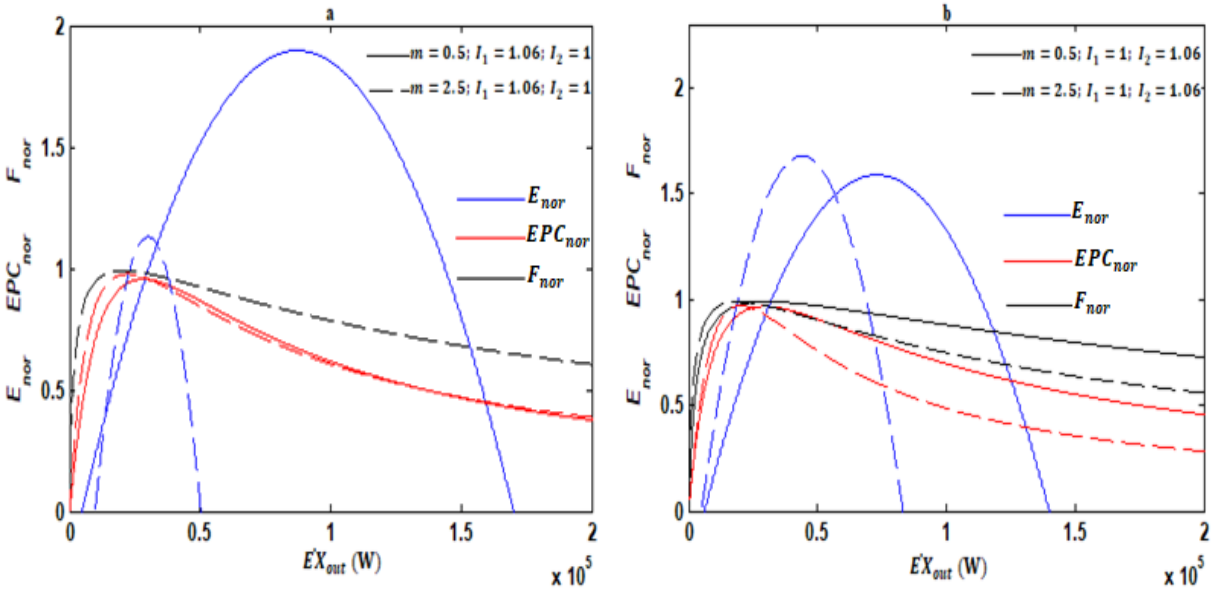

Fig. 3.51. Effects of the ratio of the rejected heat of the absorber to the condenser on the dimensionless E_{nor}, EPC_{nor} and F_{nor} with respect to the $E\dot{X}_{out}$ objective function.

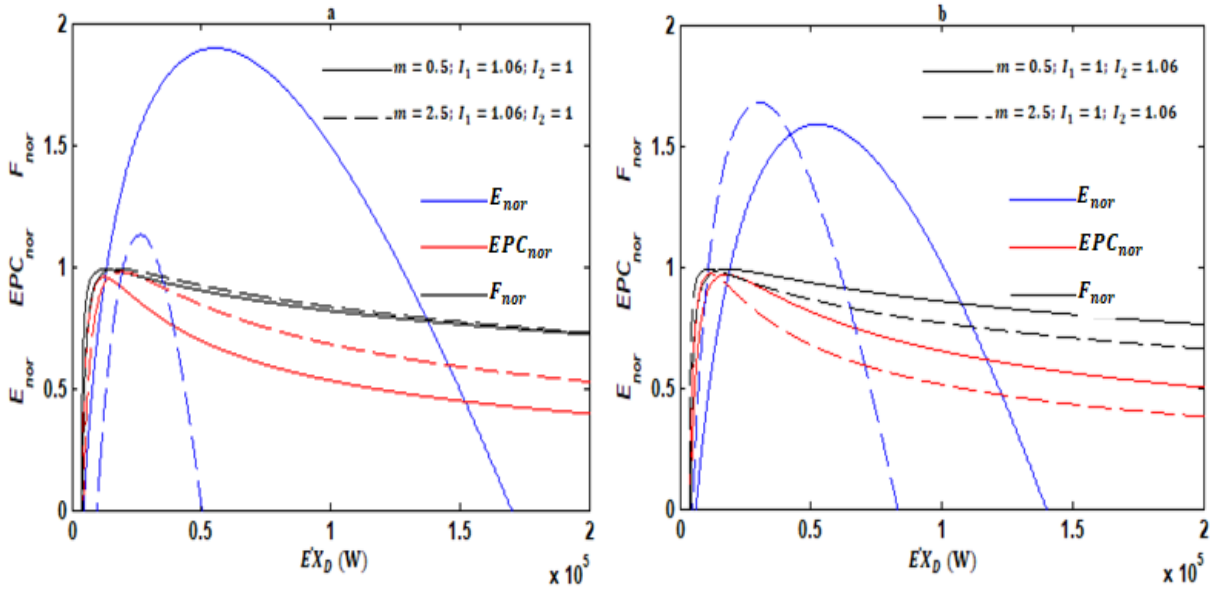

Fig. 3.52. Effects of the ratio of the rejected heat of the absorber to the condenser on the dimensionless E_{nor}, EPC_{nor} and F_{nor} with respect to the $\dot{E}X_D$ objective function.

The influences of the ratio of the rejected heat of the absorber to the condenser (m) on the objective functions of performance E, EPC and F are shown in **Figs. 3.50-3.52**. In these figures, when the parameter m increases with each time $I_1 = 1.06$ when $I_2 = 1$ (**Figs. 3.50(a)-3.52(a)**) and $I_1 = 1$ when $I_2 = 1.06$ (**Figs. 3.50(b)-3.52(b)**).

An in-depth study of the influences of m on the FTL AHP cycle made it possible to consider an optimal reference system such that $m = 0.5$ (**Table 3.7**). On the one hand for $I_1 = 1.06$ and $I_2 = 1$we have $\psi_{EPC} = \psi_F = 1.746$, $\dot{E}X_{out-E} = 86844\,\text{W}$ and $\dot{E}X_{D-EPC} = 12332\,\text{W}$; and on the other hand $I_1 = 1$ and $I_2 = 1.06$ we have $\psi_{EPC} = \psi_F = 1.601$, $\dot{E}X_{out-E} = 72756\,\text{W}$ and $\dot{E}X_{D-EPC} = 17388\,\text{W}$.

The influences of the heat exchange rates in the absorber with the absorbent-refrigerant pair, and the condenser with the refrigerant, depend on the order of magnitude of these two exchangers relative to each other. In fact, when $\dot{Q}_A$ is lower than $\dot{Q}_C$, at the maxima of *E*, *EPC* and *F* criteria, the system is more efficient in terms of *COP* under the impact of heat losses between the generator and the absorber. At the maxima of the *EPC* and *F* criteria, the system is more efficient in terms of exergy destruction rate under the effect of the internal irreversibility factor I_1, yet at the maximum of *E* criterion the best performances are recorded under the influence of heat losses between the evaporator and the condenser. However, at the maximum of *E* criterion, the

best performances are obtained in terms of exergy output rate under the effect of I_1, whereas, the best performances are obtained at the maxima of criteria *EPC* and *F* in terms of exergy output rate under the influence of I_2. On the other hand, when $\dot{Q}_A$ is greater than $\dot{Q}_C$, at the maxima of *E*, *EPC* and *F* criteria, the system performs better in terms of *COP* under the impact of heat losses between the evaporator and the condenser. Thus, at the maximum of criterion *E*, the best performances are recorded under the influence of heat losses between the generator and the absorber. However, at the maxima of *EPC* and *F* criteria, the system is more efficient in terms of exergy destruction rate under the effect of the internal irreversibility factor I_2. However, at the maximum of criterion *E*, the best performances are obtained in terms of exergy output rate under the effect of I_2, whereas, the best performances are obtained at the maxima of *EPC* and *F* criteria in terms of exergy output rate under the influence of I_1.

Table 3.7. Comparative evaluation with *E*, *EPC* and *F* criteria of the heat losses rates under the effects of the ratio of the rejected heat of the absorber to the condenser.

	Parameters of performance	Losses rates corresponding to the E_{max} (%)	Losses rates corresponding to the EPC_{max} (%)	Losses rates corresponding to the F_{max} (%)
$I_1 = 1.06$; $I_2 = 1$; $m = 2.5$	ψ	2.84	1.54	1.54
	$\dot{E}X_{out}$	65.53	74.61	76.65
	$\dot{E}X_D$	113.24	53.79	41.66
$I_1 = 1$; $I_2 = 1.06$; $m = 2.5$	ψ	-15.77	-24.46	-24.46
	$\dot{E}X_{out}$	39.73	72.41	74.52
	$\dot{E}X_D$	73.22	-34.19	-39.1

3.7.4. Combined effects of design parameters on the optimum parameters

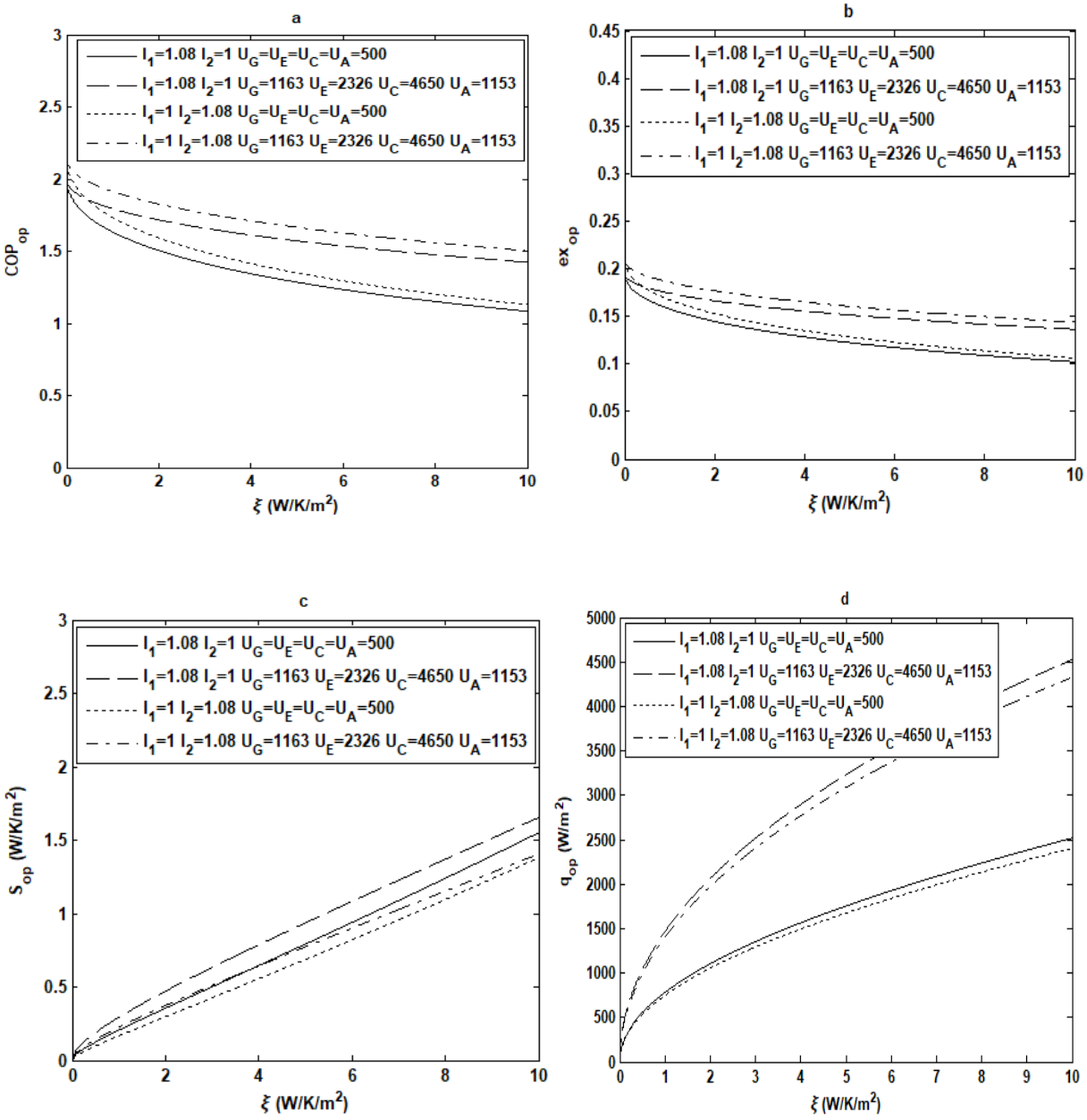

Fig. 3.53. Variations of the optimal performance criteria such as COP_{op} (a), ex_{op} (b), S_{op} (b) and q_{op} (d) with respect to the ξ (m=1.3) under the influences of the overall heat-transfer coefficient and the two internal irreversibilities.

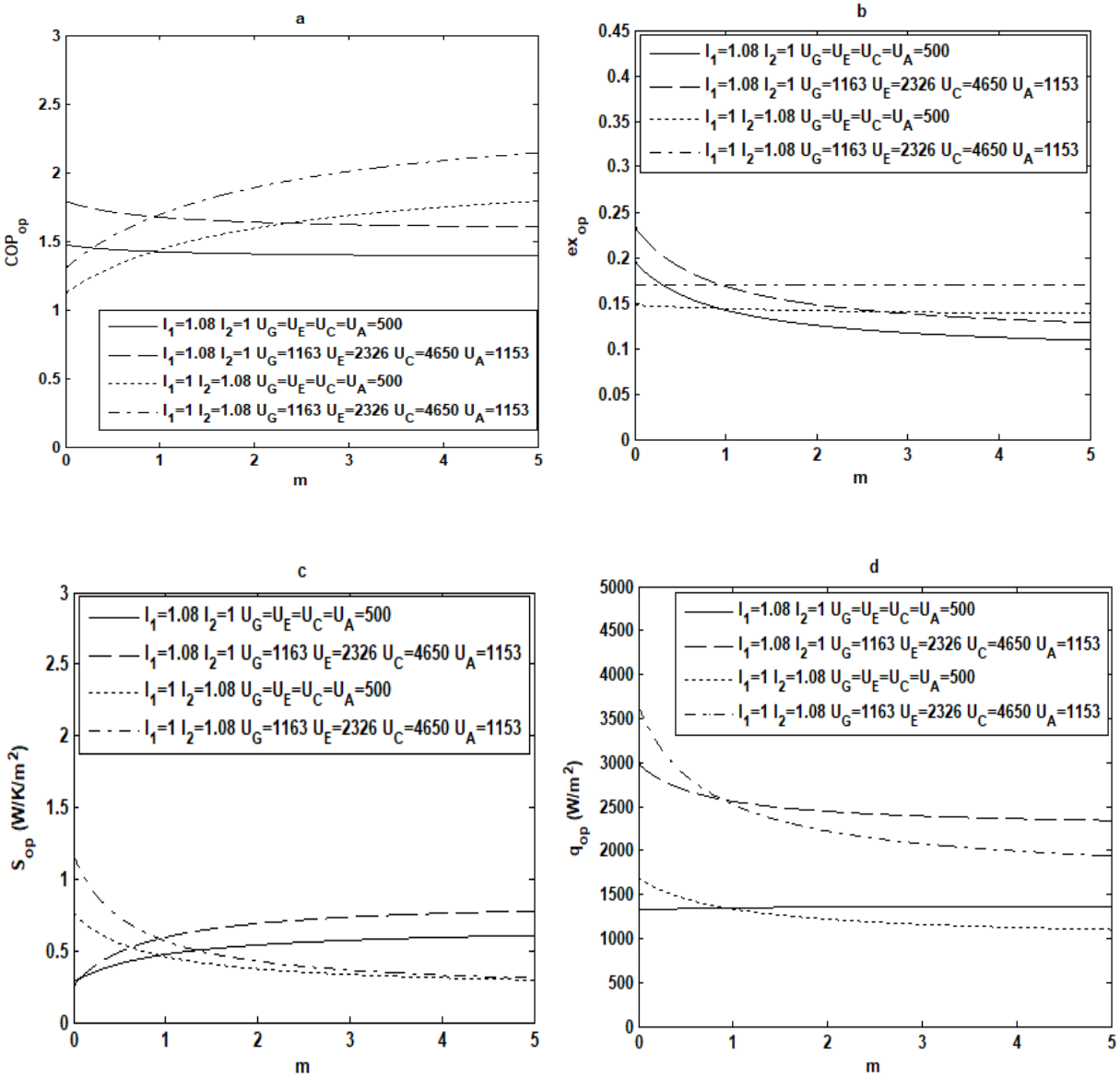

Fig. 3.54. Variations of the optimal performance criteria such as COP_{op} (a), ex_{op} (b), S_{op} (b) and q_{op} (d) with respect to the m ($\xi = 3\,\mathrm{WK^{-1}m^{-2}}$) under the influences of the overall heat-transfer coefficient and the two internal irreversibilities.

Figs. 3.53 and **3.54** show the variations of the optimal objective functions COP_{op}, ex_{op}, S_{op} and q_{op} with respect to the overall external irreversibility (ξ) and the ratio of the rejected heat of the absorber to the condenser respectively (m) according to the overall heat-transfer coefficient and two internal irreversibilities. Moreover, in **Fig. 3.53(a)** and **3.53(b)**, we observe that COP_{op} and ex_{op} decrease while S_{op} and q_{op} (**Fig. 3.53(c)** and **3.53(d)**), increase with respect to the values of ξ, when I_1 is greater than I_2 and mutually for increasing values of overall heat-transfer coefficients. However, in **Fig. 3.54** the optimal values COP_{op} and ex_{op} decrease asymptotically (**Fig. 3.54(a)**

and **3.54(b)**) when *m* increases ($I_1 > I_2$) and increase asymptotically when *m* increases ($I_1 < I_2$), this is for increasingly higher values of overall heat-transfer coefficients. Whereas the optimal values S_{op} increases, q_{op} decreases asymptotically when *m* increases ($I_1 > I_2$) and all decrease asymptotically when *m* increases ($I_1 < I_2$) this is for increasingly higher values of overall heat-transfer coefficients.

In most cases, these optimal objective functions of performance are better for higher values of overall heat-transfer coefficients of the different components. However, the exergetic losses are higher in these cases.

3.7.5. Influences of the overall heat-transfer coefficient on the *E*, *EPC* and *F* criteria

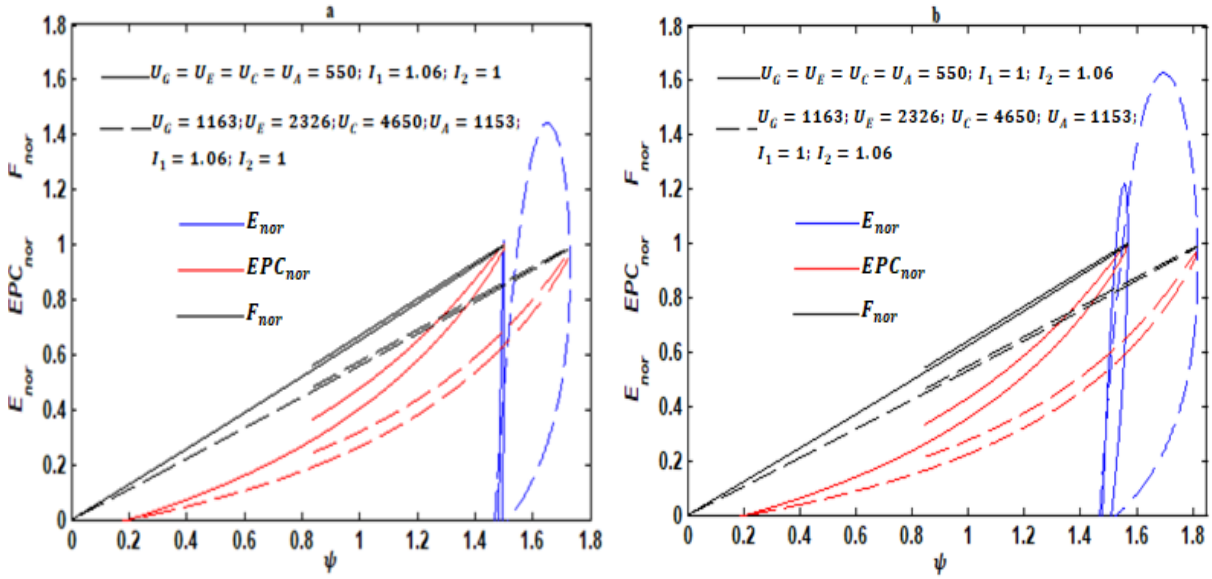

Fig. 3.55. Effects of the ratio of the overall heat-transfer coefficient on the dimensionless E_{nor}, EPC_{nor} and F_{nor} with respect to the *COP* (Ψ) objective function.

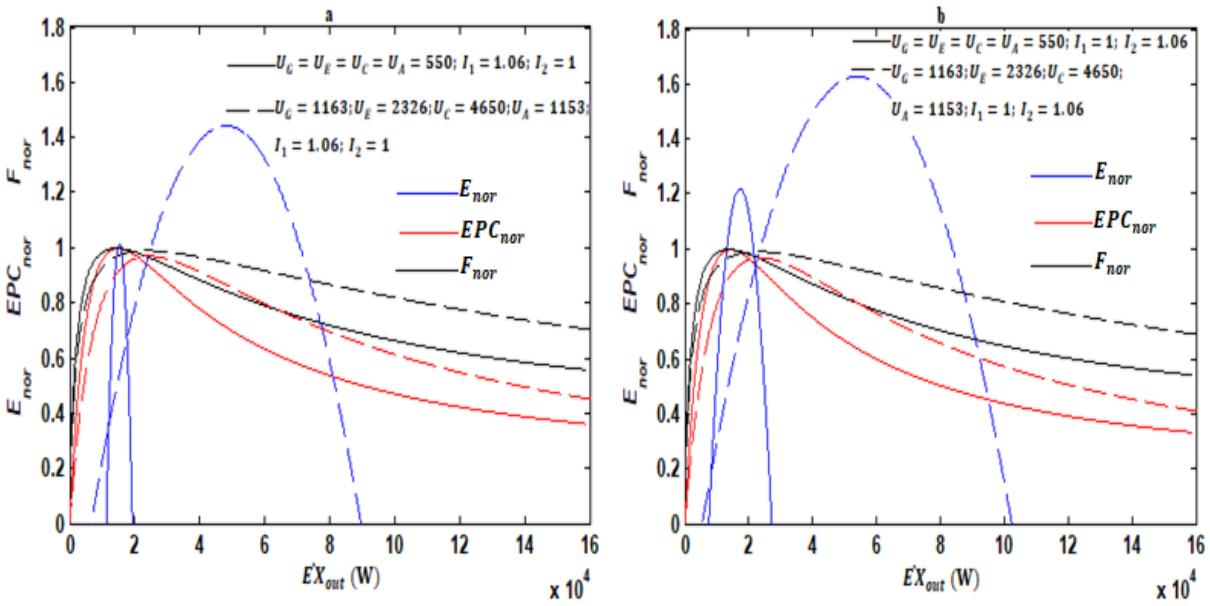

Fig. 3.56. Effects of the overall heat-transfer coefficient on the dimensionless E_{nor}, EPC_{nor} and F_{nor} with respect to the $\dot{E}X_{out}$ objective function.

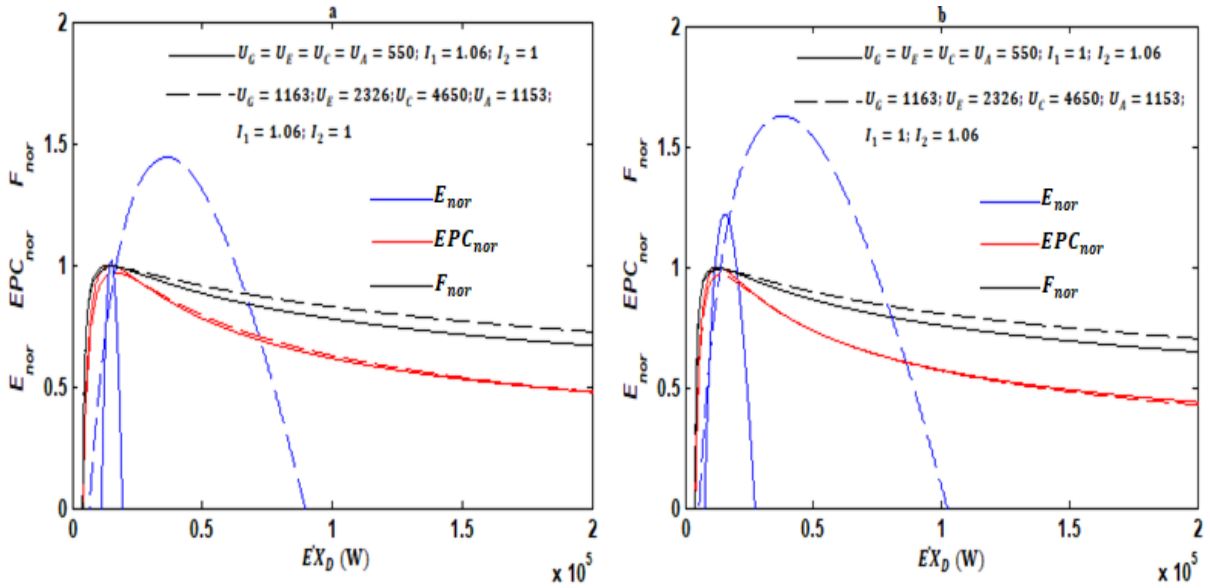

Fig. 3.57. Effects of the overall heat-transfer coefficient on the dimensionless E_{nor}, EPC_{nor} and F_{nor} with respect to the $\dot{E}X_D$ objective function.

Table 3.8 summarizes the curves **3.55(a)-3.57(a)** when $I_1 = 1$ and $I_2 = 1.06$ and the curves **3.55(b)-3.57(b)** when $I_1 = 1$ and $I_2 = 1.06$, which show the effects of the nature of the different components on the performance of the absorption cycle. In addition, these influences are taken into account on their different impacts on each of the E, EPC and F objective functions. We have taken into account two ranges of heat-transfer coefficients whose range taken as reference

Huang et al., (2008) and Ngouateu Wouagfack and Tchinda (2012a) (**Table 3.8**) is $U_G = 1163\,\mathrm{WK^{-1}m^{-2}}$; $U_E = 2326\,\mathrm{WK^{-1}m^{-2}}$; $U_C = 4650\,\mathrm{WK^{-1}m^{-2}}$ and $U_A = 1153\,\mathrm{WK^{-1}m^{-2}}$ because it communicates better optimal performance values to the system. When $I_1 = 1.06$ and $I_2 = 1$ ($\psi_{EPC} = \psi_F = 1.73$, $\dot{E}X_{out-E} = 47895\,\mathrm{W}$ and $\dot{E}X_{D-F} = 15720\,\mathrm{W}$) and when $I_1 = 1$ and $I_2 = 1.06$ ($\psi_{EPC} = \psi_F = 1.817$, $\dot{E}X_{out-E} = 53641\,\mathrm{W}$ and $\dot{E}X_{D-F} = 13173\,\mathrm{W}$).

Table 3.8. Comparative evaluation with *E*, *EPC* and *F* criteria of the heat losses rates under the effects of the heat-transfer coefficients.

	Parameters of performance	Losses rates corresponding to the E_{max} (%)	Losses rates corresponding to the EPC_{max} (%)	Losses rates corresponding to the F_{max} (%)
$I_1 = 1.06$; $I_2 = 1$; $U_G = U_E = U_C = U_A = 550\ \mathrm{WK^{-1}m^{-2}}$	ψ	13.28	13.18	13.18
	$\dot{E}X_{out}$	68.16	69.30	70.62
	$\dot{E}X_D$	-4.91	-8.35	-12.24
$I_1 = 1$; $I_2 = 1.06$; $U_G = U_E = U_C = U_A = 550\ \mathrm{WK^{-1}m^{-2}}$	ψ	14.28	13.71	13.71
	$\dot{E}X_{out}$	67.86	73.55	74.66
	$\dot{E}X_D$	17.36	-4.49	-8.46

As a result, the FTL AHP cycle system assumes small fluctuations in the optimal values of the COP when using materials constituting the heat exchangers with increasingly low heat-transfer coefficients. Furthermore, the performance of the system is greatly affected in terms of optimal exergy output rate and optimal specific heating load. On the other hand, the optimal exergy destruction rate is better in this configuration.

3.7.6. Influences of the Thermo-economic parameter (k) on the EPC, E and F objective functions

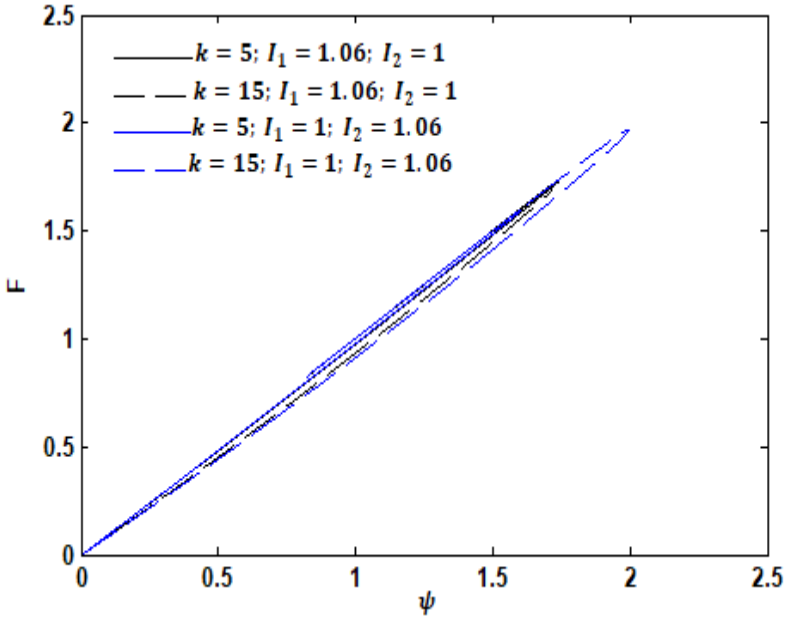

Fig. 3.58. Effects of thermo-economic factor on the *F* criterion with respect to the *COP* (ψ) objective function.

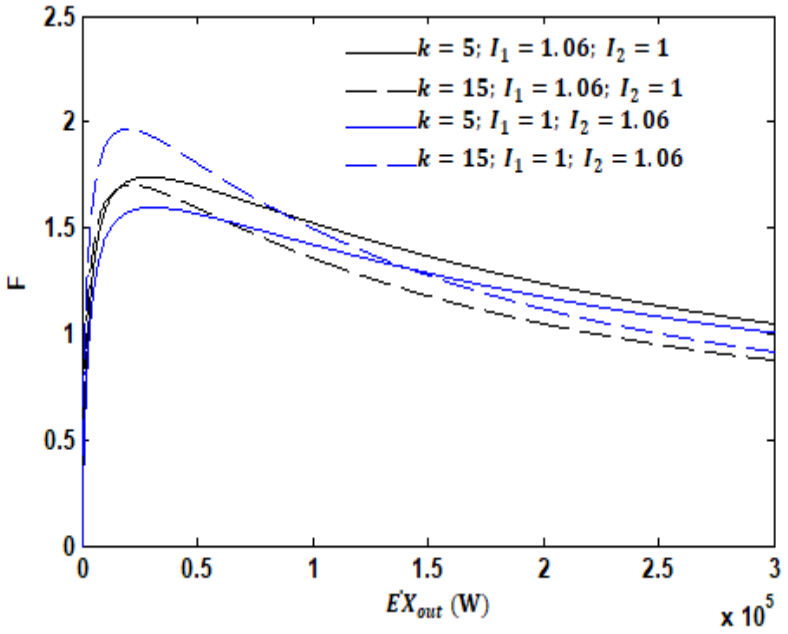

Fig. 3.59. Effects of thermo-economic factor on the *F* criterion with respect to the $\dot{E}X_{out}$ objective function.

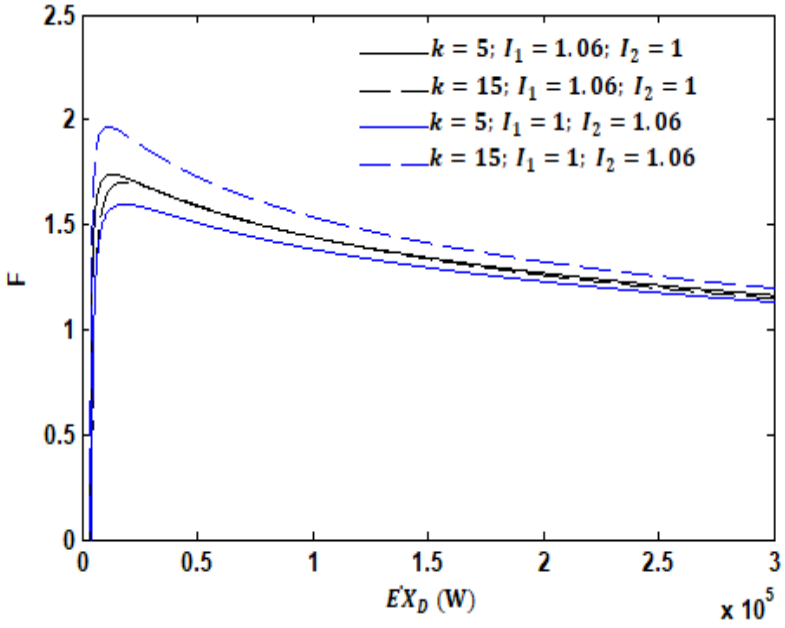

Fig. 3.60. Effects of thermo-economic factor on the *F* criterion with respect to the $\dot{EX}_D$ objective function.

The curves showing the evolution of the thermo-economic objective function with respect to the COP, the exergy output rate and the exergy destruction rate, respectively, are shown **Figs. 3.58-3.60**. The curves presenting the *F* criterion with resoect to the COP (**Fig. 3.58**) are loops from the origin. This confers two different values of the thermo-economic criterion corresponding to the same value of the COP. In **Figs. 3.59** and **3.60**, *F* criterion grows abruptly before gradually decreasing as the exergy output rate and exergy destruction rate increase. Also, when the economic parameter *k* takes larger values, the *F* objective function increases under the impact of heat losses in the evaporator-condenser connection and decreases under the impact of heat losses in the generator-absorber connection.

However, the optimum economic performance is obtained for a minimum total heat-exchange area and a maximum exergy input rate for a minimum effect of heat losses in the generator-absorber connection.

3.8. Conclusion

The investigations carried out throughout this work led to the multi-objective analysis and optimization of THR AHP and FTL AHP. On the one hand, we analyzed the performance of cycles at THR by the objective thermo-ecological function (ECOP) and then at FTL by the objective exergetic function (EPC). On the other hand, in order to be able to make a more objective synthesis, we compared three decisive performance criteria namely the ecological, exergy and economic criteria with three and four heat tanks each time. This considering the real operating conditions which are subject to the two kinds of irreversibility, that is to say external irreversibilities and

internal irreversibilities. Nevertheless, an isolated and then comparative study of the advantages and drawbacks at maximum of each performance criterion according to the corresponding optimal performance parameters such as the coefficient of performance, the entropy generation rate, the specific heating load, the heat exchange surface area, the exergy output rate and exergy destruction rate. This being, the analysis of finite time thermodynamics and the flowchart optimization method as analysis and precision tools made it possible to obtain the significant results.

Several important aspects to be addressed are:

• For FTL cycles it appears that, the optimal objective functions *EPC*, *ECOP* and *E* are better for higher values of overall heat-transfer coefficients of the different components. However, the exergetic losses are higher in these cases.

• For FTL cycles it appears that, at the maximum of the *E* objective function, a higher specific heating load has been found than the maximum of the *EPC* and *ECOP* objective functions. In addition, the optimal functions of performance at the maximum *E* criterion are higher under the influence of the internal irreversibility factor I_2.

• For THR and FTL cycles it appears that, the highest maximum values of the thermo-economic criterion correspond to a low cost on investment (low heat exchange area) and a high cost on the energy consumed (heat input from the generator heat source is high). This promotes minimal exergy destruction rate for certain values of the specific heating load and exergy output rate.

• The influences of heat leakages and heat resistances are more pronounced than the heat losses characterized by internal irreversibility factors I_1 and I_2. Furthermore, under the influences of design parameters, the THR AHP cycle presents a significant advantage at the maxima of the *F* and the *EPC* criteria in terms of coefficient of performance. Nevertheless, the THR AHP cycle presents a significant advantage at the maximum of the *EPC* in terms of exergy destruction rate and at the maximum of the *E* in terms of specific heating load and exergy output rate.

• The heat losses in the condenser-evaporator assembly have more detrimental effects on the performance of the THR AHP cycle. Nevertheless, in the FTL AHP the heat losses in the generator-absorber assembly have more detrimental effects for certain values of *m*.

GENERAL CONCLUSION AND PROSPECTS

The investigations carried out throughout this work led to the multi-objective analysis and optimization of THR AHP and FTL AHP. On the one hand, we analyzed the performance of cycles at THR by the objective thermo-ecological function (ECOP) and then at FTL by the objective exergetic function (EPC). On the other hand, in order to be able to make a more objective synthesis, we compared three decisive performance criteria namely the ecological, exergetic and economic criteria with three and four heat reservoirs each time. This considering the real operating conditions which are subject to the two kinds of irreversibility, that is to say external irreversibilities and internal irreversibilities. Also, external irreversibilities are manifested by the finite difference temperature between the system and the environment and the direct heat leakages which sink towards the source, yet internal irreversibilities are manifested by the non-isentropic transformations, the friction between the working fluid and the walls of the heat exchangers and pressure drop. Nevertheless, an isolated and then comparative study of the advantages and drawbacks at maximum of each performance criterion according to the corresponding optimal performance parameters such as the coefficient of performance, the entropy generation rate, the specific heating load, the heat exchange surface area, the exergy output rate and exergy destruction rate. This being so, the analysis of finite time thermodynamics and the flowchart optimization method as analysis and precision tools made it possible to obtain two significant blocks of results. The aspects noted in the first block of results are as follows:

i) For THR cycles it appears that, the *ECOP* criterion over the *E* criterion has a significant advantage in terms of specific entropy generation rate.

ii) For FTL cycles it appears that, the minimum exergy losses and an optimal specific heating load are recorded for $0.5 \leq m \leq 1.5$.

iii) For FTL cycles it appears that, the optimal objective functions *EPC*, *ECOP* and *E* are better for higher values of overall heat-transfer coefficients of the different components. However, the exergetic losses are higher in these cases.

iv) For FTL cycles it appears that, at the maximum of the *EPC* and *ECOP* objective functions, a low specific entropy generation rate and a better *COP* compared to the maximum of *E* objective function are obtained.

v) For FTL cycles it appears that, at the maximum of the *E* objective function, a higher specific heating load has been found than the maximum of the *EPC* and *ECOP* objective functions. In addition, the optimal functions of performance at the maximum *E* criterion are higher under the influence of the internal irreversibility factor I_2.

Then the aspects underlined in the second block are the following:

i) For THR and FTL cycles it appears that, the highest maximum values of the thermo-economic criterion correspond to a low cost on investment (low heat exchange area) and a high cost on the energy consumed (heat input from the generator heat source is high). This promotes minimal exergy destruction rate for certain values of the specific heating load and exergy output rate.

ii) The influences of heat leakages and heat resistances are more pronounced than the heat losses characterized by internal irreversibility factors I_1 and I_2. Furthermore, under the influences of design parameters, the THR AHP cycle presents a significant advantage at the maxima of the *F* and the *EPC* criteria in terms of coefficient of performance. Nevertheless, the THR AHP cycle presents a significant advantage at the maximum of the *EPC* in terms of exergy destruction rate and at the maximum of the *E* in terms of specific heating load and exergy output rate.

iii) The heat losses in the condenser-evaporator assembly have more detrimental effects on the performance of the THR AHP cycle. Nevertheless, in the FTL AHP the heat losses in the condenser-evaporator assembly have more detrimental effects for $0 < m \leq 1$, though the heat losses in the generator-absorber assembly have more detrimental effects for $m > 1$.

(iv) FTL AHP systems are more efficient when the heat rates exchanged of the absorber and condenser heat exchangers are close.

The evaluation protocol obtained leads to concrete results for the design of real absorption heat pumps by making a compromise between economic, exergetic and ecological gains.

We project to produce an ammonia-water hybrid prototype, functioning with thermal solar and the fuel cells. However, we will be able to study the ecological, exergetic and economic aspects according to a practical protocol.

REFERENCES:

Açikkalp, E., Ahmadi, M.H., 2018. Exergetic ecological index as a new exergetic indicator and an application for the heat engines. Therm. Sci. Eng. Progress 8, 204-219.

Aguilar-Jiménez, J.A., Velazquez-Limon, N., Lopez-Zavala, R., Gonzalez-Uribe, L.A., Islas, S., Gonzalez, E., Ramirez, L., Beltran, R., 2020. Optimum operational strategies for a solar absorption cooling system in an isolated school of Mexico. Int. J. Refrig. 112, 1-13.

Ahmadi, M.H., Ahmadi, M.A., 2016. Multi objective optimization of performance of three-heat-source irreversible refrigerators based algorithm NSGAII. Ren. Sust. Energy Rev. 60, 784–794.

Ahmadi, M.H., Ahmadi, M.A., Mehrpooya, M., Hosseinzade, H., Feidt, M., 2014a. Thermodynamic and thermo-economic analysis and optimization of performance of irreversible four-temperature-level absorption refrigeration. Energy Conv. Manag. 88, 1051–1059.

Ahmadi, M.H., Ahmadi, M.A., Mehrpooya, M., Sameti, M., 2015. Thermo-ecological analysis and optimization performance of an irreversible three-heat-source absorption heat pump. Energy Conv. Manag. 105, 1125–1137.

Ahmadi, M., Ahmadi, M.A., Pourfayaz, F., Bidi, M., 2016. Thermodynamic analysis and optimization for an irreversible heat pump working on reversed Brayton cycle. Energy Conv. Manag. 110, 260-267.

Ahmadi, P., Dincer, I., Rosen, M.A., 2014b. Thermoeconomic multi-objective optimization of a novel biomass-based integrated energy system. Energy 68, 958–970.

Ally, M.R., Sharma, V., 2018. Variability of absorption heat pump efficiency for domestic water heating and space heating based on time-weighted bin analysis. Appl. Therm. Eng. 130, 515–527.

Andresen, B., 2011. Current trends in finite-time thermodynamics. Angew. Chem. Int. Ed. 50 (12), 2690-2704.

Angulo-Brown F., 1991. An ecological optimization criterion for finite-time heat engines. J. Appl. Phys. 69, 7465.

Asadi, J., Amani, P., Amani, M., Kasaeian, A., Bahiraei, M., 2018. Thermo-economic analysis and multi-objective optimization of absorption cooling system driven by various solar collectors. Energy Convers. Manag. 173, 715-727.

Bejan, A., 1996. Entropy generation minimization: The new thermodynamics of finite-size devices and finite-time processes. J. Appl. Phys. 79 (3), 1191-1218.

Bhardwaj, P.K., Kaushik, S.C., and Jain, S., 2001. Finite time heat transfer and thermodynamic optimization of an irreversible Rankine cycle air-conditioning system. Published in International Conference on “Emerging Technologies in Air-conditioning and Refrigeration” organized by ISHRAE and ASHRAE in New Delhi, ACRECONF-2001 September 26–28, New Delhi, India, 398–408.

Bhardwaj, P.K., Kaushik, S.C., Jain, S., 2003a. Finite Time Thermodynamic Optimization of an Irreversible Rankine Cycle Heat Pump System. Indian J. Pure Appl. Phys. 41, 515–521.

Bhardwaj, P.K., Kaushik, S.C., Jain, S., 2003b. Finite time optimization of an endoreversible Vapour absorption refrigeration system. Energy Conv. Manag. 44, 1131-1144.

Bhardwaj, P.K., Kaushik, S.C., Jain, S., 2005. General performance characteristics of an irreversible vapour absorption refrigeration system using finite time thermodynamic approach. Int. J. Therm. Sci. 44, 189-196.

Bi, Y., Chen, L., Sun, F., 2008. Heating load density and COP optimizations of an endoreversible air heat-pump. Applied Energy 85, 607–617.

Cengel, Y.A., Boles, M.A., 2006. Thermodynamics. An Engineering approach. 5th edition. McGraw Hill.

Chaves Fortes, A.F., Carvalho, M., da Silva, J.A.M., 2018. Environmental impact and cost allocations for a dual product heat pump. Energy Conv. Manag. 173, 763–772.

Chen, J., 1998. Minimum power input of irreversible Stirling refrigerator for given cooling load. Energy Conv. Manag. 39 (12), 1255–1263.

Chen, J., 1999. The general performance characteristics of an irreversible absorption heat pump operating between four-temperature-level. J. Phys. D: Appl. Phys. 32, 1428–1433.

Chen, L., Wu, C., Sun, F., 1998a. Optimization of steady flow heat pumps. Energy Conv. Manag. 39 (5–6), 445–452.

Chen, L., Wu, C., Sun, F., 1998b. Cooling load versus COP characteristics for an irreversible air refrigeration. Energy Conv. Manag. 39 (1–2), 117–125.

Chen, L., Sun, F., Ni, N. Wu, C., 1998c. Optimal configuration of a class of two-heat-reservoir refrigeration cycles. Energy Conv. Manag. 39 (8), 767–773.

Chen, L., Wu, C., Sun, F., 1999a. Finite time thermodynamic optimization or entropy generation minimization of energy systems. J. Non-Equilib. Thermodyn. 24 (4), 327-359.

Chen, L., Sun, F., 2004. Advances in Finite Time Thermodynamics: Analysis and Optimization. Nova Science Publishers, New York.

Chen, L., Wu, C., Sun, F., 1997. Heat Transfer effect on the specific heating load of heat pumps. Appl. Therm. Eng. 17, 103-110.

Chen, L., Wu, C., Sun, F., Cao, S., 1999b. Maximum profit performance of a three-heat-reservoir heat pump. Int. J. Energy Res. 23, 773-777.

Chen, L., Ni, N., Wu, C., Sun, F., 1999c. Performance analysis of a closed regenerated Brayton heat pump with internal irreversibilities. Int. J. Energy Res. 23, 1039-1050.

Chen, L., Li, J., Sun, F., Wu, C., 2008. Performance optimization for a two-stage thermoelectric heat-pump with internal and external irreversibilities. Appl. Energy 85, 641-649.

Chen, L., Qin, X., Sun, F., Wu, C., 2005a. Irreversible absorption heat-pump and its optimal performance. Appl. Energy 81, 55–71.

Chen, L., Qin, X., Sun, F.R., 2007a. Model of irreversible finite heat capacity heat reservoir absorption heat transformer cycle and its application. Proc. IMechE C: J. Mech. Eng. Sci. 221 (C12), 1643–1652.

Chen, L., Xiaoqin, Z., Sun, F., Wu, C., 2007b. Exergy-based ecological optimization for a generalized irreversible Carnot heat-pump. Appl. Energy 84, 78–88.

Chen, L., Zheng, T., Sun, F., Wu, C., 2005b. Performance limits of real absorption refrigerators. J. Energy Inst. 78(3), 139-144.

Chen, L., Zheng, T., Sun, F., Wu, C., 2006. Irreversible four-temperature-level absorption refrigerator. Sol. Energy 80 (3), 347–360.

Chen, L., Sun, F., Wu, C., 2005c. Thermo-economics for endoreversible heat-engines. Appl. Energy 81, 388–396.

Chen, L., Zhang, W., Sun, F., 2007c. Power, efficiency, entropy-generation rate and ecological for a class of generalized optimization for a class of generalized irreversible universal heat-engine cycles. Appl. Energy 84, 512–525.

Chen, L., Ge, Y.L., Qin, X., Xie, Z.H., 2019. Exergy-based ecological optimization for a four-temperature level absorption heat pump with heat resistance, heat leakage and internal irreversibility. Int. J. Heat Mass Transf. 129, 855-861.

Curzon, F.L., Ahlborn, B., 1975. Efficiency of a Carnot engine at maximum power output. American J. Phys. 43, 22–24.

Dai, D., Liu, Z., Yuan, F., Long, R., Liu, W., 2019. Finite time thermodynamic analysis of a solar duplex Stirling refrigerator. Appl. Therm. Eng. 156, 597–605.

Dixit, M., Arora, A., Kaushik, S.C., 2017. Thermodynamic and thermoeconomic analyses of two stage hybrid absorption compression refrigeration system. Appl. Therm. Eng. 113, 120-131.

Farshi, G.L., Mahmoudi, S.M.S., Rosen, M.A., Yari, M., Amidpour, M., 2013. Exergoeconomic analysis of double effect absorption refrigeration systems. Energy Conv. Manag. 65, 13–25.

Feidt, M., 2010. Thermodynamics applied to reverse cycle machines, a review. Int. J. Refrig. 33 (7), 1327-1342.

Feidt, M., 2013. Evolution of thermodynamic modelling for three and four heat reservoirs reverse cycle machines: a review and new trends. Int. J. Refrig. 36 (1), 8-23.

Figaj, R., Szubel, M., Przenzak, E., Filipowicz, M., 2019. Feasibility of a small-scale hybrid dish/flat-plate solar collector system as a heat source for an absorption cooling unit. Appl. Therm. Eng. 163, 114399.

Frikha, S., Abid, M.S., 2016. Performance optimization of irreversible combined Carnot refrigerator based on ecological criterion. Int. J. Refrig. 62, 153 – 165.

Ge, Y.L., Chen, L.G., Sun, F., 2016. Progress in finite time thermodynamic studies for internal combustion engine cycles. Entropy 18 (4), 139.

Goktun, S., 1998. Performance Analysis of an irreversible cogeneration heat pump cycle. Int. J. Energy Res. 22, 1299-1304.

Huang, Y., Sun, D., Kang, Y., 2008. Performance optimization for an irreversible four-temperature-level absorption heat pump. Int. J. Therm. Sci. 47, 479-485.

Hu, B., Li, Y., Wang, R.Z., Cao, F., Xing, Z., 2018. Real-time Minimization of Power Consumption for Air-Source Transcritical CO_2 Heat Pump Water Heater System. Int. J. Refrig. 85, 395-408.

Kato, Y., Sasaki, Y., Yoshizawa, Y., 2005. Magnesium oxide/water chemical heat pump to enhance energy utilization of a cogeneration system. Energy 30, 2144–2155.

Kaushik, S.C., Kumar, P., and Khaliq, A., 1999. Analysis of an endoreversible Rankine Cycle Cooling System. Energy Opportunities xiv (1&2), 20–29.

Kaushik, S.C., Tyagi, S.K., 2002. Finite time thermodynamic analysis of a non-isentropic regenerative Brayton heat engine. Int. J. Solar Energy 22, 141–151.

Kaushik, S.C., Kumar, P., Jain, S., 2000. A Parametric Study based on Finite Time Thermodynamic Analysis of a Solar-Engine driven Air-conditioning System. SESI Journal, 10(2), 63–78.

Kaushik, S.C., Kumar, S., 2000a. Finite time thermodynamic analysis of an endoreversibble Stirling heat engine with regenerative losses. Energy 25, 989–1003.

Kaushik, S.C., Kumar, S., 2000b. Finite time thermodynamic evaluation of irreversible Ericsson and Stirling heat pump cycles, Proceedings of 4th Minsk International Seminar on Heat Pipes, Heat Pumps & Refrigerators, Minsk, Belarus 113–126.

Kaushik, S.C., Kumar, S., 2001. Finite time thermodynamic evaluation of irreversible Ericsson and Stirling heat engines. Energy Conv. Manag. 42, 295–312.

Kaushik, S.C., Tyagi, S.K., Bose, S.K., Singhal, M.K., 2002a. Performance evaluation of irreversible Ericsson and Stirling heat pump cycles. Int. J. Therm. Sci. 41, 193–200.

Kaushik, S.C., Kumar, P., Jain, S., 2002b. Finite Time Optimization of Irreversible Air conditioning System Using Method of Lagrangian Multiplier. J. Energy Environ. 2, 53–61.

Kaushik, S.C., Arora, A., 2009. Energy and analysis of single effect and series flow double effect water–lithium bromide absorption refrigeration systems. Int. J. Refrig. 32, 1247-1258.

Kaushik, S.C., Arora, R., Kumar, R., 2016. Thermo-economic optimization and parametric study of an irreversible regenerative Brayton cycle. J. Therm. Eng. 2(4), 861-870.

Kaushik, S.C., Tyagi, S.K., Kumar, P., 2018. Finite Time Thermodynamics of Power and Refrigeration Cycles. Springer, New York.

Kaynakli, O., Kilic, M., 2007. Theoretical study on the effect of operating conditions on performance of absorption refrigeration system. Energy Convers. Manag. 48, 599-607.

Kilic, M., Kaynakli, O., 2007. Second law-based thermodynamic analysis of water-lithium bromide absorption refrigeration system. Energy 32, 1505-1512.

Kodal, A., Sahin, B., Ekmekci, I., Yilmaz, T., 2003a. Thermoeconomic optimization for irreversible absorption refrigerators and heat pumps. Energy Conv. Manag. 44, 109-123.

Kodal, A., Sahin, B., 2003b. Finite size thermoeconomic optimization for irreversible heat engines. Int. J. Therm. Sci. 54, 209-219.

Kodal, A., Sahin, B., Erdil, A., 2002. Performance analysis of a two-stage irreversible heat pump under maximum heating load per unit total cost conditions. Exergy an Int. J. 2, 159–166.

Kodal, A., Sahin, B., Oktem, A.S., 2000a. Performance analysis of two stage combined heat pump system based on thermo-economic optimization criterion. Energy conv. Manag. 41, 1989-1998.

Kodal, A., Sahin, B., Yilmaz, T., 2000b. Effect of internal irreversibility and heat leakage on the finite time thermoeconomic performance of refrigerators and heat pumps, Energy Conv. Manag. 41, 607–619.

Leonzio, G., 2017. Mathematical model of absorption and hybrid heat pump. Chinese J. Chem. Eng. 25(10), 1492-1504.

Li, Q.Y., Chen, Q., Zhang, X., 2013. Performance analysis of a rooftop wind solar hybrid heat pump system for buildings. Energy and Buildings 65, 75–83.

Liu, F., Sui, J., Liu, T., Jin. H., 2017. Performance investigation of a combined heat pump transformer operating with water/lithium bromide. Energy Conv. Manag. 140, 295–306.

Lostec, B.L., Millette, J., Galanis, N., 2010. Finite time thermodynamics study and exergetic analysis of ammonia-water absorption systems. Inter. J. Therm. Sci. 49, 1264-1276.

Mastrullo, R., Renno, C.A., 2010. Thermoeconomic model of a photovoltaic heat pump. Appl. Therm. Eng. 30, 1959–1966.

Medjo Nouadje, B.A., Ngouateu Wouagfack, P.A., Tchinda, R., 2014. Influence of two internal irreversibilities on the new thermo-ecological criterion for three-heat-source refrigerators. Int. J. Refrig. 38, 118-127.

Medjo Nouadje, B.A., Ngouateu Wouagfack, P.A., Tchinda, R., 2016. Finite-time thermodynamics optimization of an irreversible parallel flow double-effect absorption refrigerator. Int. J. Refrig. 67, 433-444.

Misra, R.D., Sahoo, P.K., Sahoo, S., Gupta, A., 2003. Thermoeconomic optimization of a single effect water/LiBr vapour absorption refrigeration system. Int. J. Refrig. 26, 158–169.

Misra, R.D., Sahoo, P.K., Gupta, A., 2005. Thermoeconomic evaluation and optimization of a double-effect H2O/LiBr vapour-absorption refrigeration system. Int. J. Refrig. 28, 331–343.

Misra, R.D., Sahoo, P.K., Gupta, A., 2006. Thermoeconomic evaluation and optimization of an aqua-ammonia vapour-absorption refrigeration system. Int. J. Refrig. 29, 47–59.

Mortazavi, M., Schmid, M., Moghaddam, S., 2017. Compact and efficient generator for low grade solar and waste heat driven absorption systems. Appl. Energy 198, 173-179.

Ngouateu Wouagfack, P.A., Tchinda R., 2011a. Performance optimization of three-heat-source irreversible refrigerators based on a new thermo-ecological criterion. Int. J. Refrig. 34, 1008-1015.

Ngouateu Wouagfack, P.A., Tchinda, R., 2011b. Irreversible three-heat-source refrigerator with heat transfer law of $Q\alpha\Delta\left(T^{-1}\right)$ and its performance optimization based on $ECOP$ criterion. Energy System 2, 359–376.

Ngouateu Wouagfack, P.A., Tchinda R., 2012a. The new thermo-ecological performance optimization of an irreversible three-heat-source absorption heat pump. Int. J. Refrig. 35, 79-87.

Ngouateu Wouagfack, P.A., Tchinda, R., 2012b. Optimal ecological performance of a four-temperature-level absorption heat pump. Int. J. Therm. Sci. 54, 209-219.

Ngouateu Wouagfack, P.A., Tchinda, R., 2013. Finite-time thermodynamics optimization of absorption refrigeration systems: a review. Ren. Sust. Energy Rev. 21, 524–536.

Ngouateu Wouagfack, P.A., Tchinda R., 2014. Optimal performance of an absorption refrigerator based on maximum ECOP. Int. J. Refrig. 40, 404-415.

Ni, N., Chen, L., Wu, C., Sun, F., 1999. Performance analysis for endoreversible closed regenerated Brayton heat pump cycles. Energy Conv. Manag. 40, 393–406.

Ozel, G., Acikkalp, E., Savas, A.F., Yamik, H., 2016. Comparative Analysis of Thermoeconomic Evaluation Criteria for an Actual Heat Engine. J. Non-Equilib. Thermodyn. DOI 10.1515/jnet-2015-0053.

Qin, X., Chen, L., Ge, Y., Sun, F., 2013. Finite time thermodynamic studies on absorption thermodynamic cycles: A state of the arts review. Arabian J. Sci. Eng. 38 (3), 405-419.

Qin, X., Chen, L., Ge, Y., Sun, F., 2015. Thermodynamic modeling and performance analysis of the variable-temperature heat reservoir absorption heat pump cycle. Phys. A: Stat. Mech. Appl. 436, 788–797.

Qin, X., Chen, L., Sun, F., He, L., 2007. Model of real absorption heat pump cycle with a generalized heat transfer law and its performance. Proc. IMechE A: J. Power Energy 221 (A7), 907–916.

Qin, X.; Chen, L., Sun, F., Wu, C., 2004a. An absorption heat-transformer and its optimal performance. Appl. Energy 78, 329-346.

Qin, X., Chen, L., Sun, F., Wu C., 2004b. Optimal performance of an endoreversible four-heat-reservoir absorption heat-transformer. Open Syst. Inf. Dyn. 11 (2), 147-159.

Qin, X., Chen, L., Sun, F., Wu, C., 2006. Performance of an endoreversible four-heat-reservoir absorption heat pump with a generalized heat transfer law. Int. J. Therm. Sci. 45, 627-633.

Qin, X., Chen, L., Sun, F., Wu, C., 2005. Thermoeconomic optimization of an endoreversible four-heat reservoir absorption-refrigerator. Appl. Energy 81(4), 420-433.

Qin, X., Chen, L., Sun, F., Wu, C., 2008. Performance of real absorption heat-transformer with a generalised heat transfer law. Appl. Therm. Eng. 28, 767-776.

Qin, X., Chen, L., Sun, F., 2010. Thermodynamic modeling and performance of variable-temperature heat reservoir absorption refrigeration cycle. Int. J. Exergy 7 (4), 521–534.

Qin, X., Chen, L., Xia, S., 2017. Ecological performance of four-temperature-level absorption heat transformer with heat resistance, heat leakage and internal irreversibility. Int. J. Heat Mass Transf. 114, 252–257.

Qureshi, B.A., Syed, M. Z., 2015. Thermoeconomic considerations in the allocation of heat transfer inventory for irreversible refrigeration and heat pump systems. Int. J. Refrig. 54, 67-75.

Rivera, W., Best, R., Cardoso, M.J., Romero, R.J., 2015. A Review of Absorption Heat Transformers. Appl. Therm. Eng. 91, 654-670.

Romero, R.J., Rivera, W., Gracia, J., Best, R., 2001. Theoretical comparison of performance of an absorption heat pump system for cooling and heating operating with an aqueous ternary hydroxide and water/lithium bromide. Appl. Therm. Eng. 21, 1137-1147.

Sadatsakkak, S.A., Ahmadi, M.H., Ahmadi, M.A., 2015. Thermodynamic and thermo-economic analysis and optimization of an irreversible regenerative closed Brayton cycle. Energy Convers. Manag. 94, 124-129.

Sahin, B., Kodal, A., Ekmekci, I., Yilmaz, T., 1997. Exergy optimization for an endoreversible cogeneration cycle. Energy 22, 551-557.

Sarbu, I., 2014. A review on substitution strategy of non-ecological refrigerants from vapour compression-based refrigeration, air-conditioning and heat pump systems. Int. J. Refrig. 46, 123-141.

Sarkar, J., Bhattacharyya, S., Gopal, M.R., 2005. Transcritical CO_2 heat pump systems: exergy analysis including heat transfer and fluid flow effects. Energy Convers. Manag. 46, 2053-2067.

Sieniutycz, S., Salamon, P., 1990. Advances in Thermodynamics. Volume 4: Finite Time Thermodynamics and Thermoeconomics. Taylor & Francis, New York.

Silveira, J.L., Tuna, C.E., 2003. Thermoeconomic analysis method for optimization of combined heat and power systems. Part I. Prog. Energy Combust. Sci. 29, 479–485.

Silveira, J.L., Tuna, C.E. 2004. Thermoeconomic analysis method for optimization of combined heat and power systems. Part II. Prog. Energy Combust. Sci. 30, 673–678.

Su, H., Gong, G., Wang, C., Zhang, Y., 2017. Thermodynamic Optimization of an Irreversible Carnot Refrigerator with heat recovery reservoir. Appl. Therm. Eng. 110, 1624-1634.

Sun, F., Qin, X., Chen, L., Wu, C., 2005. Optimization between heating load and entropy-production rate for endoreversible absorption heat-transformers. Appl. Energy 81(4), 434-448.

Talbi, M.M., Agnew, B., 2000. Exergy analysis: an absorption refrigerator using lithium bromide and water as the working fluids. Appl. Therm. Eng. 20, 619–630.

Tyagi, S.K., Chen, J., Hua, B., 2004a. Performance evaluation and parametric study of irreversible Carnot heat pump and refrigerator cycles. Proceedings of 3rd International Symposium on Heat Transfer Enhancement and Energy Conservation, Guangzhou, China.

Tyagi, S.K., Chen, J., Kaushik, S.C., 2004b. Thermoeconomic optimization and parametric study of an irreversible Stirling heat pump cycle. Int. J. Therm. Sci. 43, 105–112.

Tyagi, S.K., Zhou, Y., Chen, J., 2004c. Optimum criteria on the performance of an irreversible Braysson heat engine based on the new thermoeconomic approach. Entropy Int. J. 6, 244–256.

Tyagi, S.K., Chen, J., Lin, G., Kaushik, S.C., 2005. Ecological optimization of an irreversible Ericsson cryogenic refrigerator cycle. Int. J. Energy Res. 29, 1191-1204.

Tyagi, S.K., Chen, G.M., Wang, Q., Kaushik, S.C., 2006. A new thermoeconomic approach and parametric study of irreversible regenerative Brayton refrigeration cycle. Int. J. Refrig. 29, 1167–1174.

Ust, Y., Karakurt, A.S., 2014. Analysis of a cascade refrigeration system (CRS) by using different refrigerant couples based on the exergetic performance coefficient (EPC) criterion. DOI 10.1007/s13369-014-1335-9.

Ust, Y., Sahin, B., Kodal, A., Akcay, I.H., 2006a. Ecological coefficient of performance analysis and optimization of an irreversible regenerative Brayton heat engine. Appl. Energy 83, 558-572.

Ust, Y., Sahin, B., Kodal, A., 2006b. Performance analysis of an irreversible Brayton heat engine based on ecological coefficient of performance criterion. Int. J. of Therm. Sci. 45, 94-101.

Ust, Y., Sahin, B., Kodal. A., 2007. Optimization of a dual cycle cogeneration system based on a new exergetic performance criterion. Appl. Energy 84, 1079–1091.

Ust, Y., Arslan, F., Ozsari, I., 2017. A comparative thermo-ecological performance analysis of generalized irreversible solar-driven heat engines. Rene. Energy 113, 1242–1249.

Wang D., Liu Y., Kou Z., Yao L., Lu Y., Tao L., Xia P., 2019. Energy and exergy analysis of an air-source heat pump water heater system using CO2/R170 mixture as an azeotropy refrigerant for sustainable development. Int. J. Refrig. 106, 628-638.

Wang, J., li, S., Zhang, G., Yang, Y., 2019. Performance investigation of a solar-assisted hybrid combined cooling, heating and power system based on energy, exergy, exergo-economic and exergo-environmental analyses. Energy Convers. Manag. 196, 227-241.

Wang, L., Bu, X., Wang, H., Ma, Z., Ma, W., Li, H. 2018. Thermoeconomic evaluation and optimization of LiBr-H2O double absorption heat transformer driven by flat plate collector. Energy Convers. Manag. 162, 66–76.

Wei, F., Lin, G., Chen J., Bruck, E., 2011. Performance characteristics and parametric optimization of an irreversible magnetic Ericsson heat-pump. Phys. B: Condens. Matter 406, 633–639.

Wu, S., Lin, G., Chen, J., 2005. Optimum thermoeconomic and thermodynamic performance characteristics of an irreversible three-heat-source heat pump. Rene. Energy 30, 2257–2271.

Xia, D., Chen, L., Sun F., Wu, C., 2007. Endoreversible four-reservoir chemical pump. Appl. Energy 84, 56–65.

Xiling, Z., Lin, F., Shigang, Z., 2011. General thermodynamic performance of irreversible absorption heat pump. Energy Convers. Manag. 52, 494–499.

Xu, L., 2016. Thermodynamic Analysis of Stirling Heat Pump based on Thermoeconomic Optimization Criteria. MATEC Web Conf. 61, 01010. DOI: 10.1051/matecconf/20166101010.

Xu, Z.Y., Wang, R.Z., 2018. Comparison of absorption refrigeration cycles for efficient air-cooled solar cooling. Sol. Energy 172(1), 14-23.

Xu, Z., Guo, J., Lin, G., Chen, J., 2016. Optimal thermoeconomic performance of an irreversible regenerative ferromagnetic Ericsson refrigeration cycle. J. Magn. Magn. Mater. 409, 71–79.

Yuksel, Y. E., Ozturk, M., 2017. Thermodynamic and thermoeconomic analyses of a geothermal energy based integrated system for hydrogen production. Int. J. Hydrogen Energy 42, 2530-2546.

Yu, J., Li, Z., Chen, E., Xu, Y., Chen, H., Wang, L., 2019. Experimental assessment of solar absorption-subcooled compression hybrid cooling system. Solar Energy 185, 245-254.

Zare, V., Mahmoudi, S.M.S., Yari, M., Amidpour, M., 2012. Thermoeconomic analysis and optimization of an ammonia-water power/cooling cogeneration cycle. Energy 47, 271–283.

Ziegler, F., 2002. State of the art in sorption heat pumping and cooling technologies. Int. J. Refrig. 25, 450-459.

Zheng, T., Chen, L., Sun, F., Wu, C., 2004. The influence of heat resistance and heat leak on the performance of a four-heat-reservoir absorption refrigerator with heat transfer law of $Q \propto \Delta(T^{-1})$. Int. J. Therm. Sci. 43 (12), 1187–1195.

Zheng, X., Shi, R., Wang, Y., You, S., Zhang, H., Xia, J., Wei, S., 2019. Mathematical modeling and performance analysis of an integrated solar heating and cooling system driven by parabolic trough collector and double-effect absorption chiller. Energy Build. 202, 109400.

RESUME ETENDU

1. Problématique

La climatisation, La conservation (réfrigération des médicaments, matériels médicaux et denrées alimentaires) et la lutte contre le réchauffement climatique de la planète constituent un défi majeur dans le Monde principalement dans la sous-région d'Afrique subsaharienne et au Cameroun. Ce qui a conduit les chercheurs et les ingénieurs à développer des systèmes de production de froid (air conditionné, réfrigération, congélation) et de chauffage mieux adaptés. Nous avons de nos jours les cycles de Carnot, de réfrigération à compression de vapeur, de réfrigération en cascade et multiétage, de réfrigération à gaz (Brayton, Ericsson et Stirling), d'adsorption, de dessiccation et d'absorption. Cependant, les cycles les plus répandus étant les cycles à compression de vapeur car ces derniers sont plus performants en terme de coefficient de performance. Par contre, ils ont trois inconvénients majeurs tels que le bruit sonore lors du fonctionnement, la forte consommation d'électricité et leurs réfrigérants sont des polluants qui participent aux changements climatiques. Ceci étant, l'industrie du froid s'est vue développée d'autres systèmes pour remédier à ces problèmes. Un de ces systèmes est la machine à absorption soucieuse de l'environnement tout en utilisant des sources d'énergies renouvelables (solaire, géothermique, biomasse etc.) et d'autres sources de chaleur telles que les piles à combustible. En plus d'utiliser de faibles quantités d'énergie, les cycles à absorption peuvent fonctionner à partir des sources d'énergie issues des pertes de chaleur industrielle. Ces systèmes fonctionnent grâce à la faculté qu'ont certains liquides comme de l'eau (absorbant) d'absorber et de désorber de la vapeur comme de l'ammoniac ou du bromure de lithium (fluide frigorigène). Néanmoins, il existe plusieurs modèles de machines à absorption dont les machines à absorption simple effet, les machines à absorption double effet, les machines à absorption multiétage, les machines à cycle Générateur- absorbeur-échangeurs, etc. Ceci entraine une autre ère, celle de « l'optimisation » car ces machines ont un rendement moins élevé que celles des machines à compression de vapeur.

Dans le cadre de cette thèse, nous nous intéressons aux pompes à chaleur à absorption simple effet (AHP) avec trois réservoirs thermiques (THR) et quatre réservoirs thermiques (FTL). Tout cela nous amène à réaliser une optimisation multi-objective dans les conditions réelles de fonctionnement (résistances thermiques, fuites de chaleur et pertes de chaleur).

Historiquement, dans la littérature la recherche a systématiquement évolué vers l'optimisation à l'aide de la thermodynamique des temps finis (FTT). Par conséquent, Chen (1999), Kato et al. (2005), Chen et al. (2005a), Qin et al. (2006, 2007, 2015), Xia et al. (2007), Bi et al. (2008), Huang et al. (2008) et Xiling et al. (2011) sur les AHP, Wei et al. (2011) sur la HP magnétique d'Ericsson, Bhardwaj et al. (2003, 2005), Zheng et al. (2004), Chen et al. (2005b, 2006), Qin et al. (2010) et Kaushik et al. (2018) sur les ARs, Qin et al. (2004a, 2004b, 2008) et

Chen et al. (2007a) sur les AHT, ont analysé ces systèmes endoréversibles et irréversibles en utilisant le coefficient de performance, la puissance spécifique de chauffage et la puissance spécifique de réfrigération comme fonctions objectives. Ensuite, les performances des systèmes thermodynamiques sont étudiées en considérant l'impact environnemental avec les pertes de chaleur, les fuites de chaleur et les résistances thermiques dans les différents composants. Ces paramètres sont dérivés de la deuxième loi de la thermodynamique et initiés par Ust et al. (2006a, 2006b) sur les moteurs thermiques irréversibles de Brayton en utilisant le critère thermo-écologique. Ils sont suivis par Ngouateu Wouagfack et Tchinda (2011a, 2011b, 2014), Medjo Nouadje et al. (2014, 2016) et Ahmadi et Ahmadi (2016) avec les AR irréversibles, puis Ngouateu Wouagfack et Tchinda (2012a, 2012b) et Ahmadi et al. (2015) avec les AHP irréversibles et Ahmadi et al. (2016) avec un cycle inversé de Brayton. Parallèlement, le critère écologique (E) basé sur les mêmes considérations est d'abord utilisé par Angulo-Brown (1991) et suivi par Sun et al. (2005), Chen et al. (2007b, 2019), Qin et al. (2017) et Frikha et Abid (2016). De plus, l'approche exergétique en plus des considérations précédentes prend en compte l'énergie utile consommée par le cycle thermodynamique (Sahin et al., 1997; Talbi et Agnew, 2000; Kilic et Kaynakli, 2007; Kaushik et Arora, 2009; Lostec et al., 2010; Farshi et al., 2013). Cependant, le critère de performance exergétique (EPC) utilisé par Ust et al. (2007) et Liu et al. (2017) sur les ARs, permet lui aussi d'évaluer les performances exergétiques des systèmes thermodynamiques. Par ailleurs, l'optimisation des systèmes thermiques par l'approche thermo-économique tient compte du coût sur l'investissement avec des paramètres tels que les aires d'échange de chaleur, les capacités thermiques et du coût sur la consommation. Kodal et al. (2000, 2002, 2003) ont utilisé cette approche sur les AHP simple effet et les AHP à deux étages, suivis de Silveira et Tuna (2003, 2004) sur les systèmes combinés de chaleur et d'électricité. Ensuite, Misra et al. (2003, 2005) sur les ARs simple effet et double effet entrainés par la paire H_2O/LiBr, Qin et al. (2005) sur les ARs endoréversibles, Durmayaz et al. (2004) sur les systèmes thermiques, Wu et al. (2005) sur la AHP irréversible, Qureshi et Syed (2015) sur les AHP et AR. Zare et al. (2012) et Ahmadi et al. (2014b) ont mené une étude thermo-économique et exergétique respectivement sur un cycle de cogénération ammoniac-eau et sur des systèmes multi-génération utilisant l'algorithme génétique évolutif. De ce fait, chaque approche a été examinée en utilisant à chaque fois un critère d'optimisation. Cependant, il est important de considérer simultanément les influences de deux irréversibilités internes dues aux pertes de chaleur (Xiling et al., 2011 utilisant le COP et la puissance spécifique de chauffage comme fonctions objectives et Medjo Nouadje et al., 2014 utilisant le critère thermo-écologique comme fonction objective sur les THR AR), de l'irréversibilité externe générale due aux fuites de chaleur et aux résistances thermiques.

Ceci étant, la considération multi-objective et la double irréversibilité interne apporte les limites et les avantages présentés par l'optimisation de chaque fonction objective en considérant une irréversibilité interne globale.

Cette thèse constitue donc une contribution à l'optimisation des pompes à chaleur à absorption avec trois réservoirs thermiques (THR AHP) et des pompes à chaleur à absorption avec quatre réservoirs thermiques (FTL AHP) simple effet. En utilisant la FTT et un algorithme flowchart (Su et al., 2017; Chen et al., 2019), nous avons réalisé une optimisation multi-objective en utilisant des critères thermo-écologiques, écologiques, exergétiques et thermo-économiques en tenant compte des irréversibilités externes et irréversibilités internes.

Les principaux objectifs sont:

i) Optimisation thermo-écologique des THR AHP en tenant compte des irréversibilités externes et de la double irréversibilité interne.

ii) Optimisation exergétique des FTL AHP en tenant compte des irréversibilités externes, de deux paramètres d'irréversibilité interne, du ratio de chaleur rejetée entre l'absorbeur et le condenseur et de la nature du matériau des échangeurs de chaleur.

iii) Optimisation écologique, exergétique et thermo-économique des THR AHP en tenant compte des irréversibilités externes et de deux irréversibilités internes.

iv) Optimisation écologique, exergétique et thermo-économique des FTL AHP en tenant compte des irréversibilités externes, de deux paramètres d'irréversibilité interne, du ratio de chaleur rejetée entre l'absorbeur et le condenseur et de la nature du matériau des échangeurs de chaleur.

2. Matériels et méthodes

Dans le cas de l'optimisation en considérant une seule fonction objective, la fonction thermo-écologique (ECOP) est optimisée pour les THR AHP et la fonction exergétique (EPC) est optimisée pour FTL AHP. La première est définie comme le ratio entre la puissance de chauffage sur le taux de génération d'entropie multiplié par la température de l'environnement, et la seconde est définie comme le ratio entre le taux d'exergie à la sortie sur le taux d'exergie détruite. Cependant, la différence entre un système THR AHP et un système FTL AHP est que la température du fluide est la même dans l'absorbeur et le condenseur pour un système THR AHP. Chacune de ces fonctions objectives est obtenue en fonction de la température du fluide dans les différents composants tels que le générateur, l'évaporateur, l'absorbeur et le condenseur en considérant la surface totale des échanges de chaleur constante. En effectuant les dérivées de celles-ci dans l'environnement de la plate-forme Maple et en tenant compte des conditions extrémales. Nous obtenons les expressions analytiques maximales de chaque fonction *ECOP* et

EPC avec les paramètres optimaux de performance correspondants tels que le coefficient de performance, la puissance spécifique de chauffage, le taux d'entropie générée, l'aire des surfaces d'échange de chaleur et la fonction écologique. Ceci est obtenu en tenant compte des paramètres d'irréversibilité externe et des deux facteurs d'irréversibilité interne.

Dans le cas de l'optimisation multi-objective en considérant trois fonctions objectives, les fonctions écologique (E), exergétique (EPC) et thermo-économique (F) qui sont optimisées et comparées. La fonction écologique est définie comme la différence entre le taux d'exergie à la sortie et le taux d'entropie générée tant dis que la fonction thermo-économique est définie comme le ratio de la charge chauffage sur le coût de l'investissement et le coût de l'énergie consommée. En utilisant la thermodynamique des temps finis, nous avons obtenu une relation liant le coefficient de performance, la charge spécifique de chauffage, l'aire des surfaces d'échange de chaleur, les facteurs d'irréversibilité externes et les deux facteurs d'irréversibilité interne. Cette relation est exploitée dans l'algorithme flowchart à fin de déterminer les points de fonctionnement optimaux du système THR AHP d'une part et FTL AHP d'autre part.

3. Résultats et discussion

Les travaux menés tout au long de cette thèse ont conduit à l'analyse et à l'optimisation multi-objective des THR AHP et FTL AHP. D'une part, nous avons analysé les performances des cycles THR par la fonction thermo-écologique objective (ECOP) puis FTL par la fonction exergétique objective (EPC). D'autre part, afin de pouvoir faire une synthèse plus objective, nous avons comparé trois critères de performance décisifs à savoir les critères écologiques, exergétiques et économiques avec trois et quatre réservoirs de chaleur à chaque fois. Cette synthèse tient compte des conditions réelles de fonctionnement qui sont soumises aux deux types d'irréversibilité, c'est-à-dire les irréversibilités externes et les irréversibilités internes. De plus, les irréversibilités externes se manifestent par la différence finie de température entre le système et l'environnement. Par contre, les irréversibilités internes se manifestent par les transformations non isentropiques, le frottement entre le fluide et les parois des échangeurs de chaleur et les chutes de pression. Néanmoins, une étude isolée puis comparative des avantages et inconvénients au maximum de chaque critère de performance en fonction des paramètres de performance optimaux correspondants tels que le coefficient de performance, le taux de génération d'entropie, la charge spécifique de chauffage, l'aire des surfaces d'échange thermique, le taux d'exergie à la sortie et taux d'exergie détruite. Cela étant, l'analyse de la thermodynamique des temps finis et la méthode d'optimisation flowchart comme outils d'analyse et de précision ont permis d'obtenir deux blocs de résultats significatifs.

Les aspects notés dans le premier bloc de résultats sont les suivants:

i) Pour les cycles THR, il apparaît que le critère *ECOP* par rapport au critère *E* présente un avantage significatif en termes de taux de génération d'entropie spécifique.

ii) Pour les cycles FTL, il apparaît que les pertes exergétiques minimales et une puissance de chauffage spécifique optimale sont enregistrées pour $0.5 \le m \le 1.5$.

iii) Pour les cycles FTL, il apparaît que les fonctions objectives optimales *EPC*, *ECOP* et *E* sont meilleures pour des valeurs plus élevées des coefficients globaux de transfert de chaleur des différents composants. Cependant, les pertes exergétiques sont plus importantes dans ces cas.

iv) Pour les cycles FTL, il apparaît qu'au maximum des fonctions d'objectives *EPC* et *ECOP*, un taux de génération d'entropie faible et un meilleur *COP* par rapport au maximum de la fonction d'objective *E* sont obtenus.

v) Pour les cycles FTL, il apparaît qu'au maximum de la fonction objective *E*, une charge spécifique de chauffage plus élevée a été trouvée par rapport au maximum des fonctions objectives *EPC* et *ECOP*. De plus, les fonctions optimales de performance au critère *E* maximum sont plus élevées sous l'influence du facteur d'irréversibilité interne I_2.

Ensuite, les aspects soulignés dans le deuxième bloc sont les suivants:

i) Pour les cycles THR et FTL, il apparaît que les valeurs maximales les plus élevées du critère thermo-économique correspondent à un faible coût d'investissement (faible surface d'échange thermique) et un coût élevé sur l'énergie consommée (l'apport de chaleur venant du générateur est haut). Cela favorise un taux d'exergie détruite minimal pour certaines valeurs de la charge de chauffage spécifique et du taux d'exergie à la sortie.

ii) Les influences des fuites de chaleur et des résistances thermiques sont plus prononcées que les pertes de chaleur caractérisées par des facteurs d'irréversibilité internes I_1 et I_2. De plus, sous l'influence des paramètres de conception, le cycle THR AHP présente un avantage significatif aux maxima des critères *F* et *EPC* en termes de coefficient de performance. Néanmoins, le cycle THR AHP présente un avantage significatif au maximum de *EPC* en termes de taux de destruction exergétique et au maximum de *E* en termes de charge calorifique spécifique et de débit de sortie exergétique.

iii) Les pertes de chaleur dans l'ensemble condenseur-évaporateur ont des effets plus néfastes sur les performances du cycle THR AHP. De plus, dans les FTL AHP, les pertes de chaleur dans l'ensemble condenseur-évaporateur ont des effets plus néfastes pour $0 < m \le 1$, bien que les pertes de chaleur dans l'ensemble générateur-absorbeur aient des effets plus néfastes pour $m > 1$.

iv) Les systèmes FTL AHP sont plus efficaces lorsque les taux d'échange de chaleur dans les échangeurs de chaleur absorbeur et condenseur sont proches.

4. Conclusion

Les travaux présentés tout au long de ce mémoire de thèse ont porté sur l'optimisation écologique, exergétique et économique des pompes à chaleur à trois et à quatre réservoirs thermiques. Une revue de la littérature a permis de montrer l'utilisation de la thermodynamique des temps finis dans les différents systèmes thermodynamiques, ainsi que les analyses des performances des pompes à chaleur à absorption par les critères écologique, exergétique et thermo-économique. Cependant, pour cette étude, nous avons considéré non plus un paramètre d'irréversibilité interne comme dans la littérature mais deux paramètres d'irréversibilité interne tels que l'irréversibilité interne de l'assemblage évaporateur-condenseur et l'irréversibilité interne de l'assemblage générateur-absorbeur, ainsi qu'un paramètre général d'irréversibilité externe. Il en ressort que les pertes de chaleur dans l'assemblage évaporateur-condenseur ont des effets plus néfastes dans les performances des pompes à chaleur à absorption fonctionnant avec trois réservoirs thermiques. Pourtant, les effets des pertes de chaleur observées dans les pompes à chaleur à absorption munies de quatre réservoirs thermiques dépendent de l'écart des taux de transfert de chaleur dans l'absorbeur et le condenseur. De plus, le système est économe en terme d'exergie détruite et écologique en terme d'exergie à la sotie.

PUBLICATIONS OF THESIS

1. Published papers

(i) **Fossi Nemogne, R.L.**, Medjo Nouadje, B.A., Ngouateu Wouagfack, P.A., Tchinda, R., **2019**. Thermo-ecological analysis and optimization of a three-heat-reservoir absorption heat pump with two internal irreversibilities and external irreversibility. **Int. J. Refrig. 106, 447-462**. doi:10.1016/j.ijrefrig.2019.06.017.

(ii) **Fossi Nemogne, R.L.**, Ngouateu Wouagfack, P.A., Medjo Nouadje, B.A., Tchinda, R., **2020**. Exergetic, ecological and thermo-economic (3E) optimization of an absorption heat pump with heat resistance, heat leakage and two internal irreversibilities: Comparison. **Int. J. Refrig. 112, 251-461**. doi:10.1016/j.ijrefrig.2019.12.016.

(iii) **Fossi Nemogne, R.L.**, Ngouateu Wouagfack, P.A., Medjo Nouadje, B.A., Tchinda, R., **2021**. Multi-objective optimization and analysis of a performance of a four-heat-reservoir absorption heat pump with multi-irrevesibilities. **Energy Convers. Manag. 234, 113967**. Doi: 10.1016/j.enconman.2021.113967.

2. Submitted papers

(iv) Medjo Nouadje, B.A., **Fossi Nemogne, R.L.**, Ngouateu Wouagfack, P.A., Thiam P., Tchinda, R., 2021. Exergy analysis and optimization of a four-temperature-level absorption heat pump based on finite-time-thermodynamics. (**In progress**).

(v) **Fossi Nemogne, R.L.**, Medjo Nouadje, B.A., Ngouateu Wouagfack, P.A., Tchinda, R., 2021. Finite time thermodynamics optimization and analysis of absorption heat pumps: A review and new trends. (**In progress).**

International Journal of Refrigeration 106 (2019) 447–462

Contents lists available at ScienceDirect

International Journal of Refrigeration

journal homepage: www.elsevier.com/locate/ijrefrig

Thermo-ecological analysis and optimization of a three-heat-reservoir absorption heat pump with two internal irreversibilities and external irreversibility

Rodrigue Léo Fossi Nemogne[a,*], Brigitte Astrid Medjo Nouadje[b,c], Paiguy Armand Ngouateu Wouagfack[d], Réné Tchinda[b,c]

[a] Energy, Electrical Systems and Electronics Laboratory, Department of physics, University of Yaounde I, PO Box 812, Yaounde, Cameroon
[b] Laboratory of Mechanical and Modelisation of Physical Systems, Department of physics, University of Dschang, PO Box 67, Dschang, Cameroon
[c] Industrial and Energy Systems Engineering Laboratory, University institute of Technology Fotso Victor, University of Dschang, PO Box 134, Bandjoun, Cameroon
[d] Department of Renewable Energy, Higher Technical Teachers' Traning College, University of Buea, PO Box 249, Buea Road, Kumba, Cameroon

ARTICLE INFO

Article history:
Received 15 February 2019
Revised 21 May 2019
Accepted 11 June 2019
Available online 13 June 2019

Keywords:
Irreversibilities
Absorption heat pump
Three-heat-reservoir
Optimization
Ecological coefficient of performance

ABSTRACT

The investigations carried out in this work concern the optimization and the thermodynamic analysis of an absorption heat pump with multi-irreversibilities and provided with three-heat-reservoir mainly using the thermo-ecological criterion as objective function. The thermodynamic analysis of the first and second laws of thermodynamics and the linear law of heat-transfer allowed us to evaluate and optimize the objective functions of performance such as: the specific heating load, the coefficient of performance, the specific entropy generation rate, the ecological coefficient of performance and the heat-transfer areas of the various components. These allowed us to study the variations of these criteria according to the design parameters and the temperatures of the working fluid in the components. From this study, it follows that the optimal system implies a maximum thermo-ecological coefficient, a minimum entropy production rate corresponding to a certain value of the specific heating load, while maintaining a system which limits the losses between the condenser and the evaporator. Moreover, the consideration of the two internal irreversibilities, the external irreversibility and the losses of the heat resistances is very close to a real absorption heat pump and allows a more precise and objective study rather than in the optimization and the design of an absorption system like an endoreversible system.

Analyse thermo-écologique et optimisation d'une pompe à chaleur à absorption à trois réservoirs thermiques avec deux irréversibilités internes et irréversibilité externe

Mots-clés: Irréversibilités; Pompe à chaleur à absorption; Triple réservoir thermique; Optimisation; Coefficient de performance écologique

1. Introduction

The heat pump is a device which has been used for a long time. The production of heat has gradually become very important in our daily lives. It is found in various applications such as drying of food, air conditioning of buildings and vehicles, heating of hot water, industry etc. Heating is an important process in the world's electricity consumption and this continues to increase, especially with the climate changes which have an important effect on the planet. Studies are being conducted to solve the environmental pollution issues associated with heat production systems such as an absorption heat pump (AHP) which is studied in this manuscript. On the one hand, research may consist of find-

* Corresponding author.
E-mail address: rodriguefossi@yahoo.fr (R. Léo Fossi Nemogne).

https://doi.org/10.1016/j.ijrefrig.2019.06.017
0140-7007/

Nomenclature

A	total heat-transfer area (m^2)
COP	coefficient of performance (dimensionless)
$ECOP$	ecological coefficient of performance (dimensionless)
E	ecological criterion (W)
h	overall heat-transfer coefficient ($WK^{-1}m^{-2}$)
I	internal irreversibility parameter (dimensionless)
K	thermal conductivity (WK^{-1})
$\dot{Q}$	rate of heat-transfer (W)
q	specific heating load (Wm^{-2})
S	specific entropy generation rate ($WK^{-1}m^{-2}$)
T	temperature (K)
U	overall heat-transfer coefficient ($WK^{-1}m^{-2}$)

Abbreviations

AHP	absorption heat pump
AR	absorption refrigerator
COP	coefficient of performance
ECOP	ecological coefficient of performance
FTT	finite time thermodynamics
HP	heat pump
HT	heat transformer
THR	three-heat-reservoir

Greek symbols

ε	coefficient of performance for reversible three-heat-source heat pump (dimensionless)
ξ	heat leakage coefficient ($WK^{-1}m^{-2}$)
π	specific heating load (Wm^{-2})
$\dot{\sigma}$	entropy generation rate (WK^{-1})

Subscripts

1	working fluid in generator
2	working fluid in evaporator
3	working fluid in absorber and condenser
A	absorber
C	condenser
E	evaporator
env	environment
G	generator
L	heat leakage
max	maximum *ECOP*
max, E	maximum E
O	absorber and condenser
op	at maximum ECOP
r	for an reversible three-heat-reservoir heat pump

Superscripts

*	at maximum E

ing less polluting fluids such as carbondioxide, light hydrocarbons (propane, butane), water, ammonia, etc. (Sarkar et al., 2005; Bi et al., 2012; Sarbu, 2014). On the other hand, researchers are looking at systems with high energy efficiency and stability in the field of physics and engineering while having a low environmental impact (Sieniutycz and Salamon, 1990; Bejan, 1996; Chen et al., 1999; Chen and Sun, 2004; Feidt, 2010, 2013; Andresen, 2011; Qin et al., 2013; Rivera et al., 2015; Ngouateu Wouagfack and Tchinda, 2013; Su et al., 2017; Ge et al., 2016). This is why the optimization by the thermo-ecological approach considering the objective function ecological coefficient of performance (ECOP) is necessary. This approach was initiated by Ust et al. (2006a, 2006b) on irreversible Brayton heat engines. This time we use it taking into account the influences of the two internal irreversibilities, the overall external irreversibility and the heat resistances.

The optimization of endoreversible and irreversible absorption systems were previously studied under the basis of the coefficient of performance (COP) and the specific heating or cooling load as objective functions, without really worrying about the amount of heat emitted in the environment. This is the case of Chen (1999) on heat pumps (HP) with four-temperature-level, Bi et al. (2008) on air heat pumps, Xia et al. (2007) on a four-source chemical pump. Kato et al. (2005) on the working fluid of a cogeneration heat pump, Qin et al. (2004a, 2004b, 2006, 2008), respectively on heat transformers, endoreversible four-heat-reservoir absorption heat transformers, endoreversible HPs with four-temperature-level and real heat transformers. Chen et al. (2005) and Huang et al. (2008) on irreversible AHPs and Bhardwaj et al. (2003, 2005) on gas absorption refrigerators, Kaushik et al. (2018) on the refrigeration cycle, Wei et al. (2011) on magnetic HP of Ericsson, Xiling et al. (2011) on the AHP with two internal irreversibilities. Chen (1999), Bi et al. (2008), Xia et al. (2007), Kato et al. (2005), Qin et al. (2004a, 2004b, 2006, 2008), Chen et al. (2005), Huang et al. (2008), Bhardwaj et al. (2003, 2005), Kaushik et al. (2018), Wei et al. (2011) and Xiling et al. (2011) have evaluated the maximum COP and the corresponding optimal specific load or the maximum specific load and the corresponding optimal COP, using finite time thermodynamics (FTT). However, the heat capacities of the components, the internal irreversibility by dissipation and the external irreversibility by heat leakage influence the performances of the AHP (Qin et al., 2007, 2015), AR (Zheng et al., 2004; Chen et al., 2005a; 2006; Qin et al., 2010) and AHT (Chen et al., 2007a). The effects of the previous design parameters on the two-stage semi-conductive thermoelectric devices using the COP and the specific heating load are analyzed with respect to the working electric current (Chen et al., 2008; 2016). In addition, the optimization of absorption systems taking into account the cost of product investment and the cost of consumption further complements the previous approach. This new study is based on the objective thermo-economic function introduced by Kodal et al. (2000, 2002, 2003) on AHP and two-stage AHPs. It is the ratio of the specific heating or cooling load to the sum of the cost of the investment and the cost of the energy consumed. This objective function allows to optimize the performances of a system taking into account the cost energy consumed. Qin et al. (2005) used this thermo-economic criterion on the endoreversible four-heat-reservoir AR taking into account the design parameters, then Qureshi and Syed (2015) used this criterion to show the effects of internal irreversibility on the system in order to optimize AHP and AR with working fluid pairs such as NH_3/H_2O and $LiBr/H_2O$. In addition, the usefulness of another approach to the optimization of irreversible AHP is important, especially an approach that takes into account the impact on the environment. Angulo-Brown (1991), Sun et al. (2005), Chen et al. (2007, 2019), Qin et al. (2017) and Frikha and Abid (2016), used the ecological objective function as a performance criterion. It is defined as the difference between the specific heating or cooling load and the degraded load by the system or the loss rate of availability, which gives it values that can be negative. The negative values that this function can obtain when the loss rate of availability is significant show that the system is not ecologically reliable. Ust et al. (2006a, 2006b), proposed a new thermo-ecological criterion called ecological coefficient of performance which is the ratio between the specific heating or cooling load and the loss rate of available (product of the entropy generation rate and the temperature of the environment). They are followed using FTT on irreversible systems by Ngouateu Wouagfack and Tchinda (2011a, 2011b, 2014) and Medjo Nouadje et al. (2014, 2016) with the ARs then Ngouateu Wouagfack and Tchinda (2012a, 2012b) with AHP. The latter analytically maximized the thermo-ecological objective

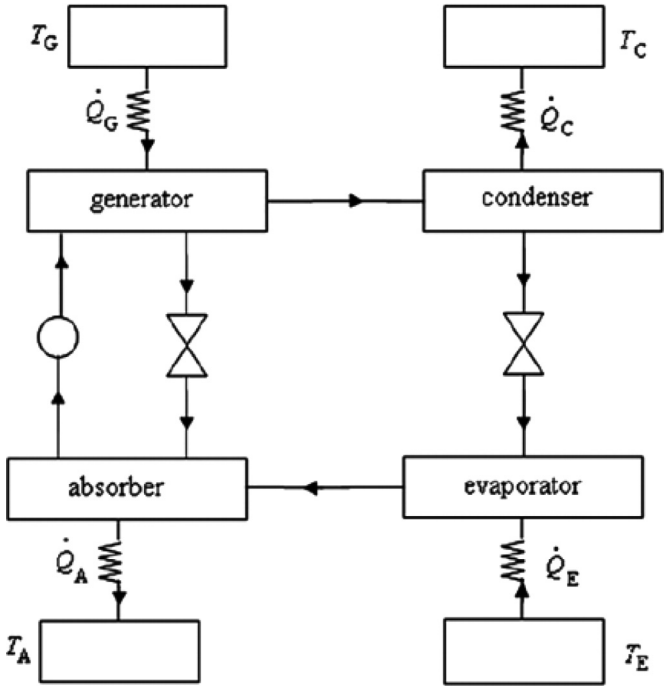

Fig. 1. Symbolic diagram of an AHP (Medjo Nouadje et al., 2014).

function corresponding to the various optimal performance criteria under the influences of the losses of the heat resistance, heat leakage and irreversibilities and discussed a practical and optimal operating region. On the other hand, Ahmadi et al. (2015, 2016) worked respectively on irreversible AHP and those working on an inverse Brayton cycle by applying the evolutionary genetic algorithm on the ECOP objective function, they found an optimal Pareto front of functioning.

As a matter of fact, the effects of two internal irreversibilities so far by the thermo-ecological decisive function (ECOP) approach has been studied by Medjo Nouadje et al. (2014) on the ARs. However, by applying the first and the second law of finite time thermodynamics (FTT) and the linear heat transfer law on heat transfer rates, we will study and discuss on optimizing the performance of an AHP three-heat-reservoir (THR) with multi-irreversibilities. This time we will model the ECOP criterion analytically and evaluate its maximum value corresponding to the optimal working fluid temperatures in the different components. Then, to obtain the different optimal parameters of the corresponding performance and to draw their curves which will make it possible to discuss on the influences of the two internal irreversibilities, the overall external irreversibility and the losses of the heat resistances.

2. Thermodynamic analysis of an irreversible absorption heat pump with three-heat-reservoir

2.1. Application of the first law of thermodynamics and Newton's law of heat-transfer

The AHP is a thermodynamic system in which undergoes a thermodynamic transformation with closed cycle. Thus, we will be able to apply the first law of thermodynamics to the AHP under these conditions. In Fig. 1, $\dot{Q}_G$ (heat input from the generator heat source), $\dot{Q}_E$ (heat input to evaporator), $\dot{Q}_A$ (heat output to the absorber heat sink) and $\dot{Q}_C$ (rejected heat from the condenser) are the quantities exchanged between the working fluid and the four components expressed in (W).

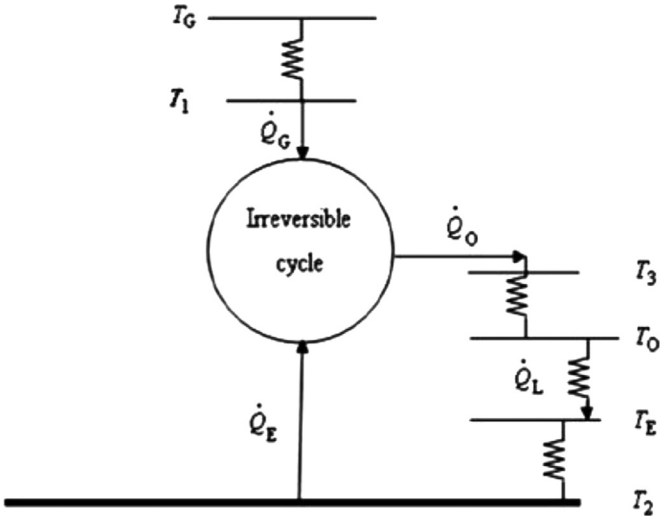

Fig. 2. The irreversible cycle model of a three-heat-reservoir AHP (Ahmadi et al., 2015).

The first law of thermodynamics can be written from Fig. 2 using the Refs. Ngouateu Wouagfack and Tchinda (2011a, 2011b, 2012a, 2012b, 2014), Medjo Nouadje et al. (2014, 2016) and Ahmadi et al. (2015, 2016).

$$\dot{Q}_G + \dot{Q}_E - \dot{Q}_C - \dot{Q}_A = 0 \tag{1}$$

By considering $\dot{Q}_O = \dot{Q}_C + \dot{Q}_A$, Eq. (1) becomes:

$$\dot{Q}_G + \dot{Q}_E - \dot{Q}_O = 0 \tag{2}$$

The Newton's law of heat transfer states that the heat exchanged between a wall of heat-transfer area S of a solid body at the temperature T and the surrounding fluid are deduced from Refs. Chen et al. (2005b), Huang et al. (2008), Ngouateu Wougfack and Tchinda (2011a, 2012a, 2012b, 2014), Medjo Nouadje et al. (2014, 2016), Ahmadi et al. (2015).

$$\dot{Q} = hS\Delta T \tag{3}$$

We deduce the heat-transfer law in the different components:

$$\dot{Q}_G = U_G A_G (T_G - T_1) \tag{4}$$

$$\dot{Q}_E = U_E A_E (T_E - T_2) \tag{5}$$

$$\dot{Q}_O = U_O A_O (T_3 - T_O) \tag{6}$$

with

$$A_O = A_A + A_C \text{ and } T_O = T_A = T_C \tag{7}$$

The heat loss due to the influence of the surrounding environment thanks to the convective exchange of the heat resistances (Ngouateu Wouagfack and Tchinda, 2012a) are evaluated between the absorber-condenser assembly and the evaporator:

$$\dot{Q}_L = K_L (T_O - T_E) \tag{8}$$

A_G, A_E, A_A, A_C and A_O are the heat-transfer areas of the heat exchangers in the generator, the evaporator, the absorber, the condenser and the absorber-condenser assembly respectively and are expressed in (m^2). U_G, U_E and U_O are the coefficients of heat transfer by convection in $(Wm^{-2}K^{-1})$, respectively, of the generator, the evaporator and the absorber-condenser assembly. $\dot{Q}_L$ in (W) and K_L the thermal conductivity of the heat leakage in (WK^{-1}).

Moreover the total heat-transfer area of the heat exchangers is evaluated by the relation (9):

$$A = A_G + A_E + A_O \tag{9}$$

2.2. Application of the second law of thermodynamics

Historically, the irreversibility of certain phenomena gave rise to the second law of thermodynamics. As a result, when there is degradation of energy at the time of a transformation, it is known as irreversible thus the importance and utility of the extensive size entropy. The application of the second law of thermodynamics to the system is due to actual operating considerations of AHP. These considerations lead to two internal irreversibilities factors I_1 and I_2 which represent the heat loss rate generated during the passage of the working fluid respectively between the absorber and the generator and between the condenser and the evaporator. By applying the second law of thermodynamics still called Clausius inequality as in the Refs. Ngouateu Wougfack and Tchinda (2011a, 2011b, 2012a) and Medjo Nouadje et al. (2014) we obtain:

$$\oint \frac{\delta \dot{Q}}{T} = \frac{\dot{Q}_G}{T_1} + \frac{\dot{Q}_E}{T_2} - \frac{\dot{Q}_O}{T_3} < 0 \tag{10}$$

where T_1, T_2 and T_3 are the temperatures of the working liquid, respectively, in the generator, the evaporator and the absorber-condenser assembly in (K).

By introducing the two internal irreversibilities into Eq. (10), we obtain a quantitative and qualitative entropy relation assessment which will enable us to minimize the degradation of energy and the influences of the irreversibilities in our system. We obtain:

$$\frac{\dot{Q}_G}{T_1} = \frac{\dot{Q}_A}{I_1 T_3}\ (I_1 \geq 1)$$
$$\frac{\dot{Q}_E}{T_2} = \frac{\dot{Q}_C}{I_2 T_3}\ (I_2 \geq 1) \tag{11}$$

Considering Eqs. (10) and (11), we obtain for an irreversible system ($I_1 > 1$ and $I_2 > 1$):

$$\frac{\dot{Q}_G}{T_1} + \frac{\dot{Q}_E}{T_2} - \frac{\dot{Q}_A}{I_1 T_3} - \frac{\dot{Q}_C}{I_2 T_3} = 0 \tag{12}$$

For a system with an internal irreversibility used in the Refs. Ngouateu Wouagfack and Tchinda (2011a, 2012a), Eq. (12) becomes:

$$\frac{\dot{Q}_G}{T_1} + \frac{\dot{Q}_E}{T_2} - \frac{\dot{Q}_O}{I T_3} = 0 \tag{13}$$

While for an endoreversble system ($I_1 = I_2 = 1$), Eq. (12) becomes:

$$\frac{\dot{Q}_G}{T_1} + \frac{\dot{Q}_E}{T_2} - \frac{\dot{Q}_O}{T_3} = 0 \tag{14}$$

3. Thermodynamic study of the performance criteria of an irreversible absorption heat pump with three-heat-reservoir

3.1. The coefficient of performance (COP)

By using Eqs. (2, 4–9) and (12), the COP of an irreversible AHP is following:

$$COP = \frac{\dot{Q}_O - \dot{Q}_L}{\dot{Q}_G} = \frac{\dot{Q}_O}{\dot{Q}_G}\left(1 - \frac{\dot{Q}_L}{\dot{Q}_O}\right) = \frac{T_3(I_1T_2 - I_2T_1)}{T_1(T_2 - I_2T_3)}(1 - \xi(T_O - T_E) \times \left(\frac{T_1(T_2 - I_2T_3)}{U_G(T_G - T_1)T_3(I_1T_2 - I_2T_1)} + \frac{T_2(I_1T_3 - T_1)}{U_E(T_E - T_2)T_3(I_1T_2 - I_2T_1)} + \frac{1}{U_O(T_3 - T_O)}\right)\right) \tag{15}$$

where $\xi = K_L/A$ is a heat leakage coefficient by the system and is expressed in $(WK^{-1}m^{-2})$.

3.2. The specific heating load (q)

The Specific heating load is obtained from Eqs. (4)–(9):

$$q = \frac{\dot{Q}_O - \dot{Q}_L}{A} = \left(\frac{T_1(T_2 - I_2T_3)}{U_G(T_G - T_1)T_3(I_1T_2 - I_2T_1)} + \frac{T_2(I_1T_3 - T_1)}{U_E(T_E - T_2)T_3(I_1T_2 - I_2T_1)} + \frac{1}{U_O(T_3 - T_O)}\right)^{-1} - \xi(T_O - T_E) \tag{16}$$

3.3. Specific entropy generation rate (S)

The specific entropy generation rate is the entropy produced per unit of heat-transfer area generated by the system. The specific entropy generation rate is as follows of Eqs. (4)–(8) and (12):

$$S = \frac{\dot{\sigma}}{A} = \frac{\frac{\dot{Q}_O - \dot{Q}_L}{T_O} - \frac{\dot{Q}_G}{T_G} - \frac{\dot{Q}_E - \dot{Q}_L}{T_E}}{A} = \left(\frac{1}{T_E} - \frac{1}{T_O}\right)\left(\xi(T_O - T_E) + \left(\zeta_r \frac{T_1(T_2 - I_2T_3)}{T_3(I_1T_2 - I_2T_1)} - 1\right)\left(\frac{T_1(T_2 - I_2T_3)}{U_G(T_G - T_1)T_3(I_1T_2 - I_2T_1)} + \frac{T_2(I_1T_3 - T_1)}{U_E(T_E - T_2)T_3(I_1T_2 - I_2T_1)} + \frac{1}{U_O(T_3 - T_O)}\right)^{-1}\right) \tag{17}$$

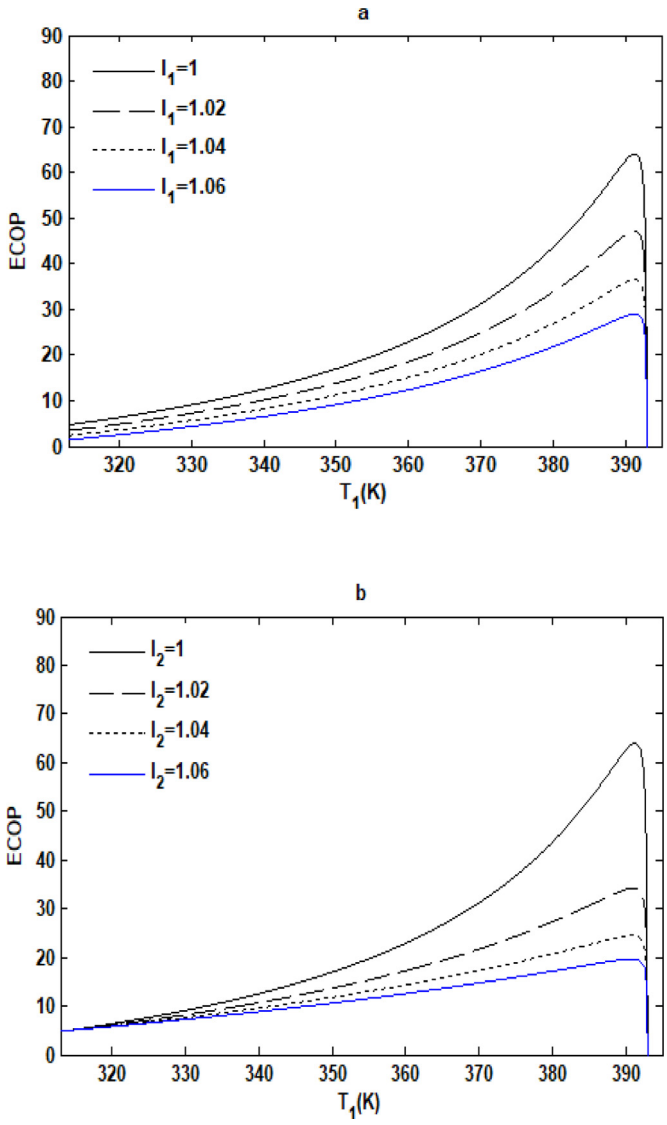

Fig. 3. Variation of *ECOP* objective function with respect to the temperature T_1 of the working fluid in the generator when $I_2 = 1$ for various I_1 (a); when $I_1 = 1$ for various I_2 (b).

Where $\zeta_r = (1 - \frac{T_E}{T_G})/(1 - \frac{T_E}{T_O})$ is the coefficient of performance of a heat pump ideal cycle with three-heat-reservoir. $\dot{\sigma}$ being the entropy generated by the system described in Fig. 2 and is expressed in (WK^{-1}) and S in $(WK^{-1}m^{-2})$.

3.4. Exergy-based ecological criterion (E)

Exergy-based ecological function (Angulo-Brown, 1991; Sun et al., 2005; Chen et al., 2007b, 2019; Qin et al., 2017; Frikha and Abid, 2016) is given by:

$$E = \left(\dot{Q}_O - \dot{Q}_L\right)\left(1 - \frac{T_{env}}{T_0}\right) - T_{env}\dot{\sigma} = A\left(\begin{array}{c}\xi(T_0 - T_E)\left(\frac{2T_{env}}{T_0} - \frac{T_{env}}{T_0} - 1\right) + \left(1 - \frac{T_{env}}{T_0} - T_{env}\left(\frac{1}{T_E} - \frac{1}{T_O}\right)\left(\zeta_r \frac{T_1(T_2 - I_2T_3)}{T_3(I_1T_2 - I_2T_1)} - 1\right)\right) \\ \left(\frac{T_1(T_2 - I_2T_3)}{U_G(T_G - T_1)T_3(I_1T_2 - I_2T_1)} + \frac{T_2(I_1T_3 - T_1)}{U_E(T_E - T_2)T_3(I_1T_2 - I_2T_1)} + \frac{1}{U_O(T_3 - T_O)}\right)^{-1}\end{array}\right) \quad (18)$$

Where the term $(\dot{Q}_O - \dot{Q}_L)(1 - \frac{T_{env}}{T_0})$ represents the output exergy of the THR AHP cycle and $T_{env}\dot{\sigma}$ is the exergy destroyed or the loss rate of availability.

3.5. Ecological coefficient of performance (ECOP)

The ecological coefficient of performance given by Refs. Kodal et al. (2003), Qureshi and Syed (2015), Chen et al. (2007), Qin et al. (2017), Frikha and Abid (2016) and Ngouateu Wouagfack and Tchinda (2011a, 2011b, 2014) of an irreversible AHP THS is the ratio between the specific heating load and the exergy loss (product of the entropy generation rate and the temperature of the environment). The ECOP

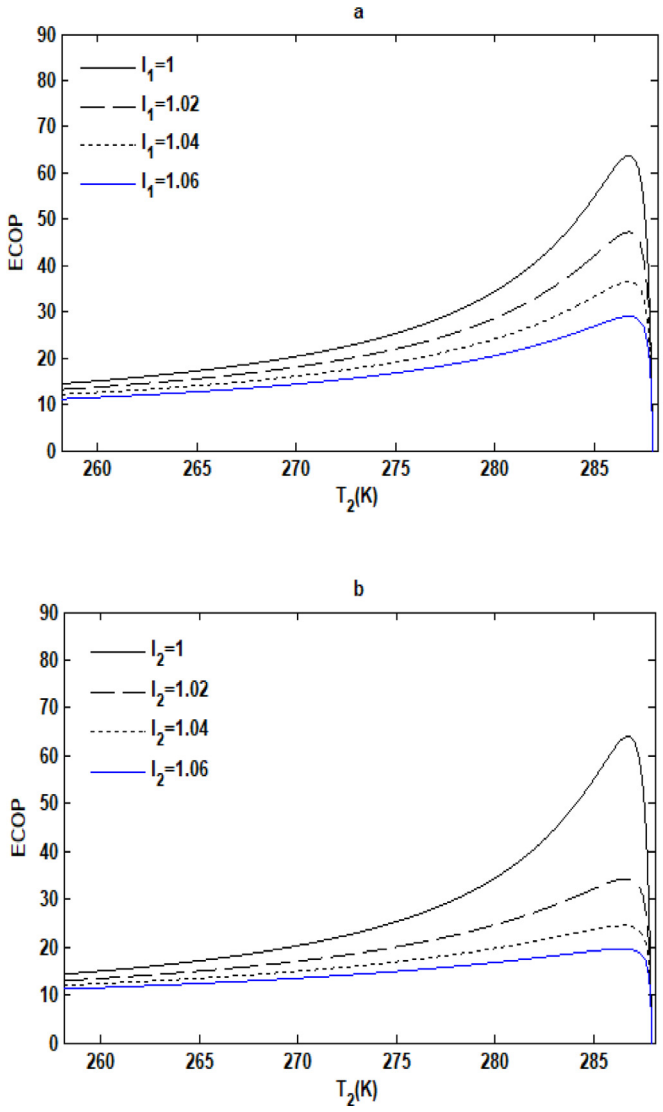

Fig. 4. Variation of *ECOP* objective function with respect to the temperature T_2 of the working fluid in the evaporator when $I_2 = 1$ for various I_1 (a) when $I_1 = 1$ for various I_2 (b).

characterizes the impact of energy lost on the environment.

$$ECOP = \frac{\dot{Q}_O - \dot{Q}_L}{T_{env}\dot{\sigma}} = \frac{1}{T_{env}\left(\frac{1}{T_E} - \frac{1}{T_O}\right)}\left(\frac{\zeta_r \frac{T_1(T_2 - I_2T_3)}{T_3(I_1T_2 - I_2T_1)}}{1 - \xi(T_O - T_E)\left(\frac{T_1(T_2 - I_2T_3)}{U_G(T_G - T_1)T_3(I_1T_2 - I_2T_1)} + \frac{T_2(I_1T_3 - T_1)}{U_E(T_E - T_2)T_3(I_1T_2 - I_2T_1)} + \frac{1}{U_O(T_3 - T_O)}\right)} - 1\right)^{-1} \tag{19}$$

When $I_1 = I_2 = I$ we find the results of Ngouateu Wouagfack and Tchinda (2012a).

3.6. Optimization of an absorption heat pump with multi-irreversibilities

Maximum ecological coefficient of performance (*ECOP*) and maximum Exergy-based ecological criterion (*E*)

$$\text{Let, } a = \frac{I_1T_3}{T_1};\ b = \frac{I_2T_3}{T_2} \text{ and } c = T_3 \tag{20}$$

we can rewrite in a simpler way *ECOP* objective function of performance.

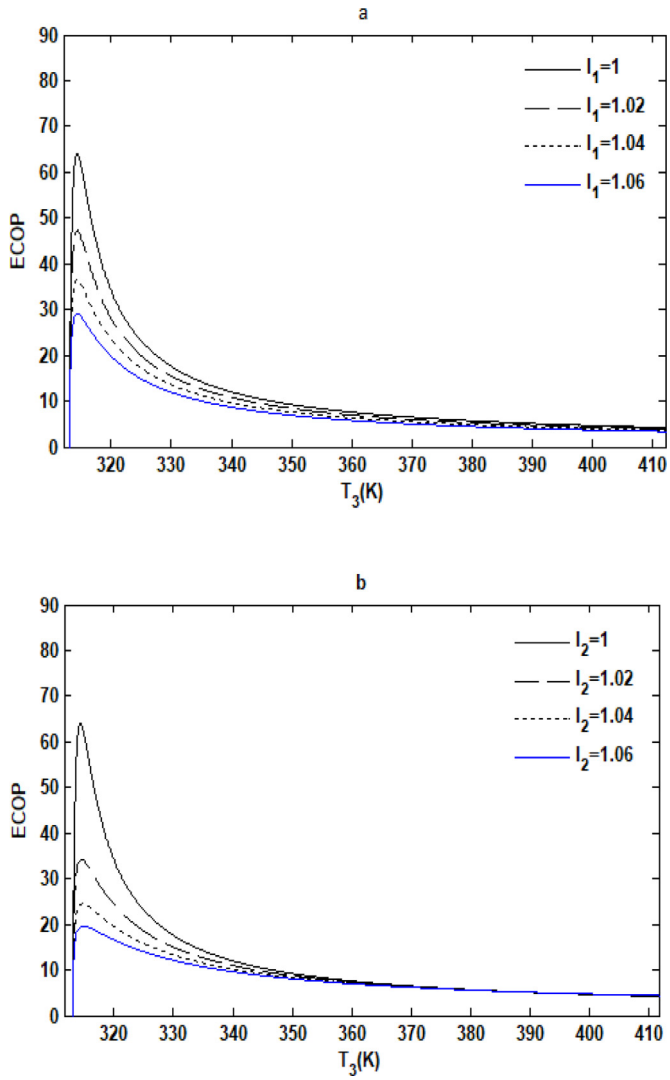

Fig. 5. Variation of *ECOP* objective function with respect to the temperature T_3 of the working fluid in the absorber and the condenser assembly when $I_2 = 1$ for various I_1 (a); when $I_1 = 1$ for various I_2 (b).

$$ECOP = \frac{1}{T_{env}\left(\frac{1}{T_E} - \frac{1}{T_O}\right)}\left(\frac{\zeta_r\left(\frac{1-b}{a-b}\right)}{1 - \frac{\xi(T_O - T_E)}{b-a}\left(\frac{a(b-1)}{U_G(aT_G - I_1 c)} + \frac{b(1-a)}{U_E(bT_E - I_2 c)} + \frac{b-a}{U_O(c - T_O)}\right)} - 1\right)^{-1} \tag{21}$$

The optimization of the system must reach the maximum values of *ECOP* objective function, which implies that one must determine the optimal temperatures up stream T_{1op}, T_{2op} and T_{3op}. $ECOP_{\max}$ corresponds to the maximum of *ECOP* objective function obtained by solving the first order partial differentials equations to the variables *a*, *b* and *c*.

$$\frac{\partial ECOP}{\partial a} = 0;\ \frac{\partial ECOP}{\partial b} = 0 \text{ and } \frac{\partial ECOP}{\partial c} = 0 \tag{22}$$

However, the optimization of the system using exergy-based ecological objective function makes it possible to obtain the corresponding optimal performance parameters. At the maximum criterion *E* that is $E_{\max,E}$ we have $T_1{}^*$, $T_2{}^*$, $T_3{}^*$, COP^*, S^* and $q^*.E_{\max,E}$ is obtained by solving the partial differential equation.

$$\frac{\partial E}{\partial a} = 0;\ \frac{\partial E}{\partial b} = 0 \text{ and } \frac{\partial E}{\partial c} = 0 \tag{23}$$

By solving Eqs. (22) and (23) and substituting their values of the variables *a*, *b* and *c* into Eq. (20), we obtain the following double equality:

$$\sqrt{I_1 U_G}\left(\frac{T_G}{T_1} - 1\right) = \sqrt{I_2 U_E}\left(\frac{T_E}{T_2} - 1\right) = \sqrt{U_O}\left(1 - \frac{T_O}{T_3}\right) \tag{24}$$

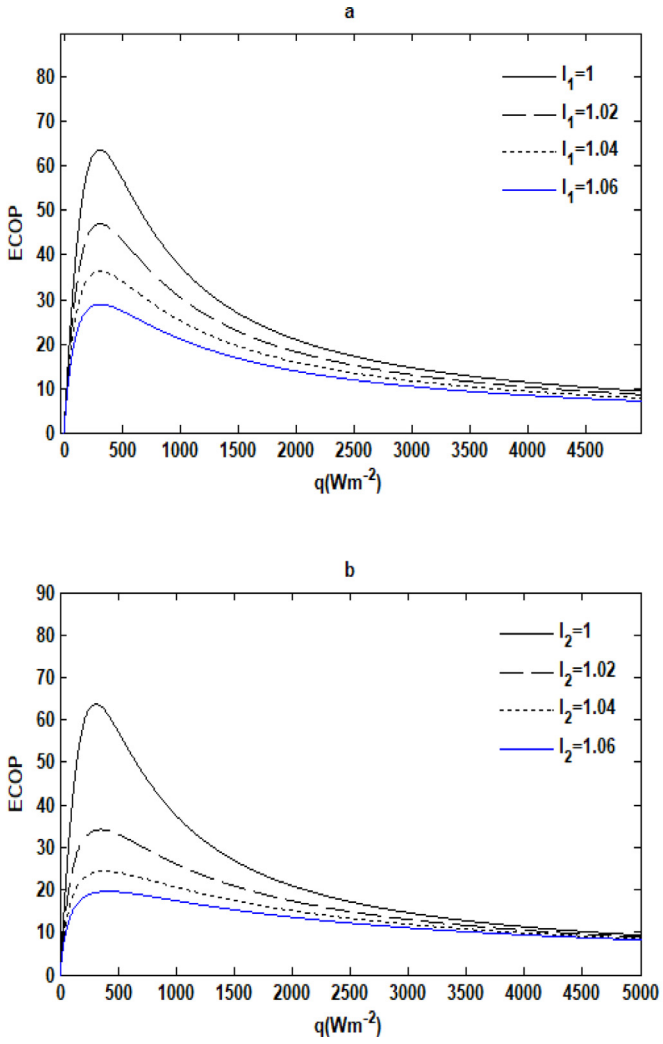

Fig. 6. Effects of internal irreversibility I_1 (a) of the generator-absorber assembly and of the internal irreversibility I_2 (b) of the evaporator-condenser assembly on the *ECOP* objective function with respect to the q objective function.

Using the relationships (22) and (24), optimal temperatures at maximum *ECOP* are obtained;

$$T_{1op} = \frac{I_1 T_G}{b_1\left(1 - \frac{T_O}{D}\right) + I_1}$$

$$T_{2op} = \frac{I_2 T_E}{b_2\left(1 - \frac{T_O}{D}\right) + I_2}$$

$$T_{3op} = D \tag{25}$$

where $D = \dfrac{(I_2 U_O T_E - \xi (T_O - T_E)(b_2 + I_2) b_2) T_O + \sqrt{(I_2 U_O (I_2 T_O - T_E) + \xi (T_O - T_E)(b_2 + I_2)^2) I_2 (T_O - T_E) T_E T_O \xi}}{I_2 U_O T_E - \xi (T_O - T_E)(b_2 + I_2)^2}$ and

$$b_1 = \sqrt{\frac{I_1 U_O}{U_G}},\ b_2 = \sqrt{\frac{I_2 U_O}{U_E}} \tag{26}$$

Substituting Eqs. (25) into Eqs. (15)–(19) yields the maximum ECOP:

$$ECOP_{\max} = \frac{1}{T_{env}\left(\frac{1}{T_E} - \frac{1}{T_O}\right)} \left(\frac{\zeta_r T_G (T_E - b_2 (D - T_O) - I_2 D) U_O (D - T_O)}{U_O (D - T_O)((D - T_O)(T_E b_1 - T_G b_2) + D(I_1 T_E - I_2 T_G)) - \xi (T_O - T_E)(\beta U_0 + (D - T_O)(T_E b_1 - T_G b_2) + D(I_1 T_E - I_2 T_G))} - 1 \right)^{-1} \tag{27}$$

and the optimal coefficient of performance (COP_{op}), the optimal specific heating load (q_{op}) and the optimal specific entropy generation rate (S_{op}) at the maximum ECOP conditions, respectively, as:

$$COP_{op} = \frac{U_O (D - T_O)((D - T_O)(T_E b_1 - T_G b_2) + D(I_1 T_E - I_2 T_G)) - \xi (T_O - T_E)(\beta U_0 + (D - T_O)(T_E b_1 - T_G b_2) + D(I_1 T_E - I_2 T_G))}{T_G (T_E - b_2 (D - T_O) - I_2 D) U_O (D - T_O)} \tag{28}$$

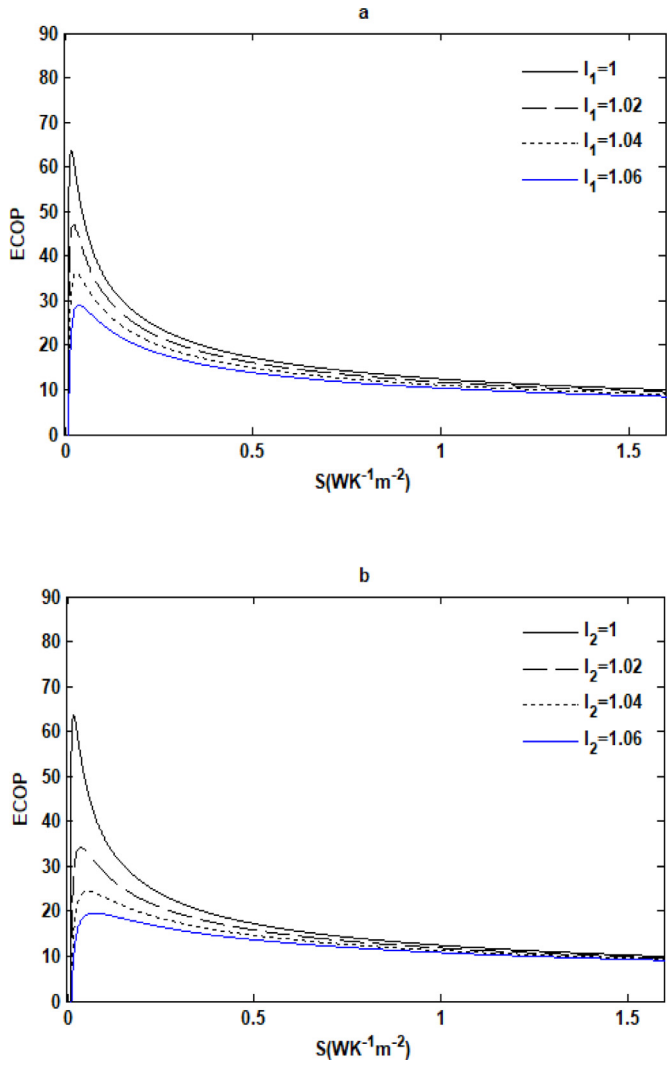

Fig. 7. Effects of internal irreversibility I_1 (a) of the generator-absorber assembly and of the internal irreversibility I_2 (b) of the evaporator-condenser assembly on the *ECOP* objective function with respect to the *S* objective function.

$$q_{op} = \frac{U_O(D-T_O)((D-T_O)(T_E b_1 - T_G b_2) + D(I_1 T_E - I_2 T_G))}{\beta U_0 + (D-T_O)(T_E b_1 - T_G b_2) + D(I_1 T_E - I_2 T_G)} - \xi\,(T_O - T_E) \tag{29}$$

$$S_{op} = \left(\frac{1}{T_E} - \frac{1}{T_O}\right)\left(\xi\,(T_O - T_E) + \frac{(\zeta_r T_G(T_E - b_2(D-T_O) - I_2 D) - (D-T_O)(T_E b_1 - T_G b_2) - D(I_1 T_E - I_2 T_G))U_O(D-T_O)}{\beta U_0 + (D-T_O)(T_E b_1 - T_G b_2) + D(I_1 T_E - I_2 T_G)}\right) \tag{30}$$

with

$$\beta = \frac{U_E b_2(b_1(D-T_O) + I_1 D)(T_E - b_2(D-T_O) - I_2 D) + U_G b_1(b_2(D-T_O) + I_2 D)(b_1(D-T_O) + I_1 D - T_G)}{U_G U_E b_1 b_2} \tag{31}$$

From Eqs. (2), (4)–(6), (9) and (25) we find that, when THR AHP is operated in the state of maximum ECOP, the relations between the heat-transfer areas of the heat exchangers and the total heat-transfer area are determined by:

$$\frac{(A_G)_{op}}{A} = \frac{U_E U_O b_2(b_1(D-T_O) + I_1 D)(b_2(D-T_O) + I_2 D - T_E)}{U_E U_O b_2(b_1(D-T_O) + I_1 D)(b_2(D-T_O) + I_2 D - T_E) + U_G U_E b_1 b_2 U_G b_1(T_G(b_2(D-T_O) + I_2 D) - T_E(b_1(D-T_O) + I_1 D)) + U_G U_O b_1(b_2(D-T_O) + I_2 D)(T_G - b_1(D-T_O) - I_1 D)} \tag{32}$$

$$\frac{(A_E)_{op}}{A} = \frac{U_G U_O b_1(b_2(D-T_O) + I_2 D)(b_1(D-T_O) + I_1 D - T_G)}{U_G U_O b_1(b_2(D-T_O) + I_2 D)(b_1(D-T_O) + I_1 D - T_G) + U_G U_E b_1 b_2(T_E(b_1(D-T_O) + I_1 D) - T_G(b_2(D-T_O) + I_2 D)) - U_E U_O b_2(b_1(D-T_O) + I_1 D)(b_2(D-T_O) + I_2 D - T_E)} \tag{33}$$

$$\frac{(A_O)_{op}}{A} = \frac{U_G U_E b_1 b_2(T_G(b_2(D-T_O) + I_2 D) - T_E(b_1(D-T_O) + I_1 D))}{U_G U_E b_1 b_2(T_G(b_2(D-T_O) + I_2 D) - T_E(b_1(D-T_O) + I_1 D)) + U_E U_O b_2(b_1(D-T_O) + I_1 D)(b_2(D-T_O) + I_2 D - T_E) - U_G U_O b_1(b_2(D-T_O) + I_2 D)(b_1(D-T_O) + I_1 D - T_G)} \tag{34}$$

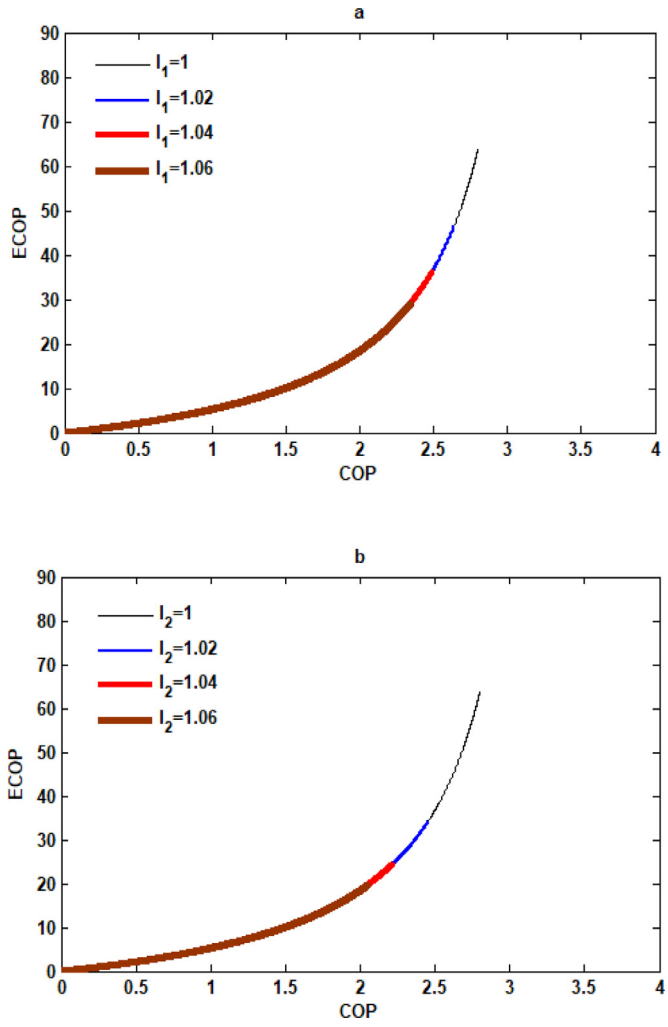

Fig. 8. Effects of internal irreversibility I_1 (a) of the generator-absorber assembly and of the internal irreversibility I_2 (b) of the evaporator-condenser assembly on the *ECOP* objective function with respect to the *COP* objective function.

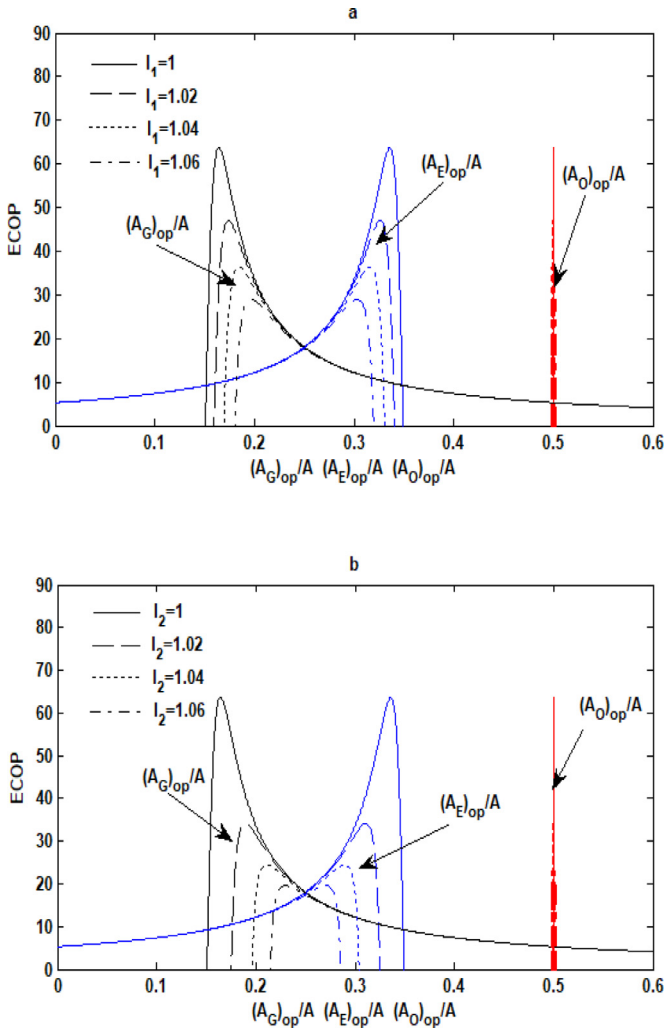

Fig. 9. Effects of internal irreversibility I_1 (a) of the generator-absorber assembly and of the internal irreversibility I_2 (b) of the evaporator-condenser assembly on the *ECOP* objective function with respect to the heat-transfer areas of the heat exchangers $(A_O)_{op}/A$, $(A_G)_{op}/A$ and $(A_E)_{op}/A$ objective functions.

4. Results and discussion

We will consider numerical data from Ngouateu Wouagfack and Tchinda (2012a) and Ahmadi et al. (2015) and model a THR AHP.

$T_G = 393\text{K}$, $T_E = 288\text{K}$, $T_O = 313\text{K}$, $T_{env} = 290\text{K}$, $U_G = U_E = U_O = 500\text{WK}^{-1}\text{m}^{-2}$, $\xi = 1.082\text{WK}^{-1}$.

4.1. Effects of temperatures of the working fluid in the different components

Figs. 3–5 show the variations of the *ECOP* objective function with respect to the temperatures T_1, T_2 and T_3 which respectively represent the temperatures of working fluid in the generator, the evaporator and the absorber-condenser assembly. In Figs. 3(a), 4(a) and 5(a) I_2 is set ($I_2 = 1$) for different values of I_1 and in Figs. 3(a), 4(a) and 5(a) I_1 is set ($I_1 = 1$) for different values of I_2. The *ECOP* gradually increases with increase in the temperatures T_1 and T_2 before reaching its maximum in Figs. 3 and 4. However *ECOP* decreases abruptly after reaching its maximum value when T_3 increases in Fig. 5. As a result, when $T_1 < T_{1op}$, $T_2 < T_{2op}$ and $T_3 > T_{3op}$ the system is less ecological and losses are more accentuated and more when $T_1 > T_{1op}$, $T_2 > T_{2op}$ and $T_3 < T_{3op}$, the system is unstable. However, the $ECOP_{\max}$ is more affected in the system for the same values of the optimum temperatures in the condenser-evaporator assembly by the irreversibility factor I_2 than in the absorber-generator by the irreversibility factor I_1.

4.2. Influences of design parameters

4.2.1. Influences of two internal irreversibilities I_1 and I_2

The effects of internal irreversibilities I_1 and I_2 on the *ECOP* objective function with respect to the specific heating load, the specific entropy generation rate, the coefficient of performance (*COP*) and heat-transfer areas of the heat exchangers are shown respectively in Figs. 6–9. For progressively large values of I_1 and I_2, we make the following observations. In Figs. 6 and 7, we observe that the maximum of the objective function *ECOP* is reached for a certain value of the specific heating load (q) Fig. 6 and a minimum of the specific entropy generation rate (S) Fig 7. This *ECOP* objective function decreases gradually when the internal irreversibility parameters I_1 and I_2 increase. Moreover, from the definition of *COP* and *ECOP* in Eqs. (15) and (18), respectively, we obtain a relation between these two objective functions $ECOP = \frac{COP}{T_{env}((\frac{1}{T_O}-\frac{1}{T_E})COP-(\frac{1}{T_G}-\frac{1}{T_E}))}$. This equation makes it possible to obtain Fig. 8 and shows that the *ECOP* increases as *COP* also increases. The analysis of the performance of the AHP shows that the objective

Table 1
Real AHP maximum values from the ecological coefficient of performance ($ECOP_{max}$) versus the endoreversible system ($I_1 = I_2 = 1$ and $\xi = 1.082$) for different values of I_1 and I_2.

Percentage (%) of $ECOP_{max}$	$I_1 = 1.00$	$I_1 = 1.02$	$I_1 = 1.04$	$I_1 = 1.06$	$I_1 = 1.08$
$I_2 = 1.00$	100.00	73.79	57.01	45.35	36.78
$I_2 = 1.02$	53.56	44.59	37.58	31.96	27.35
$I_2 = 1.04$	38.28	33.34	29.18	25.63	22.56
$I_2 = 1.06$	30.67	27.38	24.49	21.94	19.66
$I_2 = 1.08$	26.12	23.68	21.49	19.52	17.72

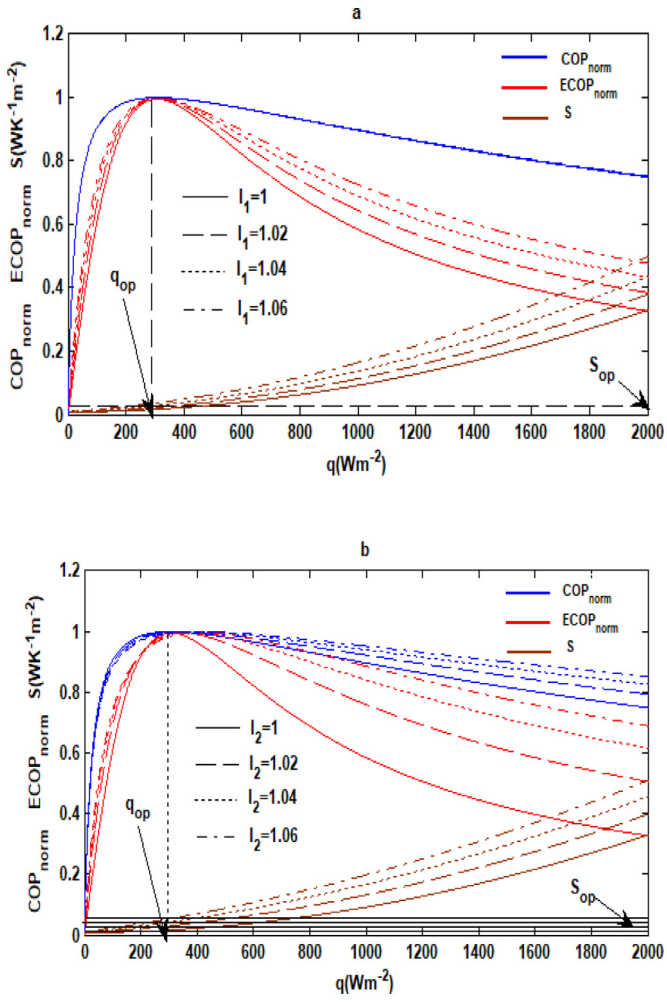

Fig. 10. Variation of the non-dimensional *ECOP* objective function, the non-dimensional *COP* objective function and entropy generation rate according to the specific heating load: (a) $I_2 = 1$ when I_1 varies and (b) $I_1 = 1$ when I_2 varies.

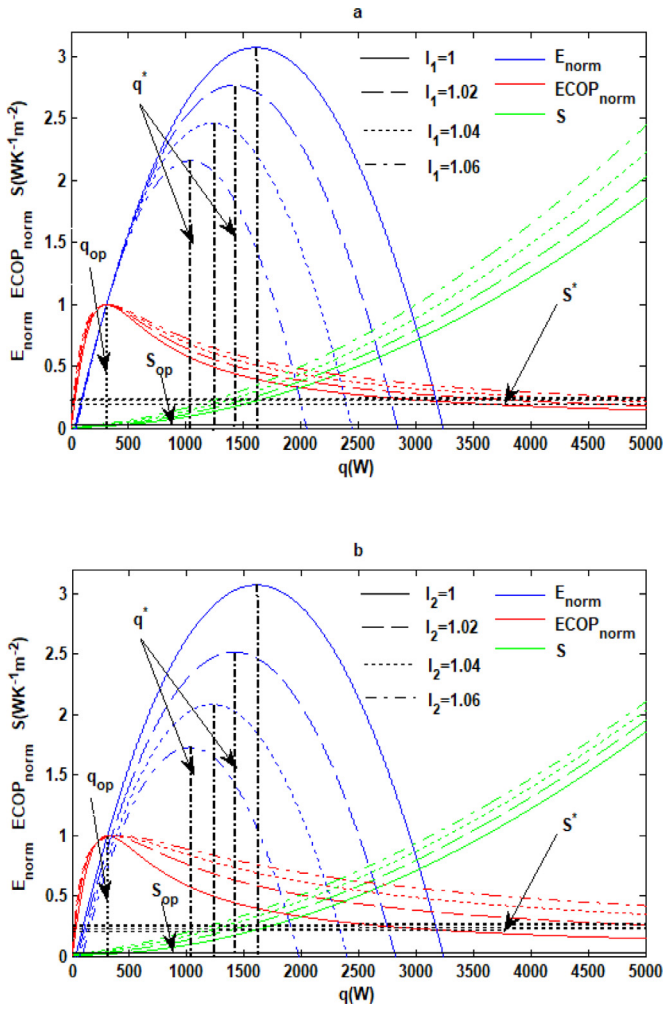

Fig. 11. Variation of the non-dimensional *ECOP* objective function, the non-dimensional *E* objective function and entropy generation rate according to the specific heating load: (a) $I_2 = 1$ when I_1 varies and (b) $I_1 = 1$ when I_2 varies.

function *COP* is always such that $COP < 3$ for any maximum value of the objective function *ECOP* which corresponds to an optimal system. Among others, Fig. 9 shows that the maximum of the objective function *ECOP* varies symmetrically with respect to the optimum heat transfer areas $(A_G)_{op}$ of the generator and $(A_E)_{op}$ of the evaporator. This means that the $ECOP_{\max}$ values decrease when the $(A_G)_{op}$ values increase while the $(A_E)_{op}$ values decrease. However, the $ECOP_{\max}$ values decrease always leaving the optimal values of $(A_O)_{op}$ constant of the absorber-condenser assembly. Fig. 10 shows variations of the normalized *ECOP* ($ECOP_{nor} = ECOP/ECOP_{max}$), normalized *COP* ($COP_{nor} = COP/COP_{op}$), and *S* with respect to the *q* for different values of I_1 and I_2. It is observed that at the point of optimal functioning of the system, the optimal values of COP_{op}, q_{op}, S_{op}, T_{1op}, T_{2op}, T_{3op}, $(A_G)_{op}$, $(A_E)_{op}$ and $(A_O)_{op}$, the maximum values of *ECOP* and *COP* coincide. Yet these last two objective functions have a different physical meaning. Ngouateu Wouagfack and Tchinda (2011a, 2012a, 2012b, 2014) made this observation between *ECOP* and *COP* for AR and AHP having three and four heat reservoirs with internal irreversibility. Same for Medjo Nouadje et al. (2014) for THR AR and two internal irreversibilities. Also, the maximum of the *ECOP* and *COP* objective functions correspond to a certain value of *q* for minimum value of *S* according to the variations of I_1 and I_2. However, Fig. 11 shows variations of the normalized *ECOP* ($ECOP_{norm} = ECOP/ECOP_{\max}$), normalized *E* ($E_{norm} = E/E_{\max,E}$), and *S* with respect to the *q* for different values of I_1 and I_2. It is observed that when the THR cycle operates under the maximum *ECOP* values conditions ($ECOP_{\max}$)on the one

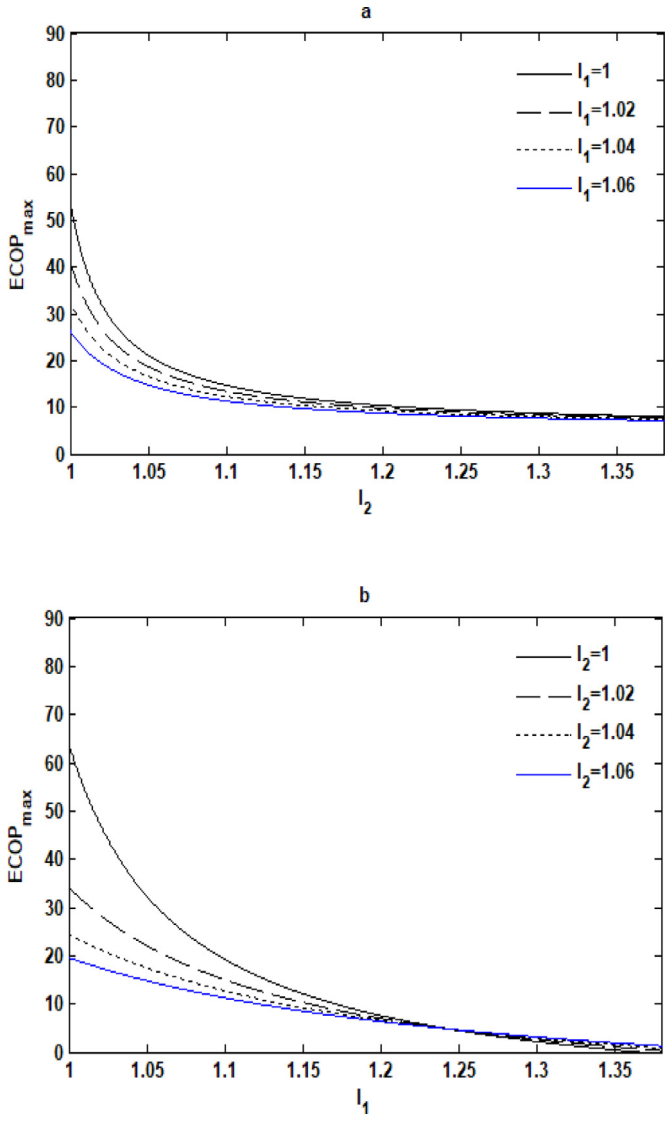

Fig. 12. Effects of internal irreversibility I_2 (a) of the generator-absorber assembly and of the internal irreversibility I_1 (b) of the evaporator-condenser assembly on the $ECOP_{max}$ maximal objective function respectively for certain values of I_1 (a) and I_2 (b).

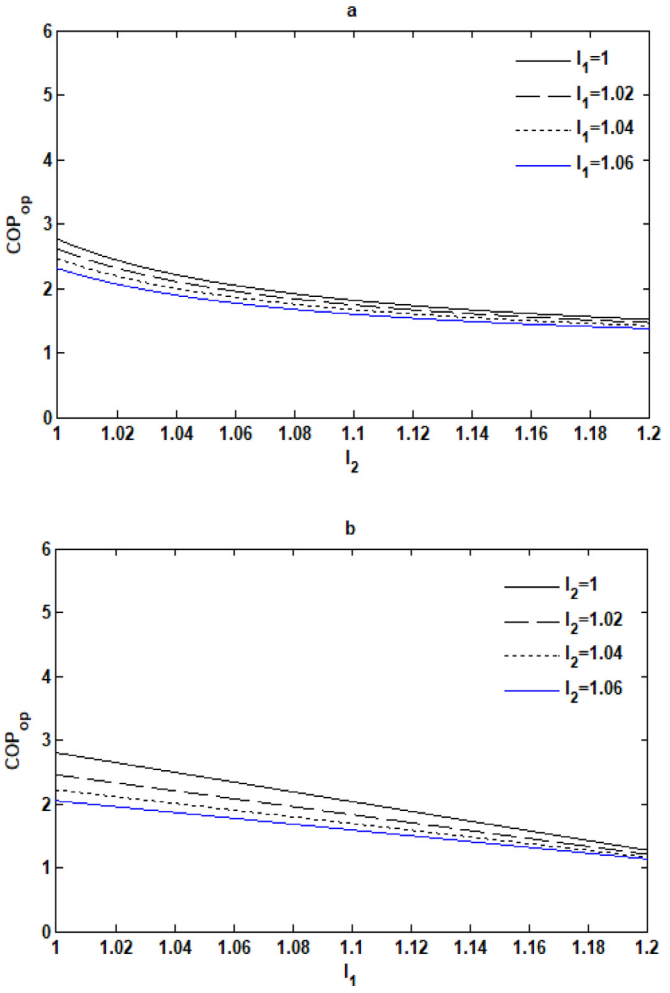

Fig. 13. Effects of internal irreversibility I_2 (a) of the generator-absorber assembly and of the internal irreversibility I_1 (b) of the evaporator-condenser assembly on the COP_{op} optimal objective function respectively for certain values of I_1 (a) and I_2 (b).

hand and maximum E values on the other hand (E_{max}), $q_{op} < q^*$ and $S_{op} < S^*$. q_{op} and q^* being the optimal specific heating load at $ECOP_{max}$ and $E_{max,E}$ respectively and S_{op} and S^* being the optimal specific entropy generation rate at $ECOP_{max}$ and $E_{max,E}$, respectively. The results show that the system operating under maximum $ECOP$ conditions has a significant advantage over the maximum E conditions in terms of specific entropy generation rate. Otherwise, under maximum E conditions has a significant advantage over the maximum $ECOP$conditions in terms of specific heating load. The results obtained by Ngouateu Wouagfack and Tchinda (2011b) show that the THR cycle operating at maximum $ECOP$ values conditions has a significant advantage over the maximum E values and maximum specific cooling load values conditions concerning the specific entropy generation rate and coefficient of performance. Figs. 12–16 show variations of the $ECOP_{max}$ maximal objective function and the COP_{op}, q_{op}, S_{op}, $(A_G)_{op}$, $(A_E)_{op}$ and $(A_O)_{op}$ optimal objective functions corresponding to the maximum of $ECOP$. These variations with respect to I_2 for different values of I_1 on the one hand Figs. 12(a)–16(a) and I_1 for different values of I_2 on the other hand Figs. 12(b)–16(b). $ECOP_{max}$ decreases rapidly, COP_{op} and $(A_E)_{op}$ decreases gradually while S_{op} and $(A_G)_{op}$ increases, q_{op} and $(A_O)_{op}$ remains constant when the parameters I_1 and I_2 increase. As a result, $ECOP_{max}$ and COP_{op} are better for values of I_1 and I_2 close to the unit corresponding to the endoreversible system with a specific entropy generation rate S_{op} minimum for a certain value of the specific heating load q_{op} and heat-transfer areas of heat exchangers $(A_G)_{op}$, $(A_E)_{op}$ and $(A_O)_{op}$.

The preceding figures can be summarized in Table 1, which shows how the maximum ecological coefficient of performance varies according to the internal irreversibilities I_1 and I_2, respectively, of the generator-absorber assembly and the evaporator-condenser assembly. We can also deduce that the optimal functioning of a real AHP is less efficient than an endoreversible AHP. Which for an obtained $ECOP_{max}$ ($I_1 = I_2 = 1$ and $\xi = 1.082 WK^{-1}m^{-2}$) we have certain value of the specific heating load $q_{op} = 307 Wm^{-2}$, a minimum entropy generation rate $S_{op} = 0.0165 WK^{-1}m^{-2}$ and a maximum coefficient of performance $COP_{max} = 2.8$ (According to Eqs. (26)–(28).

As a whole, Figs. 3(a)–16(a) and Figs. 3(b)–16(b) show that the factor of internal irreversibility I_2 of the condenser-evaporator assembly characterized by the loss rate, the losses of heat resistance, the friction, the singularity points and the turbulence of the working fluid has a more unfavorable impact on the performance of the system.

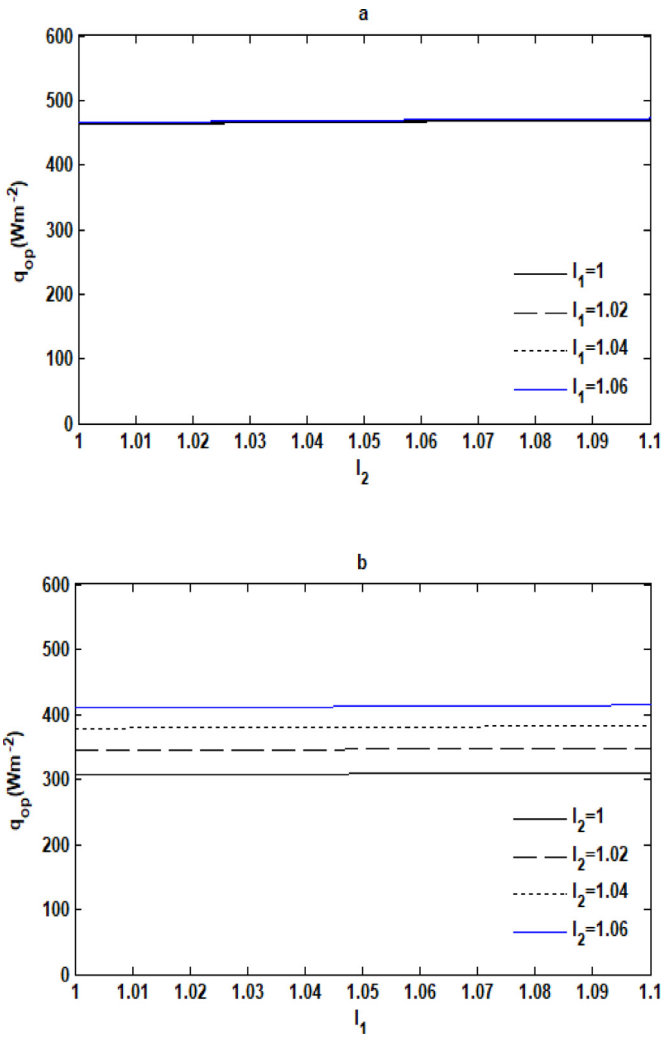

Fig. 14. Effects of internal irreversibility I_2 (a) of the generator-absorber assembly and of the internal irreversibility I_1 (b) of the evaporator-condenser assembly on the q_{op} optimal objective function, respectively, for certain values of I_1 (a) and I_2 (b).

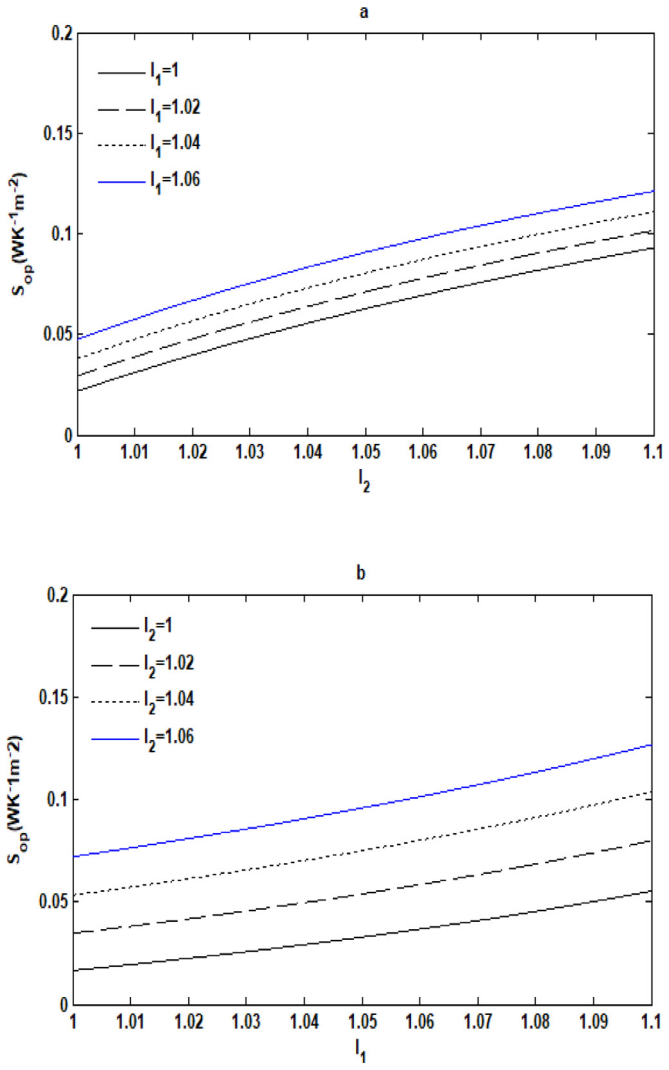

Fig. 15. Effects of internal irreversibility I_2 (a) of the generator-absorber assembly and of the internal irreversibility I_1 (b) of the evaporator-condenser assembly on the S_{op} optimal objective function respectively for certain values of I_1 (a) and I_2 (b).

4.2.2. Influences of heat leakage coefficient (ξ)

Figs. 17–19 show the variations of the ECOP objective function respectively with respect to the specific entropy generation rate (S), the specific heating load (q) and the heat-transfer areas of the heat exchangers (A_G, A_E, A_O). These variations are presented under the effect of external irreversibility or heat leakage coefficient (ξ). External irreversibility affects the performance parameters of the AHP cycle the same way that the two internal irreversibilities factors affect these parameters, that is quantitatively and qualitatively. However, the effects of heat loss and internal irreversibility (I_2) of the condenser-evaporator assembly are greater.

5. Conclusion

In this paper, a thermo-ecological optimization study is carried out to determine the optimal operating and design parameters of a multi-irreversible absorption heat pump with three-heat-reservoir. This criterion is defined by the application of the first and second laws of thermodynamics. It is based on quantities such as the load lost by the system, the specific heating load, the specific entropy generation rate, the external irreversibility and the two internal irreversibilities. As a result, the maximum of *ECOP* corresponds to the optimal values of the load lost by the system, the specific heating load, the specific entropy generation rate, the heat-transfer areas of the heat exchangers and the minimum of the internal and external irreversibilities. However, the system is less ecologically efficient in the condenser-evaporator assembly than in the generator-absorber assembly because of a greater influence of internal irreversibility I_2. In addition, the *ECOP* criterion over the *E* criterion has a significant advantage in terms of specific entropy generation rate. This is why, we can say that the ideal ecological coefficient of performance of the system corresponds to a maximum of the coefficient of performance (*COP*), a certain value of the specific heating load, a minimum of the specific entropy generation rate and the two internal irreversibilities equal to unity: in this case we are dealing with an endoreversible system. This value of *ECOP* objective function is almost impossible to achieve experimentally in the operating conditions because the system is a real system. We can nevertheless find a compromise between the specific heating load, the specific entropy generation rate, the two internal irreversibilities and the external irreversibility so that the value obtained from the *ECOP* is the most suitable.

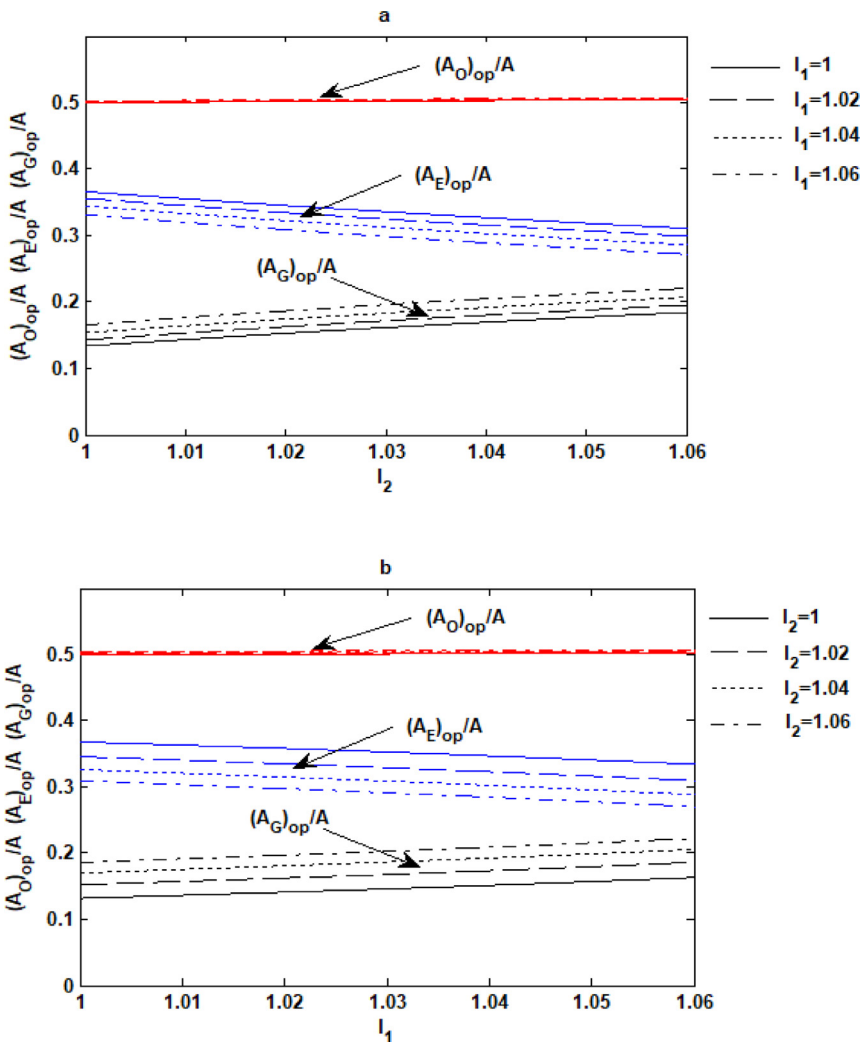

Fig. 16. Effects of internal irreversibility I_2 (a) of the generator-absorber assembly and of the internal irreversibility I_1 (b) of the evaporator-condenser assembly on the $(A_O)_{op}/A$, $(A_G)_{op}/A$ and $(A_E)_{op}/A$ optimal objective functions respectively for certain values of I_1 (a) and I_2 (b).

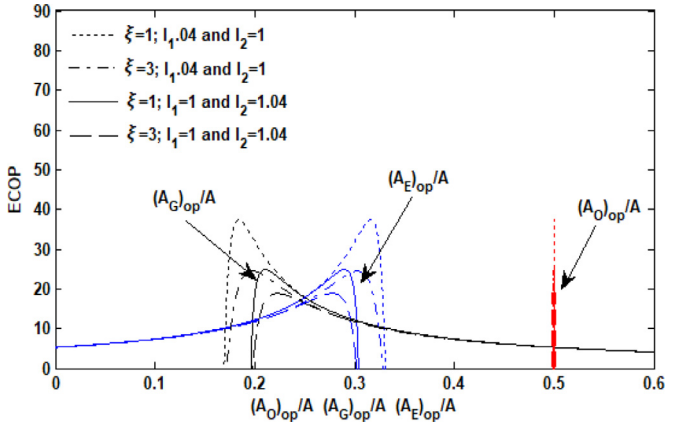

Fig. 17. Effects of heat leakage coefficient ξ on the *ECOP* objective function with respect to the $(A_O)_{op}/A$, $(A_G)_{op}/A$ and $(A_E)_{op}/A$ objective functions.

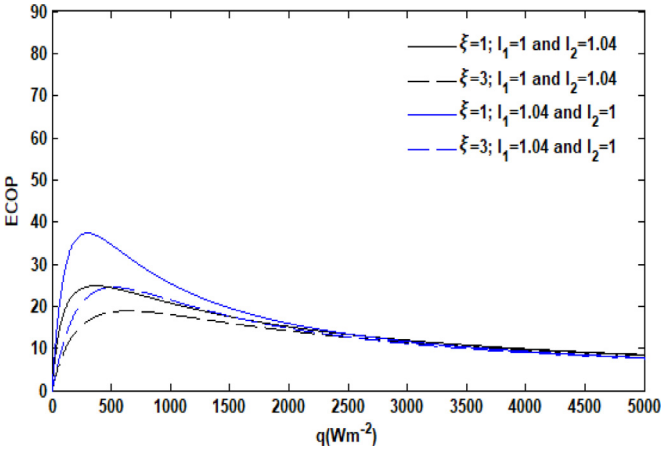

Fig. 18. Effects of heat leakage coefficient ξ on the *ECOP* objective function with respect to the q objective function.

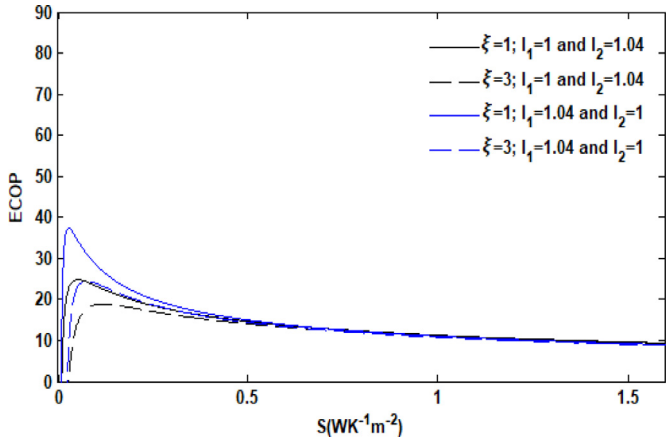

Fig. 19. Effects of heat leakage coefficient ξ on the *ECOP* objective function with respect to the *S* objective function.

Declaration of Competing Interest

The authors declare no conflicts of interest.

Acknowledgments

The authors are grateful to the Energy, Electrical Systems and Electronics Laboratory of the University of Yaounde I and the Industrial and Energy Systems Engineering Laboratory of the University Institute of Technology Fotso Victor. The authors want to thank the reviewers for their constructive comments that help to improve the quality of the paper. In particular, the author Rodrigue Léo Fossi Nemogne wishes to thank the unconditional and invaluable support of his mother, Rachel Tsangui Kembou epse Fossi.

Funding

This research did not receive any specific grant from funding agencies in the public, commercial, or not-for-profit sectors.

References

Ahmadi, M.H., Ahmadi, M.A., Mehrpooya, M., Sameti, M., 2015. Thermo-ecological analysis and optimization performance of an irreversible three-heat-source absorption heat pump. Energy Convers. Manag. 105, 1125–1137.
Ahmadi, M., Ahmadi, M.A., Pourfayaz, F., Bidi, M., 2016. Thermodynamic analysis and optimization for an irreversible heat pump working on reversed Brayton cycle. Energy Convers. Manag. 110, 260–267.
Andresen, B., 2011. Current trends in finite-time thermodynamics. Angew. Chem. Int. Ed. 50 (12), 2690–2704.
Angulo-Brown, F., 1991. An ecological optimization criterion for finite-time heat engines. J. Appl. Phys. 69, 7465.
Bejan, A., 1996. Entropy generation minimization: the new thermodynamics of finite-size devices and finite-time processes. J. Appl. Phys. 79 (3), 1191–1218.
Bi, Y., Chen, L., Sun, F., 2012. Thermodynamic optimization for crystallization process of gas hydrate. Int. J. Energy Res. 36, 269–276.
Bi, Y., Lingen Chen, L., Sun, F., 2008. Heating load density and COP optimizations of an endoreversible air heat-pump. Appl. Energy 85, 607–617.
Bhardwaj, P.K., Kaushik, S.C., Jain, S., 2003. Finite time optimization of an endoreversible vapour absorption refrigeration system. Energy Convers. Manag. 44, 1131–1144.
Bhardwaj, P.K., Kaushik, S.C., Jain, S., 2005. General performance characteristics of an irreversible vapour absorption refrigeration system using finite time thermodynamic approach. Int. J. Therm. Sci. 44, 189–196.
Chen, J., 1999. The general performance characteristics of an irreversible absorption heat pump operating between four-temperature-level. J. Phys. D: Appl. Phys. 32, 1428–1433.
Chen, L., Ge, Y.L., Qin, X., Xie, Z.H., 2019. Exergy-based ecological optimization for a four-temperature-level absorption heat pump with heat resistance, heat leakage and internal irreversibility. Int. J. Heat Mass Transf. 129, 855–861.
Chen, L., Meng, F.K., Sun, F., 2016. Thermodynamic analyses and optimizations for thermoelectric devices: the state of the arts. Sci. China: Technol. Sci. 59 (3), 442–455.
Chen, L., Qin, X., Sun, F.R., 2007a. Model of irreversible finite heat capacity heat reservoir absorption heat transformer cycle and its application. Proc. IMechE C: J. Mech. Eng. Sci. 221 (C12), 1643–1652.
Chen, L., Sun, F., 2004. Advances in Finite Time Thermodynamics: Analysis and Optimization. Nova Science Publishers, New York.
Chen, L., Wu, C., Sun, F., 1999. Finite time thermodynamic optimization or entropy generation minimization of energy systems. J. Non-Equilib. Thermodyn. 24 (4), 327–359.
Chen, L., Zheng, T., Sun, F., Wu, C., 2006. Irreversible four-temperature-level absorption refrigerator. Sol. Energy 80 (3), 347–360.
Chen, L., Zheng, T., Sun, F., Wu, C., 2005a. Performance limits of real absorption refrigerators. J. Energy Inst. 78 (3), 139–144.
Chen, L., Qin, X., Sun, F., Wu, C., 2005b. Irreversible absorption heat-pump and its optimal performance. Appl. Energy 81, 55–71.
Chen, L., Xiaoqin, Z., Sun, F., Wu, C., 2007b. Exergy-based ecological optimization for a generalized irreversible Carnot heat-pump. Appl. Energy 84, 78–88.
Chen, L., Li, J., Sun, F., Wu, C., 2008. Performance optimization for a two-stage thermoelectric heat-pump with internal and external irreversibilities. Appl. Energy 85, 641–649.
Feidt, M., 2013. Evolution of thermodynamic modelling for three and four heat reservoirs reverse cycle machines: a review and new trends. Int. J. Refrig. 36 (1), 8–23.
Feidt, M., 2010. Thermodynamics applied to reverse cycle machines, a review. Int. J. Refrig. 33 (7), 1327–1342.
Frikha, S., Abid, M.S., 2016. Performance optimization of irreversible combined Carnot refrigerator based on ecological criterion. Int. J. Refrig. 62, 153–165.
Ge, Y.L., Chen, L.G., Sun, F., 2016. Progress in finite time thermodynamic studies for internal combustion engine cycles. Entropy 18 (4), 139.
Huang, Y., Sun, D., Kang, Y., 2008. Performance optimization for an irreversible four-temperature-level absorption heat pump. Int. J. Therm. Sci. 47, 479–485.
Kato, Y., Sasaki, Y., Yoshizawa, Y., 2005. Magnesium oxide/water chemical heat pump to enhance energy utilization of a cogeneration system. Energy 30, 2144–2155.
Kaushik, S., Tyagi, S.K., Kumar, P., 2018. Finite Time Thermodynamics of Power and Refrigeration Cycles. Springer, New York.
Kodal, A., Sahin, B., Oktem, A.S., 2000. Performance analysis of two stage combined heat pump system based on thermo-economic optimization criterion. Energy Convers. Manag. 41, 1989–1998.
Kodal, A., Sahin, B., Erdil, A., 2002. Performance analysis of a two-stage irreversible heat pump under maximum heating load per unit total cost conditions. Exergy Int. J. 2, 159–166.
Kodal, A., Sahin, B., Ekmekci, I., Yilmaz, T., 2003. Thermoeconomic optimization for irreversible absorption heat pump. Energy Convers. Manag. 44, 109–123.
Medjo Nouadje, B.A., Ngouateu Wouagfack, Tchinda, R., 2014. Influence of two internal irreversibilities on the new thermo-ecological criterion for three-heat–source refrigerators. Int. J. Refrig. 38, 118–127.
Medjo Nouadje, B.A., Ngouateu Wouagfack, P.A., Tchinda, R., 2016. Finite-time thermodynamics optimization of an irreversible parallel flow double-effect absorption refrigerator. Int. J. Refrig. 67, 433–444.
Ngouateu Wouagfack, P.A., Tchinda, R., 2011a. Performance optimization of three--heat-source irreversible refrigerators based on a new thermo-ecological criterion. Int. J. Refrig. 34, 1008–1015.
Ngouateu Wouagfack, P.A., Tchinda, R., 2011b. Irreversible three-heat-source refrigerator with heat transfer law of $Q\alpha$; $\Delta(T^{-1})$ and its performance optimization based on ECOP criterion. Energy Syst. 2, 359–376.
Ngouateu Wouagfack, P.A., Tchinda, R., 2012a. The new thermo-ecological performance optimization of an irreversible three-heat-source absorption heat pump. Int. J. Refrig. 35, 79–87.
Ngouateu Wouagfack, P.A., Tchinda, R., 2012b. Optimal ecological performance of a four-temperature- level absorption heat pump. Int. J. Therm. Sci. 54, 209–219.
Ngouateu Wouagfack, P.A., Tchinda, R., 2013. Finite-time thermodynamics optimization of absorption refrigeration systems: a review. Renew. Sustain. Energy Rev. 21, 524–536.
Ngouateu Wouagfack, P.A., Tchinda, R., 2014. Optimal performance of an absorption refrigerator based on maximum ECOP. Int. J. Refrig. 40, 404–415.
Qin, X., Chen, L., Ge, Y., Sun, F., 2013. Finite time thermodynamic studies on absorption thermodynamic cycles: a state of the arts review. Arab. J. Sci. Eng. 38 (3), 405–419.
Qin, X., Chen, L., Sun, F., Wu, C., 2004a. An absorption heat-transformer and its optimal performance. Appl. Energy. 78, 329–346.
Qin, X., Chen, L., Sun, F., Wu, C., 2004b. Optimal performance of an endoreversible four-heat-reservoir absorption heat-transformer. Open Syst. Inf. Dyn. 11 (2), 147–159.
Qin, X., Chen, L., Sun, F., Wu, C., 2006. Performance of an endoreversible four-heat-reservoir absorption heat pump with a generalized heat transfer law. Int. J. Therm. Sci. 45, 627–633.
Qin, X., Chen, L., Sun, F., Wu, C., 2008. Performance of real absorption heat-transformer with a generalised heat transfer law. Appl. Therm. Eng. 28, 767–776.
Qin, X., Chen, L., Ge, Y., Sun, F., 2015. Thermodynamic modeling and performance analysis of the variable-temperature heat reservoir absorption heat pump cycle. Phys. A: Stat. Mech. Appl. 436, 788–797.
Qin, X., Chen, L., Xia, S., 2017. Ecological performance of four-temperature-level absorption heat transformer with heat resistance, heat leakage and internal irreversibility. Int. J. Heat Mass Transf. 114, 252–257.

Qin, X., Chen, L., Sun, F., He, L., 2007. Model of real absorption heat pump cycle with a generalized heat transfer law and its performance. Proc. IMechE A: J. Power Energy 221 (A7), 907–916.
Qin, X., Chen, L., Sun, F., 2010. Thermodynamic modeling and performance of variable-temperature heat reservoir absorption refrigeration cycle. Int. J. Exergy 7 (4), 521–534.
Qin, X., Chen, L., Sun, F., Wu, C., 2005. Thermoeconomic optimization of an endoreversible four-heat reservoir absorption-refrigerator. Appl. Energy 81 (4), 420–433.
Qureshi, B.A., Syed, M.Z., 2015. Thermoeconomic considerations in the allocation of heat transfer inventory for irreversible refrigeration and heat pump systems. Int. J. Refrig. 54, 67–75.
Rivera, W., Best, R., Cardoso, M.J., Romero, R.J., 2015. A review of absorption heat transformers. Appl. Therm. Eng. 91, 654–670.
Sarkar, J., Bhattacharyya, S., Gopal, M.R., 2005. Transcritical CO_2 heat pump systems: exergy analysis including heat-transfer and fluid flow effects. Energy Convers. Manag 46, 2053–2067.
Sarbu, I., 2014. A review on substitution strategy of non-ecological refrigerants from vapour compression based refrigeration, air-conditioning and heat pump systems. Int. J. Refrig. 46, 123–141.
Su, H., Gong, G., Wang, C., Zhang, Y., 2017. Thermodynamic optimization of an irreversible carnot refrigerator with heat recovery reservoir. Appl. Therm. Eng. 110, 1624–1634.
Sun, F., Qin, X., Chen, L., Wu, C., 2005. Optimization between heating load and entropy -production rate for endoreversible absorption heat-transformers. Appl. Energy 81 (4), 434–448.
Sieniutycz, S., Salamon, P., 1990. Advances in Thermodynamics. Volume 4: Finite Time Thermodynamics and Thermoeconomics. Taylor & Francis, New York.
Ust, Y., Sahin, B., Kodal, A., Akay, I.H., 2006a. Ecological coefficient of performance analysis and optimization of an irreversible regenerative brayton heat engine. Appl. Energy 83, 558–572.
Ust, Y., Sahin, B., Ali., Kodal, 2006b. Performance analysis of an irreversible Brayton heat engine based on ecological coefficient of performance criterion. Int. J. Therm. Sci. 45, 94–101.
Wei, F., Lin, G., Chen, J., Bruck, E., 2011. Performance characteristics and parametric optimization of an irreversible magnetic ericsson heat-pump. Phys. B: Condens. Matter 406, 633–639.
Xia, D., Chen, L., Sun, F., Wu, C., 2007. Endoreversible four-reservoir chemical pump. Appl. Energy 84, 56–65.
Xiling, Z., Lin, F., Shigang, Z., 2011. General thermodynamic performance of irreversible absorption heat pump. Energy Convers. Manag. 52, 494–499.
Zheng, T., Chen, L., Sun, F., Wu, C., 2004. The influence of heat resistance and heat leak on the performance of a four-heat-reservoir absorption refrigerator with heat transfer law of $Q \propto \Delta(T^{-1})$. Int. J. Therm. Sci. 43 (12), 1187–1195.

International Journal of Refrigeration 112 (2020) 251–261

Contents lists available at ScienceDirect

International Journal of Refrigeration

journal homepage: www.elsevier.com/locate/ijrefrig

Exergetic, ecological and thermo-economic (3E) optimization of an absorption heat pump with heat resistance, heat leakage and two internal irreversibilities: Comparison

Rodrigue Léo Fossi Nemogne[a,*], Paiguy Armand Ngouateu Wouagfack[b], Brigitte Astrid Medjo Nouadje[c,d], Réné Tchinda[c,d]

[a] Energy, Electrical Systems and Electronics Laboratory, Department of Physics, University of Yaounde I, PO Box 812, Yaounde, Cameroon
[b] Department of Renewable Energy, Higher Technical Teachers' Training College, University of Buea, PO Box 249, Buea Road, Kumba, Cameroon
[c] Research Unit for Mechanics and Modeling Physical Systems, Department of Physics, University of Dschang, PO Box 67, Dschang, Cameroon
[d] Research Unit in Industrial Systems and the Environment, University institute of Technology Fotso Victor, University of Dschang, PO Box 134, Bandjoun, Cameroon

ARTICLE INFO

Article history:
Received 8 October 2019
Revised 26 November 2019
Accepted 15 December 2019
Available online 18 December 2019

Keywords:
Flowchart optimization
Absorption heat pump
Exergy-based ecological criterion
Exergetic performance criterion
Thermo-economic criterion

ABSTRACT

The multi-objective optimization of a three-heat-reservoir absorption heat pump (THR AHP) is used mainly considering three objective functions: exergetic performance criterion (*EPC*), exergy-based ecological criterion (*E*) and thermo-economic criterion (*F*). Indeed, the exergy, ecological and thermo-economic criteria are highlighted analytically. This is done by using the law of convective heat exchanges between the working fluid and the different components and finite time thermodynamics analysis. This is to determine the optimum operating points of the system by minimizing exergy destruction rate, the environmental impact and the costs of capital and energy consumed. Also, the parameters taken into account influencing the performance of the absorption heat pump are the heat resistances, the heat leakages, the thermo-economic parameter and the two internal irreversibility factors in particular that between the evaporator-condenser assembly. However, the Flowchart optimization methodology made it possible to deduce that the system presents a significant advantage at the maxima of the *F* and the *EPC* criteria in terms of coefficient of performance. Nevertheless, the THR AHP presents a significant advantage at the maximum of the *EPC* in terms of exergy destruction rate and at the maximum of the *E* in terms of specific heating load and exergy output rate.

Optimisation exergétique, écologique et thermo-économique (3E) d'une pompe à chaleur à absorption en utilisant la résistance thermique, les fuites thermiques et deux irréversibilités internes: comparaison

Mots-clés: Optimisation du diagramme de flux; Pompe à chaleur à absorption; Critère écologique basé sur l'exergie; Critère de performance exergétique; Critère thermo-économique

1. Introduction

Increasing global warming over the last decade has led to the use of heating, cooling and air conditioning systems in industries, transportation and building, which are more concerned with the environment. In addition, because absorption systems are more energy efficient, they are also environmentally conscious with less polluting and use more environmentally friendly working fluids (Ally and Sharma, 2018; Hu et al., 2018; Sarbu, 2014). This is why it is necessary to design systems that take into account the exergy, ecological and economic aspects (3E) under optimal

* Corresponding author.
E-mail address: rodriguefossi@yahoo.fr (R.L. Fossi Nemogne).

https://doi.org/10.1016/j.ijrefrig.2019.12.016
0140-7007/

Nomenclature

A	heat-transfer area, (m^2)
C	cost, (price unit)
COP	coefficient of performance, (dimensionless)
E	exergy-based ecological criterion, (W)
EPC	exergetic performance criterion, (dimensionless)
ex	exergetic efficiency, (dimensionless)
$\dot{EX}$	exergy rate, (W)
F	thermo-economic criterion, (dimensionless)
I	internal irreversibility parameter, (dimensionless)
k	thermo-economic parameter, (Wm^{-2})
K	thermal conductivity, (WK^{-1})
m	distribution of the total rate of rejected heat between the absorber and the condenser, (dimensionless)
q	specific heating load, (Wm^{-2})
$\dot{Q}$	heat transfer rate, (W)
S	specific entropy generation rate, ($WK^{-1}m^{-2}$)
T	temperature, (K)
U	heat-transfer coefficient, ($WK^{-1}m^{-2}$)

Greek symbols

ξ	heat leakage coefficient, ($WK^{-1}m^{-2}$)
π	heating load, (W)
$\dot{\sigma}$	entropy generation rate, (WK^{-1})
ψ	coefficient of performance, (dimensionless)

Subscripts

1	working fluid in generator; capital cost for the unit heat-transfer area
2	working fluid in evaporator; unit cost of energy
3	working fluid in absorber and condenser
A	absorber
C	condenser
D	destruction
E	evaporator; at maximum E
e	energy consumed
env	environment
EPC	at maximum EPC
F	at maximum F
G	generator
i	investment
in	input
L	heat leakage
max	maximum
O	absorber and condenser
op	optimal
out	output

Abbreviations

AHP	absorption heat pump
AHT	absorption heat transformer
AR	absorption refrigeration
COP	coefficient of performance
ECOP	ecological coefficient of performance
EPC	exergetic performance criterion
FTT	finite time thermodynamics
FTL	four-temperature-level
HP	heat pump
HT	heat transformer
THR	three-heat-reservoir

operating conditions. Moreover, the optimization of AHP and other thermal systems becomes crucial for research. This is because the demand is increasing and for a better quality, especially in the industry with the use of renewable energy sources as a source of power (Mastrullo and Renno, 2010; Li et al., 2013; Dixit et al., 2017; Leonzio, 2017; Yuksel and Ozturk, 2017; Wang et al., 2018). Also with the design of energy efficient systems in the field of physics and engineering (Sieniutycz and Salamon, 1990; Bejan, 1996; Chen et al., 1999; Chen and Sun, 2004; Feidt, 2010, 2013; Andresen, 2011; Qin et al., 2013; Ngouateu Wouagfack and Tchinda, 2013; Rivera et al., 2015; Ge et al., 2016; Su et al., 2017; Chaves Fortes et al., 2018; Wang et al., 2019). This being so, the combined optimization approach by the three decisive objective functions F, E and EPC using finite time thermodynamics (FTT) aims to significantly improve the design and operation of AHPs. These criteria are each characterized by:

i) The exergetic performance criterion (EPC), which is the exergy output rate per unit exergy destruction rate or loss rate of availability.
ii) The ecological function (E) which is the difference between exergy output rate and the loss rate of availability.
iii) The thermo-economic function (F) which is the specific heating or cooling or mechanical load per unit sum of cost on the investment and the cost of the energy consumed.

However, research has systematically evolved towards optimization using the FTT. Therefore, Chen (1999), Kato et al. (2005), Chen et al. (2005a), Qin et al. (2006, 2007, 2015), Xia et al. (2007), Bi et al. (2008), Huang et al. (2008) and Xiling et al. (2011) on AHP, Wei et al. (2011) on magnetic HP of Ericsson, Bhardwaj et al. (2003, 2005), Zheng et al. (2004), Chen et al. (2005b, 2006), Qin et al. (2010) and Kaushik et al. (2018) on AR, Qin et al. (2004a, 2004b, 2008) and Chen et al. (2007a) on AHT, have analyzed these endoreversible and irreversible systems using the coefficient of performance, the specific heating load and the specific cooling load as objective functions. Then, the performances are studied considering the environmental impact with the heat losses, the heat leakage and the heat resistances in the various components. These parameters are derived from the second law of thermodynamics and initiated by Ust et al. (2006a, 2006b) on irreversible Brayton heat engines using the thermo-ecological criterion. They are followed by Ngouateu Wouagfack and Tchinda (2011a, 2011b, 2014), Medjo Nouadje et al. (2014, 2016) and Ahmadi and Ahmadi (2016) with the irreversible ARs, then Ngouateu Wouagfack and Tchinda (2012a, 2012b), Ahmadi et al. (2015) and Fossi Nemogne et al. (2019) with irreversible AHP and Ahmadi et al. (2016) with an inverse Brayton cycle. At the same time, the ecological criterion (E) based on the same considerations is first used by Angulo-Brown (1991) and followed by Sun et al. (2005), Chen et al. (2007b, 2019), Qin et al. (2017) and Frikha and Abid (2016). Moreover, the exergetic approach in addition to the previous considerations takes into account the useful energy consumed by the thermodynamic cycle (Sahin et al., 1997; Talbi and Agnew, 2000; Kilic and Kaynakli, 2007; Kaushik and Arora, 2009; Lostec et al., 2010; Farshi et al., 2013) and the EPC criterion used by Ust et al. (2007) and Liu et al. (2017) on the ARs, complements the previous criteria. However, the optimization of thermal systems by the thermo-economic approach makes use of the cost on the investment with the parameters such as the areas of heat exchange, the thermal capacities and the cost on the consumption with the load rate consumed. Kodal et al. (2000, 2002, 2003) used this approach on AHP and two-stage AHP, followed by Silveira and Tuna (2003, 2004) on combined heat and power systems. Then, Misra et al. (2003, 2005) on single-effect and double-effect H_2O/LiBr, Qin et al. (2005) on endoreversible ARs, Durmayaz et al. (2004) on thermal systems, Wu et al. (2005) on irreversible AHP, Qureshi and Syed (2015) on AHP and AR. Zare et al. (2012) and Ahmadi et al. (2014b) conducting a thermo-economic and exergy study on an ammonia-water power/cooling cogeneration cycle and on multi-generation systems respectively using the evolutionary genetic algorithm. Therefore,

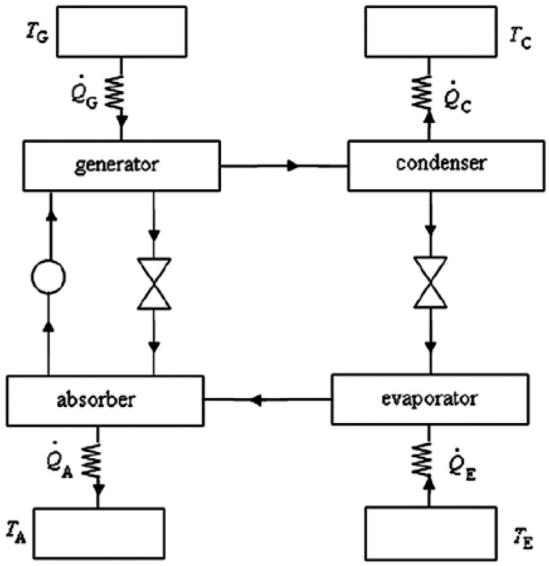

Fig. 1. Symbolic diagram of an AHP (Fossi Nemogne et al., 2019).

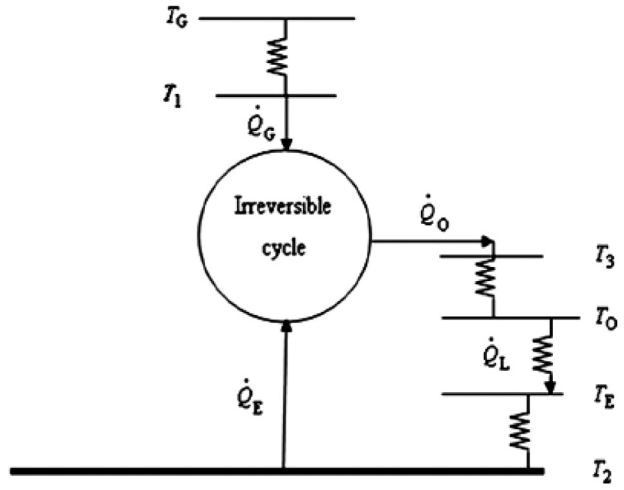

Fig. 2. The irreversible cycle model of a three-heat-reservoir AHP (Fossi Nemogne et al., 2019).

each approach has been examined using each time an optimization criterion. However, it is important to consider simultaneously the influences of two internal irreversibilities due to heat losses (Xiling et al., 2011 using COP and specific heating load as objective functions, Medjo Nouadje et al., 2014 and Fossi Nemogne et al., 2019 using the thermo-ecological criterion as objective function on THR AR and AHP respectively), of the overall external irreversibility due to heat leakages and heat resistances. This being the case, the consideration (3E) brings the limitation and the advantages presented by the optimization of each objective function.

In this paper, we will from the FTT, determine the optimal operating points of a THR AHP corresponding to the maximum of each respective objective function E, EPC and F and discuss, while using the Flowchart optimization algorithm (Su et al., 2017; Chen et al., 2019).

2. Irreversible absorption heat pump cycle model

2.1. Finite time thermodynamics

The real operating conditions of the AHP in Fig. 1 take into consideration the heat resistances, the heat leakages and the heat losses represented by two internal irreversibility factors. However, another consideration is taken into account by reducing the temperature level of the working fluid in the absorber which is equal to that in the condenser ($T_A = T_C$). The irreversible cycle of a THR AHP as shown in Fig. 2 allows us to write the first law of thermodynamics. In addition, the localized heat leakages in the absorber, condenser and evaporator heat exchangers makes it possible to model a cycle by relying on the refs. Ngouateu Wouagfack and Tchinda (2011a, 2011b, 2012a, 2012b, 2014), Medjo Nouadje et al. (2014, 2016), Ahmadi et al. (2015, 2016) and Fossi Nemogne et al. (2019), we obtain

$$\dot{Q}_G + \dot{Q}_E - \dot{Q}_O = 0 \text{ such that } \dot{Q}_O = \dot{Q}_C + \dot{Q}_A \tag{1}$$

and Newton's linear heat transfer law which is expressed between the heat exchangers and the working fluid is as follows.

$$\begin{aligned} \dot{Q}_G &= U_G A_G (T_G - T_1) \\ \dot{Q}_E &= U_E A_E (T_E - T_2) \\ \dot{Q}_O &= U_O A_O (T_3 - T_O) \end{aligned} \tag{2}$$

with $A_O = A_A + A_C$ and $T_O = T_A = T_C$

In addition, heat leakage from the THR AHP cycle is expressed as follows (Ngouateu Wouagfack and Tchinda, 2012a; Fossi Nemogne et al., 2019)

$$\dot{Q}_L = K_L (T_O - T_E) \tag{3}$$

K_L is the thermal resistance or thermal conductivity of heat leakage and is expressed in (WK^{-1}). It is important to evaluate the total heat exchange area of the heat exchangers of irreversible absorption cycles, especially for optimal operation. The total heat exchange area is:

$$A = A_G + A_E + A_O \tag{4}$$

The second law of thermodynamics or Clausius' inequality is useful to follow the steps of the thermodynamic cycle during its process in order to quantify the different types of losses.

$$\oint \frac{\delta \dot{Q}}{T} = \frac{\dot{Q}_G}{T_1} + \frac{\dot{Q}_E}{T_2} - \frac{\dot{Q}_O}{T_3} < 0 \tag{5}$$

The temperatures T_1, T_2 and T_3 are the temperatures of the working fluid respectively in the generator, the evaporator and the absorber and the condenser assembly, are expressed in (K). To rewrite the second law, we introduce the two internal irreversibilities I_1 and I_2 of Refs. Xiling et al. (2011), Medjo Nouadje et al. (2014) and Fossi Nemogne et al. (2019) which represent the losses created during heat exchange respectively between the absorber and the generator and between the condenser and the evaporator. These heat losses are characterized by the following internal irreversibility factors:

$$\frac{\dot{Q}_G}{T_1} = \frac{Q_A}{I_1 T_3} (I_1 \geq 1) \text{ and } \frac{\dot{Q}_E}{T_2} = \frac{Q_C}{I_2 T_3} (I_2 \geq 1) \tag{6}$$

Considering Eq. (6) and Eq. (5) we obtain

$$\frac{\dot{Q}_G}{T_1} + \frac{\dot{Q}_E}{T_2} - \frac{Q_A}{I_1 T_3} - \frac{Q_C}{I_2 T_3} = 0 \tag{7}$$

2.2. Characteristics parameters

The coefficient of performance (COP) and the specific heating load are obtained for

$$\text{THR AHP } \psi = \pi / \dot{Q}_G = \left(\dot{Q}_O - \dot{Q}_L\right)/\dot{Q}_G \text{ and } q = \pi / A = \left(\dot{Q}_O - \dot{Q}_L\right)/A \tag{8}$$

The Eqs. (1) and (8) of the AHP cycle provide the heat-transfer rates derived from the coefficient of performance and the heating load

$$\dot{Q}_G = \pi/\psi$$
$$\dot{Q}_E = \pi\left(1-\frac{1}{\psi}\right)+\dot{Q}_L$$
$$\dot{Q}_O = \pi+\dot{Q}_L \tag{9}$$

and Eqs. (2) and (9) the temperatures of the working fluid yields

$$T_1 = T_G - \frac{\pi}{U_G A_G \psi}$$
$$T_2 = T_E - \frac{\pi\left(1-\frac{1}{\psi}\right)+\dot{Q}_L}{U_E A_E}$$
$$T_3 = T_O + \frac{\pi+\dot{Q}_L}{U_O A_O} \tag{10}$$

Substituting Eqs. (9) and (10) into Eq. (7) we obtain another expression of the second law of thermodynamics deriving from the heating load, coefficient of performance, two internal irreversibility factors, heat leakage, heat-transfer areas of heat exchangers and convective heat exchange coefficients in the different components. This expression is obtained from that of Qin et al. (2007) and Chen et al. (2019) who established an expression between the heating load and the coefficient of performance by considering an overall internal irreversibility in FTL AHP and Qin et al. (2017) in turn established a similar expression in FTL AHTs always with an overall internal irreversibility.

$$\psi\left(\frac{T_O}{\pi+\dot{Q}_L}+\frac{1}{U_O A_O}\right)^{-1} - I_1\left(\frac{T_G}{\pi}-\frac{1}{U_G A_G \psi}\right)^{-1} - I_2\left(\frac{T_E}{\pi(\psi-1)+\dot{Q}_L\psi}-\frac{1}{U_E A_E \psi}\right)^{-1} = 0 \tag{11}$$

3. Performance analysis and optimization

3.1. Exergetic performance criterion and exergy-based ecological criterion

The exergy output rate of the system THR AHP cycle is as follows

$$\dot{E}\underset{out}{X} = \left(\dot{Q}_O-\dot{Q}_L\right)\left(1-\frac{T_{env}}{T_O}\right) = \pi\left(1-\frac{T_{env}}{T_O}\right) \tag{12}$$

The exergy input rate of the system THR AHP cycle

$$\dot{E}\underset{in}{X} = \dot{Q}_G = \frac{\pi}{\psi} \tag{13}$$

and the exergy destruction rate or the loss rate of availability

$$\dot{E}\underset{D}{X} = T_{env}\dot{\sigma} = T_{env}\left(\frac{\dot{Q}_O-\dot{Q}_L}{T_O}-\frac{\dot{Q}_G}{T_G}-\frac{\dot{Q}_E-\dot{Q}_L}{T_E}\right) = T_{env}\pi\left(\frac{1}{T_O}-\frac{T_E+(\psi-1)T_G}{T_E\psi}\right) \tag{14}$$

where $\dot{\sigma}$ is the entropy generation rate is expressed in (WK^{-1})

As a result, exergy-based ecological function has been previously used by Huang et al. (2008), Chen et al. (2007b, 2019), Frikha and Abid (2016), Qin et al. (2017) and Fossi Nemogne et al. (2019) on absorption systems yields

$$E = \dot{E}\underset{out}{X} - \dot{E}\underset{D}{X} = T_{env}\pi\left(\frac{1}{T_{env}}-\frac{2}{T_O}+\frac{T_E+(\psi-1)T_G}{T_E\psi}\right) \tag{15}$$

We can define the exergetic efficiency which is the exergy output rate per unit exergy input rate. Previously, authors such as Ust et al. (2007), Kilic and Kaynakli (2007), Kaushik and Arora (2009) and Liu et al. (2017) used and analyzed the thermal systems with this criterion. By the way, using the Eqs. (12) and (13) we have

$$ex = \frac{\dot{E}X_{out}}{\dot{E}X_{in}} = \psi\left(1-\frac{T_{env}}{T_O}\right) \tag{16}$$

Also, the exergetic performance criterion (EPC) used by Ust et al. (2007) is established as the exergy output rate per unit loss rate of availability and allows a careful measurement of the energy required, added to the impact on the environment. Using Eqs. (12) and (14), we obtain:

$$EPC = \frac{\dot{E}X_{out}}{\dot{E}X_D} = \frac{1-\frac{T_{env}}{T_O}}{\frac{1}{T_O}-\frac{T_E+(\psi-1)T_G}{T_G T_E \psi}} \tag{17}$$

3.2. Thermo-economic criterion

The thermo-economic criterion stated by Kodal et al. (2000, 2002, 2003) and followed by Ahmadi et al. (2014a), is the heating load per unit sum of the cost on the investment and the cost of the energy consumed. It takes into account the location of the system and the load to be provided by it.

$$f = \frac{\pi}{C_i+C_e} \tag{18}$$

$$\text{where, } C_i = k_1 A \text{ and } C_e = k_2\ \dot{Q}_G \tag{19}$$

C_i is the cost of the investment in AHP and depends proportionally on the total heat exchange area. C_e is the cost of energy consumed and is proportionally dependent on the heat input rate. Again k_1 and k_2 the capital cost for the unit heat-transfer area and the unit cost of energy, respectively. Considering $k = k_1/k_2$ as a thermo-economic parameter of dimension (Wm^{-2}), and substituting Eq. (19) into Eq. (18) we obtain

$$F = k_2 f = \frac{1}{\frac{k}{q}+\frac{1}{\psi}} \tag{20}$$

3.3. Optimization

3.3.1. Special cases

Eq. (11) can be written in many other forms neglecting the internal and external irreversibility factors.

The first case, where the heat resistances and the heat leakages which represent the flow of heat leaving the medium to be heated for the environment during the thermodynamic cycle are neglected. It follows that the heat leakage coefficient nullifies ($K_L = 0 \Rightarrow K_L/A = \xi = 0$), Eq. (11) becomes

$$\psi\left(\frac{T_O}{\pi}+\frac{1}{U_O A_O}\right)^{-1} - I_1\left(\frac{T_G}{\pi}-\frac{1}{U_G A_G \psi}\right)^{-1} - I_2\left(\frac{T_E}{\pi(\psi-1)}-\frac{1}{U_E A_E \psi}\right)^{-1} = 0 \tag{21}$$

The second case, where the heat losses are neglected ($I_1 = I_2 = 1$) that is to say for an endoreversible system, Eq. (11) becomes

$$\psi\left(\frac{T_O}{\pi+\dot{Q}_L}+\frac{1}{U_O A_O}\right)^{-1} - \left[\left(\frac{T_G}{\pi}-\frac{1}{U_G A_G \psi}\right)^{-1} + \left(\frac{T_E}{\pi(\psi-1)+\dot{Q}_L\psi}-\frac{1}{U_E A_E \psi}\right)^{-1}\right] = 0 \tag{22}$$

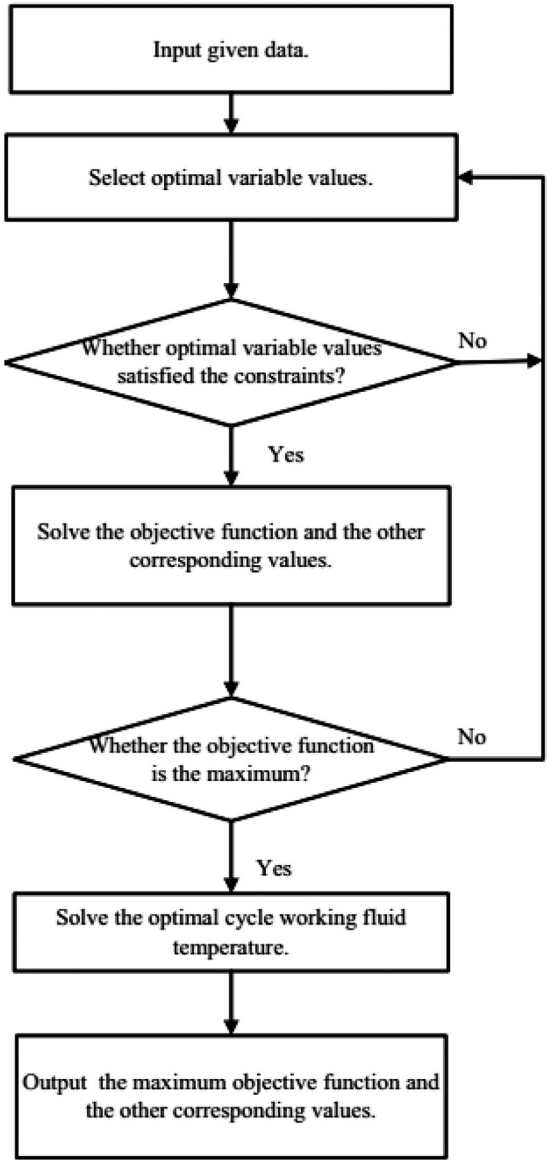

Fig. 3. The optimization flowchart (Chen et al., 2019).

The third case, where the heat resistances, the heat leakages and the heat losses are neglected ($K_L = 0 \Rightarrow K_L/A = \xi = 0$ and $I_1 = I_2 = 1$) that is to say for a reversible system, Eq. (11) becomes

$$\psi\left(\frac{T_0}{\pi} + \frac{1}{U_0 A_0}\right)^{-1} - \left[\left(\frac{T_G}{\pi} - \frac{1}{U_G A_G \psi}\right)^{-1} + \left(\frac{T_E}{\pi(\psi - 1)} - \frac{1}{U_E A_E \psi}\right)^{-1}\right] = 0 \quad (23)$$

3.3.2. Flowchart optimization

The three decisive objective functions taken into consideration for our work are the thermo-economic criterion (F), the exergy-based ecological function (E) and the ecological performance criterion (EPC). The maximum values of each objective function EPC, E, and F can be evaluated using the flowchart optimization algorithm (Fig. 3) thus used by the Refs. Su et al. (2017) and Chen et al. (2019). We obtain the maximum value of the exergetic performance criterion $EPC_{\max}$ which corresponds to the optimal values ψ_{EPC}, A_{EPC}, q_{EPC}, $EX_{out-EPC}$ and EX_{D-EPC}. Then we determine the maximum value of the exergy-based ecological criterion $E_{\max}$ which corresponds to the optimal values ψ_E, A_E, q_E, EX_{out-E} and EX_{D-E}. Finally, in the same way, we obtain the maximum values of the thermo-economic criterion $F_{\max}$ to which correspond the optimal values ψ_F, A_F, q_F, EX_{out-F} and EX_{D-F}.

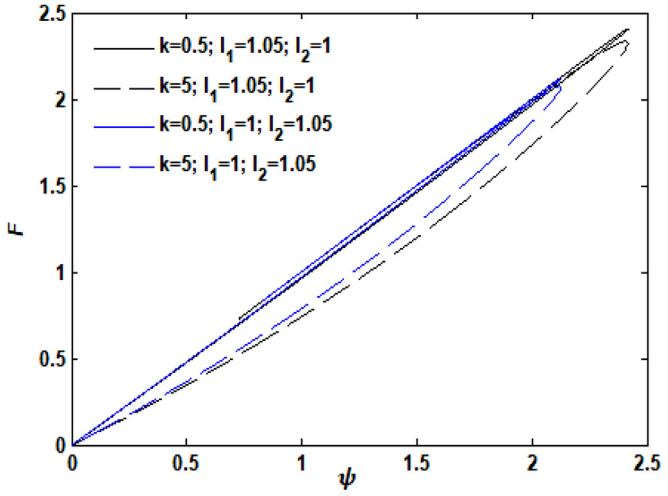

Fig. 4. Effects of thermo-economic factor on the F criterion with respect to the COP (ψ) objective function.

4. Results and discussion

4.1. Numerical applications

The numerical values below allowed to perform numerical analyzes and to plot the curves of the variations of the different objective functions E, EPC and F according to COP, q, EX_{out} and EX_D. This is under the influences of the dissipation effects, heat resistances and internal and external irreversibility factors. In a general framework, these values are taken from the Ref. literature (Fossi Nemogne et al., 2019) and are the following: $T_G = 393$K; $T_E = 288$K; $T_A = 313$K; $T_C = 313$K; $A = 100\text{m}^2$; $\xi = K_L/A = 1.082\text{Wm}^{-2}\text{K}^{-1}$. In addition, in Figs. 7–13, $k = 5$.

4.2. Influences of the design parameters on the EPC, E and F criteria

4.2.1. The thermo-economic parameter (k)

Among the three decisive objective functions F, E and EPC, the thermo-economic parameter only affects the objective function F. Again, when the capital cost increases and the cost of the consumed energy decreases, thereafter thermo-economic parameter k increases while F decreases. The variations of the thermo-economic criterion (F) with respect to the coefficient of performance (ψ), the exergy output rate (EX_{out}) and the exergy destruction rate (EX_D) respectively were plotted under the influences of thermo-economic parameter k in Figs. 4–6. In Fig. 4, the thermo-economic F objective function increases as the COP increases and the curves obtained are loops passing through the origin which are less and less sharp when the thermo-economic parameter values k increase. So much so that in Figs. 5 and 6, the criterion F increases rapidly near its maximum before decreasing asymptotically thereafter, especially in Fig. 6, this when k increases. It is useful to observe that when k increases, the maximum of the objective function F is lower. Whereas the specific heating load, the exergy output rate and the exergy destruction rate have higher optimal corresponding values.

However, it is crucial in the optimization of the THR AHP by the objective function F that we have maximum values of F,

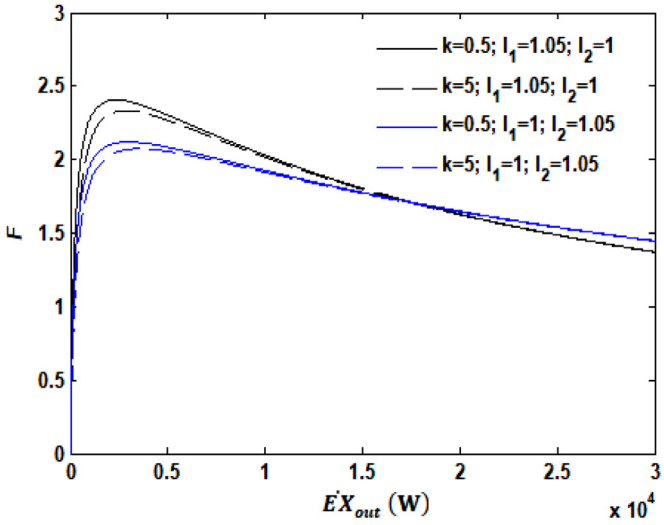

Fig. 5. Effects of thermo-economic factor on the F criterion with respect to the EX_{out} objective function.

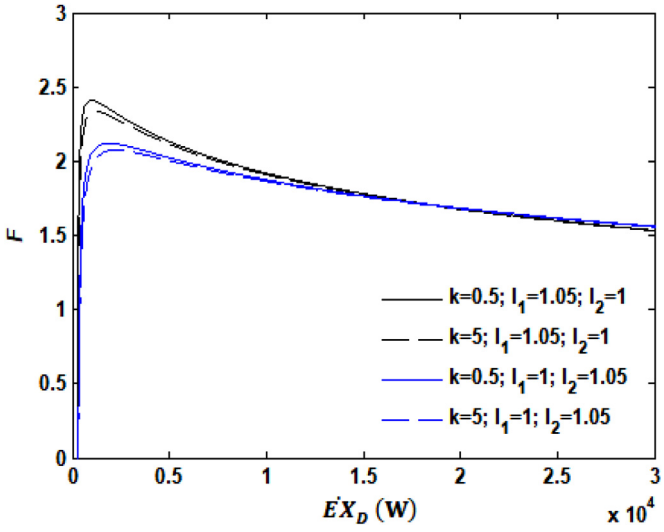

Fig. 6. Effects of thermo-economic factor on the F criterion with respect to the $\dot{EX}_D$ objective function.

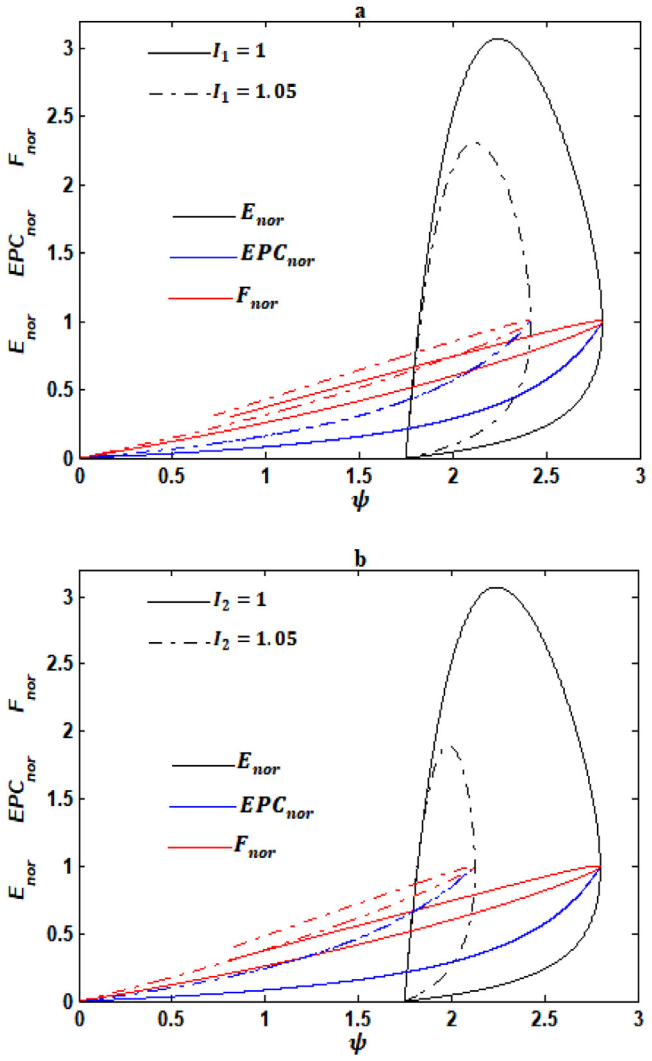

Fig. 7. Effects of internal irreversibility I_1 (a) of the generator-absorber assembly and of the internal irreversibility I_2 (b) of the evaporator-condenser assembly on the dimensionless E_{nor}, EPC_{nor} and F_{nor} with respect to the COP (ψ) objective function.

corresponding to a minimum exergy destruction rate for certain values of the specific heating load and the exergy output rate.

4.2.2. The two internal irreversibility factors I_1 *and* I_2

In Figs. 7–10, the dimensionless or normalized values $E_{nor}(E_{nor} = E/E_{op}$ where E_{op} is the optimal value of E corresponding to the value of E when F and EPC are at their maximum values, and E varies to $E_{\max}$), EPC_{nor} ($EPC_{nor} = EPC/EPC_{\max}$) and F_{nor} ($F_{nor} = F/F_{\max}$) has a curve with respect to ψ, q, EX_{out} and EX_D. These characterizes the influences of the two internal irreversibility factors I_1 and I_2 on the exergy-based ecological function E, exergetic performance coefficient EPC and thermo-economic function F criteria. Unlike the increase of k values, when the parameters I_1 and I_2 increase, then:

i) The maximum of each criterion F, E and EPC decreases with decreasing values of the corresponding optimal coefficient of performance ψ (Fig. 7).
ii) The maximum of each criterion F and E decreases with decreasing values of the corresponding optimum objective functions of performance q and EX_{out} (Figs. 8 and 9 respectively). Whereas the maximum of the objective function EPC decreases with the gradual increasing values of the corresponding optimum objective functions of performance q and EX_{out} (Figs. 8 and 9 respectively).
iii) The maximum of the objective function E decreases with the decreasing values of the corresponding optimal exergy destruction rate EX_D (Fig. 10). Whereas the maximum of each criterion F and EPC decreases with the abrupt increasing values of the corresponding optimal exergy destruction rate EX_D (Fig. 10).

Under optimal operating conditions, optimization parameters ψ, q, EX_{out} and EX_D related to the maximum of the exergy-based ecological function E and for an endoreversible system ($I_1 = I_2 = 1$) are taken as references because they have the highest values: $\psi_{EPC} = \psi_F = 2.80$, $q_E = 1603\text{Wm}^{-2}$, $EX_{out-E} = 11779\text{W}$ and $EX_{D-E} = 6324\text{W}$. Also, two cases are taken into account.

In the first case where $I_1 = 1.05$ and $I_2 = 1$, we make the following observations. ψ_F and ψ_{EPC} are both lower than the highest coefficient of performance value by 13.65%, whereas ψ_E is lower by a rate of 24.33%, in Fig. 7(a). q_E, q_F and q_{EPC} are lower than the highest specific heating load value by rates of 29.60%, 76.29% and

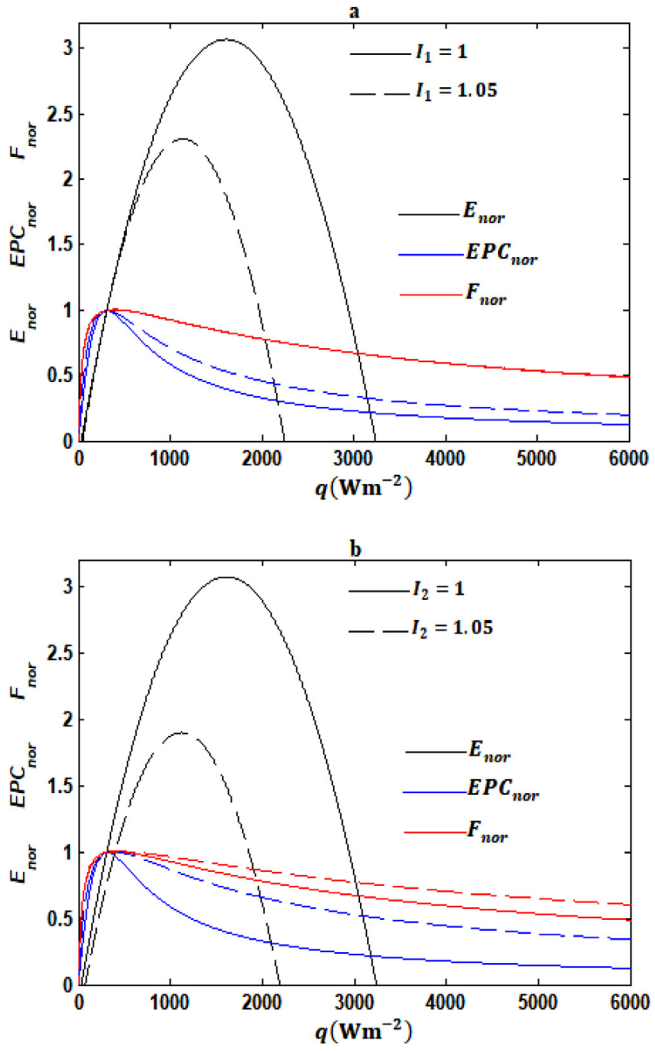

Fig. 8. Effects of internal irreversibility I_1 (a) of the generator-absorber assembly and of the internal irreversibility I_2 (b) of the evaporator-condenser assembly on the dimensionless E_{nor}, EPC_{nor} and F_{nor} with respect to the q objective function.

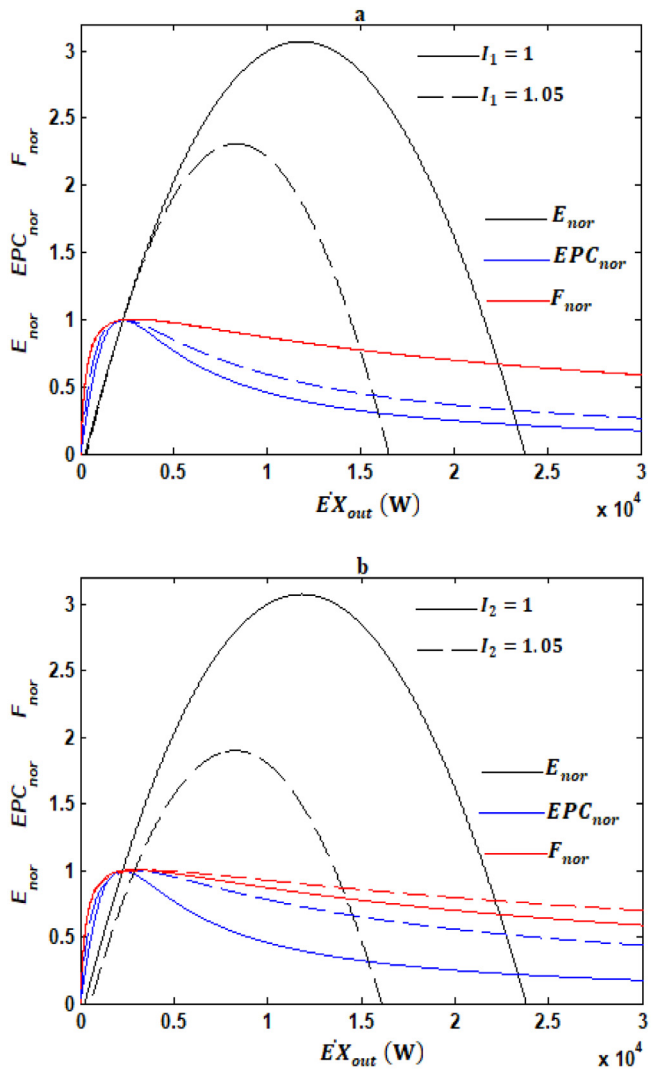

Fig. 9. Effects of internal irreversibility I_1 (a) of the generator-absorber assembly and of the internal irreversibility I_2 (b) of the evaporator-condenser assembly on the dimensionless E_{nor}, EPC_{nor} and F_{nor} with respect to the $\dot{EX}_{out}$ objective function.

80.85% respectively, in Fig. 8(a). $\dot{EX}_{out-E}$, $\dot{EX}_{out-F}$ and $\dot{EX}_{out-EPC}$ are lower than the highest specific exergy output rate value which is itself proportional to the specific heating load by rates of 29.60%, 76.29% and 80.85% respectively, in Fig. 9(a). On the other hand, $\dot{EX}_{D-EPC}$, $\dot{EX}_{D-F}$ and $\dot{EX}_{D-E}$ are lower than the highest exergy destruction rate value by rates of 85.01%, 81.20% and 16.90% respectively, in Fig. 10(a).

In the second case where $I_1 = 1$ and $I_2 = 1.05$, we make the following observations. ψ_F and ψ_{EPC} are both lower than the highest coefficient of performance value by a rate of 24.22%, whereas ψ_E is lower by a rate of 29.08%, in Fig. 7(b). q_E, q_F and q_{EPC} are lower than the highest specific heating load value by rates of 30.31%, 70.51% and 75.55% respectively, in Fig. 8(b). $\dot{EX}_{out-E}$, $\dot{EX}_{out-F}$ and $\dot{EX}_{out-EPC}$ are lower than the highest specific exergy output rate value by rates of 30.31%, 70.51% and 75.55% respectively, in Fig. 9(b). On the other hand, $\dot{EX}_{D-EPC}$, $\dot{EX}_{D-F}$ and $\dot{EX}_{D-E}$ are lower than the highest exergy destruction rate value by rates of 71.39%, 65.30% and 2.67% respectively, in Fig. 10(b).

From this we deduce that, the impact of heat losses on system performance between the condenser and the evaporator characterized by the internal irreversibility factor I_2 is greater than that between the generator and the absorber characterized by the internal irreversibility factor I_1. This is manifested by highest maximum values of the objective functions F, EPC and E which correspond to the best optimal performance of the parameters ψ, q, $\dot{EX}_{out}$ and $\dot{EX}_D$, under the influence of I_1. Furthermore, under the effects of the two internal irreversibility factors, THR AHP cycle has a significant advantage at the maxima of the F and the EPC criteria in terms of coefficient of performance. Nevertheless, the system has a significant advantage at the maximum of the EPC in terms of exergy destruction rate, and at the maximum of the E criterion in terms of specific heating load and exergy output rate.

4.2.3. Heat leakage and heat resistance

Figs. 11–13 show the variations of the dimensionless E_{nor}, EPC_{nor} and F_{nor} with respect to the objective functions of performance ψ, $\dot{EX}_{out}$ and $\dot{EX}_D$ respectively. These characterizes the influences of the heat resistances and heat leakages on the exergy-based ecological function E, exergetic performance coefficient EPC and thermo-economic function F criteria. In these figures, when the parameter ξ increases with each time $I_1 = 1.05$ when $I_2 = 1$ and $I_1 = 1$ when $I_2 = 1.05$, then:

i) The maximum of each objective function F, E and EPC decreases with decreasing values of the corresponding optimal coefficient of performance ψ (Fig. 11).

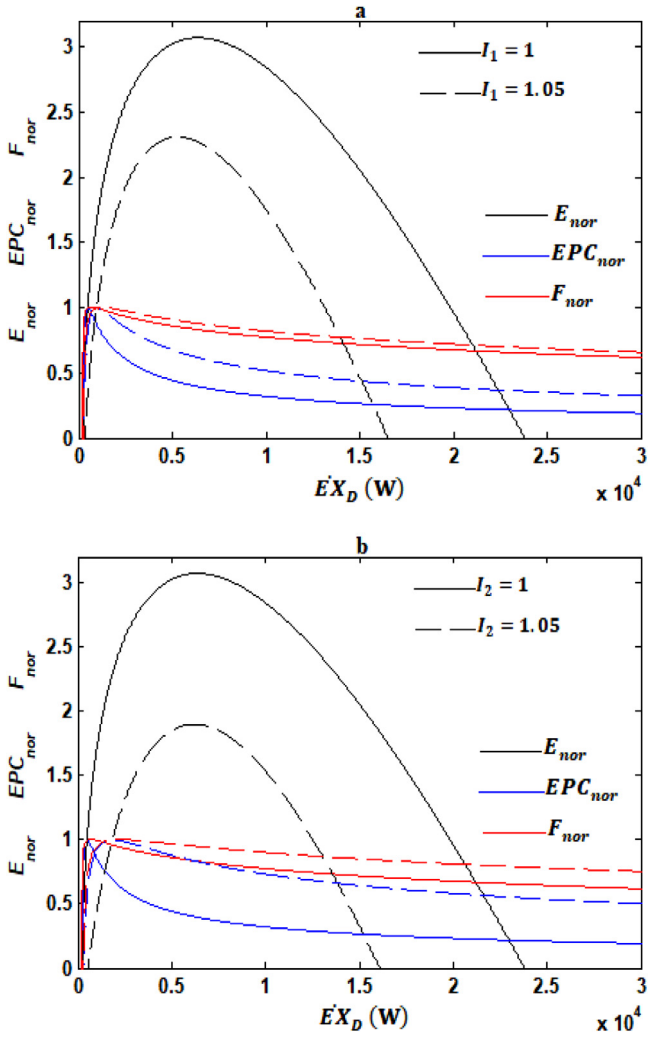

Fig. 10. Effects of internal irreversibility I_1 (a) of the generator-absorber assembly and of the internal irreversibility I_2 (b) of the evaporator-condenser assembly on the dimensionless E_{nor}, EPC_{nor} and F_{nor} with respect to the EX_D objective function.

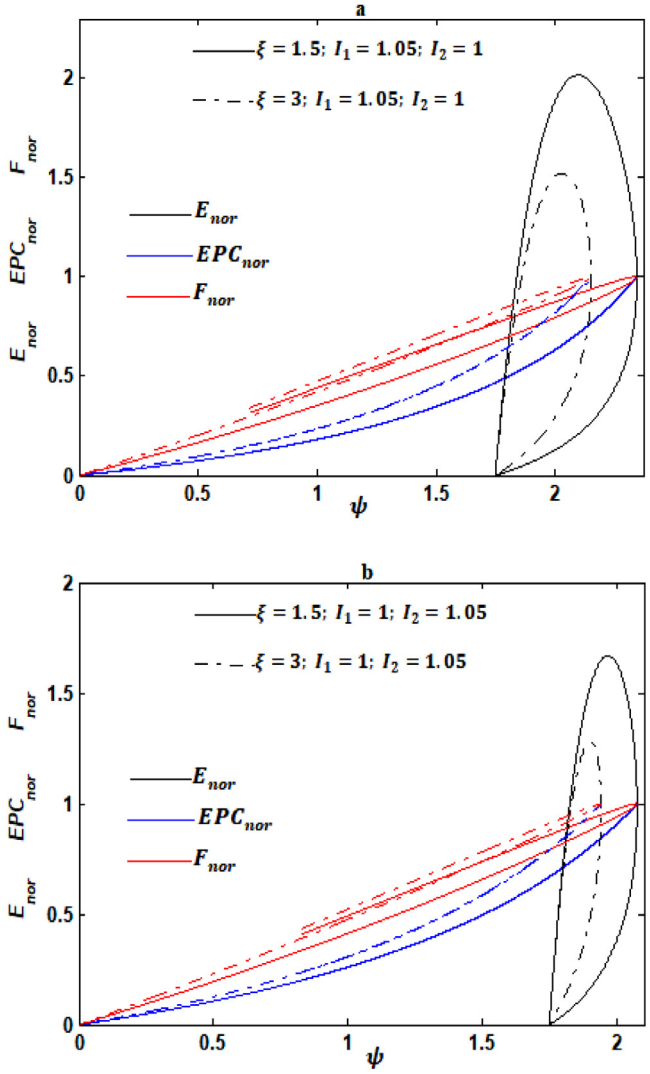

Fig. 11. Effects of heat leakage coefficient ξ on the dimensionless E_{nor}, EPC_{nor} and F_{nor} with respect to the COP (ψ) objective function.

ii) The maximum of each objective function F and EPC decreases with increasing values of the corresponding optimal exergy output rate $\dot{EX}_{out}$ (Fig. 12). Whereas the maximum of the objective function E decreases with the gradual decreasing values of the corresponding optimal exergy output rate $\dot{EX}_{out}$ (Fig. 12).

iii) The maximum of each objective functions F and EPC decreases with the abrupt increasing values of the corresponding optimal exergy destruction rate $\dot{EX}_D$ (Fig. 13), while the maximum of the objective function E decreases with the gradual increasing values of the corresponding optimal exergy destruction rate $\dot{EX}_D$ (Fig. 13).

To explore the effects of heat leakage and heat resistances, the optimal reference system is chosen according to whether $K_L = 0 \Rightarrow K_L/A = \xi = 0$ with in the first case $I_1 = 1.05$ when $I_2 = 1$ ($\psi_{EPC} = 2.88$, $q_E = 1156 \mathrm{W m^{-2}}$, $\dot{EX}_{out-E} = 8492\mathrm{W}$ and $\dot{EX}_{D-E} = 5038\mathrm{W}$) and in the second case $I_2 = 1.05$ when $I_1 = 1$ ($\psi_{EPC} = 2.44$, $q_E = 1144 \mathrm{W m^{-2}}$, $\dot{EX}_{out-E} = 8408\mathrm{W}$ and $\dot{EX}_{D-E} = 5938\mathrm{W}$).

Firstly ($\xi = 1.5$, $I_1 = 1.05$ and $I_2 = 1$); ψ_F and ψ_{EPC} are both lower than the highest coefficient of performance value by 18.87%, whereas ψ_E is lower by a rate of 27.23%, in Fig. 11(a). $\dot{EX}_{out-E}$, $\dot{EX}_{out-F}$ and $\dot{EX}_{out-EPC}$ are lower than the highest exergy output rate value which is itself proportional to the specific heating load by rates of 3.25%, 63.09% and 68.63% respectively, in Fig. 12(a). However, $\dot{EX}_{D-EPC}$ and $\dot{EX}_{D-F}$ are lower than the highest exergy destruction rate value by rates 75.22% and 70.62% respectively, in Fig. 13(a). Whereas $\dot{EX}_{D-E}$ is greater than the highest exergy destruction rate value by a rate 6% in Fig.13(a).

On the other hand ($\xi = 1.5$, $I_1 = 1$ and $I_2 = 1.05$); ψ_F and ψ_{EPC} are both lower than the highest coefficient of performance value by 15.07%, whereas ψ_E is lower by a rate of 19.44%, in Fig. 11(b). $\dot{EX}_{out-E}$, $\dot{EX}_{out-F}$ and $\dot{EX}_{out-EPC}$ are lower than the highest exergy output rate value which is itself proportional to the specific heating load by rates of 3.28%, 53.38% and 59.55% respectively, in Fig. 12(b). However, $\dot{EX}_{D-EPC}$ and $\dot{EX}_{D-F}$ are lower than the highest exergy destruction rate value by rates of 61.58% and 70.62% respectively, in Fig. 13(b). Whereas $\dot{EX}_{D-E}$ is greater than the highest exergy destruction rate value by rate 5.08% in Fig. 13(b).

We deduce that under the effects of the heat leakage and heat resistances, the THR AHP cycle has a significant advantage at the maxima of the F and the EPC criteria in terms of coefficient of performance. Nevertheless, the THR AHP cycle has a significant advantage at the maximum of the EPC, in terms of exergy destruction rate. Also, the system has a significant advantage at the maximum of the E, in terms of specific heating load and exergy output rate. Moreover, the effects of heat resistances and heat leakages are

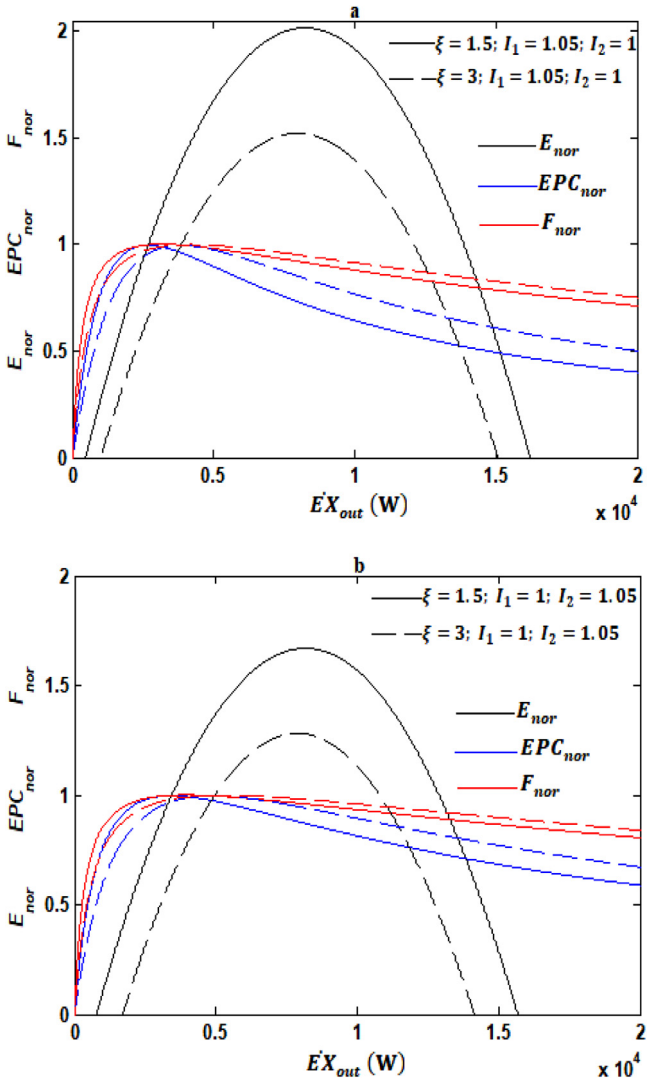

Fig. 12. Effects of heat leakage coefficient ξ on the dimensionless E_{nor}, EPC_{nor} and F_{nor} with respect to the $\dot{E}X_{out}$ objective function.

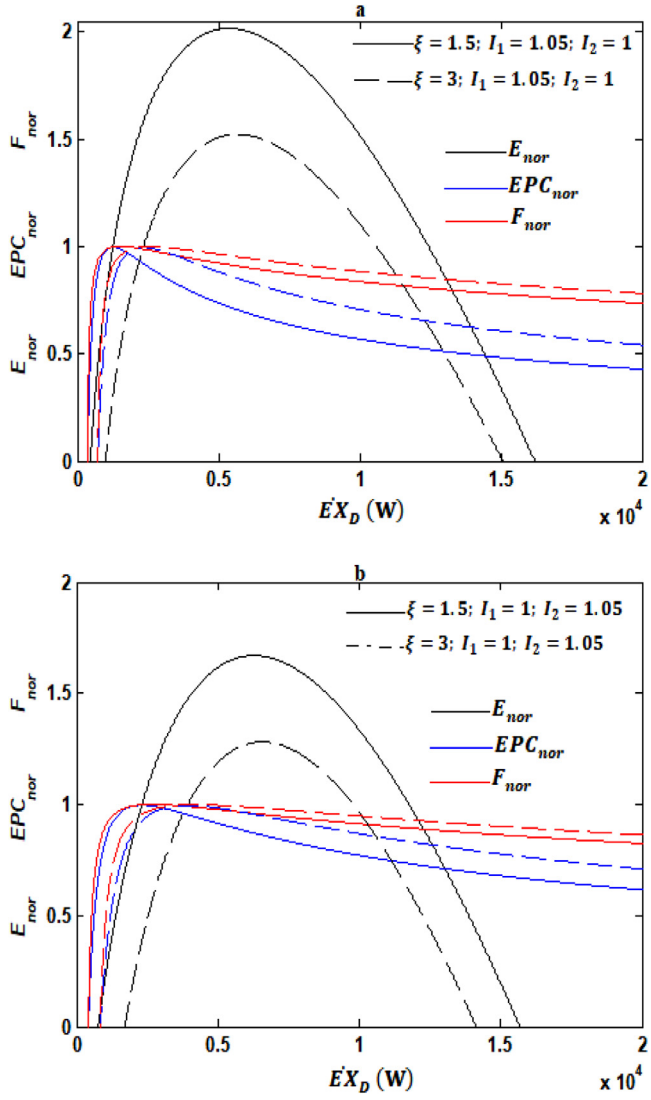

Fig. 13. Effects of heat leakage coefficient ξ on the dimensionless E_{nor}, EPC_{nor} and F_{nor} with respect to the $\dot{E}X_D$ objective function.

more pronounced than the effects of internal irreversibility factors, on the performance of THR AHP.

5. Conclusion

In this paper, the optimization of AHP from three objective functions such as the exergetic performance criterion (EPC), the exergy-based ecological function (E) and the thermo-economic function (F) under the influences of several design parameters has been carried out. Nevertheless, a comparative study of the advantages and drawbacks of each performance criterion was made according to the corresponding optimal performance parameters such as the coefficient of performance, the specific heating load, the exergy output rate and the exergy destruction rate. As a result, the finite time thermodynamics analysis and the Flowchart optimization method allowed us to obtain consistent, significant and precise results. The three important aspects to be addressed are:

- The highest maximum values of the thermo-economic criterion correspond to a low cost on investment (low heat exchange area) and a high cost on the energy consumed (heat input from the generator heat source is high). This promotes minimal exergy destruction rate for certain values of the specific heating load and exergy output rate.
- The influences of heat leakages and heat resistances are more pronounced than the heat losses characterized by internal irreversibility factors I_1 and I_2. Furthermore, under the influences of design parameters, the THR AHP cycle presents a significant advantage at the maxima of the F and the EPC criteria in terms of coefficient of performance. Nevertheless, the THR AHP cycle presents a significant advantage at the maximum of the EPC in terms of exergy destruction rate and at the maximum of the E in terms of specific heating load and exergy output rate.
- The heat losses in the condenser-evaporator assembly have more detrimental effects on the performance of the THR AHP cycle.

The evaluation protocol obtained leads to concrete results for the design of real absorption heat pumps by making a compromise between economic, exergetic and ecological gains.

Declaration of Competing Interest

The authors declare no conflicts of interest.

Acknowledgments

The authors are grateful to the Energy, Electrical Systems and Electronics Laboratory of the University of Yaounde I. The authors equally thank the reviewers for their constructive comments that help to improve the quality of the paper. In particular, the author Rodrigue Léo Fossi Nemogne wishes to thank the unconditional and mighty support, Mr. and Mrs. Tsopgni and Landry Tcheho.

Funding

This research did not receive any specific grant from funding agencies in the public, commercial, or not-for-profit sectors.

References

Ahmadi, M.H., Ahmadi, M.A., 2016. Multi objective optimization of performance of three-heat-source irreversible refrigerators based algorithm NSGAII. Renew. Sustain. Energy Rev. 60, 784–794.
Ahmadi, M.H., Ahmadi, M.A., Mehrpooya, M., Hosseinzade, H., Feidt, M., 2014a. Thermodynamic and thermo-economic analysis and optimization of performance of irreversible four-temperature-level absorption refrigeration. Energy Convers. Manag. 88, 1051–1059.
Ahmadi, M.H., Ahmadi, M.A., Mehrpooya, M., Sameti, M., 2015. Thermo-ecological analysis and optimization performance of an irreversible three-heat-source absorption heat pump. Energy Convers. Manag. 105, 1125–1137.
Ahmadi, M., Ahmadi, M.A., Pourfayaz, F., Bidi, M., 2016. Thermodynamic analysis and optimization for an irreversible heat pump working on reversed Brayton cycle. Energy Convers. Manag. 110, 260–267.
Ahmadi, P., Dincer, I., Rosen, M.A., 2014b. Thermoeconomic multi-objective optimization of a novel biomass-based integrated energy system. Energy 68, 958–970.
Ally, M.R., Sharma, V., 2018. Variability of absorption heat pump efficiency for domestic water heating and space heating based on time-weighted bin analysis. Appl. Therm. Eng. 130, 515–527.
Andresen, B., 2011. Current trends in finite-time thermodynamics. Angew. Chem. Int. Ed. 50 (12), 2690–2704.
Angulo-Brown, F., 1991. An ecological optimization criterion for finite-time heat engines. J. Appl. Phys. 69, 7465.
Bejan, A., 1996. Entropy generation minimization: the new thermodynamics of finite-size devices and finite-time processes. J. Appl. Phys. 79 (3), 1191–1218.
Bhardwaj, P.K., Kaushik, S.C., Jain, S., 2003. Finite time optimization of an endoreversible vapour absorption refrigeration system. Energy Convers. Manag. 44, 1131–1144.
Bhardwaj, P.K., Kaushik, S.C., Jain, S., 2005. General performance characteristics of an irreversible vapour absorption refrigeration system using finite time thermodynamic approach. Int. J. Therm. Sci. 44, 189–196.
Bi, Y., Lingen Chen, L., Sun, F., 2008. Heating load density and cop optimizations of an endoreversible air heat-pump. Appl. Energy 85, 607–617.
Chaves Fortes, A.F., Carvalho, M., da Silva, J.A.M., 2018. Environmental impact and cost allocations for a dual product heat pump. Energy Convers. Manag. 173, 763–772.
Chen, J., 1999. The general performance characteristics of an irreversible absorption heat pump operating between four-temperature-level. J. Phys. D: Appl. Phys. 32, 1428–1433.
Chen, L., Ge, Y.L., Qin, X., Xie, Z.H., 2019. Exergy-based ecological optimization for a four-temperature level absorption heat pump with heat resistance, heat leakage and internal irreversibility. Int. J. Heat Mass Transf. 129, 855–861.
Chen, L., Qin, X., Sun, F.R., 2007a. Model of irreversible finite heat capacity heat reservoir absorption heat transformer cycle and its application. Proc. IMechE C: J. Mech. Eng. Sci. 221 (C12), 1643–1652.
Chen, L., Qin, X., Sun, F., Wu, C., 2005a. Irreversible absorption heat-pump and its optimal performance. Appl. Energy 81, 55–71.
Chen, L., Wu, C., Sun, F., 1999. Finite time thermodynamic optimization or entropy generation minimization of energy systems. J. Non-Equilib. Thermodyn. 24 (4), 327–359.
Chen, L., Sun, F., 2004. Advances in Finite Time Thermodynamics: Analysis and Optimization. Nova Science Publishers, New York.
Chen, L., Xiaoqin, Z., Sun, F., Wu, C., 2007b. Exergy-based ecological optimization for a generalized irreversible Carnot heat-pump. Appl. Energy 84, 78–88.
Chen, L., Zheng, T., Sun, F., Wu, C., 2005b. Performance limits of real absorption refrigerators. J. Energy Inst. 78 (3), 139–144.
Chen, L., Zheng, T., Sun, F., Wu, C., 2006. Irreversible four-temperature-level absorption refrigerator. Sol. Energy 80 (3), 347–360.
Dixit, M., Arora, A., Kaushik, S.C., 2017. Thermodynamic and thermoeconomic analyses of two stage hybrid absorption compression refrigeration system. Appl. Therm. Eng. 113, 120–131.
Durmayaz, A., Sogut, O.S., Sahin, B., Yavuz, H., 2004. Optimization of thermal systems based on finite-time thermodynamics and thermoeconomics. Prog. Energy Combust. Sci. 30, 175–217.
Farshi, G.L., Mahmoudi, S.M.S., Rosen, M.A., Yari, M., Amidpour, M., 2013. Exergoeconomic analysis of double effect absorption refrigeration systems. Energy Convers. Manag. 65, 13–25.
Feidt, M., 2010. Thermodynamics applied to reverse cycle machines, a review. Int. J. Refrig. 33 (7), 1327–1342.
Feidt, M., 2013. Evolution of thermodynamic modelling for three and four heat reservoirs reverse cycle machines: a review and new trends. Int. J. Refrig. 36 (1), 8–23.
Fossi Nemogne, R.L., Medjo Nouadje, B.A., Ngouateu Wouagfack, P.A., Tchinda, R., 2019. Thermo-ecological analysis and optimization of a three-heat-reservoir absorption heat pump with two internal irreversibilities and external irreversibility. Int. J. Refrig. 106, 447–462.
Frikha, S., Abid, M.S., 2016. Performance optimization of irreversible combined Carnot refrigerator based on ecological criterion. Int. J. Refrig. 62, 153–165.
Ge, Y.L., Chen, L.G., Sun, F., 2016. Progress in finite time thermodynamic studies for internal combustion engine cycles. Entropy 18 (4), 139.
Huang, Y., Sun, D., Kang, Y., 2008. Performance optimization for an irreversible four-temperature-level absorption heat pump. Int. J. Therm. Sci. 47, 479–485.
Hu, B., Li, Y., Wang, R.Z., Cao, F., Xing, Z., 2018. Real-time minimization of power consumption for air-source transcritical CO_2 heat pump water heater system. Int. J. Refrig. 85, 395–408.
Kato, Y., Sasaki, Y., Yoshizawa, Y., 2005. Magnesium oxide/water chemical heat pump to enhance energy utilization of a cogeneration system. Energy 30, 2144–2155.
Kaushik, S.C., Arora, A., 2009. Energy and analysis of single effect and series flow double effect water–lithium bromide absorption refrigeration systems. Int. J. Refrig. 32, 1247–1258.
Kaushik, S., Tyagi, S.K., Kumar, P., 2018. Finite Time Thermodynamics of Power and Refrigeration Cycles. Springer, New York.
Kilic, M., Kaynakli, O., 2007. Second law-based thermodynamic analysis of water-lithium bromide absorption refrigeration system. Energy 32, 1505–1512.
Kodal, A., Sahin, B., Ekmekci, I., Yilmaz, T., 2003. Thermoeconomic optimization for irreversible absorption heat pump. Energy Convers. Manag. 44, 109–123.
Kodal, A., Sahin, B., Erdil, A., 2002. Performance analysis of a two-stage irreversible heat pump under maximum heating load per unit total cost conditions. Exergy Int. J. 2, 159–166.
Kodal, A., Sahin, B., Oktem, A.S., 2000. Performance analysis of two stage combined heat pump system based on thermo-economic optimization criterion. Energy Convers. Manag. 41, 1989–1998.
Leonzio, G., 2017. Mathematical model of absorption and hybrid heat pump. Chin. J. Chem. Eng. 25 (10), 1492–1504.
Li, Q.Y., Chen, Q., Zhang, X., 2013. Performance analysis of a rooftop wind solar hybrid heat pump system for buildings. Energy Build. 65, 75–83.
Liu, F., Sui, J., Liu, T., Jin, H., 2017. Performance investigation of a combined heat pump transformer operating with water/lithium bromide. Energy Convers. Manag. 140, 295–306.
Lostec, B.L., Millette, J., Galanis, N., 2010. Finite time thermodynamics study and exergetic analysis of ammonia-water absorption systems. Int. J. Therm. Sci. 49, 1264–1276.
Mastrullo, R., Renno, C.A., 2010. Thermoeconomic model of a photovoltaic heat pump. Appl. Therm. Eng. 30, 1959–1966.
Medjo Nouadje, B.A., Ngouateu Wouagfack, P.A., Tchinda, R., 2014. Influence of two internal irreversibilities on the new thermo-ecological criterion for three-heat–source refrigerators. Int. J. Refrig. 38, 118–127.
Medjo Nouadje, B.A., Ngouateu Wouagfack, P.A., Tchinda, R., 2016. Finite-time thermodynamics optimization of an irreversible parallel flow double-effect absorption refrigerator. Int. J. Refrig. 67, 433–444.
Misra, R.D., Sahoo, P.K., Gupta, A., 2005. Thermoeconomic evaluation and optimization of a double-effect H_2O/LiBr vapour-absorption refrigeration system. Int. J. Refrig. 28, 331–343.
Misra, R.D., Sahoo, P.K., Sahoo, S., Gupta, A., 2003. Thermoeconomic optimization of a single effect water/LiBr vapour absorption refrigeration system. Int. J. Refrig. 26, 158–169.
Ngouateu Wouagfack, P.A., Tchinda, R., 2011a. Performance optimization of three--heat-source irreversible refrigerators based on a new thermo-ecological criterion. Int. J. Refrig. 34, 1008–1015.
Ngouateu Wouagfack, P.A., Tchinda, R., 2011b. Irreversible three-heat-source refrigerator with heat transfer law of $Q\alpha\Delta(T^{-1})$ and its performance optimization based on *ECOP* criterion. Energy Syst. 2, 359–376.
Ngouateu Wouagfack, P.A., Tchinda, R., 2012a. The new thermo-ecological performance optimization of an irreversible three-heat-source absorption heat pump. Int. J. Refrig. 35, 79–87.
Ngouateu Wouagfack, P.A., Tchinda, R., 2012b. Optimal ecological performance of a four-temperature-level absorption heat pump. Int. J. Therm. Sci. 54, 209–219.
Ngouateu Wouagfack, P.A., Tchinda, R., 2013. Finite-time thermodynamics optimization of absorption refrigeration systems: a review. Renew. Sustain. Energy Rev. 21, 524–536.
Ngouateu Wouagfack, P.A., Tchinda, R., 2014. Optimal performance of an absorption refrigerator based on maximum ECOP. Int. J. Refrig. 40, 404–415.
Qin, X., Chen, L., Ge, Y., Sun, F., 2013. Finite time thermodynamic studies on absorption thermodynamic cycles: a state of the arts review. Arab. J. Sci. Eng. 38 (3), 405–419.
Qin, X., Chen, L., Ge, Y., Sun, F., 2015. Thermodynamic modeling and performance analysis of the variable-temperature heat reservoir absorption heat pump cycle. Phys. A: Stat. Mech. Appl. 436, 788–797.

Qin, X., Chen, L., Sun, F., He, L., 2007. Model of real absorption heat pump cycle with a generalized heat transfer law and its performance. Proc. IMechE A: J. Power Energy 221 (A7), 907–916.
Qin, X., Chen, L., Sun, F., Wu, C., 2004a. An absorption heat-transformer and its optimal performance. Appl Energy 78, 329–346.
Qin, X., Chen, L., Sun, F., Wu, C., 2004b. Optimal performance of an endoreversible four-heat-reservoir absorption heat-transformer. Open Syst. Inf. Dyn. 11 (2), 147–159.
Qin, X., Chen, L., Sun, F., Wu, C., 2006. Performance of an endoreversible four-heat-reservoir absorption heat pump with a generalized heat transfer law. Int. J. Therm. Sci. 45, 627–633.
Qin, X., Chen, L., Sun, F., Wu, C., 2005. Thermoeconomic optimization of an endoreversible four-heat reservoir absorption-refrigerator. Appl. Energy 81 (4), 420–433.
Qin, X., Chen, L., Sun, F., Wu, C., 2008. Performance of real absorption heat-transformer with a generalised heat transfer law. Appl. Therm. Eng. 28, 767–776.
Qin, X., Chen, L., Sun, F., 2010. Thermodynamic modeling and performance of variable-temperature heat reservoir absorption refrigeration cycle. Int. J. Exergy 7 (4), 521–534.
Qin, X., Chen, L., Xia, S., 2017. Ecological performance of four-temperature-level absorption heat transformer with heat resistance, heat leakage and internal irreversibility. Int. J. Heat Mass Transf. 114, 252–257.
Qureshi, B.A., Syed, M.Z., 2015. Thermoeconomic considerations in the allocation of heat transfer inventory for irreversible refrigeration and heat pump systems. Int. J. Refrig. 54, 67–75.
Rivera, W., Best, R., Cardoso, M.J., Romero, R.J., 2015. A review of absorption heat transformers. Appl. Therm. Eng. 91, 654–670.
Sahin, B., Kodal, A., Ekmekci, I., Yilmaz, T., 1997. Exergy optimization for an endoreversible cogeneration cycle. Energy 22, 551–557.
Sarbu, I., 2014. A review on substitution strategy of non-ecological refrigerants from vapour compression-based refrigeration, air-conditioning and heat pump systems. Int. J. Refrig. 46, 123–141.
Sieniutycz, S., Salamon, P., 1990. Advances in Thermodynamics. Volume 4: Finite Time Thermodynamics and Thermoeconomics. Taylor & Francis, New York.
Silveira, J.L., Tuna, C.E., 2003. Thermoeconomic analysis method for optimization of combined heat and power systems. Part I. Progr. Energy Combust. Sci. 29, 479–485.
Silveira, J.L., Tuna, C.E., 2004. Thermoeconomic analysis method for optimization of combined heat and power systems. Part II. Prog. Energy Combust. Sci. 30, 673–678.
Su, H., Gong, G., Wang, C., Zhang, Y., 2017. Thermodynamic optimization of an irreversible Carnot refrigerator with heat recovery reservoir. Appl. Therm. Eng. 110, 1624–1634.
Sun, F., Qin, X., Chen, L., Wu, C., 2005. Optimization between heating load and entropy-production rate for endoreversible absorption heat-transformers. Appl. Energy 81 (4), 434–448.
Talbi, M.M., Agnew, B., 2000. Exergy analysis: an absorption refrigerator using lithium bromide and water as the working fluids. Appl. Therm. Eng. 20, 619–630.
Ust, Y., Sahin, B., Ali, K., Akay, I.H., 2006a. Ecological coefficient of performance analysis and optimization of an irreversible regenerative Brayton heat engine. Appl. Energy 83, 558–572.
Ust, Y., Sahin, B., Ali, K., 2006b. Performance analysis of an irreversible Brayton heat engine based on ecological coefficient of performance criterion. Int. J. Therm. Sci. 45, 94–101.
Ust, Y., Sahin, B., Kodal, A., 2007. Optimization of a dual cycle cogeneration system based on a new exergetic performance criterion. Appl. Energy 84, 1079–1091.
Wang, D., Liu, Y., Kou, Z., Yao, L., Lu, Y., Tao, L., Xia, P., 2019. Energy and exergy analysis of an air-source heat pump water heater system using CO_2/R170 mixture as an azeotropy refrigerant for sustainable development. Int. J. Refrig. doi:10.1016/j.ijrefrig.2019.03.007.
Wang, L., Bu, X., Wang, H., Ma, Z., Ma, W., Li, H., 2018. Thermoeconomic evaluation and optimization of LiBr-H_2O double absorption heat transformer driven by flat plate collector. Energy Convers. Manag. 162, 66–76.
Wei, F., Lin, G., Chen, J., Bruck, E., 2011. Performance characteristics and parametric optimization of an irreversible magnetic Ericsson heat-pump. Phys. B: Condens. Matter 406, 633–639.
Wu, S., Lin, G., Chen, J., 2005. Optimum thermoeconomic and thermodynamic performance characteristics of an irreversible three-heat-source heat pump. Renew. Energy 30, 2257–2271.
Xia, D., Chen, L., Sun, F., Wu, C., 2007. Endoreversible four-reservoir chemical pump. Appl. Energy 84, 56–65.
Xiling, Z., Lin, F., Shigang, Z., 2011. General thermodynamic performance of irreversible absorption heat pump. Energy Convers. Manag. 52, 494–499.
Yuksel, Y.E., Ozturk, M., 2017. Thermodynamic and thermoeconomic analyses of a geothermal energy based integrated system for hydrogen production. Int. J. Hydrog. Energy 42, 2530–2546.
Zare, V., Mahmoudi, S.M.S., Yari, M., Amidpour, M., 2012. Thermoeconomic analysis and optimization of an ammonia-water power/cooling cogeneration cycle. Energy 47, 271–283.
Zheng, T., Chen, L., Sun, F., Wu, C., 2004. The influence of heat resistance and heat leak on the performance of a four-heat-reservoir absorption refrigerator with heat transfer law of $Q \propto \Delta(T^{-1})$. Int. J. Therm. Sci. 43 (12), 1187–1195.

Energy Conversion and Management 234 (2021) 113967

Contents lists available at ScienceDirect

Energy Conversion and Management

journal homepage: www.elsevier.com/locate/enconman

Multi-objective optimization and analysis of performance of a four-temperature-level multi-irreversible absorption heat pump

Rodrigue Léo Fossi Nemogne [a,*], Paiguy Armand Ngouateu Wouagfack [b], Brigitte Astrid Medjo Nouadje [c,d], Réné Tchinda [c,d]

[a] Electrical Systems and Electronics Laboratory, Department of Physics, University of Yaounde I, PO Box 812, Yaounde, Cameroon
[b] Department of Renewable Energy, Higher Technical Teachers' Traning College, University of Buea, PO Box 249, Buea Road, Kumba, Cameroon
[c] Research Unit for Mechanics and Modeling Physical Systems, Department of Physics, University of Dschang, PO Box 67, Dschang, Cameroon
[d] Research Unit in Industrial Systems and the Environment, University Institute of Technology Fotso Victor, University of Dschang, PO Box 134, Bandjoun, Cameroon

ARTICLE INFO

Keywords:
Exergy-based ecological criterion
Exergetic performance criterion
Thermo-economic criterion
Optimization
Absorption heat pump
Multi-irreversibilities

ABSTRACT

Performance analysis and multi-objective optimization based on finite-time thermodynamics are conducted in this paper for an absorption heat pump operating between four temperature levels. The exergy-based ecological (E), the exergetic performance (EPC) and the thermo-economic (F) criteria were considered as the objective functions. The maxima of the three objective functions and the corresponding optimal conditions were obtained by applying the flowchart optimization methodology. The influences of some design factors such as the economic indicators, internal irreversibility parameters, heat-transfer coefficients of heat exchangers and the distribution ratio rate of the total heat-reject quantity between the absorber and the condenser on the maxima of the exergy-based ecological (E), the exergetic performance (EPC) and the thermo-economic (F) objective functions and the corresponding optimal parameters have been analyzed and discussed. The results show that: (i) Materials with a low heat-transfer coefficient significantly affect the performance of the system. (ii) The detrimental effects of internal irreversibilities depend on the order of magnitude of the optimal heat-transfer rates in the absorber and the condenser. Finally, (iii) the optimum performance has been obtained for certain values of the heat exchange surface area and the exergy input rate from an economic point of view.

1. Introduction

Absorption heat pumps offer an undeniable environmental advantage over vapour compression heat pumps because they use environmentally friendly refrigerants. In addition, they also have the ability to operate with waste heat from various industries. However, they have a low coefficient of performance compared to vapour compression heat pumps. That is why many optimization studies on the basis of finite-time thermodynamics have been investigated on these systems to improve their performance [1–11]. In these referenced works, the coefficient of performance and heating load were considered as performance criteria to determine the efficiency bounds of various absorption heat pump cycles. Both energy criteria apply only the first law of thermodynamics and do not give the performance limits from the ecological point of view. The exergy-based ecological criterion (E) and exergetic performance criterion (EPC) which consider both the first and the second law of thermodynamics were then defined and applied to absorption heat pumps and heat transformers by some authors [12–21]. They obtained the optimal ecological and exergetic relationships and established for various absorption heat pump cycles the best compromise between the heating load and its dissipations. The ecological and exergetic criteria (E and EPC) do not take into account the investment cost as well as the consumption and maintenance costs of the absorption heat pumps. [23–30] proposed the thermo-economic criterion (F). They derived the performance limits with respect to the economical aspect: reduction of the cost in the design of the absorption heat pumps and reduction of their thermal consumption of energy. None of the previous works carried out the multi-objective optimization of the absorption heat pumps by considering at the same time the exergy-based ecological, exergetic performance and thermo-economic criteria.

Very recently Fossi Nemogne et al. [31] performed a multi-objective optimization of three-temperature-level absorption heat pumps by considering the ecological, exergetic performance and thermo-economic criteria as objective functions. By applying the flowchart optimization methodology [16,32], they determined the maxima of these three

* Corresponding author.
E-mail address: rodriguefossi@yahoo.fr (R.L. Fossi Nemogne).

https://doi.org/10.1016/j.enconman.2021.113967
Received 16 October 2020; Received in revised form 16 October 2020; Accepted 15 February 2021

Nomenclature

Symbols

A	heat-transfer area, m^2
C	cost, *ncu*
E	exergy-based ecological criterion, W
EPC	exergetic performance criterion, –
$\dot{E}X$	exergy rate, W
F	thermo-economic criterion $Wncu^{-1}$
I	internal irreversibility factor, –
k_1	capital costs for the unit heat-transfer area, $ncum^{-2}$
k_2	capital costs for the unit energy consumed, $ncuW^{-2}$
K	thermal conductance, WK^{-1}
m	distribution of the total rate of rejected heat -between the absorber and the condenser
q	specific heating load, Wm^{-2}
$\dot{Q}$	heat-exchange rate, W
S	entropy production rate,WK^{-1}
T	temperature
U	heat-transfer coefficient, $WK^{-1}m^{-2}$

Greek symbols

Δ	entropy production in a component, WK^{-1}
ξ	heat leakage coefficient, $WK^{-1}m^{-2}$
π	heating load, W
ψ	coefficient of performance, –

Subscripts

1	working fluid in generator
2	working fluid in evaporator
3	working fluid in condenser
4	working fluid in absorber
A	absorber
C	condenser
D	destruction
e	for the energy consumed cost
E	evaporator, at maximum, *E*
env	environment
EPC	at maximum, *EPC*
F	at maximum, *F*
G	generator
i	for the investment cost
in	input
L, L1, L2	heat leakage
max	maximum
out	output

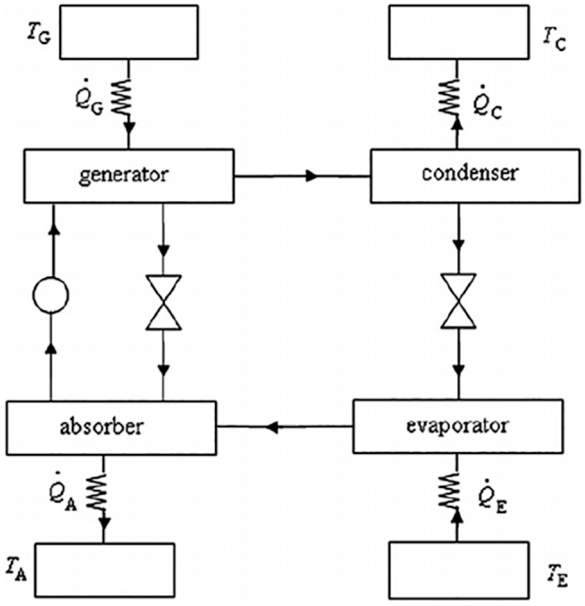

Fig. 1. Symbolic diagram of an absorption heat pump [14].

objective functions and the corresponding optimal conditions. They show that the three-heat-reservoir heat pump presents a significant advantage at the maxima of the ecological, exergetic performance and thermo-economic objective functions in terms of coefficient of performance, exergy destruction rate, specific heating load and exergy output rate.

In this paper, the 3E optimization technique [31] is extended to an irreversible four-temperature-level absorption heat pump which more closely models a real absorption heat pump.

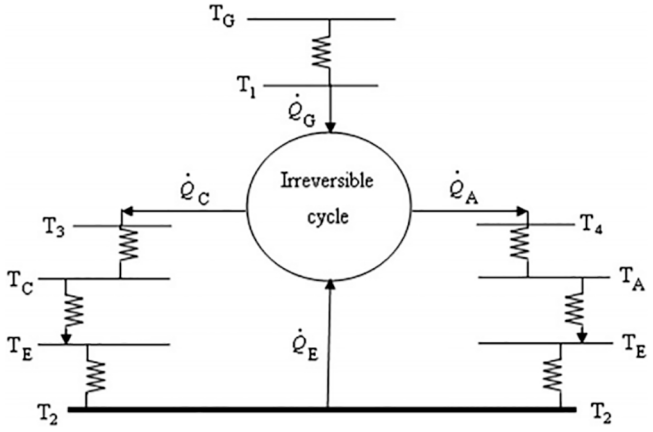

Fig. 2. The irreversible cycle model of a four-temperature-level absorption heat pump [14].

2. Model of the irreversible cycle of a single-effect absorption heat pump with four temperature levels

2.1. System description

The symbolic diagram summarizing the operation principle of the absorption heat pump is shown in Fig. 1 [14]. The liquid rich solution mixture coming from the absorber is compressed by a pump. It is evaporated in the generator due to heat input rate $\underset{G}{Q}$ to separate the refrigerant from the absorbent. While the resulting weak absorbent-refrigerant mixture goes to the absorber, the high pressure refrigerant vapour is condensed in the condenser to a sub-cooled liquid due to a discharge of heat rate $\underset{C}{Q}$ to the medium to be heated. The sub-cooled liquid is expanded and then evaporated in the evaporator by extracting heat rate $\underset{E}{Q}$ from the environment (heat sink). The vapour that emanates is super-heated and finally absorbed in the absorber in the

weak absorbent-refrigerant mixture by liberating heat rate $\underset{A}{Q}$ to the medium to be heated. In what follows, the absorbent-refrigerant pair used is that of the water-ammonia pair according to the temperatures considered in the various heat exchangers.

Some considerations are made to approximate the operating conditions of the proposed system to real ones. Firstly, the influences of internal dissipations during the flow of the absorbent-refrigerant mixture from the absorber to the generator under a high pressure and flow of the refrigerant from the condenser to the evaporator under a low pressure expansion are considered. Secondly, the influences of external irreversibility of finite-rate heat-transfer due to finite temperature differences between the generator, condenser, evaporator and absorber and heat sources as shown in Fig. 2 [14] are also taken into account.

2.2. Investigations on the first and second laws of thermodynamics

The first law of thermodynamics is deduced from Fig. 2 as follows [15,16,19]:

$$\underset{G}{Q} + \underset{E}{Q} - \underset{C}{Q} - \underset{A}{Q} = 0 \tag{1}$$

Considering the Newton's law of heat transfer one can write [17–31]:

$$\underset{G}{Q} = U_G A_G (T_G - T_1);\ \underset{E}{Q} = U_E A_E (T_E - T_2);\ \underset{C}{Q} = U_C A_C (T_3 - T_C);\ \underset{A}{Q} = U_A A_A (T_4 - T_A)$$

Besides, the rate of heat leakage from the heated reservoirs at temperatures T_C and T_A to the

environment at temperature T_E is expressed as [14]:

$$\underset{L}{Q} = \underset{L1}{Q} + \underset{L2}{Q} = K_L(T_C - T_E) + K_L(T_A - T_E) \tag{3}$$

where K_L is the thermal conductance due to heat leakage in $\left(WK^{-1}\right)$.

The total of heat-transfer area in the heat exchangers such as generator, evaporator, absorber and condenser is:

$$A = A_G + A_E + A_A + A_C \tag{4}$$

The internal dissipations of the working fluid are one of the main sources of irreversibility which can decrease the coefficient of performance and the heating load of absorption heat pump. The second law of thermodynamics describes this irreversibility due to the internal dissipation of the working substance and is written as [15,16,19]:

$$\Delta S_A + \Delta S_C - \Delta S_G - \Delta S_E > 0 \tag{5}$$

where, $\Delta S_A = \underset{A}{\dot{Q}}/T_4;\ \Delta S_C = \underset{C}{\dot{Q}}/T_3;\ \Delta S_E = \underset{E}{\dot{Q}}/T_2\ ;\Delta S_G = \underset{G}{\dot{Q}}/T_1.$

T_1, T_2, T_3 and T_4 in (K) represent the working fluid temperatures in the generator, evaporator, condenser and absorber, respectively. By introducing the internal irreversibility factors I_1 and I_2 for absorber-generator assembly and condenser-evaporator assembly respectively [17,31] Eq. (5) becomes:

$$\Delta S_A + \Delta S_C - I_1 \Delta S_G - I_2 \Delta S_E = 0 \tag{6}$$

where $I_1 = \Delta S_A/\Delta S_G\ (I_1 \geqslant 1)\ and\ I_2 = \Delta S_C/\Delta S_E\ (I_2 \geqslant 1)$

2.3. Performance indicators

The coefficient of performance ψ represents the amount of heat supplied to the surrounding to be heated compared to the amount of heat input. Though, the specific heating load q represents the flow of heat supplied to the surrounding to be heated per unit area (Wm^{-2}). They are given as follows [31]:

$$\psi = \pi/\dot{Q}_G = \left(\dot{Q}_C + \dot{Q}_A - \dot{Q}_L\right)\Big/\dot{Q}_G \text{and}\ q = \pi/A = \left(\dot{Q}_C + \dot{Q}_A - \dot{Q}_L\right)\Big/A \tag{8}$$

where the heating load π represents the heat rate supplied to the medium to be heated (W).

By combining Eqs. (1) and (8) the heat transfer rates in the irreversible four-temperature-level absorption heat pumps are obtained:

$$\dot{Q}_G = \pi/\psi;\ \dot{Q}_E = \pi\left(1 - \frac{1}{\psi}\right) + \dot{Q}_L;\ \dot{Q}_C = \left(\pi + \dot{Q}_L\right)\Big/(m+1);\ \dot{Q}_A = m\left(\pi + \dot{Q}_L\right)\Big/(m+1) \tag{9}$$

as well as the working fluid temperatures in the generator, evaporator, condenser and absorber from Eqs. (2) and (9):

$$T_1 = T_G - \frac{\pi}{U_G A_G \psi};\ T_2 = T_E - \frac{\pi\left(1 - \frac{1}{\psi}\right) + \underset{L}{\dot{Q}}}{U_E A_E};\ T_3 = T_C + \frac{\pi + \underset{L}{\dot{Q}}}{U_C A_C (m+1)};\ T_4 = T_A + \frac{m\left(\pi + \underset{L}{\dot{Q}}\right)}{U_A A_A (m+1)}$$

where $m = \dot{Q}_A/\dot{Q}_C$is the ratio of the rejected heat rate between the absorber and the condenser.

By substituting Eqs. (9) and (10) into Eq. (7), an optimal generalized expression between the design indicators (the internal dissipations factors, heat leaks, heat transfer coefficients, ratio of the heat rate rejected between the absorber and the condenser) and the performance parameters (the coefficient of performance and heating load) of an irreversible four-temperature-level absorption heat pump integrating the two laws of thermodynamics is obtained:

$$\left(\frac{1}{U_C A_C} + \frac{T_C(1+m)}{\pi + \dot{Q}_L}\right)^{-1} + \left(\frac{1}{U_A A_A} + \frac{T_A(1+m)}{m\left(\pi + \dot{Q}_L\right)}\right)^{-1} + I_1\left(\frac{1}{U_G A_G} - \frac{T_G \psi}{\pi}\right)^{-1} + I_2\left(\frac{1}{U_E A_E} - \frac{T_E}{\pi\left(1 - \frac{1}{\psi}\right) + \dot{Q}_L}\right)^{-1} = 0 \tag{11}$$

3. System performance and improvement tools

3.1. Exergy-based ecological criterion

The exergy-based ecological criterion (E) is expressed as the difference between the exergy output rate and exergy destruction rate [12,16,19,31]:

$$E = \underset{out}{EX} - \underset{D}{EX} \tag{12}$$

where the exergy output rate and exergy destruction rate are expressed respectively:

$$\underset{out}{EX} = \left(\underset{C}{Q} - \underset{L1}{Q}\right)\left(1 - \frac{T_{env}}{T_C}\right) + \left(\underset{A}{Q} - \underset{L2}{Q}\right)\left(1 - \frac{T_{env}}{T_A}\right) = \pi\left(1 - \frac{T_{env}}{m+1}\left(\frac{1}{T_C} + \frac{m}{T_A}\right)\right) + \frac{K_L T_{env}}{m+1}(T_A - mT_C + (m-1)T_E)\left(\frac{1}{T_A} - \frac{1}{T_C}\right) \tag{13}$$

$$\underset{D}{EX} = T_{env}\dot{\sigma} = T_{env}\left(\frac{\underset{C}{Q} - Q_{L1}}{T_C} + \frac{\underset{A}{Q} - Q_{L2}}{T_A} - \frac{\underset{G}{Q}}{T_G} - \frac{\underset{E}{Q} - \underset{L}{Q}}{T_E}\right)$$
$$= \frac{T_{env}}{m+1}\left(\pi\left(\frac{1}{T_C} + \frac{m}{T_A} - \frac{m+1}{\psi T_G} + \frac{m+1}{T_E}\left(\frac{1}{\psi} - 1\right)\right) - K_L(T_A - mT_C + (m-1)T_E)\left(\frac{1}{T_A} - \frac{1}{T_C}\right)\right) \quad (14)$$

In Eq. (14) $\dot{\sigma}$ represents the entropy production rate expressed in (WK^{-1}).

By substituting Eqs. (13) and (14) into Eq. (12), the exergy-based ecological function of a multi-irreversible four-temperature-level absorption heat pump is derived:

$$E = \pi\left(1 - T_{env}\left(2\left(\frac{1}{T_C} + \frac{m}{T_A}\right) - \frac{1}{\psi T_G} + \frac{1}{T_E}\left(\frac{1}{\psi} - 1\right)\right)\right) + \frac{2K_L T_{env}}{m+1}(T_A - mT_C + (m-1)T_E)\left(\frac{1}{T_A} - \frac{1}{T_C}\right) \quad (15)$$

3.2. Exergetic performance criterion

The exergetic performance criterion (EPC) accounts for the amount of exergy supplied by the system during a cycle compared to the amount of exergy destruction [21–31]. Using Eqs. (13) and (14) yields:

$$EPC = \frac{\underset{out}{EX}}{\underset{D}{EX}} = \frac{\pi\left(1 - \frac{T_{env}}{m+1}\left(\frac{1}{T_C} + \frac{m}{T_A}\right)\right) + \frac{K_L T_{env}}{m+1}(T_A - mT_C + (m-1)T_E)\left(\frac{1}{T_A} - \frac{1}{T_C}\right)}{\frac{T_{env}}{m+1}\left(\pi\left(\frac{1}{T_C} + \frac{m}{T_A} - \frac{m+1}{\psi T_G} + \frac{m+1}{T_E}\left(\frac{1}{\psi} - 1\right)\right) - K_L(T_A - mT_C + (m-1)T_E)\left(\frac{1}{T_A} - \frac{1}{T_C}\right)\right)} \quad (16)$$

3.3. Thermo-economic criterion

The thermo-economic criterion that provides information on the amount of heat supplied to the medium to be heated compared to the investment and the energy consumed costs is written as [25,31]:

$$F = \frac{\pi}{C_i + C_e} \quad (17)$$

where, $C_i = k_1 A$ and $C_e = k_2 \underset{G}{Q}$

C_i represents the investment cost and depends proportionally to the total heat-transfer area in the external heat reservoirs of the heat exchangers. C_e is the energy consumed cost and depends proportionally to the heat input rate. C_i and C_e have the value of the national currency unit (ncu). $k_1 = C_i/A$ and $k_2 = C_e/\underset{G}{Q}$ are the capital costs for the unit heat-transfer area and the unit energy consumed respectively [31]. Eq. (17) becomes:

$$F = \frac{1}{\frac{k_1}{q} + \frac{k_2}{\psi}} \quad (19)$$

3.4. Improvement

3.4.1. Exception examples

As mentioned in Section 2.3, Eq. (11) is the optimal generalized expression of a four-temperature-level absorption heat pump cycle. It includes the optimal performances of the irreversible three-temperature-level absorption heat pump cycle, the exoreversible, endoreversible and reversible four-temperature-level absorption heat pump cycles. From Eq. (11) we can therefore obtain the following configurations:

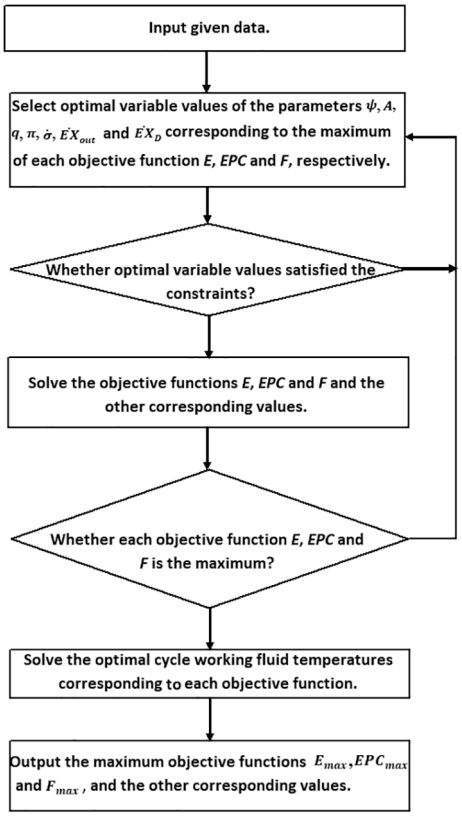

Fig. 3. The flowchart.

Eventuality 1, the irreversible three-temperature-level absorption heat pump cycle: $m = 1$ ($\underset{C}{\dot{Q}} = \underset{A}{\dot{Q}}$), $I_1 \neq 1$, $I_2 \neq 1$ and $K_L \neq 0$

$$\left(\frac{1}{U_C A_C} + \frac{2T_C}{\pi + \underset{L}{\dot{Q}}}\right)^{-1} + \left(\frac{1}{U_A A_A} + \frac{2T_A}{\left(\pi + \underset{L}{\dot{Q}}\right)}\right)^{-1} + I_1\left(\frac{1}{U_G A_G} - \frac{T_G\psi}{\pi}\right)^{-1} + I_2\left(\frac{1}{U_E A_E} - \frac{T_E}{\pi\left(1 - \frac{1}{\psi}\right) + \underset{L}{\dot{Q}}}\right)^{-1} = 0 \quad (20)$$

Eventuality 2, the exoreversible four-temperature-level absorption heat pump cycle: $K_L = 0$, $I_1 \neq 1$, $I_2 \neq 1$ and $m \neq 1$

$$\left(\frac{1}{U_C A_C} + \frac{T_C(1+m)}{\pi}\right)^{-1} + \left(\frac{1}{U_A A_A} + \frac{T_A(1+m)}{m\pi}\right)^{-1} + I_1\left(\frac{1}{U_G A_G} - \frac{T_G\psi}{\pi}\right)^{-1} + I_2\left(\frac{1}{U_E A_E} - \frac{T_E}{\pi\left(1 - \frac{1}{\psi}\right)}\right)^{-1} = 0 \quad (21)$$

Eventuality 3, the reversible four-temperature-level absorption heat pump cycle: $K_L = 0$, $I_1 = I_2 = 1$ and $m \neq 1$

$$\left(\frac{1}{U_C A_C} + \frac{T_C(1+m)}{\pi}\right)^{-1} + \left(\frac{1}{U_A A_A} + \frac{T_A(1+m)}{m\pi}\right)^{-1} + \left(\frac{1}{U_G A_G} - \frac{T_G\psi}{\pi}\right)^{-1} + \left(\frac{1}{U_E A_E} - \frac{T_E}{\pi\left(1 - \frac{1}{\psi}\right)}\right)^{-1} = 0 \quad (22)$$

Table 1
Parameters used in the model of the four-temperature-level absorption heat pump multi irreversible.

parameter	value
Temperature in generator, evaporator, condenser and absorber respectively, T(K)	413, 283, 333, 313 [9,14]
Heat-transfer coefficient of generator, evaporator, condenser and absorber respectively, U(WK^{-1}m^{-2})	1163, 2326, 4650, 1153 [9,14]
Distribution of the total rejected heat rate between the absorber and the condenser, m(-)	1.3 [9,14]
Total heat-transfer area of the external heat reservoirs in the heat exchangers, A(m^2)	100 [31]
Thermal conductance linked to heat leaks, K_L(WK^{-1})	300 [31]
Heat leakage coefficient, ξ(WK^{-1}m^{-2})	3 [9,14]
Economic parameters respectively, k_1(ncum^{-2}) and k_2(ncuW^{-1})	25, 5 [31]

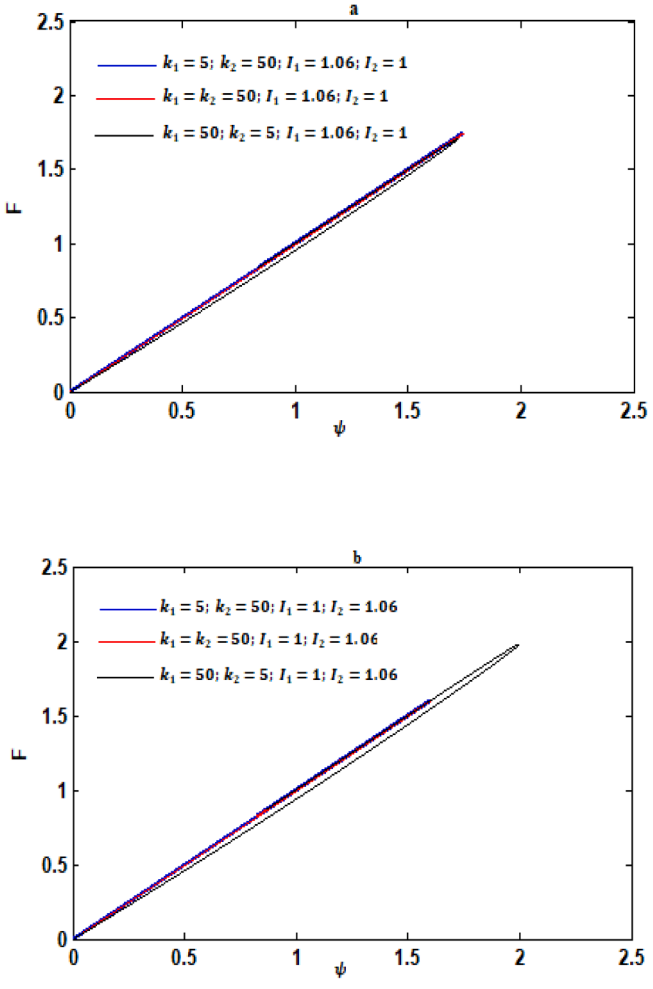

Fig. 4. Variations of the thermo-economic function (F) with respect to the coefficient of performance (ψ) for different values of economic parameters k_1 *and* k_2 the capital costs for the unit heat-transfer area and the unit energy consumed, respectively.

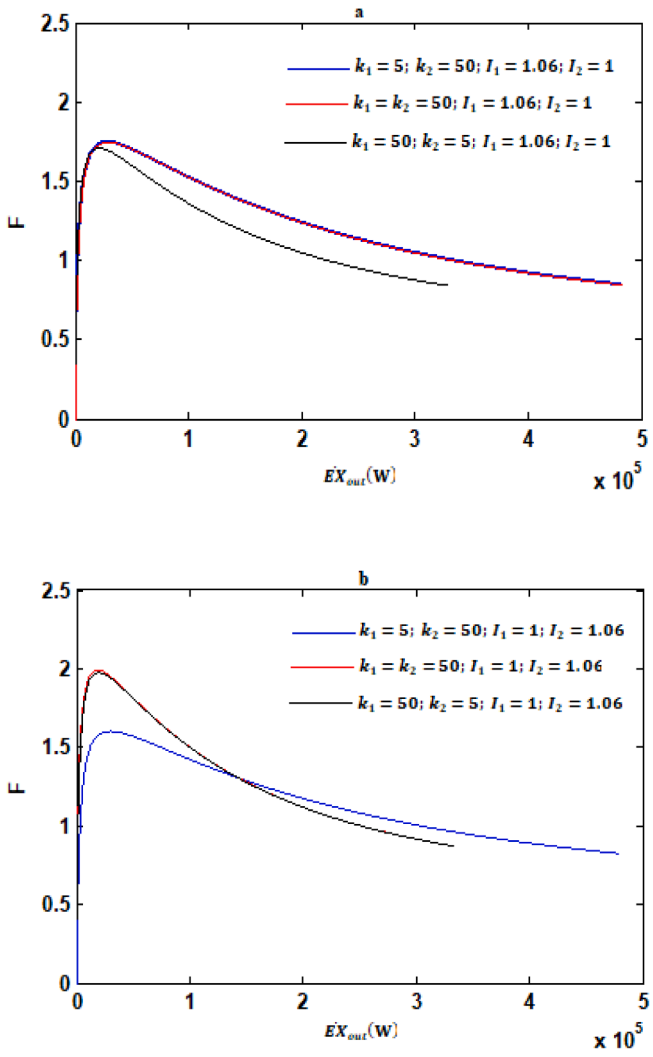

Fig. 5. Variations of the thermo-economic criterion (F) with respect to the exergy output rate ($\dot{EX}_{out}$) for different values of economic parameters k_1 *and* k_2 the capital costs for the unit heat-transfer area and the unit energy consumed, respectively.

Eventuality 4, the endoreversible four-temperature-level absorption heat pump cycle: $K_L \neq 0$, $I_1 = I_2 = 1$ and $m \neq 1$

$$\left(\frac{1}{U_C A_C} + \frac{T_C(1+m)}{\pi + \dot{Q}_L}\right)^{-1} + \left(\frac{1}{U_A A_A} + \frac{T_A(1+m)}{m\left(\pi + \dot{Q}_L\right)}\right)^{-1} + \left(\frac{1}{U_G A_G} - \frac{T_G \psi}{\pi}\right)^{-1} + \left(\frac{1}{U_E A_E} - \frac{T_E}{\pi\left(1 - \frac{1}{\psi}\right) + \dot{Q}_L}\right)^{-1} = 0 \quad (23)$$

3.4.2. Flowchart improvement

The maxima of the exergy-based ecological (E), exergetic performance (EPC) and thermo-economic (F) objective functions and the corresponding optimal temperatures, coefficient of performance, heating load, exergy output rate and exergy destruction rate are determined by using the flowchart algorithm as processed in Fig. 3. Recently, this algorithm was used by Su et al. [32] to optimize an irreversible Carnot refrigerator, Chen et al. [16] to improve the four-temperature-level absorption heat pump performances using the exergy-based ecological criterion as objective function and Fossi Nemogne et al. [31] to obtain a

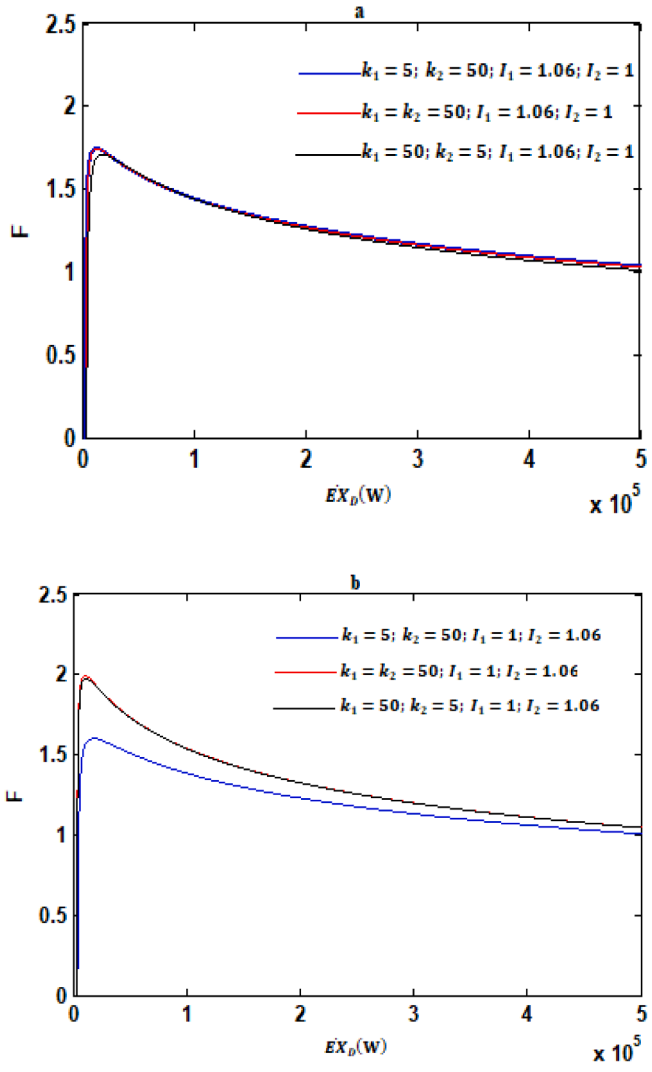

Fig. 6. Variations of the thermo-economic criterion (F) with respect to the exergy destruction rate ($\dot{E}X_D$) for different values of economic parameters k_1 *and* k_2 the capital costs for the unit heat-transfer area and the unit energy consumed, respectively.

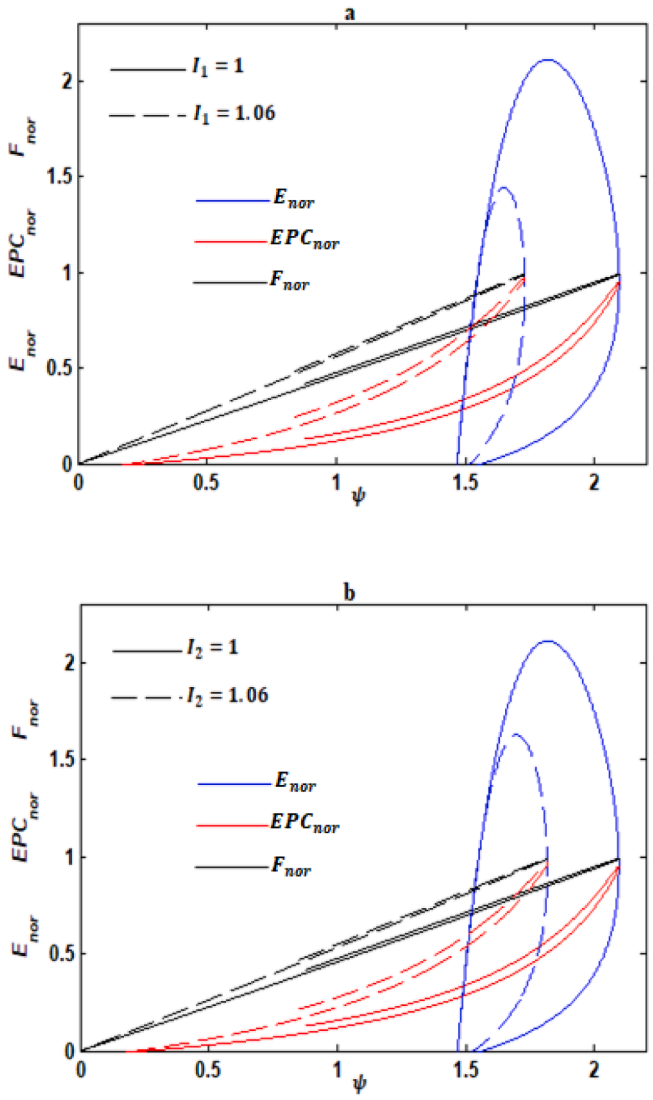

Fig. 7. Optimum characteristic curves of the ecological (E_{nor}), exergetic (EPC_{nor}) and thermo-economic (F_{nor}) normalized objective functions with respect to the coefficient of performance (ψ) for different I_1 values of the generator-absorber connection (a) and for different I_2 values of the evaporator-condenser connection (b).

compromise for optimal operations of a three-heat-reservoir absorption heat-pump.

4. Results and discussion

4.1. Numerical values

We have considered the numerical values given in Table 1.

4.2. Impacts of the design indicators on the exergy-based ecological, exergetic performance and economic criteria

Figs. 4–15 below describe the influences of some design indicators such as the thermo-economic factor, internal irreversibility parameters, heat-transfer coefficients of the heat-exchangers and distribution ratio rate of the total heat-reject quantity between the absorber and the condenser on the maxima of the exergy based-ecological (E), exergetic performance (EPC) and thermo-economic (F) objective functions and the corresponding optimal parameters. Figs. 4-6 present the variations of the thermo-economic objective function with respect to the coefficient of performance, exergy output rate and exergy destruction rate for different values of the economic factors k_1 *and* k_2. Figs. 7–15 illustrate the curves of the normalized exergy-based ecological $E_{nor}(E_{nor} = E/E_{op}$ where E_{op} is the optimal value of the exergy-based ecological function E corresponding to the maxima of thermo-economic F and exergetic performance EPC objective functions), normalized exergetic performance $EPC_{nor}(EPC_{nor} = EPC/EPC_{max})$ and normalized thermo-economic function $F_{nor}(F_{nor} = F/F_{max})$ with respect to the coefficient of performance ψ, exergy output rate EX_{out} and exergy destruction rate $\frac{EX}{D}$, respectively. This for different values of internal irreversibility factors I_I and I_2, heat-transfer coefficients U_G, U_E, U_C, U_A and ratio of the rejected heat rate of the absorber to the condenser m. Figs. 4–15 are obtained by varying the three objective functions and the coefficient of performance, exergy output rate and exergy destruction rate with respect to working fluid temperatures T_1, T_2, T_3 and T_4. The values of working fluid temperatures are taken around their optimal values calculated from the Flow-chart Algorithm. The optimal working fluid temperatures are those which maximize the three objective functions. Figs. 4–15 all demonstrate that the three objective functions considered in the present work can reach their maximum value with respect to the coefficient of performance, exergy output rate and exergy destruction rate. They also

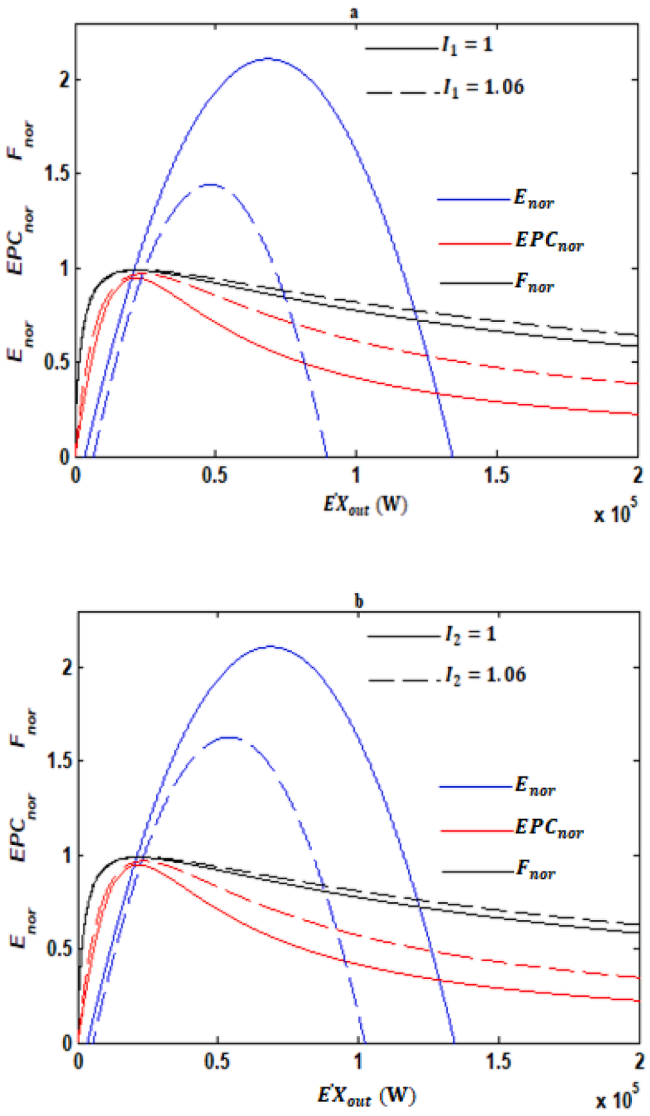

Fig. 8. Optimum characteristic curves of the ecological (E_{nor}), exergetic (EPC_{nor}) and thermo-economic (F_{nor}) normalized objective functions with respect to the exergy output rate ($\dot{EX}_{out}$) for different I_1 values of the generator-absorber connection (a) and for different I_2 values of the evaporator-condenser connection (b).

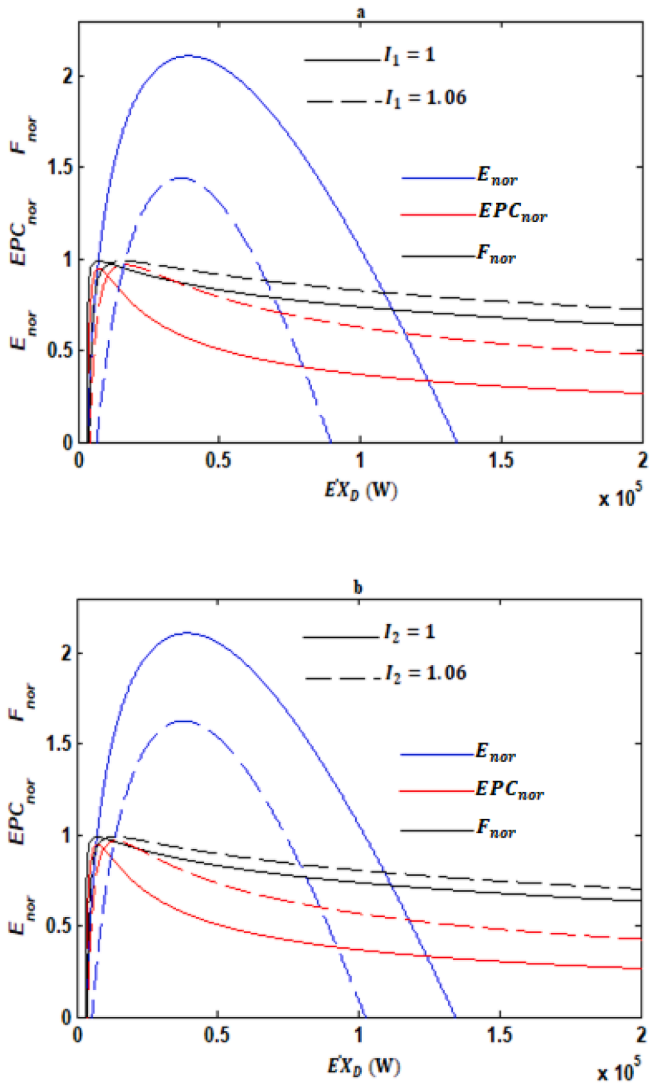

Fig. 9. Optimum characteristic curves of the ecological (E_{nor}), exergetic (EPC_{nor}) and thermo-economic (F_{nor}) normalized objective functions with respect to the exergy destruction rate ($\dot{EX}_D$) for different I_1 values of the generator-absorber connection (a) and for different I_2 values of the evaporator-condenser connection (b).

indicate that the variations of the three objective functions with respect to the coefficient of performance are loops.

4.2.1. *Impacts of the economic factors k_1 and k_2*

It is observed from Figs. 4–6 that when the capital cost for unit heat-transfer area k_1 is greater than or equal to the capital cost for the unit energy consumed k_2, the thermo-economic objective function increases under the impact of heat losses in the evaporator-condenser assembly (Fig. 4 (b)-6 (b)) and decreases under the impact of heat losses in the generator-absorber assembly (Fig. 4 (a)-6 (a)).

It follows that, the maximum economic performance is obtained for a specific range of values of the total heat transfer area and the exergy input rate. Also, by reducing heat losses from the generator-absorber assembly.

4.2.2. *Impact of the internal irreversibility factors I_1 and I_2*

Figs. 7–9 shows that the heat losses at the generator-absorber and condenser-evaporator assemblies characterized by I_1 and I_2 respectively strongly affect the maximum of the exergy-based ecological function (E_{max}). The effects are light on the maxima of exergetic performance (EPC_{max}) and thermo-economic (F_{max}) objectives functions.

The numerical results presented in Table 2 are derived from Figs. 7–9. It gives an overview of the effects of I_1 and I_2 on the optimal coefficient of performance, exergy output rate and exergy destruction rate.

It is shown from Table 2 that for fixed I_1 and I_2, the optimal coefficients of performance of the four-temperature-level absorption heat pump operating at EPC_{max} and F_{max}conditions are the same. It is also observed that the system has a significant benefit in terms of exergy destruction rate when it operates at EPC_{max} and F_{max} conditions. However, it is more efficient with respect to the coefficient of performance when functioning at E_{max} conditions. Even more, the harmful impact of internal irreversibility I_1 on the system performance is greater than that of I_2 in terms of coefficient of performance at E_{max}, EPC_{max} and F_{max} operating conditions; in terms of exergy output rate at E_{max} operating conditions and in terms of exergy destruction rate at EPC_{max} and F_{max} operating conditions.

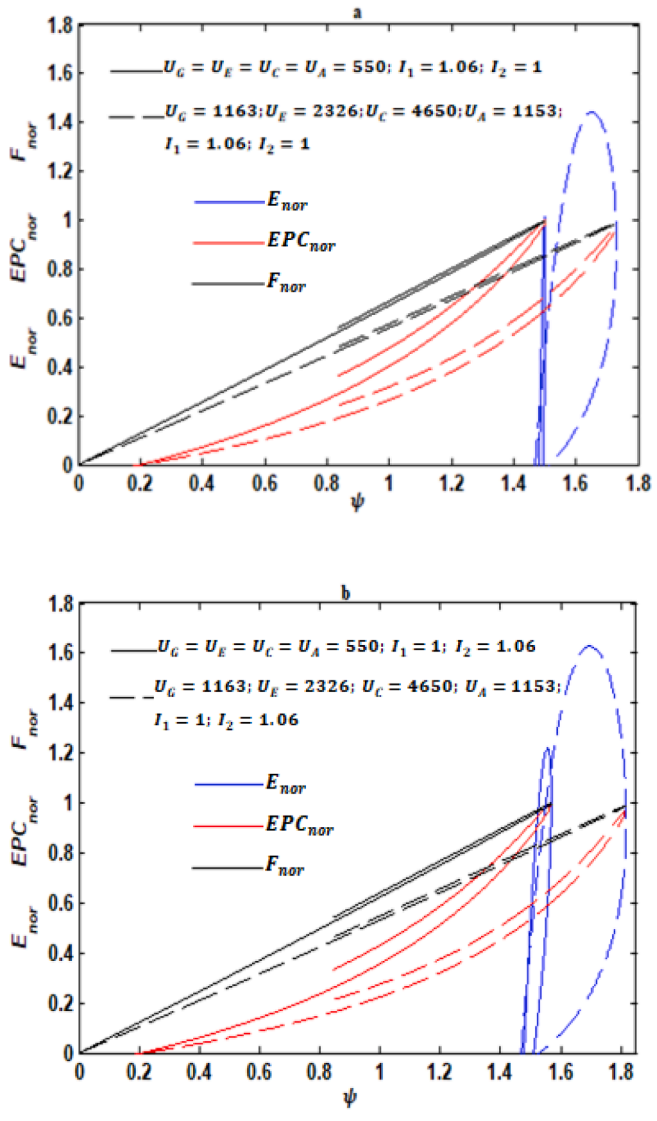

Fig. 10. Optimum characteristic curves of the ecological (E_{nor}), exergetic (EPC_{nor}) and thermo-economic (F_{nor}) normalized objective functions with respect to the coefficient of performance (ψ) for different heat-transfer coefficients values.

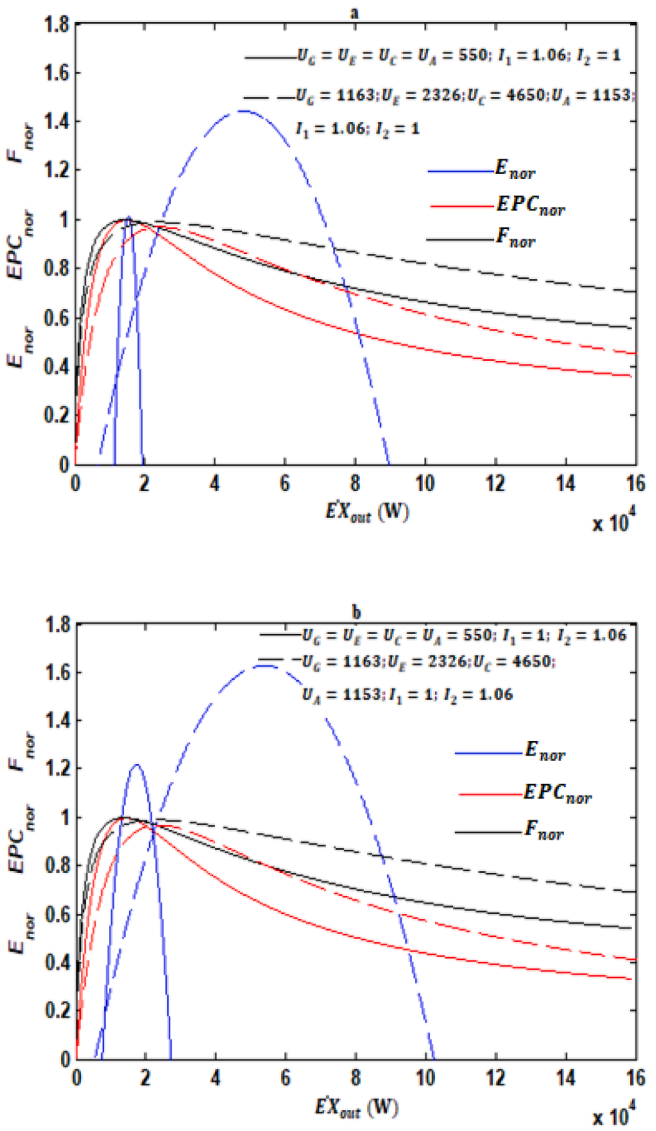

Fig. 11. Optimum characteristic curves of the ecological (E_{nor}), exergetic (EPC_{nor}) and thermo-economic (F_{nor}) normalized objective functions with respect to the exergy output rate ($\dot{EX}_{out}$) for different heat-transfer coefficients values.

4.2.3. Impact of Heat-transfer coefficients

Figs. 10–12 shows that the effects of heat transfer coefficients in the generator, evaporator, condenser and absorber are significant on the maximum of the exergy-based ecological function (E_{max}) while light on the maxima of exergetic performance (EPC_{max}) and thermo-economic (F_{max}) functions.

Table 3 summarizes Fig. 10(a), Fig. 11(a) and Fig. 12(a) when $I_1 = 1.06$, $I_2 = 1$ and Fig. 10 (b), Fig. 11(b) and Fig. 12(b) when $I_1 = 1$, $I_2 = 1.06$. It shows the effects of the nature of the main components (generator, condenser, evaporator and absorber) on the performance of the absorption heat pump cycle working at E_{max}, EPC_{max} and F_{max} conditions. We have taken into account two ranges of heat-transfer coefficients which range $U_G = 1163\,\mathrm{WK^{-1}m^{-2}}$; $U_E = 2326\,\mathrm{WK^{-1}m^{-2}}$; $U_C = 4650\,\mathrm{WK^{-1}m^{-2}}$ and $U_A = 1153\,\mathrm{WK^{-1}m^{-2}}$ is taken as reference is [9,14] because it gives better optimal performance values to the system. When $I_1 = 1.06$ and $I_2 = 1$ ($\psi_{EPC} = \psi_F = 1.73$, $EX_{out-E} = 47895\,\mathrm{W}$ and $EX_{D-F} = 15720\,\mathrm{W}$) and when $I_1 = 1$ and $I_2 = 1.06$ ($\psi_{EPC} = \psi_F = 1.817$, $EX_{out-E} = 53641\,\mathrm{W}$ and $EX_{D-F} = 13173\,\mathrm{W}$).

As a result, the four-temperature-level absorption heat pump cycle assumes small fluctuations in the optimal values of the coefficient of performance when using low heat-transfer coefficient materials in the four main heat exchangers. Furthermore, the performance of the system is greatly affected in terms of optimal exergy output rate. On the other hand, the optimal exergy destruction rate of the system are lower when it operates at E_{max}, EPC_{max} and F_{max} conditions.

4.2.4. Effects of the ratio of the rejected heat of the absorber to the condenser

The influences of the ratio of the rejected heat of the absorber to the condenser (m) on the ecological, exergetic and thermo-economic objective functions of performance are presented in Figs. 13–15. As it

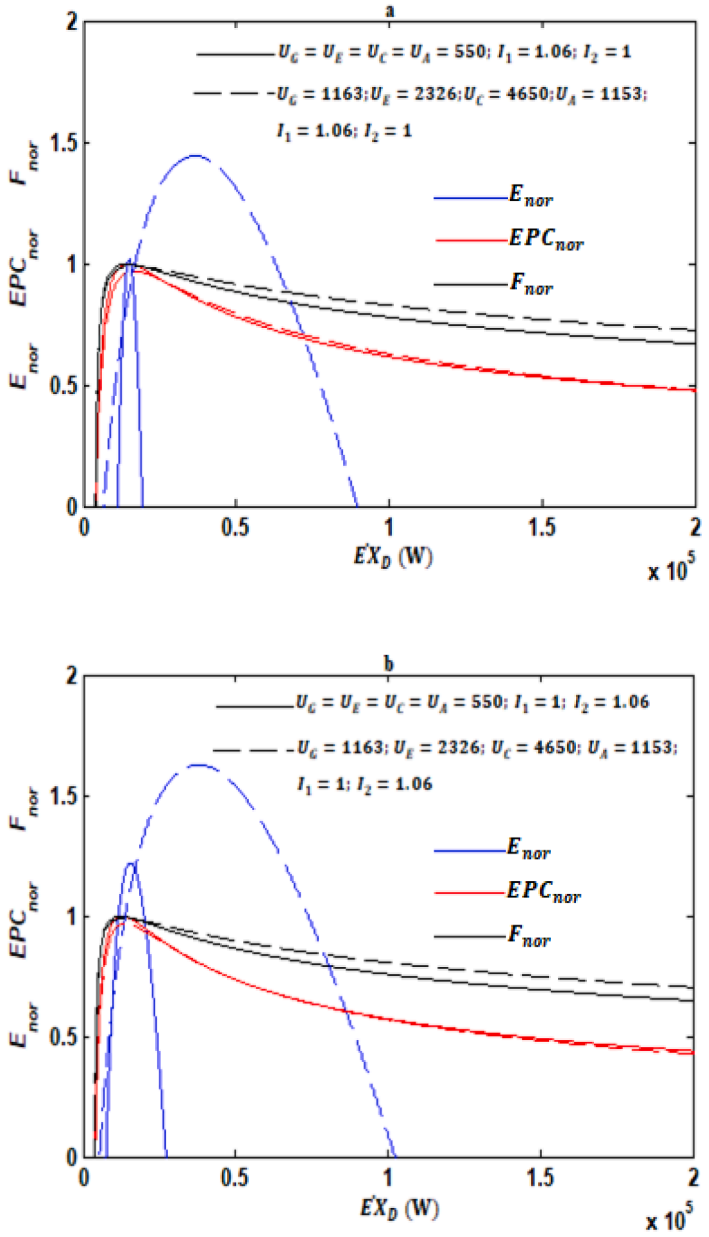

Fig. 12. Optimum characteristic curves of the ecological (E_{nor}), exergetic (EPC_{nor}) and thermo-economic (F_{nor}) normalized objective functions with respect to the exergy destruction rate ($\dot{EX}_D$) for different heat-transfer coefficients values.

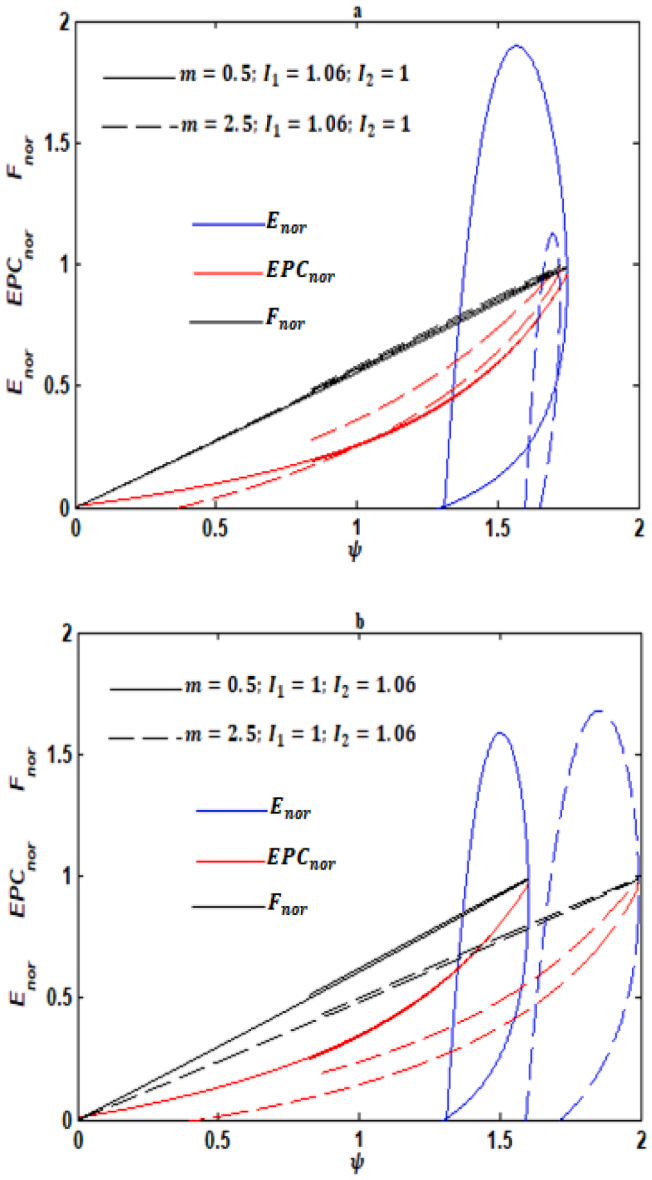

Fig. 13. Optimum characteristic curves of the ecological (E_{nor}), exergetic (EPC_{nor}) and thermo-economic (F_{nor}) normalized objective functions with respect to the coefficient of performance (ψ) for different values of the ratio of the rejected heat of the absorber to the condenser.

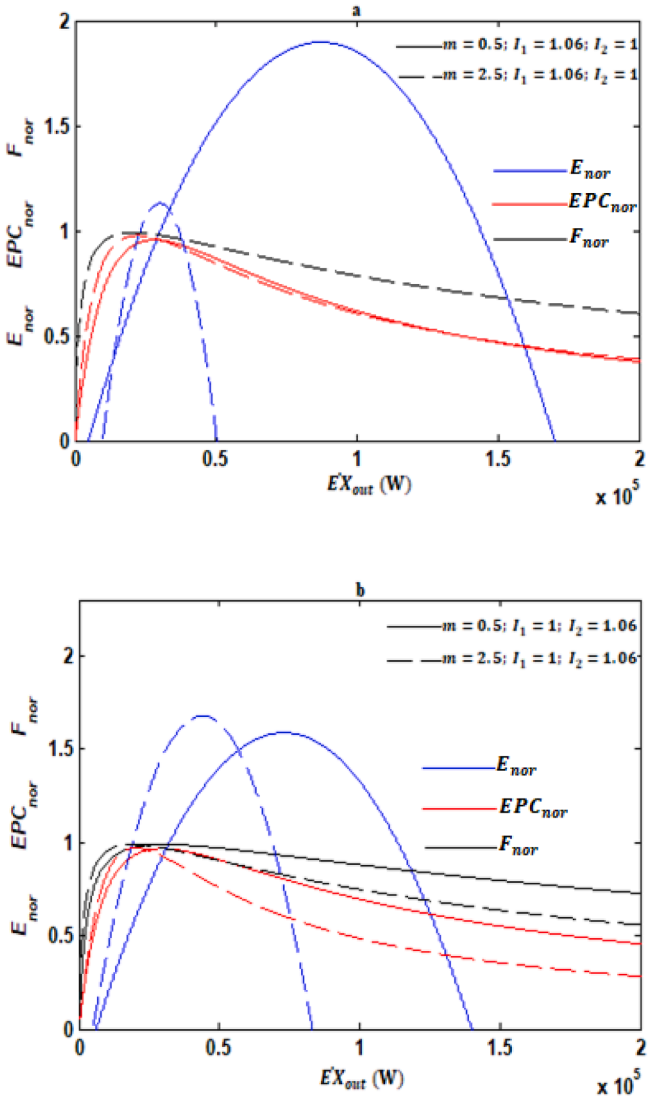

Fig. 14. Optimum characteristic curves of the ecological (E_{nor}), exergetic (EPC_{nor}) and thermo-economic (F_{nor}) normalized objective functions with respect to the exergy output rate ($\dot{EX}_{out}$) for different values of the ratio of the rejected heat of the absorber to the condenser.

can be seen in Figs. 13–15, the effects of the ratio m are significant on the maximum of the exergy-based ecological function (E_{max}) while light on the maxima of exergetic performance (EPC_{max}) and thermo-economic (F_{max}) functions.

An in-depth study of the influences of m on the four-temperature-level absorption heat pump cycle is made by considering $m = 0.5$ as optimal reference value (Table 4). On the one hand for $I_1 = 1.06$ and $I_2 = 1$ we have $\psi_{EPC} = \psi_F = 1.746$, $EX_{out-E} = 86844$W and $EX_{D-EPC} = 12332$ W ; and on the other hand $I_1 = 1$ and $I_2 = 1.06$ we have $\psi_{EPC} = \psi_F = 1.601$, $EX_{out-E} = 72756$W and $EX_{D-EPC} = 17388$ W.

The influences of the heat exchange rates in the absorber with the absorbent-refrigerant pair, and the condenser with the refrigerant, depend on the order of magnitude of these two heat exchange rate relative to each other. In fact, when the heat-exchange rate in the absorber $\dot{Q}_A$ is lower than the heat-exchange rate in the condenser $\dot{Q}_C$, at the maxima of the exergy-based ecological, exergetic performance and thermo-economic criteria, the system is more efficient in terms of coefficient of performance under the impact of heat losses between the generator and the absorber. At the maxima of the exergetic performance and thermo-economic criteria, the system is more efficient in terms of exergy destruction rate under the effect of the internal irreversibility factor I_1, yet at the maximum of exergy-based ecological criterion the best performances are recorded under the influence of heat losses between the evaporator and the condenser. However, at the maximum of exergy-based ecological criterion, the best performances are obtained in terms of exergy output rate under the effect of I_1, whereas, the best performances are obtained at the maxima of the exergetic performance and thermo-economic criteria in terms of exergy output rate under the influence of I_2. On the other hand, when the heat-exchange rate in the

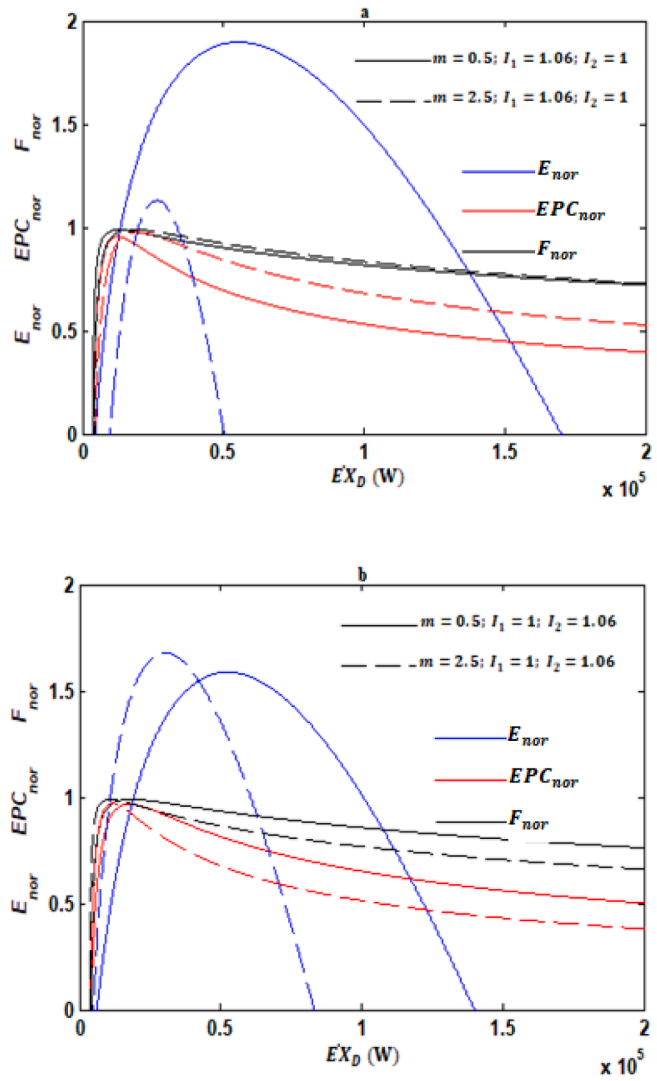

Fig. 15. Optimum characteristic curves of the ecological (E_{nor}), exergetic (EPC_{nor}) and thermo-economic (F_{nor}) normalized objective functions with respect to the exergy destruction rate ($E\dot{X}_D$) for different values of the ratio of the rejected heat of the absorber to the condenser.

absorber Q_A is greater than that in the condenser Q_C, at the maxima of the exergy-based ecological, exergetic performance and thermo-economic criteria, the system performs better in terms of coefficient of performance under the impact of heat losses between the evaporator and condenser. Thus, at the maximum of exergy-based ecological criterion, the best performances are recorded under the influence of heat losses between the generator and the absorber. However, at the maxima of the exergetic performance and thermo-economic criteria, the system is more efficient in terms of exergy destruction rate under the effects of the internal irreversibility factor I_2. However, at the maximum of exergy-based ecological criterion, the best performances are obtained in terms of exergy output rate under the effects of I_2, whereas, the best performances are obtained at the maxima of the exergetic performance and thermo-economic criteria in terms of exergy output rate under the influence of I_1.

5. Conclusion

The exergy-based ecological, exergetic performance and thermo-economic criteria were considered in this work to conduct the multi-objective optimization of a four-temperature-level absorption heat pump on the basis of finite-time thermodynamic approach. The benefits and limitations at the maximum of each objective function in terms coefficient of performance, exergy output rate and exergy destruction rate under the influences of design factors have led to the following aspects:

- The optimum economic performance is obtained for a specific range of values the exergy input rate and by reducing heat losses from the generator-absorber assembly.
- The performance of the four-temperature-level absorption heat pump cycle is unfavorable in terms of optimal exergy output rate and optimal specific heating load, when the materials which constitute the generator, evaporator, condenser and absorber have low heat-transfer coefficients. Its optimal exergy destruction rate is however better.
- Heat losses in the evaporator-condenser connection have a detrimental effect on the system, when Q_A is less than Q_C at the maximum ecological, exergetic and thermo-economic criteria in terms of coefficient of performance. The opposite effects are observed when Q_A is greater than Q_C.

So, the multi-objective optimization of the irreversible four-temperature-level absorption heat pump conducted in this paper takes into consideration several aspects that will allow the optimal design of a real single effect absorption heat pump. In particular the working fluids pair ammonia-water, the thermo-physical properties of these are similar to the considerations made.

CRediT authorship contribution statement

Rodrigue Léo Fossi Nemogne: Investigation, Conceptualization, Methodology, Software, Data curation, Writing - original draft, Writing - review & editing. **Paiguy Armand Ngouateu Wouagfack:** Visualization, Methodology, Writing - review & editing. **Brigitte Astrid Medjo Nouadje:** Visualization, Writing - review & editing. **Réné Tchinda:** Supervision.

Table 2
Comparative evaluation of the ecological E, exergetic EPC and thermo-economic F criteria with respect to the heat losses rates in the generator-absorber assembly and in the evaporator-condenser assembly (the reference is set for an endoreversible system $I_1 = I_2 = 1 K_L = 300\ \mathrm{WK}^{-1}$ [31] and $\psi_{EPC} = \psi_F = 2.095$, $EX_{out-E} = 68500\ \mathrm{W}$, $EX_{D-F} = 7062\ \mathrm{W}$).

	Parameters of performance	Losses rates corresponding to the E_{max}(%)	Losses rates corresponding to the EPC_{max}(%)	Losses rates corresponding to the F_{max}(%)
$I_1 = 1.06; I_2 = 1$	ψ	21.13	17.42	17.42
	EX_{out}	30.08	64.76	65.93
	EX_D	411.7	130.13	122.6
$I_1 = 1; I_2 = 1.06$	ψ	18.95	13.27	13.27
	EX_{out}	21.69	65.85	66.93
	EX_D	431.35	92.58	86.52

Table 3
Comparative evaluation of ecological E, exergetic EPC and thermo-economic F criteria with respect to heat losses rates under the effects of the heat-transfer coefficients.

	Parameters of performance	Losses rates corresponding to the E_{max}(%)	Losses rates corresponding to the EPC_{max}(%)	Losses rates corresponding to the F_{max}(%)
$I_1 = 1.06; I_2 = 1; U_G = U_E = U_C = U_A =$ 550 $WK^{-1}m^{-2}$	ψ	13.28	13.18	13.18
	EX_{out}	68.16	69.30	70.62
	$\frac{EX}{D}$	−4.91	−8.35	−12.24
$I_1 = 1; I_2 = 1.06; U_G = U_E = U_C = U_A =$ 550 $WK^{-1}m^{-2}$	ψ	14.28	13.71	13.71
	EX_{out}	67.86	73.55	74.66
	$\frac{EX}{D}$	17.36	−4.49	−8.46

Table 4
Comparative evaluation with ecological E, exergetic EPC and thermo-economic F criteria of the heat losses rates under the effects of the ratio of the rejected heat of the absorber to the condenser.

	Parameters of performance	Losses rates corresponding to the E_{max}(%)	Losses rates corresponding to the EPC_{max}(%)	Losses rates corresponding to the F_{max}(%)
$I_1 = 1.06; I_2 = 1; m =$ 2.5	ψ	2.84	1.54	1.54
	EX_{out}	65.53	74.61	76.65
	$\frac{EX}{D}$	113.24	53.79	41.66
$I_1 = 1; I_2 = 1.06; m =$ 2.5	ψ	−15.77	−24.46	−24.46
	EX_{out}	39.73	72.41	74.52
	$\frac{EX}{D}$	73.22	−34.19	−39.1

Declaration of Competing Interest

The authors declare that they have no known competing financial interests or personal relationships that could have appeared to influence the work reported in this paper.

Acknowledgments

The authors are grateful to the Energy, Electrical Systems and Electronics Laboratory of the University of Yaounde I. The authors equally thank the reviewers for their constructive comments that help to improve the quality of the paper.

Funding

This research did not receive any specific grant from funding agencies in the public, commercial, or not-for-profit sectors.

References

[1] Yan Z, Chen S. Finite time thermodynamic performance bound of three-heat-reservoir heat pumps. Chinese Sci Bull 1986;31:798–9.
[2] Chen J. The general performance characteristics of an irreversible absorption heat pump operating between four-temperature-level. J Phys D: Appl Phys 1999;32:1428–33.
[3] Chen L, Wu C, Sun F. Optimal coefficient of performance and heating load relationship of a three-heat-reservoir endoreversible heat pump. Energy Convers Manage 1997;38:727–33.
[4] Chen L, Qin X, Sun F, Wu C. Irreversible absorption heat-pump and its optimal performance. Appl Energy 2005;81:55–71.
[5] Qin X, Chen L, Sun F, Wu C. Performance of an endoreversible four-heat-reservoir absorption heat pump with a generalized heat transfer law. Int J Therm Sci 2006;45:627–33.
[6] Qin X, Chen L, Sun F, He L. Model of real absorption heat pump cycle with a generalized heat transfer law and its performance. Proc IMechE A: J Power Energy 2007;221(A7):907–16.
[7] Qin X, Chen L, Ge Y, Sun F. Thermodynamic modeling and performance analysis of the variable-temperature heat reservoir absorption heat pump cycle. Phys A: Stat Mech Appl 2015;436:788–97.
[8] Xia D, Chen L, Sun F, Wu C. Endoreversible four-reservoir chemical pump. Appl Energy 2007;84:56–65.
[9] Bi Y, Lingen Chen L, Sun F. Heating load density and COP optimizations of an endoreversible air heat-pump. Appl Energy 2008;85:607–17.
[10] Huang Y, Sun D, Kang Y. Performance optimization for an irreversible four-temperature-level absorption heat pump. Int J Therm Sci 2008;47:479–85.
[11] Xiling Z, Lin F, Shigang Z. General thermodynamic performance of irreversible absorption heat pump. Energy Convers Manage 2011;52:494–9.
[12] Chen L, Xiaoqin Z, Sun F, Wu C. Exergy-based ecological optimization for a generalized irreversible Carnot heat-pump. Appl Energy 2007;84:78–88.
[13] Ngouateu Wouagfack PA, Tchinda R. The new thermo-ecological performance optimization of an irreversible three-heat-source absorption heat pump. Int J Refrig 2012;35:79–87.
[14] Ngouateu Wouagfack PA, Tchinda R. Optimal ecological performance of a four-temperature-level absorption heat pump. Int J Therm Sci 2012;54:209–19.
[15] Ahmadi MH, Ahmadi MA, Mehrpooya M, Sameti M. Thermo-ecological analysis and optimization performance of an irreversible three-heat-source absorption heat pump. Energy Convers Manage 2015;105:1125–37.
[16] Chen L, Ge YL, Qin X, Xie ZH. Exergy-based ecological optimization for a four-temperature-level absorption heat pump with heat resistance, heat leakage and internal irreversibility. Int J Heat Mass Transf 2019;129:855–61.
[17] Fossi Nemogne RL, Medjo Nouadje BA, Ngouateu Wouagfack PA, Tchinda R. Thermo-ecological analysis and optimization of a three-heat-reservoir absorption heat pump with two internal irreversibilities and external irreversibility. Int J Refrig 2019;106:447–62.
[18] Patel VK, Raja BD. A comparative performance evaluation of the reversed Brayton cycle operated heat pump based on thermo-ecological criteria through many and multi objective approaches. Energy Convers Manage 2019;183:252–65.
[19] Qin X, Chen L, Xia S. Ecological performance of four-temperature-level absorption heat transformer with heat resistance, heat leakage and internal irreversibility. Int J Heat Mass Transf 2017;114:252–7.
[20] Sahin B, Kodal A, Ekmekci I, Yilmaz T. Exergy optimization for an endoreversible cogeneration cycle. Energy 1997;22:551–7.
[21] Ust Y, Sahin B, Kodal A. Optimization of a dual cycle cogeneration system based on a new exergetic performance criterion. Appl Energy 2007;84:1079–91.
[22] Lostec BL, Millette J, Galanis N. Finite time thermodynamics study and exergetic analysis of ammonia-water absorption systems. Int J Therm Sci 2010;49:1264–76.
[23] Kodal A, Sahin B, Oktem AS. Performance analysis of two stage combined heat pump system based on thermoeconomic optimization criterion. Energy convers Manage 2000;41:1989–98.
[24] Kodal A, Sahin B, Yilmaz T. Effects of internal irreversibility and heat leakage on the finite time thermoeconomic performance of refrigerators and heat pumps. Energy Convers Manage 2000;41:607–19.
[25] Kodal A, Sahin B, Ekmekci I, Yilmaz T. Thermoeconomic optimization for irreversible absorption refrigerators and heat pumps. Energy Convers Manage 2003;44:109–23.

[26] Durmayaz A, Sogut OS, Sahin B, Yavuz H. Optimization of thermal systems based on finite-time thermodynamics and thermoeconomics. Progr Energy Combust Sci 2004;30:175–217.
[27] Wu S, Lin G, Chen J. Optimum thermoeconomic and thermodynamic performance characteristics of an irreversible three-heat-source heat pump. Renew Energy 2005; 30:2257–71.
[28] Zare V, Mahmoudi SMS, Yari M, Amidpour M. Thermoeconomic analysis and optimization of an ammonia-water power/cooling cogeneration cycle. Energy 2012;47:271–83.
[29] Qureshi BA, Syed MZ. Thermoeconomic considerations in the allocation of heat transfer inventory for irreversible refrigeration and heat pump systems. Int J Refrig 2015;54:67–75.
[30] Xu L. Thermodynamic analysis of stirling heat pump based on thermoeconomic optimization criteria. MATEC Web Conf 2016;61:01010. https://doi.org/10.1051/matecconf/20166101010.
[31] Fossi Nemogne RL, Medjo Nouadje BA, Ngouateu Wouagfack PA, Tchinda R. Exergetic, ecological and thermo-economic (3E) optimization of an absorption heat pump with heat resistance, heat leakage and two internal irreversibilities: comparison. Int J Refrig 2020;112:251–61.
[32] Su H, Gong G, Wang C, Zhang Y. Thermodynamic optimization of an irreversible carnot refrigerator with heat recovery reservoir. Appl Therm Eng 2017;110: 1624–34.